

# **Study of Human Cripto-1 in Oncogenic Molecular Interactions**

**A Thesis**

**Submitted in Partial Fulfillment of the  
Requirements for the Degree of**

**DOCTOR OF PHILOSOPHY**

*by*

**SATENDRA SINGH GURJAR**



**Department of Biosciences and Bioengineering,  
Indian Institute of Technology Guwahati,  
Guwahati-781039, Assam, India**

**March 2021**



# **Study of Human Cripto-1 in Oncogenic Molecular Interactions**

**A Thesis**

**Submitted in Partial Fulfillment of the  
Requirements for the Degree of**

**DOCTOR OF PHILOSOPHY**

*by*

**SATENDRA SINGH GURJAR**



**Department of Biosciences and Bioengineering,  
Indian Institute of Technology Guwahati,  
Guwahati-781039, Assam, India**

**March 2021**



विद्यां ददाति विनयं,  
विनयाद् याति पात्रताम्।  
पात्रत्वात् धनमाप्नोति,  
धनात् धर्मं ततः सुखम्॥

*Hitopadesha verse 5*

Knowledge gives discipline,  
from discipline comes worthiness,  
from worthiness one gets wealth,  
from wealth (one does) good deeds,  
from that (comes) joy.

*Hitopadesha verse 5*



**INDIAN INSTITUTE OF TECHNOLOGY GUWAHATI**

**DEPARTMENT OF BIOSCIENCES AND  
BIOENGINEERING**

---

**STATEMENT**

I do hereby declare that the research findings of this thesis is the result of research work carried out by me in the Department of Biosciences and Bioengineering, Indian Institute of Technology Guwahati, Guwahati, India, under the supervision of Dr. Biplab Bose.

As per the general norms of reporting research findings, due acknowledgements have been made, wherever the research findings of other researchers have been cited in this thesis.

**Date:** 12 August 2021

  
12/08/21

**Satendra Singh Gurjar**

**146106043**



**INDIAN INSTITUTE OF TECHNOLOGY GUWAHATI**  
**DEPARTMENT OF BIOSCIENCES AND**  
**BIOENGINEERING**

**CERTIFICATE**

It is certified that the work described in this thesis entitled “*Study of Human Cripto-1 in Oncogenic Molecular Interactions*” by Mr. Satendra Singh Gurjar for the award of degree of Doctor of Philosophy is an authentic record of the results obtained from the research work carried out under my supervision in the Department of Biosciences and Bioengineering, Indian Institute of Technology Guwahati, India, and this work has not been submitted elsewhere for the award of any other degree.

**CERTIFIED**

*Biplab Bose*

**Biplab Bose, Ph.D.**

(Thesis Supervisor)

Date: *12/08/2021*

*Satendra Singh Gurjar*  
*12/08/21*

**Satendra Singh Gurjar**

(Candidate)

Roll No: 146106043



# ACKNOWLEDGEMENT

---

I would like to take this opportunity to express my heartfelt gratitude to my family, friends and teachers who have made my learning experience worthwhile.

First and foremost, I would like to acknowledge the pivotal role played by Dr. Biplab Bose, in my PhD tenure. I am grateful to have spent my formative years in academics under such a learned person, who inculcated in me an appreciation of science and a unique outlook towards research. During my PhD tenure, Dr. Bose not only taught me the basics of research but also inculcated in me a yearning for science and the philosophy of life. The association with Dr. Bose has been extremely inspiring, motivating me to scale critical issues during my PhD thesis work. Amongst his various features, his dedication towards the subject and tremendous breadth of knowledge stands out as commendable qualities. Furthermore, his inimitable support, moral guidance and steadfast resolve has helped me learn to face hardships head on and pull through rough patches with patience and complete this work. Most importantly, his virtues of dedication towards science, determination and unquenchable thirst for knowledge influenced my growth as a student of science.

I am grateful to my doctoral committee members, Professor Siddharth Sankar Ghosh, Professor Aiyagari Ramesh and Professor Lalit Mohan Pandey for their insightful suggestions, support and constant motivation, which has led to an improvement in the quality of my research work.

I am grateful to Professor Latha Rangan, Head of the Department of Biosciences and Bioengineering, IIT Guwahati, Professor Kannan Pakshirajan and Professor V.V. Dasu, Former Heads of the Department Biosciences and Bioengineering, IIT Guwahati for providing me the necessary facilities that helped me to pursue my research at IIT Guwahati. I am also grateful to all faculty members and staff of the Department of Biosciences and Bioengineering for supporting me throughout the Ph.D. tenure. I would like to thank Department of Biosciences and Bioengineering for providing infrastructural facility for my research work. I would also like to thank Departmental Central Instruments Facility (DCIF) for providing ambient atmosphere of research and high-end equipments to execute my experiments.

I am grateful to Professor Siddhartha Sankar Ghosh, Professor Pranab Goswami, Professor Lingaraj Sahoo and Professor Aiyagari Ramesh for providing a state-of-the-art facility at the Center for Excellence under the aegis of Program Support Grant provided by Department of Biotechnology (DBT), Government of India having high-end equipments, providing an ambient atmosphere for my research. This academic environment enabled me to execute my experiments, develop my skills and complete my Ph.D. work. I acknowledge the Department of Biotechnology (DBT), Government of India, Indian Council of Medical Research (ICMR), Ministry of Human Resource Department (MHRD) and IIT Guwahati for providing research fellowships and supporting my research through grants.

I would like to extend sincere gratitude to my lab seniors Dr. Pojul Loying, Dr. Mahesh Agarwal and Dr. Paulami Dutta and my colleague Dr. Vimalathithan Devaraj, whose intellectual contribution and motivation enabled the realization of this thesis. It has been my privilege to have worked with them. I am also thankful to my former lab members Saumya, Kaushalesh and Vishwas. It is also my pleasure to thank my current lab junior Mouli. I would also like to acknowledge Dr. Mohitosh Dey, for all the elevating discussions and knowledge he has passed on to me. I wish to thank my friend Dr. Ashok Jangra, (from NIPER Guwahati) along with my friends from IIT Guwahati including Mr. Krishan Kumar Thakur, Dr. Bapi Mandal, Dr. Bandhan Chatterjee, Dr. Anil P. Bidkar, Mrs. Shrutika Suryawanshi, Mrs. Arithra Das, Dr. Poulomi Dey, Dr. Srirupa Bhattacharya, and Mrs. Anwasha Purakayastha for supporting me through thick and thin. I would also like to thank all my batch mates for making my life in IIT Guwahati so enjoyable.

Lastly, and also most importantly, I am extremely grateful to my parents, Mrs. Mithilesh Gurjar and Mr. Veerendra Singh Gurjar who have taught me the virtues which make me who I am. They have filled my life with their unconditional love and blessings. I am thankful for the freedom, support and guidance they have given me at every step of my life. I am also thankful to my brother and sister-in-law, Mr. Suraj Singh Gurjar and Mrs. Renu Gurjar and my sister Mrs. Sapna Gurjar and brother-in-law Mr. Kushal Gurjar for their unconditional love and affection during the course of my education at every level.

**Satendra Singh Gurjar**





# CONTENTS

---

<b>Contents</b>	<b>i</b>
<b>Abbreviations</b>	<b>ix</b>
<b>List of Tables</b>	<b>xiii</b>
<b>List of Figures</b>	<b>xv</b>
<b>CHAPTER 1: Introduction</b>	<b>1</b>
<b>CHAPTER 2: Literature Review</b>	
2.1. Human Cripto-1	10
2.2. Cripto-1: Genomic Organization	11
2.3. The Differential Expression Pattern of Cripto-1	14
2.3.1. Cripto-1 in Embryogenesis	14
2.3.1.1. In Embryonic development	14
2.3.1.2. In Adult Cells (Especially in Mammary gland)	17
2.3.2. Cripto-1 in Tumourigenesis	18
2.4. Role of Cripto-1 in CSCs and ESCs Maintenance	20
2.5. Cancer Stem Cells	21
2.6. Properties of CSCs	23
2.6.1. Self-Renewal Capacity	23
2.6.2. Metastasis and CSCs	23
2.6.3. Dormancy and Quiescence of CSCs	24
2.6.4. Creation of Tumour Heterogeneity	24
2.6.5. CSCs and Tumour Vascularization	24
2.7. Pathways of Cripto-1	24
2.7.1. Nodal-Dependent Cripto-1 Signalling	25
2.7.2. Nodal-Independent Cripto-1 Signalling Pathway	27

## Contents

---

2.7.3.	Wnt Signalling Pathway	31
2.7.4.	Notch Signalling Pathway	31
2.8.	Crosstalk of the Nodal/Cripto-1 Signalling Pathway	33
2.9.	Cripto-1 and Epithelial to Mesenchymal Transition (EMT)	33
2.10.	Embryonic Stem Cells	34
2.11.	ES cells and Hypoxia	35
2.12.	Hypoxia-Inducible Factor (HIF)	36
2.12.1.	HIFs – Structure and Regulation	37
2.12.2.	HIF Isoforms	38
2.13.	Role of HIF in Embryogenesis	39
2.14.	Role of HIF-1 in MAPK/ERK and PI3K/AKT Pathways	40
2.14.1.	Interplay between HIF and ERK	40
2.14.2.	Interplay between HIF and PI3K	41
2.15.	Multidrug Resistance	41
2.15.1.	MDR Types, Their Structure and Function	42
2.16.	MDR-1 and CSCs	44
2.17.	MDR-1 and CRIPTO-1	45
2.18.	MDR-1 and HIF-1	48

### CHAPTER 3: Materials and Methods

3.1.	Bacterial Strains Maintenance and Growth	53
3.2.	Human Cell Lines: Culturing, Passaging and Stock Making	53
3.3.	Spheroid Formation	55
3.4.	Plasmid DNA Isolation	56
3.5.	Plasmid Construct	57
3.6.	CR-1 Clone Confirmation by Colony PCR	58
3.7.	CR-1 Clone Confirmation by Restriction Digestion	59
3.8.	Transfection of CR-1 clone Vector Constructs into Mammalian Systems	60
3.9.	RNA Extraction	61

## Contents

---

3.10.	Removal of Genomic DNA Contamination from Isolated RNA	62
3.11.	cDNA Synthesis	63
3.12.	Quantitative Real-Time PCR	65
3.13.	Protein Isolation	66
3.14.	Protein Estimation by Lowry' Method	68
3.15.	SDS Page and Western Blotting	68
3.16.	MTT Assay for Cytotoxicity	70
3.17.	Flow Cytometry	70
3.18.	Cell Proliferation Assay	71

### CHAPTER 4: Results and Discussion

4.1.	Upregulation of CR-1 Expression by TGF- $\beta$	75
4.2.	Expression of CR-1 on MAPK and PI3K Pathway Inhibition	76
4.3.	TGF-B Induced CR-1 Expression on MAPK & PI3K Pathway Blockage	78
4.4.	Induction of Cripto-1 Expression by Recombinant CR-1 in HEK293 Cells	79
4.5.	Generation of CR-1 Overexpressing Cell System	81
4.6.	Co-expression of HIF-1 $\alpha$ and MDR-1 on CR-1 Overexpression in HEK293	86
4.7.	Cripto-1 Overexpression Induced HIF-1 $\alpha$ Expression Mediated by AKT Mitogenic Pathway	89
4.8.	CR-1 Overexpression Induces the Cell Proliferation in HEK and MCF-7 Cells	90
4.9.	Effect of CR-1 Overexpression on Functional P-Glycoprotein Efflux Pump	91
4.10.	CR-1 Modulates the CSC Markers' Expression	93
4.11.	Association of Cripto-1 with Embryonic Stem Cells Markers	98

## Contents

---

4.12.	In Hypoxic-like condition, HIF-1 $\alpha$ induces the Expression of CR-1	100
4.13.	Effect of CoCl <sub>2</sub> on the Activation of AKT/ERK Pathways	101
4.14.	Expression Studies of CSC and ESC markers on Cells Subjected to CoCl <sub>2</sub> Treatment	103
4.15.	Expression of CR-1 in 2D Monolayer vs 3D Spheroids Model:	104
4.16.	Studies on the Activation of ERK and AKT Pathways in the 3D Spheroid Model	107
4.17.	The Fate of CSC and ESC Markers in the 3D Spheroids Hypoxic Model:	108
4.18.	Effect of CR-1 Overexpression on 3D Spheroids:	110
<b>CHAPTER 5: Conclusion and Future Perspectives</b>		120
<b>CHAPTER 6: Bibliography</b>		124
<b>Appendix</b>		179
<b>List of Publications</b>		186

# ABBREVIATIONS

---

<b>ANOVA</b>	Analysis of variance
<b>AKT</b>	Protein kinase B (PKB), or AKT is a serine/threonine-specific protein kinase
<b>µg</b>	Microgram
<b>µL</b>	Microliter
<b>µM</b>	Micro molar
<b>BrdU</b>	5-bromo-2'-deoxyuridine
<b>BLAST</b>	Basic local alignment search tool
<b>bp</b>	Base pair
<b>CR-1</b>	Cripto-1
<b>cDNA</b>	Complementary DNA
<b>CD24</b>	Cluster of differentiation 24 or heat stable antigen CD24
<b>CD44</b>	A cell-surface glycoprotein involved in cell–cell interactions, cell adhesion and migration
<b>CD133</b>	Known as prominin-1, is a glycoprotein that in humans is encoded by the PROM1 gene
<b>CFU</b>	Colony forming unit
<b>CMV</b>	Human cytomegalovirus (CMV)
<b>cps</b>	Counts per second
<b>CV</b>	Crystal violet
<b>C<sub>t</sub></b>	cycle threshold
<b>CSC</b>	Cancer Stem Cells
<b>DMEM</b>	Dulbecco's modified eagles' medium
<b>DMSO</b>	Dimethyl sulfoxide
<b>DNA</b>	Deoxyribonucleic Acid
<b>dNTP</b>	Deoxyribonucleotide triphosphate
<b>ECM</b>	extracellular matrix
<b>EDTA</b>	Ethylene diamine tetra acetic acid
<b>EGF</b>	Epidermal growth factor
<b>EGFR</b>	Epidermal growth factor receptor
<b>ERK</b>	Extracellular signal-regulated kinase
<b>ESC</b>	Embryonic Stem Cells

## Abbreviations

---

<b>EV</b>	Empty Vector
<b>FBS</b>	Fetal bovine serum
<b>GPI</b>	Glycosylphosphatidylinositol (GPI)
<b>GSH</b>	Glutathione
<b>GST</b>	Glutathione S-transferase
<b>GAPDH</b>	Glyceraldehyde 3-phosphate dehydrogenase
<b>h</b>	Hour
<b>HRP</b>	Horseradish peroxidase
<b>HEK</b>	Human embryonic Kidney
<b>HIF</b>	Hypoxia-Inducible Factor
<b>IC<sub>50</sub></b>	half maximal inhibitory concentration
<b>kDa</b>	Kilo Dalton
<b>Kg</b>	Kilogram
<b>MAPK</b>	Mitogen-activated protein kinases
<b>MCF7</b>	Michigan Cancer Foundation-7 breast adenocarcinoma
<b>MDR</b>	Multi Drug Resistance
<b>min</b>	Minutes
<b>mg</b>	Milligrams
<b>mL</b>	Milliliter
<b>mM</b>	Milli molar
<b>MTT</b>	3-(4,5-Dimethylthylthiazol-2-yl)-2,5-diphenyltetrazolium bromide
<b>MW</b>	Molecular weight
<b>NANOG</b>	Homeobox protein NANOG is a transcriptional factor that helps embryonic stem cells (ESCs) maintain pluripotency by suppressing cell determination factors
<b>ng</b>	Nano gram
<b>nM</b>	Nano molar
<b>nm</b>	Nanometer
<b>NTERA</b>	A clonally derived, pluripotent human embryonal carcinoma cell line
<b>OD<sub>600</sub></b>	Optical density at 600 nm
<b>OCT4</b>	octamer-binding transcription factor 4
<b>P-AKT</b>	Phospho- Protein kinase B (PKB), also known as Akt,
<b>PBS</b>	Phosphate buffered saline
<b>PCR</b>	polymerase chain reaction

## Abbreviations

---

<b>P-ERK</b>	Phosphorylated Extracellular signal-regulated kinase
<b>PI3K</b>	Phosphatidylinositol 3-kinase
<b>PIP2</b>	Phosphatidylinositol-(4,5)-bisphosphate
<b>PIP3</b>	phosphatidylinositol-(3,4,5)-triphosphate
<b>PI</b>	Propidium iodide
<b>PMSF</b>	Phenylmethanesulfonylfluoride
<b>PTEN</b>	Phosphatase and tensin homolog
<b>PVDF</b>	Polyvinylidene fluoride
<b>qRT-PCR</b>	Real-Time Quantitative Reverse Transcription PCR
<b>RBC</b>	red blood corpuscle
<b>RIPA</b>	Radioimmunoprecipitation assay
<b>RNA</b>	Ribonucleic acid
<b>rRNA</b>	Ribosomal RNA
<b>rpm</b>	Revolutions per minute
<b>RT</b>	Room Temperature
<b>SD</b>	Standard deviation
<b>SDS-PAGE</b>	sodium dodecyl sulphate–polyacrylamide gel electrophoresis
<b>SOX2</b>	SRY (sex determining region Y)-box 2, also known as SOX2
<b>TDGF</b>	Teratocarcinoma derived growth factor
<b>TGF-<math>\beta</math></b>	Transforming growth factor beta

# LIST OF TABLES

---

CHAPTER 2	Page No.
<b>Table 2.1.</b> Regulatory Factors of Cripto-1	17
<b>Table 2.2.</b> Pathways affected by Cripto-1.	26
<b>Table 2.3.</b> Examples of Proteins affected by Cripto-1 Overexpression	30
<b>CHAPTER 3</b>	<b>Page No.</b>
<b>Table 3.1..</b> List of Bacterial Strains	53
<b>Table 3.2..</b> Bacterial Culture Media	53
<b>Table 3.3.</b> Culture Conditions	54
<b>Table 3.4.</b> List of Plasmid Vectors	58
<b>Table 3.5.</b> Composition of the Reaction Mixture for Colony PCR	58
<b>Table 3.6. .</b> Composition of the Reaction Mixture for Restriction Digestion	59
<b>Table 3.7. .</b> Composition of the Reaction Mixture for DNase treatment	63
<b>Table 3.8. .</b> Reaction Mix Preparation for cDNA Synthesis	64
<b>Table 3.9. .</b> Reverse Transcription Cycling Program for cDNA Synthesis	64
<b>Table 3.10.</b> Reaction Mix Preparation for qRT-PCR	65
<b>Table 3.11.</b> Standard cycling conditions are recommended for cDNA templates for qRT-PCR.	66
<b>Table 3.12.</b> Specific properties of the components of the protease inhibitor cocktail	67

# LIST OF FIGURES

---

CHAPTER 2		Page No.
<b>Scheme 2.1.</b>	Structural representation of human Cripto-1 protein (amino acids 1-188). Cripto-1 is a membrane protein anchored to GPI that can be broken by GPIPLD and released as a soluble protein into the cells' supernatant. GPI-PLD: phospholipase D with glycosylphosphatidylinositol.	11
<b>Scheme 2.2.</b>	Schematic of Cripto-1 Signalling pathways. (adapted from (Strizzi et al., 2005) )	28
<b>Scheme 2.3.</b>	Schematic representation of the Cross talk of the Nodal/Cripto-1 signalling pathway with various other signalling pathways.	32
<b>Scheme 2.4.</b>	Schematic representation of the Cross talk of the Nodal/Cripto-1 signalling pathway with Wnt, hypoxia, Notch, Oct-4, and Nanog signalling pathways. ( <i>adapted from</i> (Caterina Bianco et al., 2010b))	37
CHAPTER 3		Page No.
<b>Scheme 3.1.</b>	Sub culturing of mammalian cell lines	54
<b>Scheme 3.2.</b>	Formation of a special semi-solid medium for culturing of 3D spheroids	55
<b>Scheme 3.3.</b>	Preparation of stable 3D spheroids	56
<b>Scheme 3.4</b>	Recombinant Plasmid DNA Isolation	57
<b>Scheme 3.5</b>	Colony PCR Protocol and Cycling Program	59
<b>Scheme 3.6</b>	Procedure of Lipofectamine based transfection	60
<b>Scheme 3.7.</b>	Total RNA Extraction by TRIZOL Method	62
<b>Scheme 3.8.</b>	Schematic illustrating DNase Treatment of RNA Samples Prior to RT-PCR.	63
<b>Scheme 3.9.</b>	Schematic illustrating the cDNA Synthesis Concept	64
<b>Scheme 3.10</b>	Schematic illustrating the protein isolation protocol	67
<b>Scheme 3.11</b>	Schematic illustrating the Protein Estimation by Lowry' method	68
<b>Scheme 3.12</b>	Schematic illustrating the Protocol for western blotting	69

## List of Tables

---

<b>Scheme 3.13</b>	Schematic illustrating the protocol of MTT assay for cytotoxicity assessment	70
<b>Scheme 3.14</b>	Schematic illustrating the Flow Cytometry protocol	71
<b>Scheme 3.15</b>	Schematic illustrating the protocol of Cell Proliferation assay	72
<b>CHAPTER 4</b>		<b>Page No.</b>
<b>Figure 4.1.</b>	Upregulation of CR-1 expression by TGF- $\beta$ in NTERA-2 cell line analyzed by Real-Time PCR: A) different concentration of TGF- $\beta$ for 24 h and B) Treatment of 10 ng/mL of TGF- $\beta$ at different time points. Data represented are the mean of a triplicate sample, and the analysis was performed by using Kruskal-Wallis analysis of variance. The fold in the expression of CR-1 was statistically significant ( $p < 0.05$ )	75
<b>Figure 4.2.</b>	Upregulation of CR-1 expression by TGF- $\beta$ in NTERA-2 cell line: A) Protein level expression of CR-1 measured by Flow cytometer on treatment with 10 ng/mL of TGF- $\beta$ for 24 h in serum-free optimum media (colour code: green- treated stained, red-untreated stained and blue-untreated unstained) and B) Real-Time PCR based mRNA expression of CR-1 on treatment with 10 ng/mL of TGF- $\beta$ . 18s rRNA was used as an endogenous control.	76
<b>Figure 4.3.</b>	Cell viability of NTERA-2 cells treated with different doses of (A) U0126 and (B) LY294002. Cells were treated for 24 h in serum-free optimum media, and cell viability was measured by MTT assays.	77
<b>Figure 4.4.</b>	Expression of CR-1 on treatment with different doses of both the inhibitors: A) U0126 and B) LY294002. NTERA-2 cells were treated in serum-free optimum media for 24 h, and expression of CR-1 was quantified by Real-Time PCR. 18s rRNA was used as an endogenous control.	77
<b>Figure 4.5.</b>	Expression of CR-1 on treatment with both the inhibitors in the presence or absence of TGF- $\beta$ : A) U0126 combined with TGF- $\beta$ and B) LY294002 combined with TGF- $\beta$ . NTERA-2 cells were treated in serum-free optimum media for 24 h, and the expression of CR-1 was quantified by Real-Time PCR. 18s rRNA was used as an endogenous control	78
<b>Figure 4.6.</b>	Components of ALK4/SMAD2/3 Pathway: Semi-quantitative PCR to check the expression of different molecules of ALK4/SMAD2/3 pathway in HEK293 cells. Here H denotes Water control, M denotes 100 BP marker, and C represents cDNA	80
<b>Figure 4.7.</b>	Expression of CR-1 on treatment with exogenous recombinant Cripto-1 protein (rCR-1). HEK239 cells were treated with 50ng/mL, and 150 ng/mL of dose in serum-free DMEM media for 72 h and expression of CR-1 was quantified by Real-Time PCR. 18s rRNA was used as an endogenous control.	81

- Figure 4.8.** Different forms of CR-1 Protein used in the study. a) Full-length human CR-1 overexpressed in HEK293 and MCF-7 cells. b) C-terminal truncated human CR-1 ( $\Delta$ CR-1) overexpressed in HEK293 and MCF-7 cells. c) Recombinant CR-1 expressed in insect expression system procured from R&D Systems. Each block in the structure represents a protein domain, and the numbers above the blocks represent the number of amino acids arranged in sequence to form the particular domain 82
- Figure 4.9.** Schematic diagram of both the recombinant constructs: A) pCI-neo-CR-1 consists of Full-length human CR-1 gene and B) pCI-neo- $\Delta$ CR-1 contains C-terminal truncated human CR-1 gene. The vector consists of the CMV promoter, Amp<sup>r</sup> (ampicillin resistance gene for bacterial selection) and Neo<sup>r</sup> (Neomycin resistance gene as mammalian cells selection marker) 83
- Figure 4.10.** Confirmation of Plasmid DNA by Restriction Digestion: A) Restriction digestion of pCI-neo-CR-1 by EcoRI. Lane 1 is 1 KB ladder; Lane 2 is digested plasmid with a fragment of 532 bp released at the bottom of the gel, and Lane 3 is an undigested circular plasmid. B) Restriction digestion of pCI-neo- $\Delta$ CR-1 by XhoI and NotI. Lane 1 is 1 KB ladder; Lane 2 is digested plasmid with a fragment of 507 bp released at the bottom of the gel, and Lane 3 is an undigested circular plasmid. 85
- Figure 4.11.** Generation of stably transfected clones: A) Expression of CR-1 in MCF-7 transfected with Full-length human CR-1 compared with untransfected MCF-7 cells. B) Expression of CR-1 in HEK293 transfected with Full-length human CR-1(HEK-CR-1) compared with untransfected HEK293 cells. C) Expression of CR-1 in MCF-7 transfected with C-terminal truncated human CR-1(MCF- $\Delta$ CR-1) compared with untransfected MCF-7 cells. Real-time PCR was used to measure the expression of CR-1 after 6-8 weeks of clonal selection by G-418 antibiotics 86
- Figure 4.12.** The expression of CR-1 was accessed by western blotting.  $\beta$ -actin and Total Smad2 were used as a loading control for MCF-7 clones and HEK293 clones, respectively. A) Protein level Expression of CR-1 in MCF-7 transfected with Full-length human CR-1 and C-terminal truncated CR-1 compared with untransfected MCF-7 cells. B) Protein level Expression of CR-1 in HEK293 transfected with Full-length human CR-1(HEK-CR-1) compared with untransfected HEK293 cells. 86
- Figure 4.13.** Co-expression of HIF-1 $\alpha$  and MDR-1 on CR-1 overexpression: A) Expression of CR-1 in HEK293 overexpressed with full-length human CR-1 by stable transfection. B) and C) represents the expression of HIF-1 $\alpha$  and MDR-1, respectively, on CR-1 overexpression in HEK293. D) Expression of CR-1 in MCF-7 overexpressed with full-length human CR-1 by stable transfection. E) and F) represents the expression of HIF-1 $\alpha$  and MDR-1, respectively, on CR-1 overexpression in MCF-7. The expression of genes was assessed by Real-Time PCR. 18s rRNA was used as endogenous control 87

- Figure 4.14.** Western blotting shows the Co-expression of HIF-1 $\alpha$  and MDR-1 on protein level in CR-1 overexpression cells: A) Expression of CR-1, HIF-1 $\alpha$  and MDR-1 in HEK-CR-1 and HEK- $\Delta$ CR1 cells as compared to HEK-EV. Lane A, B, and C represents HEK-EV, HEK-CR-1 and HEK- $\Delta$ CR1 sample, respectively. B) Expression of CR-1 and MDR-1 in MCF-CR-1 and MCF- $\Delta$ CR1 cells compared to MCF-EV. Lane A, B, and C represents MCF-EV, MCF-CR-1 and MCF- $\Delta$ CR1 sample, respectively. GAPDH was used as the loading control. 88
- Figure 4.15.** Western Blotting to detect the phosphorylation status of ERK and AKT (A) Expression of P-ERK and P-AKT in HEK-CR-1 and HEK- $\Delta$ CR1 cells compared to HEK-EV Lane A, B, and C represents HEK-EV, HEK-CR-1 and HEK- $\Delta$ CR1 sample, respectively. (B) Expression of P-ERK and P-AKT in MCF-CR-1 and MCF- $\Delta$ CR1 cells compared to MCF-EV. Lane A, B, and C represents MCF-EV, MCF-CR-1 and MCF- $\Delta$ CR1 sample, respectively. Total ERK and Total AKT were used as the loading control. 89
- Figure 4.16.** Cell proliferation assay: Cells were seeded in equal density in a 96-well plate in phenol red-free Serum media. Cells were lysed at a specific time point by adding the staining solution (composition: see methods section). Multiplate reader measured fluorescence intensity at 530 nM excitation and 620 nM emission wavelength. A) Fold change in Cell number compared between MCF-EV and MCF-CR1 B) Fold change in Cell number compared between HEK-EV between HEK-CR1 91
- Figure 4.17.** Cytotoxicity assay: To measure P-glycoprotein efflux pump activity in MCF-CR-1 cells compared to MCF-EV cells, the MTT assay was performed. A) % cell viability after treatment with different doses of Paclitaxel for 48 h B) % cell viability after treatment with different doses of Doxorubicin for 48 h. For each dose, five replicates were used, and the absorbance of DMSO dissolved formazan crystals was measured by the multiplate reader at 570 nM wavelength. 92
- Figure 4.18.** Cytotoxicity assay: To measure P-glycoprotein efflux pump activity in HEK-CR-1 cells compared to HEK-EV cells, the MTT assay was performed. A) % cell viability after treatment with different doses of Paclitaxel for 48 h B) % cell viability after treatment with different doses of Doxorubicin for 48 h. For each dose, five replicates were used, and the absorbance of DMSO dissolved formazan crystals was measured by the multiplate reader at 570 nM wavelength 92
- Figure 4.19.** CR-1 modulates the CSCs marker expression: To check this, the expression of cancer cell surface markers was measured using Real-time PCR: A) CD24, B) CD44, and C) CD133 represents the fold change in mRNA expression of HEK-CR-1 compared to HEK293 wild-type cells. While D) CD24 E) CD44 and F) CD133 represents the mRNA level expression in MCF-CR1 93

- compared to MCF-7 wild-type cells. 18s rRNA was used as endogenous control
- Figure 4.20.** Effect of rCR-1 treatment on the CSCs modulation: The HEK293 cells were treated with two different doses of rCR-1 for 72 h in serum-free DMEM media, and the expression of cancer cell surface markers was measured by using Real-time PCR: A) CD24 and B) CD44 represents the fold change in mRNA expression in rCR-1 treated HEK293 as compared to untreated cells. 18s rRNA was used as the endogenous control. 94
- Figure 4.21.** Flow cytometry analysis to detect the cell surface expression of CD24 and CD44: HEK293 treated with rCR-1 for 72 h in serum-free DMEM media and the expression of A) CD24 and B) CD44 was checked by FACS analysis. (Colour code: Red, Blue, Orange, and Green histograms represent Untreated Unstained, Untreated stained with antibody, 50 ng/mL of rCR-1 treated stained with antibody and 150ng/mL rCR-1 treated stained with antibody respectively). The increase in expression was denoted in terms of median fluorescence intensity (MFI), shown in C) MFI of CD24-FITC tagged and D) MFI of CD44-PE tagged 95
- Figure 4.22.** Dual colour flow cytometry determines the side cell population's nature on treatment with recombinant cripto-1 in HEK293 cells. The cells were stained with CD24-FITC tagged, and CD44-PE tagged. The dot plots represent A) Untreated group, B) 50 ng/mL rCR-1 treated and C) 150 ng/mL rCR-1 treated. The fluorescence spillover was removed using the compensation matrix. The percentage of CD44+/CD24+ subpopulation increases in a dose-dependent manner 96
- Figure 4.23.** Flow cytometry to detect the CSCs marker expression: The NTERA2 cells were treated with 10ng/mL of TGF- $\beta$  for 24 h in serum-free optimen media. The top row represents the expression of CD24-FITC tagged, the middle row represents the expression of CD44-PE tagged, and the bottom row represents the expression of CR-1-PE tagged 97
- Figure 4.24.** CR-1 overexpression induces the ESCs markers expression: To check this, the expression of embryonic stem cell markers was measured by using Real-time PCR: A) OCT4, B) Nanog, and C) SOX2 represents the fold change in mRNA expression in HEK-CR1 as compared to HEK293 wild-type cells. While D) OCT4, E) Nanog, and F) SOX2 represents the mRNA level expression in MCF-CR1 compared to MCF-7 wild-type cells. 18s rRNA was used as endogenous control. 99
- Figure 4.25.** Effect of rCR-1 treatment on ESCs markers expression: The HEK293 cells were treated with two different doses of rCR-1 for 72 h in serum-free DMEM media, and the expression of cancer cell surface markers was measured by using Real-time

- PCR: A) OCT4, B) Nanog and C) SOX2 represents the fold change in mRNA expression in rCR-1 treated HEK293 as compared to untreated cells. 18s rRNA was used as the endogenous control
- Figure 4.26.** Effect of Cobalt Chloride on co-expression of CR-1 and HIF-1 $\alpha$ : The HEK293 cells were treated with CoCl<sub>2</sub> for 24 h in serum DMEM media, and the mRNA expression was measured by using Real-time PCR: A) HIF-1 $\alpha$ , B) CR-1, and C) MDR-1 represents the fold change in mRNA expression in CoCl<sub>2</sub> treated HEK293 as compared to untreated cells. 18s rRNA was used as the endogenous control. 100
- Figure 4.27.** Western blotting shows the Co-expression of HIF-1 $\alpha$  and CR-1 in Cobalt chloride treated HEK293 cells: A) Expression of CR-1, HIF-1 $\alpha$  and MDR-1 on treatment with different doses of CoCl<sub>2</sub> in HEK293 cells as compared to untreated. B) Expression of CR-1 and MDR-1 on treatment with different doses of CoCl<sub>2</sub> in MCF-7 cells compared to untreated. GAPDH was used as the loading control. 101
- Figure 4.28.** Western Blotting to detect the phosphorylation status of ERK and AKT in COCl<sub>2</sub> treated HEK293 cells (A) Expression of P-ERK and P-AKT on treatment with different doses of CoCl<sub>2</sub> in HEK293 cells as compared to untreated. (B) Expression of P-ERK and P-AKT on treatment with different doses of CoCl<sub>2</sub> in MCF-7 cells compared to untreated. Total ERK and Total AKT were used as the loading control. 102
- Figure 4.29.** Effect of Cobalt Chloride on CSCs and ESCs markers: The HEK293 cells were treated with CoCl<sub>2</sub> for 24 h in serum DMEM media, and the mRNA expression was measured by using Real-time PCR: A) CD24, B) CD44, C) CD133, D) Nanog, E) OCT4, and F) SOX2 represents the fold change in mRNA expression in CoCl<sub>2</sub> treated HEK293 as compared to untreated cells. 18s rRNA was used as endogenous control. 103
- Figure 4.30.** Bright-field microscopic image showing morphological differences between HEK293 Monolayer vs 3D Spheroids. The scale bar of the image is 200  $\mu$ m. 105
- Figure 4.31** Expression of CR-1 in 2D monolayer vs 3D spheroids: The HEK293 cells were allowed to grow up to different time points, and Real-Time PCR measured the fold change in mRNA expression. A) And B) represents the induction of CR-1 expression in 3D spheroids grown for different time points. S-4, S-6 and S-8 represent the spheroids grown for 4, 6, and 8 days respectively. 18s rRNA was used as endogenous control. 105
- Figure 4.32** Co-expression of CR-1 and HIF-1 $\alpha$  in 3D spheroids shown by Real-Time PCR. The Top row bar plot represents the fold change in expression of A) CR-1, B) HIF-1 $\alpha$ , and C) MDR-1 in the HEK-CR-1 spheroids compared to HEK-CR-1 monolayer. The bottom row bar plot represents the fold change in expression of D) CR-1 E) HIF-1 $\alpha$  and D) MDR-1 in the HEK-EV spheroids compared to 106

## List of Tables

---

- the HEK-EV monolayer. 18s rRNA was used as endogenous control.
- Figure 4.33** Western blotting shows the Co-expression of HIF-1 $\alpha$  and CR-1 in 3D spheroids: **A)** Expression of CR-1, HIF-1 $\alpha$  and MDR-1 in monolayer vs spheroids comparison of HEK293 clones. **B)** Expression of CR-1, HIF-1 $\alpha$  and MDR-1 in monolayer vs spheroids comparison of MCF7 clones. GAPDH and Total AKT were used as the loading control 107
- Figure 4.34** Western Blotting to detect the phosphorylation status of ERK (**A)** Expression of P-ERK in monolayer vs spheroids comparison of HEK293 clones. (**B)** Expression of P-ERK in monolayer vs spheroids comparison of MCF-7 clones. Total ERK was used as the loading control 108
- Figure 4.35** CSCs and ESCs markers expression in 3D spheroids: The HEK293 spheroids were formed after 4 days of cell seeding. The expression of CSC and ESC markers spheroids was compared by monolayer and detected by using Real-time PCR: **A)** CD24, **B)** CD44, **C)** CD133, **D)** OCT4, **E)** Nanog, and **F)** SOX2 represents the fold change in mRNA expression in spheroids as compared to HEK293 monolayer. 18s rRNA was used as endogenous control 109
- Figure 4.36** Effect of CR-1 overexpression on 3D spheroids: The spheroids were formed after 4 days of cell seeding. The expression of CR-1, HIF-1 $\alpha$  and MDR-1 was analyzed in the HEK-CR-1 spheroids as compared to HEK293 spheroids and detected by using Real-time PCR: **A)** HIF-1 $\alpha$  **B)** CR-1 **C)** MDR-1 **D)** CD24 and **E)** OCT4 represents the fold change in mRNA expression in HEK-CR-1 spheroids as compared to HEK293 spheroids. 18s rRNA was used as endogenous control. 111



# Abstract

Human Cripto-1 (CR-1) is an Oncofetal gene that promotes cell proliferation and differentiation in the fetus, but its aberrant expression in adults leads to aggressive and highly metastatic cancer. Solid tumours are known to have the ability to thrive in a hypoxic microenvironment and frequently develop resistance to multiple drugs. Hypoxia-Inducible Factor-1 $\alpha$  (HIF-1 $\alpha$ ) is a crucial regulator of cellular processes triggered in hypoxic conditions, and Multidrug resistance protein -1(MDR-1) is involved in the emergence of resistance to a large number of drugs. In the present study, we explored the crosstalk between Cripto-1 (CR-1), Hypoxia-Inducible Factor-1 $\alpha$  (HIF-1 $\alpha$ ), and Multidrug resistance protein -1(MDR-1).

To investigate this, we used different cellular models, i.e., Cripto-1 overexpression system, Chemical induction of hypoxia-like condition by using Cobalt chloride treatment, and 3D spheroid model. Our experimental data indicate a possible co-regulation of CR-1, HIF-1 $\alpha$ , and MDR-1 in different experimental systems used in the study. We further investigated the proliferation behaviours and drug resistance of cells in the same models. Moreover, We examined the modulation of stem cell markers in our experimental system and observed possible co-regulation of common stemness molecules with the expression of Cripto-1. Further, we observed the modulation of canonical molecular signalling pathways, P-AKT and P-ERK pathways in our experimental system.

As a whole, our observations coming from multiple experiments shows that overexpression and oncogenic function of human Cripto-1 is part of an orchestrated modulation of molecular processes involving several key regulators for the genesis and progression of cancer.







## INTRODUCTION





## Introduction

Cancer is a disease in which cells have acquired the capacity to divide and expand uncontrollably, typically through genetic modifications of specific genes. (Hanahan & Weinberg, 2011). Substantial cancer origin hypotheses include tissue stem cell development, e.g. field theory, mutation, infection, chemical carcinogenesis, or epigenetic alteration. (Sell, 2010). Genetic modification in signalling pathways that regulate the cell cycle progression, apoptosis, and cell growth are popular cancer markers. Still, the degree, mechanisms, and co-occurrence of changes in these pathways vary between individual tumours and types of tumours. (Sanchez-Vega et al., 2018). Frequent genetic alterations in multiple signalling pathways, including PI3K/Akt signalling and RTK/RAS/MAP-Kinase pathway, have been reported for cancer. (Vogelstein & Kinzler, 2004). Nonetheless, the property of malignancy and the molecular lesion of cancer have been found to be in the cancer stem cell (Sell, 2010). Genetics, epigenetics, and TME are three major contributors to intratumor heterogeneity and have been postulated to regulate therapeutic resistance and tumour progression by impairing cancer cell's stemness properties. (Kreso & Dick, 2014).

According to the cancer stem cell theory, a subpopulation of cells, better known as the cancer stem cells (CSC), exists in the solid core of tumours and is also prevalent in hematopoietic origin cancers. Two fundamental principles are suggested in the stem cell theory of cancer: i) Stem cells may be found in the tissues of adults and infants; and ii) A cancer tumour consist of cells similar to the regular cell, which includes differentiated cells, stem cells and transit developing cells.(Ayob & Ramasamy, 2018; K. Wang et al., 2013). Genetic and non-genetic factors that govern the resistance to therapy, metastasis and/ or preservation of tumour microenvironment can be modulated by cancer stem cells (CSCs). (Saygin et al., 2019). These cancer stem cells (CSCs) can divide, flourish the cell population, and differentiate into normal cells.

In the early 19th century, the first idea that cancers could occur from stem cells emerged and was officially known as the embryonal rest theory of cancer (Sell, 2010). This hypothesis has shown that adult organs possess the remains of embryonic tissue. These remnant embryonic tissues began to proliferate and developing the cellular mass similar

to foetal tissues when there are a disbalance in the surrounding environment and/or tissues. (Magee et al., 2012).

CSCs can be characterized as an antecedent cell intended to be differentiated into a cancer cell (Kasai et al., 2014). Several CSC cell-surface markers (e.g. Epithelial Cell-Adhesion Molecule [EpCAM]), CD44, CD133, CR-1, CD24, Aldehyde Dehydrogenase 1 (ALDH) enzyme activity cells, and ATP-binding cassette B member 5 (ABCB5) have been identified over the years and have been shown to be useful for CSC studies. (Schulenburg et al., 2015; B. B. S. Zhou et al., 2009). The unique identification and classification of cancer is still elusive despite the availability of different CSCs markers, as CSCs can also be recognized in cells showing no CSCs marker expression. (B. B. S. Zhou et al., 2009). This suggests the need for multiple markers for the identification and classification of various types of cancer.

(CD44+CD24-/low) is the breast cancer subpopulation having high expression of CD44 and low/ no expression of CD24 were shown to be highly resistant to chemotherapy and thus promotes the relapse (Jaggupilli & Elkord, 2012; X. Li et al., 2008). For instance, CD44+ cell-specific genes in breast cancer include several recognized stem cell markers, and chemotherapy treatment has demonstrated an increment in the percentage of CD44+CD24-/low tumour cells (B. B. S. Zhou et al., 2009), The high expression level of ATP binding cassette (ABC) drug pumps is consistent with the relative resistance of these tumour-initiating cells to anticancer drugs such as paclitaxel and doxorubicin (Angelini et al., 2005) This may be due to the slow growth rate that evades the influence of fast-acting drugs on the cells. (Gasser et al., 2013; C. H. Lee, 2010)

P-glycoprotein (P-GP) encoded by the Multidrug resistance gene (MDR-1) is a 170-kD plasma membrane protein. This ATP-dependent efflux pump prevents drug accumulation into the cells, thus indirectly reducing the drugs' cytotoxicity. (Katayama et al., 2014). Active P-gp efflux pump has been reported in breast carcinomas leading to multiple drugs resistance. (Linardi & Natalini, 2006). Exploring the underlying molecular mechanism that modulates the tumour initiating cells will help to neutralize cancer cells by developing new or combination therapeutics.

CSC-specific signalling pathways offer an additional opportunity to examine CSCs in pre-clinical models. (Saygin et al. 2016). In cancer, different organs and tissues undergo various combined and regular changes in somatic cells, suggesting a possible cross-talk between pathways. (A. M. Singh et al., 2012). Extensive research has been required to explain the detailed molecular mechanism governing oncogenic modification in these pathways, essential for novel therapeutic development (Sanchez-Vega et al., 2018).

There is a subset of the cell population in humans that displays phenotypic plasticity and can divide into several lineages during embryonic development and adult life. This condition is more prevalent during embryogenesis and is limited in adult stem cells. However, phenotypic plasticity was found to reappear in cancer during tumour growth (O'Brien-Ball & Biddle, 2017). Embryogenesis is a multifaceted phenomenon that involves various growth factors for the development and differentiation of embryonic stem cells (ESC) into various functional forms of cells. Embryonic stem (ES) cells can be defined as the cells exhibiting pluripotency, immortality and capacity to develop different types of cells in the embryo and in adults on differentiation (Kasai et al., 2014). Like the aberrant embryogenesis, most germ-line cancers cells differentiate into postmitotic derivatives like mature teratoma elements on rapid multiplication. (O'Brien-Ball & Biddle, 2017)

Human Cripto-1 is a member of the Epidermal Growth Factor-Cripto-FRL-1-cryptic (EGFCFC) family of peptides, exhibiting enhanced cell proliferation, differentiation, and angiogenesis in the fetus (Caterina Bianco et al., 2010b). As a membrane-bound protein, CR-1 interacts with type I and II activin receptor and serves as a co-receptor for TGF- $\beta$  ligands like Nodal, GDF-1 and GDF-3 (Growth And Differentiation Factor-1 and 3) during early development in humans (Caterina Bianco et al., 2003; Cripto-, 2012; Souquet et al., 2012; Luigi Strizzi et al., 2007). However, Cripto-1 is also an oncofetal gene that promotes cancer cell proliferation and metastasis when expressed in adults. This later life overexpression of cripto-1 has a negative impact on the human body (Q. Liu, Cui, Yu, Bian, Qian, Hu, Ji, Yang, et al., 2017).

Cripto-1 is a type of oncofetal gene that plays a significant role in embryogenesis and malignant cancer progression. (Caterina Bianco et al., 2005; Park, Do, Han, Choi, & Kim, 2018). Besides, both embryonic stem cells and cancer cells share similar signalling

pathways, including Cripto-1 signalling (Pereira et al., 2011). | A recent report suggests the involvement of cripto-1 in the differentiation of the stem cell and its self-renewable pathway (Sousa et al., 2020)(Caterina Bianco, Strizzi, Ebert, et al., 2005) (Bianco et al., 2010). Hypoxia, Wnt-  $\beta$ /catenin, Notch signalling and TGF- $\beta$  pathway are key pathways regulated and/or influenced by CR-1 signalling (Pereira et al., 2011). Cripto-1 and its related embryonic genes are shown to overexpress in cancer and control the functions of stem cells, suggesting a link between them. (Pereira et al., 2011). A subpopulation isolated by cell sorting from human embryonic carcinoma, androgen-responsive & refractory prostate cancer and malignant melanomas shows higher cripto-1 expression and stem cell-like properties. (Cocciadiferro et al., 2009; Luigi Strizzi et al., 2007). Hence, CR-1 signalling might be a potential target for cancer therapeutics because it can help us eliminate differentiated cancer cells and undifferentiated cells stem cell like cells. (Pereira et al., 2011).

CR-1 is known to function through multiple signalling pathways, including Nodal/Alk4/SMAD2/3(Caterina Bianco et al., 2003). Alternately, Cripto-1 is also known to activate the Nodal/AIK4 independent signalling pathway. CR-1 interacts with the Glypican receptor and activates Src, which further activates the phosphoinositol-3 kinase/Akt and MAPK pathway (Cripto-, 2012; Luigi Strizzi et al., 2005). In embryonic stem cells, cripto-1 has been recognized as a pluripotency marker apart from other well-known markers like Sox-2, Oct-4, LeftyA, Tert, Nanog, and Rex-1 (Chang et al., 2010). Various transcription factors control the expression of cripto-1, including Nanog, Oct4 and SOX2 (Kashyap et al., 2009; Mahmoudian et al., 2017). Nanog and Oct4 bind to the proximal region of the transcription start site of the CR-1 promoter, and their direct involvement was noticed in the development of embryonic carcinoma(Luigi Strizzi et al., 2005). SOX2 along Oct-3/4 required for the embryonic stem cell self-renewable and pluripotency maintenance (Eini et al., 2014). Alternately, SOX2 also shows tumour suppressor properties and governs the migration and invasion in cancer cells. (Engineering & Ireland, 2015). The Cripto-1 binds as a co-receptor to form CR-1/Nodal/ALK4/ActRII receptor complex and activates Smad-2 and Smad-3 by phosphorylation which subsequently binds with Smad-4, which further activates it by phosphorylation and translocates into the nucleus (Rangel et al., 2012). This Smad 2/3/4 complex binds with CREB binding protein (CBP)/p300 to activate the downstream target genes (Pereira et al., 2011).

During early embryogenesis, stem cell differentiation, proliferation, and maintenance are regulated by various signalling pathways. Few of these pathways indicated the involvement of cripto-1 signalling, suggesting a crucial role of CR-1 in stem cell generation and maintenance. The primary pathway which acts as a common route for stem cell and Cripto-1 signalling is the Notch pathway, TGF- $\beta$  family pathways, Wnt/ $\beta$ -catenin signalling pathway, and hypoxia-inducible factor-1 alpha (HIF-1 $\alpha$ ) (De Castro et al., 2010; Souquet et al., 2012). Cripto-1 also facilitates TGF- $\beta$  family members signalling and increases Notch signalling by promoting the maturation of Notch receptors. HIF-1  $\alpha$  and GNCf are the transcription factors that are known to be active in mouse mES and human NCCIT cells and human teratocarcinoma cell line NTERA2, respectively. These transcription factors were directly or indirectly involved in the upregulation of CR-1, which induces cancer progression.

Cripto-1 is also implicated in altered stemness state, and various reports support the dynamics of stemness in both normal and cancer cells. This dynamic variation in stemness leads to change in the phenotypic equilibrium of a cell population in cancer, which varies their response to external stimuli. In a recent study, CR-1-positive populations obtained from patient-derived tumour spheroids were observed to exhibit increased expression of the genes responsible for cellular stemness. *In vivo* administration of CSC leads to increased invasion and migration of tumours, while CR-1 silencing inhibits CSC-induced tumour xenograft and arrests CSC's growth. These findings indicate an essential role of CR-1 in the regulation of the CSC compartment. However, the mechanism which is involved in CSC to non-CSC transition is not quite elucidated yet. Hence, it would be interesting to decipher the role of CR-1 in CSC generation and the mechanism involved in the dynamic transition of stem cell to non-stem cell state.

Multi-drug resistance (MDR-1) gene encodes for a kind of ABC transporter, which is responsible for the development of resistances in different cells against various drugs and similar structures (He et al., 2010; X. Wang et al., 2019). This ABC transporter prevents the accumulation and entry of drugs in the cells thereby develops resistance against several drugs. Incidence of MDR mediated by PGP has been acknowledged in various human cancers, including breast carcinomas (Kluzinska et al., 2014; Linardi & Natalini, 2006; Pojul Loying et al., 2015; Luigi Strizzi, Margaryan, Gilgur, Hardy, Normanno, et

al., 2013). The cell surface Cripto-1 prevents the cleavage of caspase-3 by different drugs. Caspase-3 disruption is a sign of apoptosis (Y. Y. Zhang et al., 2018). This anti-apoptotic property of cripto-1 was induced by TAK-1 activation followed by increased NF- $\kappa$ B-mediated Survivin activity (De Santis et al., 2000). External stimuli, like drug introduction, plays a vital role in cripto-1 induced anti-apoptotic property. Hence, targeting the CR-1 and TAK-1/NF- $\kappa$ B/Survivin pathway might be an efficient tool to reduce resistance against apoptosis during cancer (Y. Y. Zhang et al., 2018). HIF-1 $\alpha$  has been found to regulate MDR-1 (multidrug resistance-1 / ABCB1 gene) in bladder cancer cell lines (Yi Sun et al., 2016). Cripto-1 positive subpopulation isolated by cell sorting also has shown higher expression of MDR-1 in human glioblastoma cells (Poju Loying et al., 2015). These studies prompted us to explore the possible crosstalk between CR-1, HIF-1 and MDR-1.

In current work, we have thus explored the role of the Oncofetal gene cripto-1 in modulating the pathways that signal the embryonic and cancer stem cell behaviour and how this misbehaviour of molecular circuits contribute to metastasis and tumourigenesis .

## Objective

The overall objective of this thesis is to investigate the interplay between human Cripto1, Hypoxia-Inducible Factor-1 $\alpha$ , Multidrug Resistance Protein-1 and possible implications in drug resistance and cancer cell stemness.

The contents of the Ph.D. thesis entitled “Study of Human Cripto-1 in Oncogenic Molecular Interactions” have been segregated into six chapters. Chapter 1 provides an overview of the potential of Cripto-1, an Embryonic Molecule whose mistiming in expression can be a key determinant causing Cancer. Chapter 2 provides an up-to-date state-of-the-art literature report on the subject, including extensive data regarding the pathways modulating Cripto-1. Based on the all-encompassing search in the lacunae present in literature regarding Cripto-1 and its signalling pathways, the motivation as well as the materials and methods used for the execution of the experimentation are discussed in Chapter 3. The results obtained and the discussion of the outcomes of the present investigation is described in Chapter 4. An overall conclusion of the research investigation emphasizing the significant findings of the work has been included after Chapter 5.



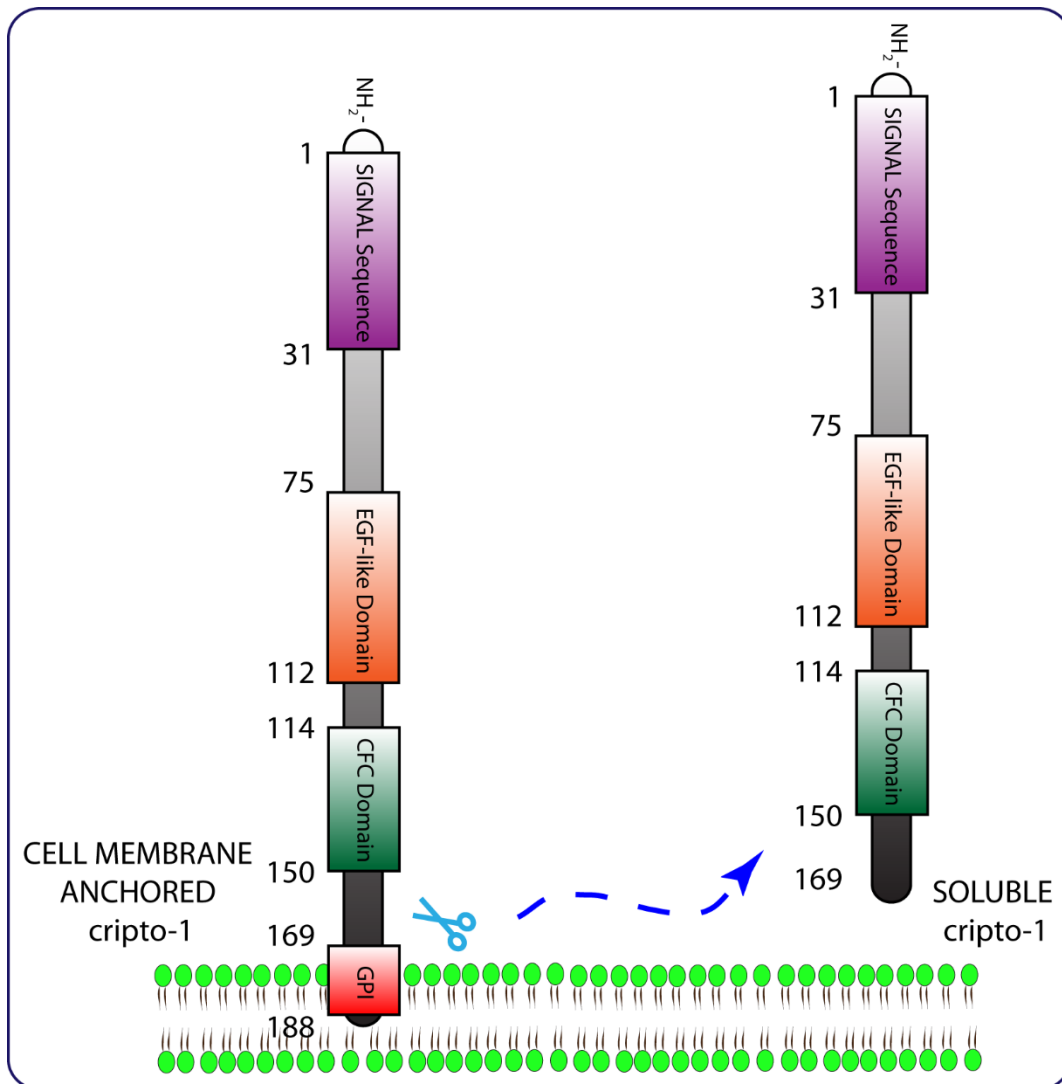




## 2.1. Human Cripto-1

Human Cripto-1 (CR-1) is a membrane-anchored glycoprotein made up of 188 amino acids and has a molecular weight of 19-36 kDa. Cripto-1 is also known as the teratocarcinoma-derived growth factor-1 and is a member of the epidermal growth factor cripto-1 FRL-1 cryptic (EGF-CFC) family and is a critical factor in early embryonic development. (Caterina Bianco, Strizzi, Normanno, et al., 2005). The human CR-1 CFC domain comprises 3 (R-S-S-R) disulfide bonds arranged in the similar pattern as like the von Willebrand factor C (VWFC)- like domains, present at the Carboxyl terminal extracellular parts of Notch ligands, Jagged1 and Jagged2 ((Foley et al., 2003; Van Vlijmen et al., 2004). Further exploration of the biochemical aspect of human CR-1 reveals that N-linked glycosylation is prominent at Asn-79 residue with more than 90% occupancy, whereas Ser-40 and Ser-161 residues act as the O-linked glycosylation site showing approximate occupancy around 80 and 40%, respectively.

The Protein size variation can be either an attribution of the cleavage of the hydrophobic moiety or the result of further modifications of protein like phosphorylation glycosylation or myristylation (Brandt et al., 1994; Minchiotti et al., 2001). Moreover, the presence of furin and stromelysin cleaving site around the N-terminal region in human CR-1 contributes to the smaller protein size(Gritsman et al., 1999; Pei & Weiss, 1995); Zhang et al., 1998). There are two different forms of human CR-1 protein, i.e., cell membrane-anchored and soluble form. However, complete EGF and CFC domain is necessary for the activity of the CR-1 protein (Adamson et al., 2002; Minchiotti et al., 2001; Yan et al., 2002). In addition, there is a GPI- modification site at the C-terminal for cleavage and attachment purposes in human CR-1 protein(Kinoshita, 2014; Zhongwu Guo, 2013). Removal of this GPI anchor stretch of residues from the COOH-terminal by enzymatic digestion with phospholipase D produces the soluble form of human Cripto-1, which is also biologically active(Galian et al., 2012; Zhongwu Guo, 2013). In various *in vivo* and reporter-based *in vitro* assays, this soluble type can also act as a co-ligand for Nodal in Nodal-dependent signalling pathway assays containing promoter sites that have binding moieties of FAST2 (FoxH1) and Smad-2 and -3(Minchiotti et al., 2001; Chunhui Xu et al., 1999; Yan et al., 2002). Therefore, Cripto-1 can act as either a protein anchored to the cell membrane or a soluble ligand (Luigi Strizzi et al., 2005). However, it is not yet known



**Scheme 2.1:** Structural representation of human Cripto-1 protein (amino acids 1-188). Cripto-1 is a membrane protein anchored to GPI that can be broken by GPIPLD and released as a soluble protein into the cells' supernatant. GPI-PLD: phospholipase D with glycosylphosphatidylinositol.

whether there are any significant implications of the qualitative or quantitative variations between Free and cell membrane bound forms of Cripto-1 on the biological activities controlled by it.

## 2.2. Cripto-1: Genomic Organization

The human teratocarcinoma derived growth factor 1 (TDGF1) gene is known as CRIPTO-1. The human Cripto-1 gene is 4.8 kb in length and comprises six exons and five introns, and has sequence elements of inverted Alu and B1, respectively and maps to chromosome 3p21.3 centromerically, close to a region that is often deleted (Caterina

Bianco & Salomon, 2010; R. Dono et al., 1991). Several alleles resulting from the amplification of groups of exons occur in the CR-1 gene in the human population. Different human CR-1 alleles have been linked to tolerance or responsiveness to different disorders, indicating that CR-1 polymorphisms could exacerbate differential genetic or environmental pressures (Jacobson & Weis, 2008). While these various alleles may be attributed to the genetic variability of the current evolutionary development of strong homologs, there may also be advantages to having CR-1 proteins of differing sizes that facilitate the binding of complexes. The human CR-1 protein is an efficient complement activation controller (Jacobson & Weis, 2008). Soluble recombinant CR-1 proteins have been known to be produced and used during increased complement activation to regulate complement activation (Noris & Remuzzi, 2013).

Between the human and mouse Cripto-1 genes, the exon-intron structure is excellently conserved in the exon4 region that consists of the EGF-like motif (Brandt et al., 1994; Ciccodicola, Dono, Obici, Simeone, Zollo, & Persico, 1989). Additionally, both the mouse and human Cripto-1 encode mRNA having comparatively short life span due to the presence of the AUUU(A)-type Kamen-like sequences in highly untranslated regions of mRNA (Caterina Bianco, Strizzi, Ebert, et al., 2005; De Castro et al., 2010; R. Dono et al., 1991). There are various other dissimilarities between murine and human CR-1. For instance, the genomic sequences 50 bp upstream of the most distal translation start sites between -610 and -1 vary between murine and human CR-1 (Baldassarre et al., 2001). In the promoter region of murine CR-1, various CAAT and TATA boxes are found, while these sequences are not found in the human CR-1 promoter sequence (Baldassarre et al., 2001; Scognamiglio et al., 1999).

The structural gene encoding the human CRIPTO protein (CR-1) corresponds to the structural gene encoding the human CRIPTO protein expressed in the undifferentiated human teratocarcinoma cells. The other (CR-3) corresponds to a complete copy of the mRNA containing seven base substitutions representing both silent and replacement substitutions in the coding region (R. Dono et al., 1991; Salomon et al., 2000). The CAP site 440 bp 5' to CR-1's is also retained in CR-3 (Moritz Hentschke et al., 2006). In several studies, analysis of the mouse CR1/CR2 genes has implicated them in various critical roles (Jacobson & Weis, 2008). The number of CR-1 related-pseudogenes also vary between mouse and human. Presently five other pseudogenes associated with human CR-1 and two with murine CR-1 are reported in the literature (X. Chen et al., 2020; Moritz Hentschke et al., 2006; Scognamiglio et al., 1999). Upon the structural and functional

comparison of genes encoding man's and mouse's CR1 and CR2 proteins, it was found that a single gene encodes these in mice while two are needed in humans for expression(Saccone et al., 1995; Scognamiglio et al., 1999).

Humans CR-1 protein expression effectively addresses many of the functions carried out by the sub primate CR-2-derived CR-1 structural domains(Jacobson & Weis, 2008). It consists of the identical SCR domains arranged to form sets of 7 SCR, called long homologous repeats (LHR), which have high homology and are thus indicative of very recent genomic development(Wong et al., 1989). In humans, Cripto-1 is found in various allelic forms, obtained by the integration of sets of exons, each comprising of genes carrying three, four, five, or six of these LHR domains encoding 190,000-300,000 Da proteins(Jacobson & Weis, 2008; Wong et al., 1989). While the presence of various allelic of CR-1 may be attributed to the current genomic modification, which results in the development of highly strong homology among various alleles, those might have advantages for binding(Ruggiero et al., 2015; Sousa et al., 2020).

Modulation of many intracellular signalling pathways, such as membrane phosphoprotein p53, nucleolin-mediated PI3K, has been related to human and mouse CR2 proteins, including responses to antigen internalization processing(Alowaidi et al., 2019; Ruggiero et al., 2015). Intronless and truncated at the 5 'end, the pseudogenes CR-2, CR-4, and CR-5 have accrued insertions point mutations, and deletions (Maria Graziella Persico et al., 1998; Scognamiglio et al., 1999).

The gene which contains the code for the expression of the human protein in teratocarcinoma cells correlates to TDGF-1(Al-Fahdawi et al., 2019; Multiforme, 2015). TDGF-3 corresponds to a full mRNA copy containing seven coding region base substitutions representing both silent and replacement substitutions(Saccone et al., 1995; Sousa et al., 2020).TDGF-1 maps on chromosome 3 from p23 to p21 location while TDGF-3 maps on the X chromosome position q21 to q22 region (Saccone et al., 1995; Scognamiglio et al., 1999).

The above human genes also map to 6p25, 3q22, and 2q37 chromosomes, individually, while CR-6 maps to chromosome 19q13.1 and the pseudogene CR-3 maps of the Xq21-q22 region of the human chromosome(N. Gene et al., 2010; Maria Graziella Persico et al., 1998). The two CR-1 pseudogenes of the mouse (CR-1-ps or TDGF-1-ps1 and CR-1-ps2 or TDGF-1-ps2) are intronless genes that have several base mutations that mark substitutions of silent and replacement amino acids and have several retroposon characteristics (Baldassarre et al., 2001; R. Dono et al., 1991; Scognamiglio et al., 1999).

CR-3, as well as CR-1-ps1, express the protein, which is functionally different from proteins expressed by CR-1 as CR-1 encodes approximately 2 kb sized major mRNA species of which differ by five amino acids (Hazrati et al., 2012).

In embryos and carcinomas, the transcripts having size varies from 1.7 – 3.5 kb are not found frequently (C Bianco, Strizzi, Normanno, et al., 2005). This might be attribution of various transcript levels modifications like alternative splicing, polyadenylation sequences, or alternative transcription initiation (Baldassarre et al., 2001; Scognamiglio et al., 1999). However, in subpopulations of breast, bladder, head and neck, lung, renal, and gastric cancer, it shows loss of heterozygosity (LOH) (D'Andrea et al., 2008; Sekido et al., 1998)

### 2.3. The Differential Expression Pattern of Cripto-1

Cripto-1 is significantly upregulated in the process of embryogenesis as well as tumorigenesis. Conversely, its level in adult tissue seems to be very minimal or negligible (De Castro et al., 2010). Cripto-1 would be a classic example of a gene that is frequently overexpressed in both the stages of development as well as in tumorigenesis (Maria Graziella Persico et al., 1998). Although the expression of Cripto-1 is lost during ES cell differentiation into the three germ layer cell types, it resurfaces at higher stages inside the cancerous cells (Luigi Strizzi et al., 2005). Nevertheless, the main factor underlying Cripto-1 re-expression in tumour cells is still to be properly identified (Hough et al., 2014). Lately, it has been identified that Cripto-1 is an indispensable part of the major essential signalling pathways related to differentiation and maintenance of stem cells and that the regulatory factors associated with Cripto-1 are described in **Table 2.1**.

#### 2.3.1 Cripto-1 in Embryogenesis

##### 2.3.1.1. In Embryonic Development

Cripto-1 may function as a co-receptor for the TGF $\beta$  component of the Nodal family during embryogenesis, regulating the development of the primitive streak as well as mesoderm and endoderm specification. (Caterina Bianco, Strizzi, Normanno, et al., 2005). Experimentation in murine and zebrafish model reveals the role of Nodal in governing the CR-1 mediated primitive streak development, Axis pattern,

mesoendoderm specification, and left-right (L/R) asymmetry formation (Ding et al., 1998; Schier & Shen, 2000; Yan et al., 2002).

Further studies revealed that EGF-CFC proteins are positively correlated with Activin Type I ALK4 (ActRIB) receptors and its co-receptor Nodal which later activates the Activin (Caterina Bianco et al., 2002; Gritsman et al., 1999; Rangel et al., 2012) Type II receptor via induction of Smad-2/Smad-3 phosphorylation leading to the formation of Smad2/3/4 complex along with FoxH11 as co-transcriptional activating agent (Caterina Bianco et al., 2002; A. M. Singh et al., 2012; Yeo & Whitman, 2001). Antivin, Lefty1 and 2 are the extracellular blockers of signalling of Vg-1 and Nodal, which regulates the Nodal activity in a concentration-dependent manner (Souquet et al., 2012; Luigi Strizzi et al., 2008). Except for the dimeric Nodal as well as Vg1/GDF-1 proteins, these proteins are monomeric. Subsequently, Antivin and Lefty also exhibit the ability to interact with multiple genes like Cripto-1, FRL-1, Nodal, and oep (Y. Chen & Schier, 2002; Sakuma et al., 2002).

Nodal and BMP may serve as cooperative antagonists via a CR-1-independent network that might be essential for the configuration of the anterior portion of neural tissue (Yeo & Whitman, 2001). In 2001, Brennan et al. have demonstrated that Nodal was able to function unilaterally irrespective of CR-1 and Smad-2 to facilitate posterior cell fate. However, obligately needed CR-1 during migration of the anterior portion of the gut endoderm (Brennan et al., 2001). Cripto-1 has often been observed to be expressed in mouse as well as human undifferentiated embryonic stem (ES) cells, which regulate pluripotency and self-renewal (Caterina Bianco et al., 2010b; Moritz Hentschke et al., 2006).

In addition, the pluripotential transcription factors Nanog and Oct-4 immediately target the downstream gene CR-1, which is re-expressed in the iPSCs (induced pluripotent stem cells) originated from mature differentiated cells programmed to express Klf4, Nanog, Oct-4, as well as c-myc (Aasen et al., 2008; Y. H. Loh et al., 2006; Yan Shi et al., 2008). CR-1 expression could also be measured by quantitative PCR as well as immunohistochemistry in ICM (inner cellular mass) of early developing fetus and trophoblast (Bandeira et al., 2014; Sebastiano et al., 2010). Such an expression tends to be strongly linked with the initial isolation and recognition of CR-1 as well as Cr-1 genes from cDNA libraries acquired respectively from the undifferentiated human NTERA2/D1 and F9 embryonic carcinoma cells (Ciccodicola, Dono, Obici, Simeone,

Zollo, & Persico, 1989; Ding et al., 1998; Rosanna Dono et al., 1993; Chunhui Xu et al., 1999).

After retinoic acid-induced differentiation, expression of both the genes is lost in NTERA2/D1 as well as in F9 cells (Ciccodicola, Dono, Obici, Simeone, Zollo, & Persico, 1989; Rosanna Dono et al., 1993; Minchiotti et al., 2001). CR-1 and cryptic is distinct from each other in their expression pattern. Cryptic is present only within differentiated mesoderm cells undergoing retinoic acid therapy and is neither found in embryonic carcinoma nor ICM stem cells (Ding et al., 1998; Klauzinska et al., 2014; Shen et al., 1997). As the blastocyst is attached to the uterine wall, the expression of CR-1 can be analyzed in an ectodermal sample of a developing embryo (Caterina Bianco, Strizzi, Normanno, et al., 2005). Furthermore, the expression of CR-1 increases as the gestation time increase to day 6.5 due to the formation of mesoderm followed by the EMT of epiblast cells. However, on day 7, the expression declines, and there is a further increase in the myocardium of the arterial trunk of the evolving heart (Ding et al., 1998; Rosanna Dono et al., 1993; Chunhui Xu et al., 1999).

CR-1 transcript may be identified throughout the epimyocardium, although not in the endocardium inside the developing heart (Salomon et al., 2000). Excluding the developing heart, very little or no expression of CR-1 mRNA has been observed in the remaining embryonic region past the 8<sup>th</sup> day (Caterina Bianco, Strizzi, Normanno, et al., 2005; Salomon et al., 2000). CR-1 mRNA expression throughout adult tissues is typically multiple folds lower than in undifferentiated F-9 mice embryonic carcinomas (Johnson et al., 1994). The epiblast cells undergo EMT, where the primitive strip cell converts into mesenchymal cells followed by migration to form mesoderm (Savagner, 2001). Various molecular signalling contributes to regulating the process of EMT, which governs the cell to ECM and cell to cell adhesion, cell migration and shape maintenance (W. Lu & Kang, 2019; Rangel et al., 2012). Embryonic lethality occurs due to impaired gastrula formation on the blockage of any of these molecular signalling (Sirard et al., 1998; Waldrip et al., 1998). Losing the ability to gastrulate and to shape sufficient germ layers results in embryonic lethality at day 7.5 in mice without CR-1 express (Cr-1<sup>-/-</sup>) (Ding et al., 1998). Embryonic fibroblasts isolated from cripto-1 null mice show no or marginal capability to migrate towards chemotactic attractants like collagen (type-1) and fibronectin, in invitro, compared to wild-type embryonic fibroblasts cells (Chunhui Xu et al., 1999). Oep/Cripto-1 controls the transcription factors like Twist, slug or snail, regulating the expression molecule

**Table 2.1:** Regulatory Factors of *Cripto-1*

Sl.No.	Type of Regulation	Identity of the Regulator	Functional Role	Target cell	Reference.
1.	Positive	HIF-1 $\alpha$	Transcription factor	Cardiomyocytes	(Caterina Bianco et al., 2009)
		TGF- $\beta$	Growth Factor	Embryonal/ Colon Carcinoma	(Caterina Bianco et al., 2008)
		Oct4	Transcription factor	ESCs	(Kazuhide Watanabe et al., 2010)
		Nanog	Transcription factor	ESCs	(Gawlik-Rzemieniewska & Bednarek, 2016)
		Wnt/ $\beta$ -catenin	Growth Factor	Colorectal Cancer/Hepatoma	(K. Wang et al., 2013)
		Netrin-1	Growth Factor (Chemotropic)	Mammary Epithelial Cells	(Mancino et al., 2009)
		Caveolin-1	Scaffolding Protein	Breast Cancer	(Nagaoka et al., 2012)
		LRH-1	Nuclear Receptor	Embryonal/ Breast Carcinoma	(Caterina Bianco et al., 2013)
		Msx2	Transcription factor	EpH4 (Mammary Epithelial Cells)	(Di Bari et al., 2009)
2.	Negative	GCNF	Nuclear Receptor	Embryonal/ Breast Carcinoma	(Caterina Bianco et al., 2013)
		BMP-4	Growth Factor	Embryonal/ Colon Carcinoma	(Mancino et al., 2008)

involved in cell mobility and cell to cell adhesion such as integrins, cadherins, netrins claudins and occludins (Caterina Bianco, Strizzi, Normanno, et al., 2005).

*In vivo* silencing of Cr-1 results in the loss of differentiating capacity of embryonic stem cells into cardiomyocytes, obtained from CR-1 null mice (Maria Cristina, Rangel Nadia, P. Castro, Hideaki Karasawa, Tadahiro Nagaoka, David S. Salomon, 2012). The mechanism that commonly happens via the Nodal-and Smad-2-dependent pathway yet does not affect the capability of embryonic stem cells to specialize into various kinds of cells(Parisi et al., 2003; Chunhui Xu et al., 1999). Furthermore, *in vivo* silencing of genes like HRG-1 erbB-2 erbB-4 results in embryonic lethality, on the 10<sup>th</sup> day, due to myocardial and endocardial deformities (Klapper et al., 1999; Chunhui Xu et al., 1999). As cripto-1 indirectly regulated the erbB4 tyrosine kinase phosphorylation(Muraoka-Cook et al., 2008; Nagaoka et al., 2012). Inhibition of CR-1 using tomoregulin-1 might provide a significant outcome as it binds to both erbB-4 and CR-1. (Klapper et al., 1999; Nagaoka et al., 2012).

### 2.3.1.2 In Adult Cells (Especially in Mammary gland)

Cripto-1 expression is marginal in adults, possibly in the stem cell present in the tissue. (Caterina Bianco et al., 2010b). The cripto-1 expression is marginal in adults, possibly in the stem cell present in the tissue(De Castro et al., 2010).CR-1 interacts with GRP78 as a co-receptor to regulate the stem cell regeneration of hematopoietic origin in the hypoxic portion of bone marrow(Miharada et al., 2011). CR-1 expression continues to be an important factor in adult tissues for the development of the mammary gland and amplifies expression while breastfeeding and lactation occurs(Salomon et al., 2000; Luigi Strizzi et al., 2007). CR-1 has been identified across varying phases of postnatal mammary gland advancement(M. Graziella Persico et al., 2001). CR-1 content increases two to three times across different pregnancy phases and remains high throughout lactation but dropped significantly through involution(Caterina Bianco, Strizzi, Normanno, et al., 2005). *In vivo* study on mice, mammary epithelium shows the regulation of CR-1 expression indicate that in ageing breeder mice with a high frequency of forming mammary tumours, the expression is increased(De Santis et al., 2000; Herrington et al., 1997). Research has identified a functional form of CR-1 in human breast milk, which clearly shows that CR-1 is a mammary gland secretory component and proposes that this variant of CR-1 may contribute to regulating the differentiation

and proliferation of milk-producing cells (C Bianco et al., 2001). In essence, the EGF-like domain of CR-1 was observed to directly associate with the mammary epithelial cells of mice, namely NMuMG and HC-11, and portions of the mammary gland tissue, implying the existence of a complementary CR-1 receptor that might regulate the functions associated with a mammary gland in pregnant as well as lactating females via autocrine control (De Santis et al., 2000; Normanno et al., 2004; Maria Graziella Persico et al., 1998; Salomon et al., 2000).

### 2.3.2. Cripto-1 in Tumourigenesis

There are several resemblances between embryonic development and tumourigenesis development. During embryonic development, the signalling pathways responsible for embryonic stem cell plasticity, propagation, and mobility often begin to act in tumour development and malignancy (De Angelis et al., 2019; Marjanovic et al., 2013). Apart from cripto-1 several morphogens which take active participation in the embryogenesis reported re-expressing in cancer progression (Dudu et al., 2004; Moritz Hentschke et al., 2006; Tabata & Takei, 2004). Cancer formation is a multi-step phenomenon involving anomalies in many metabolic processes, including division, control of the cell cycle, death of cells, proliferation, and preservation of genome due to functional differences in several genes (Caterina Bianco et al., 2010b; De Angelis et al., 2019; Hanahan & Weinberg, 2011). To comprehend the biology and establish therapeutic regimens, it is essential to explore the fundamental signalling mechanisms regulating cancer cells. Studies have shown that high levels of CR-1 expression in various kinds of cancers (Kluzinska et al., 2014). Typically, 50-80% of various forms of cancer, including colorectal, lung, ovarian, pancreatic breast and testicular germ cell tumours, express CR-1 at elevated levels (Francescangeli et al., 2015; Pilgaard et al., 2014; Chunhua Xu et al., 2014; Xue et al., 2019).

Cripto-1 plays a regulatory role in human multiple human cells in promoting stem, growth, invasion, migration, and angiogenesis, including breast, intestine, lung, testis, prostate, and pancreas stomach, ovary, and glioma cells (C Bianco, Strizzi, Normanno, et al., 2005; Francescangeli et al., 2015). Since Cripto-1 has been found to be associated with the maintenance, proliferation, angiogenesis, and invasion of cancer stem cells (CSC), it has been suspected to also be involved in the control and progression of tumorigenesis (Caterina Bianco, Strizzi, Normanno, et al., 2005; Luigi Strizzi et al., 2005,

2007; D. Wu et al., 2017). In vitro research findings have revealed that CR-1 operates as an oncogene by intensifying the invasion, migration and epithelial to mesenchymal transition of many epithelial human and mouse mammary gland cells and encourages in vitro and in vivo tumour angiogenesis (Q. Liu, Cui, Yu, Bian, Qian, Hu, Ji, Yang, et al., 2017; Nagaoka et al., 2012; Rangel et al., 2012; D. Wu et al., 2017). Nevertheless, the mechanisms behind the recurrent expression of CR-1 in cancer is still not well understood. Therefore, many Cripto-1-related signalling processes have been identified that are common to both developmental phases and tumour progression, indicating that some of the developmental pathways are reactivated, leading to tumourigenic transition and progression (Kluzinska et al., 2014; Sousa et al., 2020; Luigi Strizzi et al., 2005).

Scientists including Bianco et al. have demonstrated that Cripto-1 overexpression has a major effect on microvessel development and tumour development (Caterina Bianco, Strizzi, Normanno, et al., 2005; Normanno et al., 2004; Wechselberger et al., 2005). This observation is also corroborated by the fact that angiogenin, the activator of human vascularization, is a direct associate of Cripto-1 (Caterina Bianco, Strizzi, Normanno, et al., 2005; Caterina Bianco & Salomon, 2010).

Studies that highlight the involvement of CR-1 in development and proliferation, specifically in the gut epithelium, show that CR-1 mRNA activity is lower in disease states like gastric ulcer and IBD (inflammatory bowel disease), while increased levels of and apoptosis and necrosis eventuate (Caterina Bianco et al., 2010b; Chailier, 1999). The potential role of CR-1 in promoting or advancing in vivo CR-1 expression of mammary tumours has been investigated in various transgenic mice' mammary glands in which the enhanced expressions of CR-1 have been reported earlier to contribute to the instant progression of lesions of the mammary epithelium (Adamson et al., 2002; Maria Graziella Persico et al., 1998; Wechselberger et al., 2005).

Reproducible CR-1 overexpressing transgenic mice model of hyperplastic mammary glands has been developed, indicating the purpose of CR-1 in mammary epithelial proliferation development deregulation (Maria Graziella Persico et al., 1998; Luigi Strizzi et al., 2007; Wechselberger et al., 2005).

#### **2.4. Role of Cripto-1 in CSCs and ESCs Maintenance**

The inferred role of Cripto-1 in cancer pathogenesis has led to attempts to use it as a tumour progression biomarker (Caterina Bianco, Strizzi, Normanno, et al., 2005). Reports have suggested that the expression of CR-1 and LIF (leukaemia inhibitory factor) is regulated by the nodal via induction of Smad2/3, which governs glioma progression (Bonnet & Dick, 1997; Mancino et al., 2008). There are two distinct subpopulations (CR-1<sup>high</sup> and CR-1<sup>low</sup>) identified in Embryonal carcinoma (EC cells) and human melanoma cell lines (C8161 cells), based on cell surface expression of cripto-1 (S. Lin et al., 2017). The cell with enhanced expression of CR-1 shows the higher sphere-forming ability *in vitro*, as the same CR-1<sup>high</sup> cells, when introduced in NOD/SCID mice, give rise to the larger tumour compared to CR-1<sup>low</sup> cells (Kazuhide Watanabe et al., 2010). The CR-1<sup>+/high</sup> cells isolated from the C8161 cell subpopulation shows distinct characters like slow growth rate, smaller size, ability to form a sphere *in vitro* and have higher expression of pluripotency markers, i.e. MDR-1, Oct4 and Nanog.12 accordingly, the higher expression of CR-1 was shown to associate with upregulated expression of stemness markers like SUZ-12 and Oct4 in the patient-derived sample of prostate cancer (Kazuhide Watanabe et al., 2010). Treatment of embryonal carcinoma with recombinant human cripto-1 results in increased cellular proliferation and DNA synthesis (Das et al., 2012). Conversely, reduced cell proliferation was observed in human colon adenocarcinoma cells (HCT-8 cells) on treatment alantolactone, by blocking the collaboration between CR-1 and Activin type II-A receptor (Ying Shi et al., 2011). Cells having increased expression of CR-1 proliferate rapidly in oral squamous carcinoma cells (CORTEGOSO et al., 2017). The fast-growing tumour region contains the cell with higher CR-1 expression than surrounding slow-growing cells (Lengyel, 2010; Kazuhide Watanabe et al., 2010). As demonstrated earlier, embryonic cancer stem cells have a crucial role in the various signalling pathway. Hence, it is likely to act as a key target in cancer therapeutics.

Upregulated expression of CR-1 results in the development of a malignant tumour and stem cell-like characteristics (Ayob & Ramasamy, 2018; Luigi Strizzi, Margaryan, Gilgur, Hardy, Salomon, et al., 2013). Therefore, CR-1 overexpression can be correlated with detecting effective markers for the early prognosis of cancer onset and development. Studies in epithelial cells and stem cells suggest the precise relation between EMT and cellular stemness (W. Lu & Kang, 2019; Pastushenko & Blanpain, 2019; D. Wang et al., 2017). Moreover, there is ample evidence suggesting the involvement of CR-1 in developing stem cell phenotype and EMT (Kluzinska et al., 2014; Rangel et al., 2012).

In NTERA2/DC EC cell line, the CR-1<sup>high</sup> subpopulation exhibits the potential to initiate EMT and greater spheroids forming ability *in vitro* compared to CR-1<sup>low</sup> (Simões & Ramos, 2007). In addition, CR-1 has also been shown to regulate embryonic stem cell pluripotency both in human and mouse cell lines (Caterina Bianco et al., 2010b; Luigi Strizzi et al., 2008). Numerous studies suggest the involvement of CR-1 in cancer stem cells (CSCs) generation and maintenance in colorectal cancer (Sato et al., 2020; Y. Zhou et al., 2018) and oesophageal squamous cell carcinoma (Q. Liu, Cui, Yu, Bian, Qian, Hu, Ji, & Yang, 2017). However, the mechanism or pathway followed is yet to explore. A recent study demonstrates the upregulation of Wnt signalling by CR-1, resulting from Dvl3 stabilization, which induces the activation of  $\beta$ -catenin in the HCC cell line (Wechselberger et al., 2005; Xue et al., 2019).

Furthermore, the expression of CR-1 is regulated by Oct4 and Nanog, which are known stemness markers, in human embryonal carcinoma cells (Y. H. Loh et al., 2006; Park et al., 2018; Luigi Strizzi et al., 2008). In stem cells, Nanog transcription is induced by Nodal dependent CR-1 signalling, which creates a positive feedback loop (Rangel et al., 2012; Luigi Strizzi et al., 2007; K Watanabe et al., 2010). Development and enrichment of CSCs in tumours results in the acquisition of resistance towards chemotherapy and radiotherapy (D. Chen & Wang, 2019; L. Han et al., 2013). Increased expression of CR-1 in CSCs also correlated with resistance to chemotherapy and relapse of tumours (Alam et al., 2018; Todaro et al., 2014). Thus, targeting CR-1 along with other CSCs markers might help in better management of cancer.

## 2.5. Cancer Stem Cells

In the beginning, first cancer stem cells (CSCs) were identified in hematopoietic cancer, later on, cancer stem cells of different origins were detected like prostate, breast, colon, pancreas, head and neck and lungs (ALHulais & Ralph, 2019; Klonisch et al., 2008; Saygin et al., 2019; Sell, 2010). Cancer stem cells can be defined as a small group of progenitor cells present in cancer, capable of self-renew and enriching its population (Kashyap et al., 2009; O'Brien-Ball & Biddle, 2017; Sell, 2010). One of the specific features of the CSCs is the ability to develop tumours when introduced into immunodeficient mice. The CSCs also have differentiation properties, contributing to the heterogeneity in the cancer population, leading to more malignant and aggressive carcinoma. Various types of CSCs markers are CD133, CD44, CD24, CD90, CD200,

ALDH, ABCB5 and EpCAM etc. (Bao et al., 2013; Glumac & LeBeau, 2018; Jaggupilli & Elkord, 2012; Q. Liu, Cui, Yu, Bian, Qian, Hu, Ji, & Yang, 2017).

Genetic and epigenetic modification in cancer cells leads to the dedifferentiation of cancer cells, giving rise to cancer stem cells (Friedmann-Morvinski & Verma, 2014; Röpke et al., 2003; Yosuke Yamada et al., 2014). Several studies suggested the correlation of epithelial to mesenchymal transition with the acquisition of stem cell phenotypes (W. Lu & Kang, 2019; O'Brien-Ball & Biddle, 2017). The pathways that control stem cells' maintenance in humans are Wnt, Notch and hedgehog signalling pathways. These pathways were shown to be induced during EMT, leading to the development of stem cell-like phenotype in cancer cells (Kamdje et al., 2017; Katoh & Katoh, 2008; Takebe et al., 2011).

In breast cancer, upregulated expression of CSCs marker CD44 was observed in cells undergoing EMT (L. Li et al., 2015; H. Xu et al., 2016). Subsequently, CD44 was identified as a target for  $\beta$ -catenin (Chang et al., 2013; Uchino et al., 2010).

CSCs is also shown to have EMT like phenotype, which was proposed to induce metastasis (O'Brien-Ball & Biddle, 2017). Apart from that, CSCs were also shown to associate with cancer advancement and development resistance to radio- and chemotherapy (Cho & Kim, 2020; M. Li et al., 2012; K. Wang et al., 2013). Further, many probable mechanisms were detected to decipher the pathway involved in the induction of resistance. This resistance to therapy and inbuilt tumorigenicity helps the CSCs to induce relapse of cancer (Agliano et al., 2017; Ambudkar et al., 2003; E. W. Yu et al., 2003). There are markers of CSCs that are the determinant for a particular tissue similar to normal stem cells. For instance, Normal hematopoietic cells express  $CD34^+CD38^+$  as a surface antigen, whereas differentiated hematopoietic cells express  $CD34^+CD38^-$  as stemness markers (Edy Susanto, 2010; Hauswirth et al., 2007). Leukaemic cells expressing  $CD34^+CD38^-$  were having tumour initiation capability, while cells with  $CD34^+CD38^+$  expression were unable to do so (Bonnet & Dick, 1997; Hauswirth et al., 2007; Lapidot et al., 1994). Likewise, neural CSCs expresses nestin that is generally expressed by neural stem cells (Calabrese et al., 2007; Jin et al., 2013; Neradil & Veselska, 2015). Literature reports have suggested that stem cell properties acquired by the cell result from transformation induced by some stimulus that drives the epigenetic modifications in partially differentiated cells. Such conversion was observed in Hair follicle stem cells, where progenitor cells transform into stem cells following mechanical injury (Hsu et al., 2011). The epigenetic modifications are the possible

mechanism for the dedifferentiation of the stem cells (Lister et al., 2011). Primarily, genetically unstable cells transform and dedifferentiate into stem cells (Federici et al., 2011).

Moreover, when cells grow under the hypoxic condition, they acquire stem cell-like characteristics following reversal of differentiation state (J. Li et al., 2014). Subsequently, a study conducted on iPSCs (induced pluripotent stem cells) depicted the reprogramming of differentiated cells results in recovery of stem cell properties (Lister et al., 2011; Takahashi & Yamanaka, 2006). Recently, the adult's fibroblasts and other somatic cells were reprogrammed using cloning techniques in which stemness markers like Oct3/4, C-myc, Klf-4 and SOX2 were transduced (Nomura et al., 2012; Takahashi & Yamanaka, 2006; Wakao et al., 2012). This results in the production of a totipotent cell having the ability to form a live embryo.

Earlier, differentiation and development were understood as a one-directional or non-reversible process in which loss of stemness is bound to happen along with differentiation (Yosuke Yamada et al., 2014). However, recently understanding suggests that the gain and loss of stemness is a dynamic process and stem cell properties in CSCs are the result of the reversal of differentiation (Friedmann-Morvinski & Verma, 2014). Another study suggested that the combination of LIN28 and Nanog synergize the production of iPSCs with human fibroblast (Gillis et al., 2011). Other than this, enhanced expression of various exogenous factors is required for the generation of iPSCs (J. Yu et al., 2007), hence the origin of CSCs cannot be generalized. However, the part played by transcription factors during the production of CSCs cannot be overlooked. SOX2, ras and myc support the generation of stem cells (Herreros-Villanueva et al., 2013; Ischenko et al., 2013), while GATA4 has been reported to antagonize Nanog and inhibits the dedifferentiation process (Serrano et al., 2013).

## **2.6. Properties of CSCs**

### **2.6.1 Self-Renewal Capacity**

The phenomenon of generation new CSCs by the mitotic division of existing CSCs is called self-renewal (O'Brien-Ball & Biddle, 2017). This is one of the most essential functions of CSCs, which help in the maintenance of CSCs reservoir in both symmetric

and asymmetric cell division (Huntly & Gilliland, 2005). There is the loss of tumorigenicity and capability to relapse of the tumour when self-renewal capacity is lost.

### **2.6.2 Metastasis and CSCs**

Metastasis is the process in cancer cells move from the site of origin and enters the lymphatic and circulatory system where it continues to survive the passage later on it moves to the secondary site by leaving the circulatory system and start growing in a new local niche (Ayob & Ramasamy, 2018; Chambers et al., 2002). In 1998, a study conducted showing metastasis of approximately 80% of blood cancer cells that move out of the bloodstream and enter the lungs initiates tumour growth within one day (Luzzi et al., 1998). Nevertheless, a small number of cells succeed in making high tumour vascularization (Koop et al., 1995; Luzzi et al., 1998). The reason behind it is the majority of cells remain dormant at the secondary site, which is shown in many metastasis models (Bao et al., 2013; Hanahan & Weinberg, 2011).

### **2.6.3 Dormancy and Quiescence of CSCs**

Dormancy is the attire of metastatic cancer cells provided by quiescent cells (Sau Har Lee et al., 2020). These cells exhibit a slow growth rate and high apoptotic ability (W. Chen et al., 2016). Due to its dormancy, these cells have the ability to retain fluorescent dye, which dilutes sequentially after normal cell division (Davis et al., 2019; Naumov et al., 2006).

### **2.6.4 Creation of Tumour Heterogeneity**

The CSCs can differentiate into various forms of cells, which give rise to tumour heterogeneity (Muhammad Al-Hajj & Clarke, 2004). These cells are also known to maintain and introduce heterogeneity among the cancer cells (De Angelis et al., 2019). Furthermore, a study conducted from the patient-derived samples also proves similar phenomena (M. Al-Hajj et al., 2003).

### **2.6.5 CSCs and Tumour Vascularization**

Studies have shown that stem cells are also involved in the development of tumour vasculature (Dvorak et al., 1991; Putnam, 2014). In these studies, GSCs (GBM stem

cells) were found to have vascular tube forming ability when grown in the endothelial medium *in vitro* (Jhaveri et al., 2016; Ricci-Vitiani et al., 2010). In addition, the introduction of human GSCs into NOD/SCID mice, either by subcutaneous or orthotopic route of administration, leads to the development of a tumour xenograft with the vasculature of human origin (Ricci-Vitiani et al., 2010). Furthermore, CD133<sup>+</sup> GSCs demonstrated the ability to imitate human vascularization, which means that tumour cells with enhanced cell plasticity appear to form a vessel-like structure (Petty et al., 2007; Putnam, 2014; Qian et al., 2016).

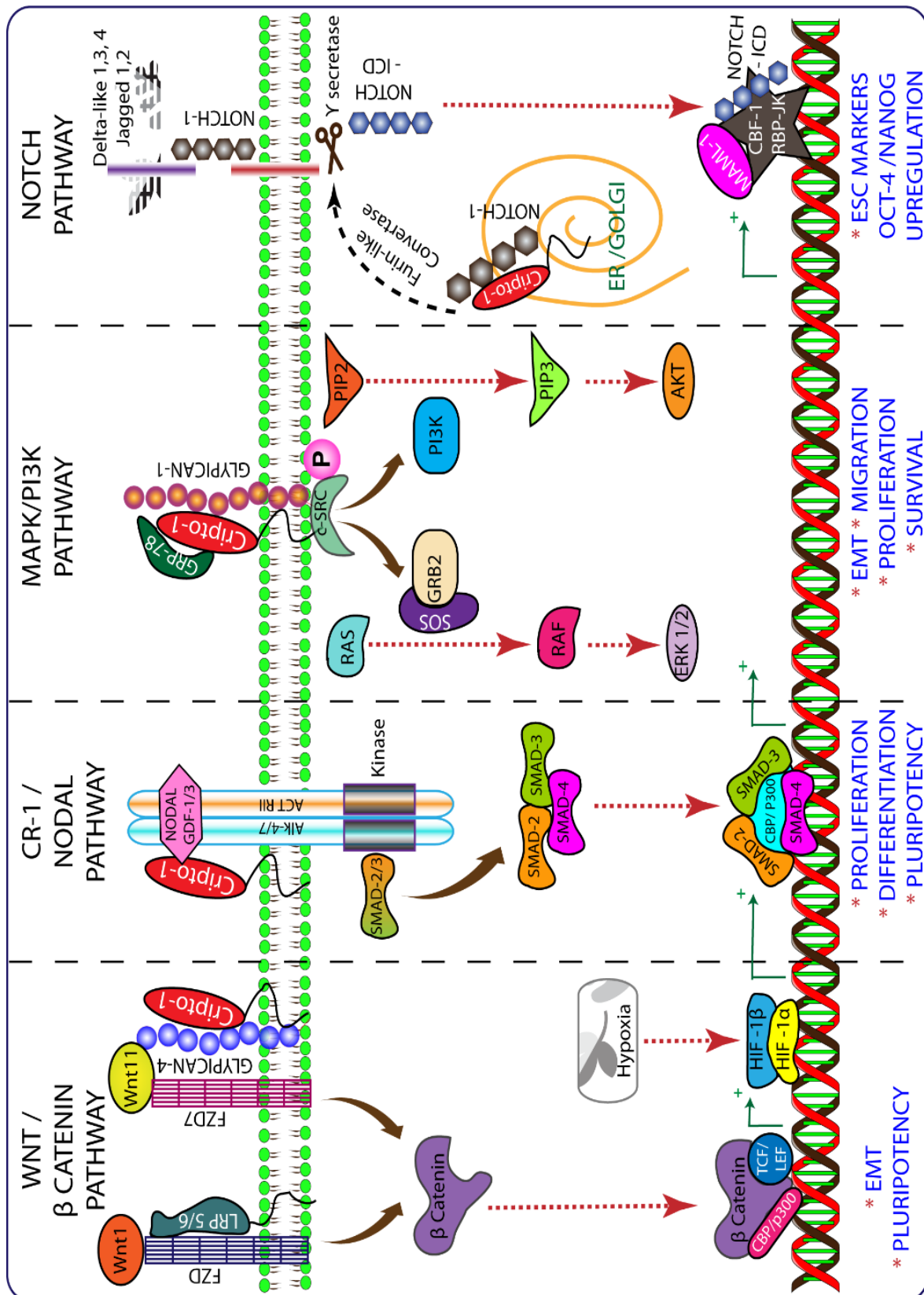
## 2.7. Pathways of Cripto-1

The science of ES cells has contributed to the appreciation of transcriptional programming, including molecular pathways which embody stem cell renewal as well as differentiation (Englund et al., 2011; Rippon & Bishop, 2004). Researches have highlighted molecular markers of genes in undifferentiated ES cells, which regulate pluripotency and self-renewal (Maria Cristina, Rangel Nadia, P. Castro, Hideaki Karasawa, Tadahiro Nagaoka, David S. Salomon, 2012). Molecular and genetic analyses have confirmed a functional relation amongst the EGF-CFC proteins and Nodal, both come under the TGF- $\beta$  superfamily (Gritsman et al., 1999; Schier & Shen, 2000). EGF-CFC proteins serve as co-receptors for Nodal as well as GDF-1 and GDF-3 (Growth and Differentiation Factors) via a complex formation between them and Activin Type II and Type I (ALK4) serine-threonine kinase receptors mostly in cell membrane niche (Caterina Bianco et al., 2002; Klauzinska et al., 2014). On binding to Nodal/GDF-1/GDF-3, Smad-2 and 3 gets phosphorylated followed by activation of type I and II receptor complex, and that in turn binds to Smad-4 and moves to the nucleus to promote the transcription of particular target genes as a transcriptional complex (Caterina Bianco et al., 2008; Gray & Vale, 2012; Sousa et al., 2020; Yeo & Whitman, 2001). The binding of CR-1

**Table 2.2.** Pathways affected by Cripto-1.

Sl. No.	Name of the Pathway	Target Pathway	Mechanism of Action	Reference
1.	Nodal/GDF1/3	Nodal/SMAD2/3-dependent signalling	Proliferation /differentiation	(Shen, 2007)

2.	GRP78	a) MAPK/AKT signalling	Proliferation /migration	(Nagaoka et al., 2012)
		b) Src/PI3K/AKT	Proliferation /migration /plasticity	(D. Wu et al., 2017)
		c) Antagonizes Activin/Nodal/TGF- $\beta$ signalling	Proliferation /migration /plasticity	(Kelber et al., 2009)
3.	Glypican-1	a) c-Src/MAPK/AKT signalling	Proliferation /migration	(Gray & Vale, 2012)
		b) Src/Ras/Raf/MAPK	Proliferation /migration /survival	(Luigi Strizzi et al., 2005)
		c) Src/PI3K/AKT	Proliferation /migration /survival	(Nagaoka et al., 2012)
4.	Nodal	MAPK/p70S6K signalling	Cardiac specification of ESCs	(Kluzinska et al., 2014)
5.	TMEFF1/ErbB4	c-Src/MAPK/AKT signalling	Stem cell self-renewal /proliferation /EMT	(Nagaoka et al., 2012)
6.	Wnt3/frizzled/LRP5/6	$\beta$ -Catenin signalling	Stem cell self-renewal /proliferation /EMT	(R. C. L. Lo et al., 2018)
7.	Wnt11/Glypican-4/frizzled	$\beta$ -Catenin signalling	Stem cell self-renewal /proliferation /EMT	(K. Wang et al., 2013)
8.	Mature Notch/Delta like 1,3,4/Jagged1,2	Notch signalling	Stem cell self-renewal /proliferation /EMT	(Mahmoudian et al., 2017)



Scheme 2.2: Schematic of Cripto-1 Signaling pathways.

with glypican-1 (a heparin sulphate proteoglycan), may enhance tyrosine kinase c-Src activity by promoting the phosphorylation of MAPK and AKT in a nodal-independent process (Caterina Bianco et al., 2008; Das et al., 2012). Cell growth, differentiation, motility, and survival are affected by the activity of the MAPK and AKT pathways (Kluzinska et al., 2014; Nagaoka et al., 2012). CR-1 can indeed suppress signalling by TGF- $\beta$ 1 and activin A/B, the other members of the TGF- $\beta$  family, which leads to tumour cell development (Seoane & Gomis, 2017). The target genes of Wnt and Notch signalling pathways are specifically involved in the progression and development of the ESCC, and the deregulation of these genes have a crucial role in tumour formation (Xiao et al., 2016).

CR-1 communicates with multiple components of different signalling pathways, particularly TGF- $\beta$ , Notch, Wnt, Nanog and Oct-4 (Kluzinska et al., 2014; Mahmoudian et al., 2017; Nagaoka et al., 2012). CR-1 is a target gene of the Wnt/ $\beta$ -catenin signalling pathway downstream to it, and its communication with Wnt may regulate diverse physiological processes, which include embryo formation, activation of EMT, cell invasion and migration (Yang et al., 2016). CR-1 is required by the Nodal to trigger the activation of Alk4 and Alk7, the serine-threonine kinase activin type I receptors as well as the activin type II receptor complex, which in effect stimulates phosphorylation of the cytoplasmic receptor-activated Smad proteins, namely Smad-2 and Smad-3, which translocate into the nucleus after complexation with Smad-4 and interact with other co-activators such as FoxH1 to initiate transcription of specific target genes. (Caterina Bianco et al., 2002; Yeo & Whitman, 2001)

### 2.7.1. Nodal Dependent Cripto-1 Signalling

CR-1 is reported being the co-receptor of Nodal, a ligand belonging to the transforming growth factor-beta (TGF- $\beta$ ) group (Caterina Bianco et al., 2002; Sakuma et al., 2002). The CR-1 regulated Nodal/ALK4/Smad-2 signalling pathway is primarily involved in embryogenesis (Caterina Bianco et al., 2002; D'Andrea et al., 2008; Kluzinska et al., 2014). Linked to several other ligands of the TGF- $\beta$  family, such as activin as well as bone morphogenetic proteins (BMPs), nodal signals via the serine/threonine kinase receptor present in the transmembrane (Caterina Bianco et al., 2003; Lonardo et al., 2011) [60]. Nodal signalling uses ActRIB (ALK4) type I activin receptors and ActRIIA and ActRIIB type II receptors, contributing to phosphorylation as well as nuclear aggregation

of Smad2 and/or Smad3 cytoplasmic signal transducers along with Smad4 (Parisi et al., 2003; Shen, 2007; Yan et al., 2002). The stimulated Smad complex associates with transcription factors present in the nucleus, such as the FAST subfamily, to elicit gene expression (Caterina Bianco et al., 2002; Massagué & Xi, 2012; Kazuhide Watanabe et al., 2010). Mutational experimentation studies suggest CR-1's ability to bind to Nodal via its EGF and CFC domain and also suggest its capability of binding to ALK4 (ActRIB) (Caterina Bianco et al., 2002; Maria Graziella Persico et al., 1998; Schier & Shen, 2000). Membrane-associated CR-1 employs Nodal to the Activin receptor complex consisting of ActRIB (ALK4) and ActRIIB (Caterina Bianco et al., 2002; Klauzinska et al., 2014; Nagaoka et al., 2012). CR-1 can also interact directly with ALK7, some other serine/threonine orphan kinase receptor that improves the capacity of ALK7 to react to Nodal (Klauzinska et al., 2014; Tsuchida et al., 2004). The various pathways of CR-1, including the Nodal/ALK4/ALK7/Smad-2, is elaborately illustrated in **Figure 2.3**. Numerous reports indicate that, apart from the activation of Nodal/ALK4/ALK7/Smad-2 and Glypican-1/c-Src/MAPK/Akt pathways, CR-1 signalling may also be in cross-talk with the wnt/ $\beta$ -catenin/Lef-1 signalling pathway (Nagaoka et al., 2012, 2013; D. Wu et al., 2017). Moreover, CR-1 has been recognized as the main target gene in the signalling cascade of wnt/ $\beta$ -catenin during the process of embryonic development (Funa et al., 2015; Nagaoka et al., 2013).

### 2.7.2 Nodal-Independent Cripto-1 Signalling Pathway

Cripto-1 being a co-receptor for Nodal, can stimulate individually both the Nodal-dependent as well as the Nodal-independent signalling pathways. It not only attaches to Glypican-1 but also provokes the activation of the c-Src/MAPK/AKT cascade, resulting in cell motility or even EMT (Caterina Bianco et al., 2003).

As a portion of the MAPK signalling pathway interceding cell proliferation, Cripto-1 has been known to phosphorylate EGFR (also known as Ser1070) or FGFR1 (also known as throughout the central repudiates malignant transformation (Alowaidi et al., 2019; Nagaoka et al., 2012; Thiery & Chopin, 1999). Nevertheless, a variety of cases of cancer include mutations in the MAPK pathways, leading to irregular signalling that impairs many processes required for cancer cells to acquire tumour forming potential.

Additionally, deregulation of MAPK signalling promotes oncogene stimulated senescence prevention and drug tolerance acquisition (Boutros et al., 2008; Dhillon et

al., 2007). PI3K/Akt signalling pathway facilitates essential cancer cell activity, including tumour development and progression, as well as tumour-related outcomes, like proliferation, development, metabolism, angiogenesis, motility, invasion, migration, autophagy as well as survival (Bononi et al., 2011; Dobbin & Landen, 2013; McAuliffe et al., 2010). Deregulation or even increased pathway activation have indeed been involved in the creation of anti-tumour immunity, including immune evasion among cancerous cells (Dituri et al., 2011). In particular, the genes regarded as important key modulators in the maintenance of undifferentiated and pluripotent conditions in ES cells include POU5F1, a POU class 5 homeobox 1, Oct-4, Nanog and Sox-2 (Jerabek et al., 2014).

These transcription factors govern the expression of several other transcriptional regulators, which also preserve or suppress lineage-specific differentiation genes. Whole genome Chip analysis has also demonstrated the existence of binding sites of Oct-4 and Nanog inside the Cripto-1 promoter region Tyr654 (Alowaidi et al., 2019; Kazuhide Watanabe et al., 2010). Cripto-1 can also regulate cell motility as well as invasion in the FA pathway by binding to ITGA, thereby facilitating the activation of the Src signal cascade, which have the components Tyr418, FAK (Tyr396) and PXN (Tyr118) (Alowaidi et al., 2019; D. Wu et al., 2017).

In conjunction, Cripto-1 could further activate the regulation of cell survival through the Src (Tyr418), FAK (Tyr396), p130CAS (Tyr410) and Bcl2 (Thr69) pathways or control the cell proliferation through the Src (Tyr418), FAK (Tyr396), p130CAS (Tyr410) c-Jun (Ser63) cascade (Alowaidi et al., 2019; D. Wu et al., 2017). Through the evaluation of ALK4<sup>-/-</sup> and/or Nodal<sup>-/-</sup> cells, Bianco et al. (2002) revealed that perhaps the activation of all the aforementioned pathways by Cripto-1 is independent of both the genes (Caterina Bianco et al., 2003; Luigi Strizzi et al., 2005). Comparably, during the activation of C-Src, which is essential to its oncogenic operation, Cripto-1 has been observed to exhibit Nodal and ALK4-independent activities in a mice epithelial mammary cells model system (Caterina Bianco et al., 2003). MAPK signal transduction regulated by Cripto-1 is also largely reliant on its ability to associate with the GRP78 endoplasmic reticulum-based heat shock protein, which is found to be significantly up-regulated on some cancer cells' surface. (Shani et al., 2008)

In essence, any intervention in the GRP78-Cripto-1 interaction hinders the activation of the Akt/MAPK pathway as this interference significantly undermines the tumorigenic

**Table 2.3.** *Examples of Proteins affected by Cripto-1 Overexpression.*

Sl. No	Protein Name	Amino Acid Residue	Pathway Involved	Carcinogenic Activity	Ref.
1.	VEGFR2	Tyr1054	ERK1/2, PI3K / Akt,	Migration and Proliferation of endothelial lymphatic cells	(Kelber et al., 2009)
			c-Raf / MAPK, PLC $\gamma$ 1 / PKC,	Malignant astrocytoma radio resistance and growth	(Gray & Vale, 2012)
			VEGF- VEGFR2-NRP1,	Maintains the tumorigenicity, viability, and self-renewal	(Knizetova et al., 2008)
			VEGFR-2/PLC $\gamma$ 1 / Akt.	Endothelial permeability, proliferation and survival;	(Dellinger & Brekken, 2011)
			ephrin-B2/PDZ- signalling	Regulation of tumour angiogenesis	(Sawamiphak et al., 2010)
2.	Akt	Thr308	PI3-kinase/Akt pathway	Survival and Growth of tumour cells	(Gao et al., 2014)
		Tyr474	Ca <sup>2+</sup> permeable AMPA receptors/Akt	Motility and Growth of glioblastoma cells	(T. Jiang & Qiu, 2003)
3.	CREB-2 (ATF4)	Ser245	PERK-ATF4	tumour development, lymph node metastasis, upregulated during tumour growth, escalated hypoxia	(Fan et al., 2014)
4.	Caveolin-1	Try14	Focal Adhesion	Cell migration, structural and signalling significance in focal adhesions	(Parat & Riggins, 2012)
5.	FAK	Try397	Focal Adhesion/ PI3 Kinase AKT	Focal Adhesion, increased motility, invasiveness, growth and survival of cancer cells. Anti-apoptosis	(Luo & Guan, 2010)

activity of Cripto-1(Gray & Vale, 2012; Miharada et al., 2011). For the Nodal-dependent activities of Cripto-1, including the activation of the Smad2/3 signal cascade, GRP78 is

important as it interferes with the proliferative potential of this pathway (Kelber et al., 2009). Furthermore, GRP78 induced activation of Akt/MAPK/c-Src signalling via Cripto-1 can result in reduced adhesion and increased proliferation in breast cancer cells which, on analysis, have exhibited reduced expression of E-cadherin (Kelber et al., 2009; Nagaoka et al., 2013). In addition to that suggested earlier, the Cripto-1-GRP78 complex has often been linked to a variety of EMT regulatory pathways, namely Notch, TGF $\beta$  and Wnt/ $\beta$ -catenin, thus serving a key role in the regulation of EMT (Rangel et al., 2012; Nagaoka et al., 2012; Gray & Vale, 2012).

### 2.7.3. Wnt Signalling Pathway

In the embryo, Cripto-1 is a downstream target gene of the canonical Wnt/ $\beta$ -catenin pathway. In combination with Frizzled 7 (Fzd7) and Glypican-4, the non-canonical Wnt11 can associate with Cripto-1 and induce the activation of the  $\beta$ -catenin pathway. Literature reveals that Cripto-1 strengthens the signalling of the canonical Wnt/ $\beta$ -catenin pathway by coupling to its co-receptors LRP5 and LRP6 (Nagaoka et al., 2013). Across both normal cells as well as cancer stem cells, the Wnt pathway plays a critical role in cell cycle regulation and self-renewal on its activation (Holland et al., 2013).

Several types of cancer have been identified with dysregulation of the Wnt/ $\beta$ -catenin pathway. However, stabilisation of the transcriptional co-activator  $\beta$ -catenin is recognized as a crucial hallmark of the progression of several tumours. The tumour associated gene expression profile is regulated by  $\beta$ -catenin by binding to the TCF/LEF-1 DNA-binding transcription factor family members.  $\beta$ -catenin, in conjunction with cadherins, is also an integral part of cell adhesion complexes and therefore plays a significant role in the regulation of EMT (Polakis et al., 2012; van der Zee et al., 2013; Kypta & Waxman, 2012). Cripto-1 has reportedly been known to specifically modulate Wnt/ $\beta$ -catenin signalling. Studies by (Nagaoka et al., 2013) have shown that Cripto-1 can attach to LRP5 as well as LRP6 (protein 5 and 6 linked to low-density lipoprotein receptors) and help promote the coupling of Wnt3a to LRP5/6, their co-receptors.

### 2.7.4. Notch Signalling Pathway

Notch is necessary for the induction of expression of Nodal as an upstream gene to Nodal (Raya et al., 2003). Notch signalling affects embryogenesis, cell differentiation, proliferation, organogenesis and apoptosis, and may end up causing carcinogenesis through deregulation (Bolós et al., 2007). In ER/Golgi membranes, Cripto-1 communicates explicitly with Notch and boosts cleavage of the extracellular domain of Notch, amplifying the signal triggered by the Notch ligand. CR-1 is a downstream target of Oct-4 and NANOG, the transcription factors that control CR-1 expression by attaching to the promoter of CR-1. Moreover, these are genes linked to stem cells that indicate that CR-1 expression can facilitate the role of NANOG and Oct-4 by implementing and sustaining their expression (C Bianco et al., 2013). It should be noted that differentiated cells can be deregulated into the pluripotent stem cell phenotype by the master transcriptional complex comprising Oct-4, Sox2, and NANOG.

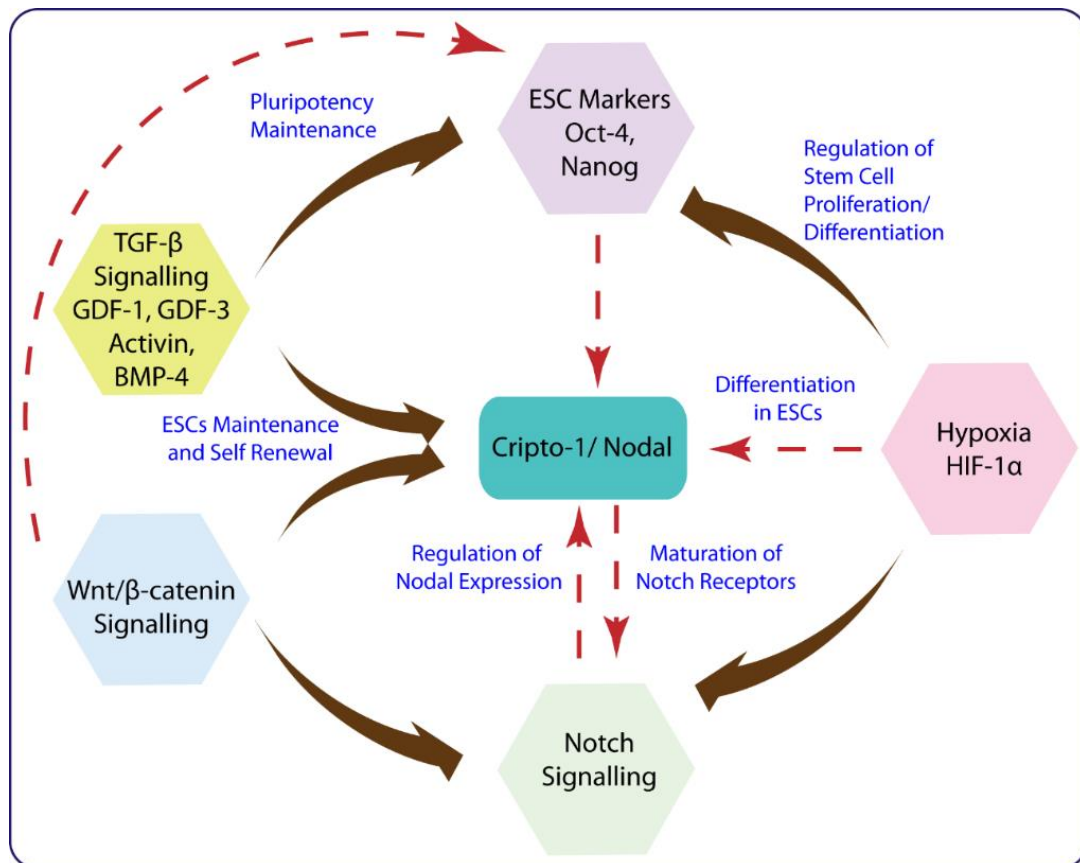
During the retinoic acid stimulated differentiation of human embryonic cancer cells subsequent to binding of GCNF to a DR0 motif in the human CR-1 promoter region, CR-1 is often explicitly inhibited mostly by the orphan nuclear germ cell receptor nuclear factor (GCNF) (M Hentschke et al., 2006). GCNF is also necessary to suppress Oct-4, Nanog as well, as Sox-2 expression against ES cell differentiation with retinoic acid (Gu, LeMenuet, et al., 2005).

In addition, by recruiting the methyl-CpG binding domain, including DNA methyltransferases, to the Oct-4 promoter, GCNF binding activates the initiation of methylation of the promoter DNA by activating epigenetic gene silencing during ES cell differentiation of the Oct4 locus (Gu et al., 2011). DR0 constituents may even bind to several other orphan nuclear receptors, like the homolog-1 liver receptor (LRH-1), which is essential for preserving Oct-4 expression within undifferentiated ES cells (Gu, Goodwin, et al., 2005). Thus, by competition within the Oct-4 promoter region for the same regulatory factor, GCNF and LRH-1 not only govern pluripotency but also differentiation of ES cells

## 2.8. Crosstalk of the Nodal/Cripto-1 Signalling Pathway

By activating an integrated framework of signalling pathways, Cripto-1 is involved in numerous cellular activities, particularly cell proliferation and motility, including angiogenesis (C Bianco, Strizzi, Ebert, et al., 2005; Xiu Feng Hu & Xing, 2005; Normanno et al., 2004). In reviewed literature, crosstalk amongst Cripto-1 and several

other canonical signalling pathways such as Wnt/ $\beta$ -catenin, hypoxia, Notch, Oct-4, and Nanog has collectively been described (Nagaoka et al., 2012). Notch specifically controls Nodal expression, and CR-1 links to all four Notch receptors indicating that a Crosstalk exists among Notch and the signalling pathways of Nodal/CR-1 (Raya et al., 2003; Luigi Strizzi et al., 2007).



**Scheme 2.3:** Schematic representation of the Cross talk of the Nodal/Cripto-1 signalling pathway with various other signalling pathways.

## 2.9. Cripto-1 and Epithelial to Mesenchymal Transition (EMT)

Cripto-1 plays a crucial role in the process of epithelial to mesenchymal transition (EMT) (Rangel et al., 2012). During this process, the differentiated epithelial cell changes to mesenchymal form following differentiation, thereby reviving its stemness property (W. Lu & Kang, 2019). Phenotypically, these mesenchymal cells show similar traits to invasive carcinoma cells. Literature suggests that EMT governs the invasion of the cell into nearby tissues, and this mechanism has consistently been related to the CSC phenotype acquisition (Pastushenko & Blanpain, 2019) (C. Chen et al., 2018) (W. Lu & Kang, 2019). Majority of cells having EMT phenotype shows CSC-like

characteristics (Abell & Johnson, 2014). Cancer cells acquire EMT to escape the chemotherapeutic and physiological stress like hypoxia and tumour microenvironment stress (Jing et al., 2019). However, the mechanism to establish the relation between CSC and EMT is not clearly understood. Various cancer cell lines, including breast, colon and cervical, showed higher expression of cripto-1 after epithelial to mesenchymal transition. Furthermore, the upregulated expression of mesenchymal markers like vimentin, N-cadherin and Twist and downregulation of epithelial marker, i.e., E-cadherin, was observed in the cripto-1 overexpression system (Di Bari et al., 2009) (C. Y. Loh et al., 2019). However, the molecular mechanism correlating the cell invasion with altered CR-1 expression is not yet clear. In vitro exposure of HUVEC cells (Human umbilical vein endothelial cells) with cripto-1 show enhanced migration, invasion and vascular tube formation (angiogenesis) on ECM like Matrigel (D. Wu et al., 2017).

The first study that illustrates the role of CR-1 in EMT was performed in the murine mammary epithelial cell line (EpH4 cells). The findings of the study revealed that EMT plays a crucial role in gastrula formation, neural crest cell migration, differentiation of tissues and regeneration (Pérez-Pomares & Muñoz-Chápuli, 2002). In the process of EMT, downregulation in E-cadherin expression results in loss of cellular contact and destruction of the complex junction, due to which the cell develops high motility.

The epithelial cell becomes spindle shape and acquires mesenchymal morphology due to an increase in expression of Vimentin (Boyer et al., 2000; Thiery, 2002) (Ackland et al., 2003; Casaroli-Marano et al., 1999; Dandachi et al., 2001; Grille et al., 2003; Steinert & Roop, 1988). In vitro study conducted on HeLa cells (Human cervical carcinoma cells) reveals that the upregulation of vimentin expression is associated with enhanced migration and invasion of the cell across the ECM coated membrane in the CR-1 overexpression system. Thereby implicates that cripto-1 induced vimentin expression give rise to a highly malignant character to the cervical carcinoma (Ebert et al., 2000).

A recent study demonstrates the effect of CR-1 on EMT induction in HC-11 (mammary epithelial cell line) and human CR-1 overexpressing transgene mice model. The presented data reveals decreased expression E-cadherin while the expression of other mesenchymal markers like N-cadherin, different isoforms of integrins vimentin and snail (zinc-finger repressor transcription factor) in both CR-1 transgene murine model and Cr-

1 overexpressing HC-11 cells (L Strizzi et al., 2004). Furthermore, enhanced phosphorylation of AKT, c-Src and focal adhesion kinase (FAK) was observed, which are known to get activate during EMT (Thiery & Chopin, 1999). Additionally, expression of the phosphorylated and inactive form of GSK-3 $\beta$  (glycogen synthetase kinase 3 $\beta$ ) and expression of active/non-phosphorylated form of  $\beta$ -catenin was observed simultaneously in both in-vivo and in-vitro CR-1 overexpressing systems. The active form of  $\beta$ -catenin interacts with E-cadherin and plays an essential role in cell-to-cell junction formation (Savagner, 2001). The expression of  $\beta$ -catenin is regulated by GSK3 $\beta$ , which governs its proteasomal degradation followed by phosphorylation.

## 2.10. Embryonic Stem Cells

Embryonic stem cells are the progenitor cells that exhibit the ability to differentiate and generate all forms of cells required for normal embryonic development(Englund et al., 2011; Rippon & Bishop, 2004). Embryonic stem cells can be an attractive target for treating various diseases using transplantation therapy and can also be used as a target for drug screening(Watt & Driskell, 2010). ES cells can also be used as a suitable model for studying embryonic development and different types of neonatal cancers(Maria Cristina, Rangel Nadia, P. Castro, Hideaki Karasawa, Tadahiro Nagaoka, David S. Salomon, 2012).

In 1981, murine embryonic stem cells were isolated from the blastocyst, which was implanted earlier by two separate groups of researchers (Evans & Kaufman, 1981; Martin, 1981). The blastocyst comprises two distinct types of cells an outer layer called trophoblast, which will give rise placenta and an inner cellular mass (ICM) that further generates all the different types of tissues of the body and a potential source of ES cells (Englund et al., 2011). Since ICM changes its form quickly and for continuous experimentations, isolated ES cells can also be grown in-vitro by maintaining ideal culture conditions. A cell having a high nuclear-to-cytoplasmic ratio, enlarged nuclei and discrete morphology proliferate at a higher rate. Besides, ES cells also exhibit a stable euploidic set of chromosomes and should also express all the pluripotency markers(Aasen et al., 2008; Gan et al., 2007).

General characteristics of human ESCs include differentiation, self-renewal, expression of pluripotent markers like Oct3/4, SOX2, Nanog, surface antigen markers like SSEA-1/3/4 and Tra-1/60/80(De Wert & Mummery, 2003; Elçin et al., 2010; Englund et al.,

2011). Another interesting characteristic of ESCs is the potential to generate teratomas in immunocompromised (SCID) mice (Inoshima et al., 2012). Along with different pluripotency markers, expression of *cripto-1* was also observed in iPSCs (induced pluripotent stem cells) obtained from different human cells (Alam et al., 2018). The *CR-1* co-expression, along with other stemness markers, provides an essential model for better understanding of the primary mechanism of ES cells in normal tissues and decoding their impact in regulation and management of cancer (ALHulais & Ralph, 2019; Q. Liu, Cui, Yu, Bian, Qian, Hu, Ji, Yang, et al., 2017).

## 2.11. ES cells and Hypoxia

Accumulating evidence suggests that normal early embryonic development occur under hypoxia condition and Oxygen play a vital role in deciding cell fate and cell differentiation (Q. Lin et al., 2008). The hypoxia microenvironment is essential for the normal biological development of embryo and required for the maintenance of adult stem cells of hematopoietic, neural and mesenchymal origin (Mohyeldin et al., 2010). Enhanced ESCs pluripotency, impaired differentiation and partial dedifferentiation followed by acquisition stem cell-like characteristics were observed in different cell lines when grown under hypoxic conditions (1 -5% O<sub>2</sub>) (Ezashi et al., 2005; Mathieu et al., 2013). Similarly, another study demonstrates the emergence of adult stem cells and cancer stem cells in in-vivo. Their in-vitro model is used to maintain dedifferentiated cells under low O<sub>2</sub> tension (Mohyeldin et al., 2010).

Furthermore, HIF-2 $\alpha$  directly bind to the promoter region of Oct4 and regulate the state of stemness in the cells (Covello et al., 2006; Hu et al., 2003). Although another study in murine ES cells reveals that overexpression of HIF-2 $\alpha$  does not impact the Oct4 expression, on the contrary, increased differentiation was observed in cardiomyocytes (Yong Sun et al., 2015). Other reports suggest the differentiation of ES cells when grown under hypoxic conditions (H. Chen et al., 2009; Sonia Prado-lopez et al., 2010).

The variation in the reports supporting differentiated and maintenance of stem can be due to differences in the cell line, experimental model and degree/duration of hypoxia as there is no ideal hypoxia condition at which the transition between stem cell to non-stem cell or vice versa. Besides, other attributes like growth factor, cofactor, or coactivator are required to properly understand stem cells to non-stem cell transition dynamics.

## 2.12. Hypoxia-Inducible Factor (HIF)

HIF-1 is a transcription factor, initially detected during the gene expression study of erythropoietin (EPO) gene expression (Semenza & Wang, 1992; Gregg L. Semenza et al., 1991). It is a member of an environmental sensor family known as bHLH-PAS (basic-helix-loop-helix-Per-Arnt-Sim) and occurs in the heterodimeric form in nature (Hogenesch et al., 1997; Peng et al., 2000; Scheuermann et al., 2009). This dimer consists of an  $\alpha$ -subunit regulated by oxygen gradient and an essential  $\beta$  subunit (Mathieu et al., 2011; Wang et al., 1995). Under normoxia, HIF-1 $\alpha$  immediately hydroxylates at the two proline residues of the O<sub>2</sub>-dependent degradation domain (ODDD) (Comerford et al., 2002; Ruas et al., 2002). This hydroxylation serves as an identification marker for the proteasomal digestion of HIF-1 $\alpha$  by (pVHL) E3 ubiquitin ligase complex (Huang et al., 1998; Jaakkola et al., 2001; Patrick H. Maxwell\* et al., 2019). Proline hydroxylase (PHD) acts as an oxygen sensor of the cell and regulates the post-translational modification on HIF (Bruick & McKnight, 2001). Presently, three different isoforms of PHD are known in mammalian cells: PHD1, also known as egg-laying defective nine homologue 2 (EGLN-2), PHD2 (EGLN-1) and PHD3 (EGLN-3) (Schofield & Ratcliffe, 2004). Other than these three isoforms, PHD4, a fourth isoform, is also found on the endoplasmic reticulum surface, which can hydroxylate HIF. PHD2 is the most researched PHD, acts as an oxygen sensor and helps in the maintenance of basal level HIF-1 $\alpha$  *in vivo*, under normoxia (Berra et al., 2003). PHDs have an absolute requirement for O<sub>2</sub> to fulfil their function because molecular O<sub>2</sub> provides the oxygen atom in the hydroxyl group during HIF-1 $\alpha$  hydroxylation (Jaakkola et al., 2001; Ruas et al., 2002). Furthermore, 2-oxoglutarate (2-OG), formed during the tricarboxylic acid (TCA) cycle, serves as a co-substrate, whereas ferrous iron (Fe<sup>2+</sup>) and ascorbate act as cofactors of the active site (Wong et al., 2013). Subsequently, Succinate acts as an oxygen atom that is formed by decarboxylation of 2-OG after hydroxylation reaction (Chandel & Budinger, 2007). PHDs inactivate in the absence of oxygen molecules and cofactors, which results in the stabilization, accumulation and nuclear translocation of the HIF-1 $\alpha$  subunit. In the nucleus, the HIF-1 $\alpha$  subunit dimerizes with the HIF-1 $\beta$  subunit (C.-J. Hu et al., 2003). The active dimer complex of HIF-1 binds to a putative DNA binding sequence known as the hypoxia-responsive element (HRE) to transactivate various downstream genes associated with HIF-1 (Wenger, 2000).

### 2.12.1 HIFs – Structure and Regulation

bHLH and PAS domains are present in both  $\alpha$  and  $\beta$  subunit of HIF-1, after which the entire protein family was named (Scheuermann et al., 2009). Formation of active dimer and binding to a specific DNA sequence is carried out by bHLH and PAS domains (Hogenesch et al., 1997). PAS domains associate directly with ligands and other cofactors and promote environmental sensing. Though the functional relevance of endogenous molecules binding is not yet clear (Scheuermann et al., 2009). Depending upon the location in the protein sequence, there are two types of ODDD that function independently: NODDD is present at N-terminal while CODDD is located at C-terminal (Ortiz-Barahona et al., 2010). These domains regulate the expression and function of HIF- $\alpha$ . The proline residues in these conserved regions hydroxylate to mark the  $\alpha$  subunit for proteolytic degradation. There are two transactivation domains present in HIF-1 $\alpha$  and HIF-2 $\alpha$  subunits which are parted by a negative regulatory region: The N-terminal transactivation domain (N-TAD) which coincides with the CODDD and the C-terminal transactivation domain (C-TAD) (B. H. Jiang et al., 1996). The C-TAD domain plays a key role in the transcription of the HIF mediated by the interaction of co-activators such as p300/CBP (a cAMP-response-element-binding protein) in its CH-1 (cysteine/histidine rich) domain. This association is regulated in an oxygen concentration-dependent manner. (Ruas et al., 2002; D. Wang et al., 2010). Studies demonstrated that the disruption of this O<sub>2</sub>-dependent association was carried out by FIH (factor inhibiting HIF) and another 2-OG-dependent hydroxylase family member. The disruption was accomplished by the hydroxylation of asparaginyl residue found in C-TAD (Lando et al., 2002). Similar to PHDs, the FIH also loses its activity under hypoxic conditions. However, some studies suggest a higher affinity of FIH toward molecular oxygen (Koivunen et al., 2004). Apart from PHDs, FIH mediated hydroxylation at asparaginyl residues in CTAD represent another process to regulate the functioning of HIF- $\alpha$  (Lisy & Peet, 2008). Besides hydroxylation, other post-translation modifications that occur on the C-TAD and other domains of the  $\alpha$  subunit, regulates the HIF-1 $\alpha$  activity. These modifications are S-nitrosylation, acetylation and SUMOylation (F. Li et al., 2007)(Dörfel et al., 2013)(J. Li et al., 2014). However, the results were not very promising as both activation and deactivation of HIF were reported after these modifications (Lisy & Peet, 2008).

### 2.12.2 HIF Isoforms

After the discovery of HIF-1, several paralogs of HIF-1 of  $\alpha$  and  $\beta$  subunits were identified using cDNA sequence homology to enrich the bHLHPAS family (C. Hu et al., 2003; Keith et al., 2012). Presently, there are 3 different HIF forms known: HIF-1 $\alpha$ , HIF-2 $\alpha$  (also known as an endothelial PAS protein 1, EPAS1) and HIF-3 $\alpha$  (Makino et al., 2002; Tian et al., 1997). Other than HIF-1 $\beta$  (ARNT), also known as aryl hydrocarbon receptor nuclear translocator, two different forms of beta subunits, i.e., ARNT2 and ARNT3, were identified (Hoffman et al., 1991) (Hogenesch et al., 1997). Out of all these isoforms, HIF-1 $\alpha$  is the only subunit that is present in almost all cell types and hence, it is the most extensively studied isoform and designed as major regulation of oxygen homeostasis. The expression of HIF-2 $\alpha$  isoform is found in endothelial cells, glial cells, type II pneumocytes, cardiomyocytes, kidney fibroblasts, interstitial cells of the pancreas and duodenum and hepatocytes (Zhao et al., 2015). Approximately 48% of amino acids sequence is similar between HIF-1 $\alpha$  and 2 $\alpha$  (Tian et al., 1997), due to this similarity, both HIF-1 $\alpha$  and 2 $\alpha$  binds to the same HRE sequence (RCGTG) in the promoter region of the target gene (Mole et al., 2009). In addition, both these subunits behave similarly with the HIF- $\beta$  subunit and undergo oxygen gradient dependent proteasomal degradation after hydroxylation by PHDs and FIH. The major difference between these subunits is the variability in the N-TAD domain, responsible for the differential selection of the transcription co-factors (Cheng-Jun Hu et al., 2007). Generally, HIF-1 activates under acute and intense hypoxia ( $< 0.1\% O_2$ ), whereas HIF-2 starts its activity under chronic and mild hypoxia ( $< 5\% O_2$ ) (Holmquist-Mengelbier et al., 2006; Z. Li et al., 2009). However, these subunits also have few common target genes like glucose transporter 1 (GLUT1) and the vascular endothelial growth factor (VEGF). Although, the sole responsibility of HIF-1 $\alpha$  is to regulate the expression genes of the glycolytic cycle, pH regulator genes and gene regulating apoptosis. Conversely, HIF-2 $\alpha$  activates the gene responsible for stemness, cell cycle, invasion and metastasis (C.-J. Hu et al., 2003; Mole et al., 2009). But it should be noted that HIF-1 $\alpha$  and HIF-2 $\alpha$  subunits activity and ability are varying with different cell types (Keith et al., 2012). On the contrary, HIF-3 $\alpha$  is different from both the other subunits due to the C-TAD domain's absence. Lack of C-TAD leads to the inability of HIF-3 $\alpha$  to bind with transcription co-activators (Makino et al., 2002). Hence it forms an incompetent complex with HIF-1 $\alpha$  subunits, thereby acts as a negative regulator by competing with the HIF-1 $\beta$  subunit (Makino et al., 2002).

### 2.13. Role of HIF in Embryogenesis

Low oxygen level is not the only feature of pathological conditions like tumour development, brain stroke and ischemic heart disease but also an essential factor in regulating embryonic development because several vital reactions are carried out hypoxia. Pluripotent cells or embryonic stem cells function naturally under hypoxia (Lin et al., 2008; Mohyeldin et al., 2010). Approximately 2 % of genes present in the human genome are predicted to act as a target gene for hypoxia (Mazure et al., 2004). *In silico* and gene profiling studies reveal more than 200 genes that are regulated by HIF-1 $\alpha$  (Benita et al., 2009; Ortiz-Barahona et al., 2010). During gastrula formation, there is a rapid proliferation of the cell, which leads to hypoxia in the microenvironment. Hence, most embryonic development occurs at low oxygen concentration, which initiates the activation of the HIF-dependent mechanism (Dunwoodie, 2009; Ezashi et al., 2005; Kotch et al., 1999). Oxygen serves as an essential morphogen in embryogenesis and plays a crucial role in the production of energy (Dunwoodie, 2009). The significance of the functional HIF system was assessed in a variety of knock-out tests. Knockout of HIF-1 $\alpha$  (HIF-1 $\alpha$   $-/-$ ) in the murine model initially resulted in impaired erythropoiesis, vascular tube defect and cardiac deformities, and finally, embryonic lethality at mid-gestation around E10.5 (Kotch et al., 1999; Yoon et al., 2006). This implies that HIF-1 $\alpha$  expression is critical for the normal development of the cardiovascular system. Furthermore, defective cephalic vascularization and neural tube defects were reported (Iyer et al., 1998). Conversely, the knockout of HIF-2 $\alpha$   $-/-$  results in insufficient catecholamine metabolism, bradycardia, vascular defect and embryonic lethality at E12.5 of gestation (Peng et al., 2000). In another study, the mice live till the neonatal stage but died due to improper lung development (Compernelle et al., 2002) or survived for few months and died due to multiple organ disorders (Scortegagna et al., 2003). Vasculogenesis is the *de novo* process for blood vessels formation, in which the progenitor cell differentiates into the endothelial cell that arranges to form a primary vascular plexus. Further, the blood vessel develops and remodels to form a functional circulatory system. There are genes that are responsible for vascular development: Vascular endothelial growth factor (VEGF)(A-D), which bind VEGF (1-3) receptors.

### 2.14. Role of HIF-1 in MAPK/ERK and PI3K/AKT Pathways

There are several signalling which is going on simultaneous in a cell system (Mylonis et al., 2006; Sang et al., 2003; Treins et al., 2005). To study these signalling, we need a robust model that activates and deactivates frequently in response to external stimuli. The transduction of these signals is carried out by phosphorylation and dephosphorylation of proteins by kinases and phosphatase enzymes, respectively (Bononi et al., 2011). For example, for HIF-1 $\alpha$  activity and nuclear accumulation, phosphorylation by p42/44 MAPK of the Ser641/643 residue is highly essential. Several signalling pathways regulate the activities of HIF (Richard et al., 1999). In tumours, HIF activation is regulated by mitogen-activated protein kinase (MAPK) signalling as it is essential for HIF-1 $\alpha$  transactivation activity. MAPK/ERK and PI3K/AKT pathways regulate the expression and activity of HIF-1 under both normoxic and hypoxic conditions. p42/p44 MAPK has also been reported to be able to modify HIF-1 $\alpha$  (Richard et al., 1999; Sang et al., 2003). Site-directed mutagenesis of MAPK phosphorylation sites, including residues Ser-641 and Ser-643, leads to a significant reduction in the phosphorylation of HIF-1 $\alpha$  (Mylonis et al., 2006).

### 2.14.1. Interplay between HIF and ERK

MAPK/ERK pathway plays an essential role in regulating and enhancing the HIF-1 $\alpha$  transactivation (Fukuda et al., 2002). At the same, there are reports of MAPK/ERK pathway activation after exposure to the hypoxic condition in many cell lines (C. Liu et al., 2005; Minet et al., 2000; (Mottet, Dumont, et al., 2003). Furthermore, experimentation like site-directed mutagenesis, mass spectrometry and in-vitro phosphorylation reveal that ERK1/2 directly phosphorylated HIF-1 at 641 and 643 positions in the serine residue. This interaction does not influence the DNA binding ability and protein stability of HIF-1 $\alpha$ . On the contrary, the phosphorylation in HIF-1 induces its localization at the subcellular level and transcriptional activity (Mylonis et al., 2006; Richard et al., 1999). Alternatively, HIF-1 demonstrates decreased transcriptional activity by dominant-negative mutation or chemical inhibition of ERK1/2 (Hur et al., 2001; Mottet, Michel, et al., 2003). NES (nuclear export signal) is a short sequence present in the close vicinity of serine residues of HIF-1.

ERK kinases have been reported to be activated during hypoxia in human microvascular endothelial cells-1 (HMEC-1) (Minet et al., 2000). ERK1 is essential for HIF-1 transactivation activity due to hypoxia. It governs the transport of HIF-1 from the nucleus

to the cytoplasm by interacting with Exportin-1/CRM1 protein (chromosomal maintenance 1) that shuttles the HIF-1 from the nucleus to the cytoplasm (Mylonis et al., 2006). When ERK1/2 is not activated, there is no phosphorylation at the serine residues, and NES is free to interact with exportin-1, which initiates the transport of HIF-1 back to the cytoplasm (Mylonis et al., 2006). In hypoxia, HIF-1 $\alpha$  phosphorylation follows an ERK-dependent pathway (Minet et al., 2000). On the contrary, the phosphorylated ERK induces the phosphorylation of HIF-1 at serine residue, which in turn block the active site of NES and preventing the interaction of exportin -1. This results in the longer localization of HIF-1 in the nucleus and increases its activity (Mylonis et al., 2008). Besides, the activation of ERK1/2 promotes the interaction of HIF-1 with its cofactor like p300/CBP and indirectly enhancing its activity (Sang et al., 2003). However, the treatment with drug targeting microtubules reduce the nuclear localization of HIF-1 and, at the same compromises its interaction with the cytoskeleton (Escuin et al., 2005).

### 2.14.2 Interplay between HIF and PI3K

Several reports suggest the involvement of PI3K in the regulation of HIF-1 (Gang et al., 2017; Mottet, Dumont, et al., 2003). Treatment with different inducers of PI3K pathways like IGF (insulin-like growth factor), EGF (epidermal growth factor) and insulin results in increased protein expression of HIF-1 and hence targeting other downstream effector genes of HIF (Dekanty et al., 2005; Secades et al., 2015; Treins et al., 2005). Further experimentation reveals that PI3K induced HIF-1 upregulation is neither due to stabilization of HIF protein nor affect the activity of PHDs or pVHL (Berra et al., 2003; Jaakkola et al., 2001). On the contrary, increased HRE activity was observed in mTOR dependent manner, which can be related to upregulated mRNA expression (Again et al., 2013). Subsequently, inhibition of the PI3K pathway by using PI3K and mTOR inhibitor not only decreases the basal expression of HIF-1 but also prevents its induction on exposure to hypoxia, by inhibiting the transactivation of HIF-1 and VEGF expression (Powis & Kirkpatrick, 2004). Alternatively, the treatment with LY294002 and wortmannin (chemical inhibitors of PI3K pathway) and dominant-negative PI3K mutant reveals decreased protein level expression HIF-1, but mRNA level expression remains unaffected (Clark et al., 2002; Tsou et al., 2015; Vlahos et al., 1994). This was attributed to decreased expression of Heat shock protein that stabilizes the HIF-1 protein (G. Zhou et al., 2004). There are no reports about HIF Phosphorylation by Akt. However, glycogen

synthase kinase 3 $\beta$  (GSK3 $\beta$ ) mediated phosphorylation has been reported, which further results in the Ubiquitination and proteasomal degradation of HIF-1 protein, bypassing its natural hydroxylation and pVHL pathway (Flügel et al., 2007).

## 2.15. Multidrug Resistance

In the treatment of cancer, multidrug resistance is a major problem. This resistance mechanism evolves with different structures and modes of action against various drugs. MDR is a significant contributor to the failure of most types of chemotherapy (Ambudkar et al., 2003; Yagüe et al., 2007). Tumour cells sensitive to broad-spectrum drugs frequently also develop resistance to more specialized groups of anti-cancer drugs.

This resistance is primarily due to the increased efflux of drugs triggered by pumps located on the cell membrane (Holohan et al., 2013; Vellonen et al., 2004). In the cell, drug accumulation takes place essentially by two mechanisms. When the genes expressing target proteins yield unique mutations or modify expression patterns, cancer cells can very well develop resistance to targeted drugs. Secondly, TME heterogeneity due to the variety and complex existence of vasculature within tumours and fluctuating hypoxia contributes to genetic heterogeneity improvement (Jing et al., 2019). Oxidative stress is induced by repeated cycles of hypoxia and reoxygenation that could trigger DNA damage in tumour cells, leading to genetic instability that contributes to the accumulation of additional mutations and genetically disparate clonal development subgroups (Brahimi-Horn et al., 2007; Harris, 2002; Shannon et al., 2003). Due to the complex shifts in TME during therapy, drug resistance may also be increased (Brahimi-Horn et al., 2007; J. Chen et al., 2014; Seidel et al., 2010; P. Xu et al., 2017). Anomalous tumour vasculature, hypoxia, reduced pH, enhanced interstitial fluid pressure, and variations in the expression of tumour suppressor genes and oncogenesis are the microenvironmental selection pressures that predispose to MDR progression (Comerford et al., 2002; P. Xu et al., 2017)

### 2.15.1. MDR Types, Their Structure and Function

Drug resistance can be caused by reduced drug absorption and increased drug efflux (Yagüe et al., 2007). Multidrug resistance (MDR) is associated with three subfamilies: ABCB (also referred to as ABCB1/MDR1/P-glycoprotein), MDR-associated protein 1

(MRP1; also referred to as ABCC1) and breast cancer resistance protein (BCRP; also referred to as ABCG2/MXR)(Lemos et al., 2008; Molinas et al., 2012; Vaidyanathan et al., 2016). All these proteins have significant and intertwining sensitivity of substrates and can also facilitate the removal of different hydrophobic compounds.

MDR1 is a membrane-bound glycoprotein expressed in the majority of tissues(Vaidyanathan et al., 2016). In most tumours, MDR1 is overexpressed and may also be triggered by chemotherapy(Vaidyanathan et al., 2016). Several reports have confirmed that increased expression of MDR1 in different cancer types is closely linked with chemotherapy malfunction (Ambudkar et al., 2003; C.-H. Choi, 2005). Drug resistance in breast, lung and prostate cancer is also correlated with MRP1 overexpression, and BCRP is also established to be correlated with resistance to chemotherapy in leukaemia and breast cancer (Doyle et al., 1998; Robey et al., 2007).

The transmembrane transporters liable for efflux of drugs predominantly belong to the family of proteins known as ABC transporters(C. H. Lee, 2010; Lemos et al., 2008; Saeed et al., 2014). There are 48 ABC genes in the human genome, and they are divided into seven subclasses (ABCA-ABCG) (Brown et al., 2006). In the acquirement of multidrug resistance (MDR) for cancer chemotherapeutics, ABCB1, ABCC1 and ABCG2 are highly active among them(Katayama et al., 2014; Kimura et al., 2007). The multidrug resistance gene 1 (*mdr1*), which consists of 28 exons and is located on the 7th chromosome, encodes ABCB1 (MDR1 or P-gp)(Ambudkar et al., 2003; Chinn & Kroetz, 2007). MDR-1 is one of the best characterized ABC transporters, a standard 190 kDa ABC transporter protein consisting of 1280 amino acids (Deeley & Cole, 1997). It is made up of two domains: a) transmembrane domains (TMDs) and b) distinctive nucleotide binding domains (NBDs) that produce energy through ATP hydrolysis for the active transport of compounds through the cell membrane (Teicher et al., 2012). There are many binding sites for ABCB1 that can adhere and syphon a wide array of different drugs substrates, including paclitaxel, doxorubicin, etoposide and vinblastine (Dumontet & Jordan, 2010; Holohan et al., 2013; Pellegrini & Budman, 2005).

In several different tumour forms, including the kidney, lung, liver, colon and rectum, elevated levels of ABCB1 expression were observed prior to chemotherapy (Labhasetwar, 2011). In comparison, in many haematological malignancies such as AML and ALL, ABCC1 or multidrug resistance-associated protein 1 (MRP1) (J. F. Lu et al., 2015) similar to ABCB1, initially low expression and then a drastically increased

expression of ABCB1 post-chemotherapy was also reported to transport out a wide variety of bioactive compounds including vinca alkaloids, epipodophyllotoxins, camptothecins, and anthracyclines (Joyce et al., 2015; X. Wang et al., 2019). ABCC1 pumps organic anionic substrates such as glutathione, glucuronide, or sulphate conjugate compounds, while ABCB1 bears amphipathic and lipid-soluble compounds (Buys et al., 2007; Lebedeva et al., 2011). In several forms of cancer, including lung, breast and prostate cancers, increased expression of ABCC1 has been reported to be correlated with resistance (Buys et al., 2007; O'Driscoll & Clynes, 2006). The main drug efflux transporter in breast cancer-related resistance is ABCG2, the breast cancer resistance protein (Dong et al., 2019; Gottesman & Pastan, 2015). In certain cancers, ABCG2 is regarded as a marker of CSCs and is also accountable for the side population effect. Both positively and negatively charged drugs, including the ones used in chemotherapy, namely mitoxantrone, bisantrene, epipodophyllotoxin, camptothecin, flavopiridol and anthracycline) and tyrosine kinase inhibitors (TKI) like imatinib and gefitinib can be transported by ABCG2. ABCG2 overexpression has also been found in many other cancer types, including lung cancer and leukaemia, in addition to breast cancer (Joyce et al., 2015; Mao & Unadkat, 2005). For their substrates and roles in tumour resistance to anticancer drugs, other ABC transporters have also been studied, offering further explanations on drug resistance mechanisms. For instance, several chemotherapy drugs, particularly doxorubicin, cisplatin, and etoposide, can be transported by ABCC2 and ABCC3, the overexpression of which can amount to multidrug resistance (Bruhn & Cascorbi, 2014; Van Der Schoor et al., 2015). ABC transporter mutations and increased expression significantly impact tumour responsiveness and the effectiveness of drugs against cancer. For appropriate drug choice and improved patient efficacy, an accurate and precise expression profiling of ABC transporters in tumours is critical (Fletcher et al., 2010; Gillet et al., 2007; Milane et al., 2011). The growth of multidrug resistance (MDR) in cancer is aided by inadequacies in systemic drug dispersion and tumour location as well as micro-environmental selection pressures (Milane et al., 2011). MDR's characteristics include irregular vascular system, hypoxia areas, ABC-transporter transactivation, aerobic glycolysis, and an elevated apoptotic cutoff point (Donnenberg & Donnenberg, 2005; J. F. Lu et al., 2015; Saraswathy & Gong, 2013).

## 2.16. MDR-1 and CSCs

There are two broad types of cancer drug resistance: innate and acquired. Multiple drug resistance (MDR) refers to a mechanism wherein one-drug resistance is followed by resistance to many drugs that vary entirely in chemical composition or mechanism of action (Donnenberg & Donnenberg, 2005). It is a crucial factor in the failure of certain forms of chemotherapy. The MDR issue in the healthcare facility could encompass two main components, one acquired during therapy and the other pre-existing at the time of diagnosis (Buys et al., 2007; Cong Liu et al., 2015). For the formulation of chemotherapeutic drugs to resolve MDR, the detection of MDR dynamics is critical. In comparison to the above-mentioned factors, the hypothesis that human tumour proliferation may be controlled by a limited population of self-renewing cancerous cells also referred to as tumour stem cells, seems to be of high significance in MDR (Cho & Kim, 2020; Milane et al., 2011). Cancer stem cells containing MDR characteristics can repopulate tumours during cancer treatment cycles, which is a significant challenge in clinical oncology (Cho & Kim, 2020; Milane et al., 2011). Genetic variation or modification of a drug target's expression may decrease the efficacy of target inhibitors, leading to tolerance. Patients who developed resistance to RAF or MEK inhibitor monotherapy have been reported to possess alterations in MAPK and variations in MEK1 or/and MEK2 (Aplin et al., 2011; Dhillon et al., 2007; Hur et al., 2001; Lugowska et al., 2015).

CSCs are a tumour subpopulation having the ability to self-renew and differentiate in order to be able to engage in tumour onset and advancement (ALHulais & Ralph, 2019; Wainwright & Scaffidi, 2017). Several cancer categories, including leukaemia, glioblastoma and pancreatic cancer, have been believed to be associated with tolerance towards chemotherapy agents. To minimize drug resistance, combination therapy targeting both CSCs and tumour cells may be necessary (Gutting et al., 2019; Mokhtari et al., 2017; X. Xu et al., 2015).

The EMT-induced multidrug resistance mechanisms are not clearly elucidated. However, recent findings indicate that EMT and CSC share some common features and that their drug resistance activity reflects various dimensions of the same phenotype (Du & Shim, 2016; Mitra et al., 2015; Shibue & Weinberg, 2017; A. Singh & Settleman, 2010). One conceivable solution is that EMT cells possess many links with cancer stem cells (CSCs) in signalling pathways, such as Wnt, Notch and Hedgehog pathways. EMT, therefore, empowers cancerous cells to gain tolerance to anti-cancer medications and avoid drug-

induced apoptosis (Katoh & Katoh, 2008). TGF- $\beta$ , for instance, is a well investigated primary cytokine in EMT whose signalling pathways are associated with drug resistance advances. TGF- $\beta$  suppression might reverse the EMT cascade and greatly increase cancer cells' responsiveness to chemotherapy (Katoh & Katoh, 2008; L. Li et al., 2015). There are also studies suggesting the association of Wnt and Hedgehog pathways with drug intolerance (McCubrey et al., 2016; Takebe et al., 2011). Aggregated data indicates that the CSCs depend on the EMT programme as a key regulator when facilitating drug resistance. Epigenetic modifications resulting from EMT stimulation encompass the CSC condition of carcinomas. A substantial contribution to anticancer biologics can be obtained by understanding the mechanistic correlation among EMT, CSC and drug tolerance (Mitra et al., 2015; Shibue & Weinberg, 2017; A. Singh & Settleman, 2010). Increased expression levels of Twist, ZEB1/2, Slug, as well as Snail upregulates ABCB1 transcriptional activity, contributing to drug resistance (Katoh & Katoh, 2008; Tsou et al., 2015). Snail, MSX2, SOX2 and ZEB1 are reported to be controlled by ABCG2, an ABC transporter intimately associated to MDR (J.-Y. Shi et al., 2004; Spasokoukotskaja et al., 1995; Månsson et al., 2003; Johansson & Karlsson, 1996). Multiple ABC vehicles participating in MDR, including ABCC1, ABCC2, ABCC4, and ABCC5, have also been listed under the EMT-TFs regulation (Kristensen et al., 1994; Furman et al., 1986; J. Wang et al., 2000).

ATP may also directly contribute towards chemotherapy hostility via purinergic receptor signalling from the cell exterior. Extracellular ATP was also reported to stimulate glucose transporter 1 expression, likely through the PI3K-AKT cascade triggered by P2X7 and hypoxia-inducible factor 1 $\alpha$ - mediated signalling (Nogales et al., 1995). Such modifications are also likely to enhance cancer cell longevity and drug tolerance. Consequently, in addition to minimizing ATP internalisation, lowering extracellular ATP concentration may increase drug efficacy by lowering relevant purinergic receptor signalling (Chandel & Budinger, 2007; Gottesman & Pastan, 1993; Teicher et al., 2012).

### 2.17. MDR-1 and CRIPTO-1

Features including cellular variability as well as plasticity, the expression of MDR1 or the aberrant expression of embryonic signalling ligands and morphogens, sometimes including Nodal, essential for self-renewal and pluripotency, indicate that a stem cell-like populace may prevail in intense melanomas (Luigi Strizzi et al., 2008; Yagüe et al.,

2007). The expression of Cripto-1, the Nodal co-receptor, in a subset of malignant melanoma samples can be used to classify potential melanoma stem cells (MSC)(Luigi Strizzi et al., 2008); Pereira et al., 2011). Perhaps in view of the fact that the application of anti-Cripto-1 antibodies on sorted Cripto-1-positive cells of the metastatic melanoma cell line C8161 has formally established a slow-growing, sphere-forming subgroup which expresses elevated levels of Oct4, Nanog and MDR1(Z. Wu et al., 2009; Zimmerer et al., 2013). The cripto-1 expression can be a good biomarker for detecting cancer stem cells in skin cancer and probably other belligerent tumours(Francescangeli et al., 2015; Klauzinska et al., 2014; Mahmoudian et al., 2017). The transcription factors Oct4 and Nanog, alongside Cripto-1, are said to control pluripotency, self-renewal, cellular involvement and the differentiation of ES cells in mice as well as humans (Y. H. Loh et al., 2006; Luigi Strizzi et al., 2008; Kazuhide Watanabe et al., 2010). In addition, Cripto-1 is said to be a specific target gene for Nanog and Oct4 in the mouse and human ES cells. The expression of the stem cell marker Cripto-1, also known as the Nodal Coreceptor, can be used to isolate cells from metastatic melanoma that appear to have stem cell-like characteristics (Strizzi et al., 2007; Pereira et al., 2011). Nodal signalling may constitute a fundamental connection for the unification of embryonic and tumorigenic signalling pathways in malignant tumours. It may include Nodal as a marker for the progression of the disease and a potential new therapeutic target. Malignant melanomas have been shown to comprise cells that express markers like MDR-1, also known as P-glycoprotein, which is responsible for multidrug resistance that is also correlated with normal nonmalignant stem cells (Fuchs et al., 1991). Expression of ABCG2 and CD133, the drug efflux transporter and stem cell marker, respectively, are suggested to be useful for the identification of a possible MSC demographic (Moitra, 2015).

Literature suggests that doxorubicin recruitment by CCRF-CEM leukaemia cancer cell results in multidrug resistant CEM/A7R cell line overexpressing MDR-1 coded P-glycoprotein (P-gp)(X. F. Hu et al., 2007). Moreover, Cripto-FRL, a Cryptic family member, on being abundantly expressed in CEM/A7R cell line, and also anti-Cripto-1 monoclonal antibodies (Mab) can inhibit CEM/A7R cell proliferation both in vitro and in established xenograft lesions in severe combined immunodeficient mice (Normanno et al., 2004; Xing et al., 2004; Y. Y. Zhang et al., 2018). Findings prove that Cripto-1 monoclonal antibodies have the ability to synergistically intensify the responsiveness of

MDR cells to P-gp like epirubicin (EPI), daunorubicin (DAU) as well as non-Pgp nucleoside analogue cytosine arabinoside substrates (AraC)(X. F. Hu et al., 2007).Cripto-1 Mab marginally impaired P-gp expression but had no effect on P-gp activity, suggesting that a P-gp-independent pathway was involved in overriding MDR(X. F. Hu et al., 2007). Lately, oncoprotein Cripto-1, a leading member belonging to the epidermal growth factor-Cripto-FRL1-Cryptic (EGF-CFC) network, has also been shown to be a critical aspect in the mediation of drug tolerance (Normanno et al., 2004). Scientists have suggested that Cripto-1 is upregulated in Pgp-positive CEM/A7R cells. Cripto-1 had first been discovered and sequenced from the teratocarcinoma cDNA expression database, and is overexpressed in certain tumours, involving its function in tumorigenesis and cancer progression (Salomon et al., 2000). Cripto-1 and MDR1 are said to be specific target genes for b-catenin, the primary mediator of the Wnt signalling pathway (Yamada et al., 2000; Morkel et al., 2003). Upregulation of MDR1 and aggregation of b-catenin have also been reported in chemically induced rats and human hepatic adenomas and adenocarcinomas (Yasuhiro Yamada et al., 1999). It is far more probable that perhaps the chemically mediated intracellular aggregation of b-catenin contributes to its nuclear translocation and attachment to the T-cell receptor as well as the lymphoid enhancer factor transcription factors that have transactivated MDR-1 and Cripto-1 along with several other Wnt target genes(Seidensticker & Behrens, 2000). These might describe why and how the DOX recruitment of Pgp-mediated MDR phenotypes in the CEM/A7R cells contributes to the concurrent activation of Cripto-1 expression. The EGF-like segment of Cripto-1 is associated with the stimulation of C-Src ras/raf/MAPK as well as PI3k/Akt/GSK-3b mediated cell proliferation and cell survival signalling pathways (Caterina Bianco et al., 2003)(Ebert et al., 1999)(Kannan et al., 1997). Constitutive stimulation of PI3K/Akt pathway facilitates MDR morphology in breast cancer, prostate cancer and acute myeloid leukaemia (AML) (Clark et al., 2002),(Grandage et al., 2005),(J. T. Lee et al., 2004). These findings indicate that the Cripto-1-activated PI3K/Act pathway in CEM/A7R cells promotes tumour growth and triggers MDR-1 phenotype by disruption of apoptosis frameworks triggered by chemotherapy.

Cancer cells can use either Cripto-1 or P-gp proteins to survive apoptosis caused by chemotherapy drugs. Cripto-1 is now classified as a therapeutic target, and the EGF-like area has been considered an effective immunotherapy intervention site (Adkins et al.,

2003; Xing et al., 2004) (Xiu Feng Hu & Xing, 2005). Anti-Cripto-1 monoclonal antibodies may exploit MDR to circumvent P-gp by activating a signal molecule to stimulate cell death in MDR cancerous cells with Cripto-1 and P-gp overexpression. The mechanisms responsible for anti-Cripto-1 Mab induced apoptotic cell death, and enhanced cytotoxicity by chemotherapeutic drugs was investigated for activation of the JNK/SAPK pathway and the inhibition of the Akt pathway (X. F. Hu et al., 2007). The JNK/SAPK pathway has been found to be triggered by anti-Cripto-1 Mab and AraC in the CEM/A7R cells, where the PI3K/Akt pathway is known to be intrinsically activated by Cripto-1 (Ebert et al., 1999). Anti-Cripto-1 Mab is likely to suppress Akt phosphorylation, a significant component of the PI3K/Akt pathway and disrupted Cripto-1/Akt/GSK-3 $\beta$  signalling pathways contributing to destabilising b-catenin and flipping Axin to trigger JNK apoptosis signalling instead of preferring Wnt signalling activation (Seung Hoon Lee et al., 2001) (Neo et al., 2000). Expression of CR-1 and MDR1 is co-induced by treatment with CR-1. In 2013, Strizzi et al., have stated that CR-1-expressing melanoma cells have a greater expression of MDR-1, the multidrug-resistant protein. In the FACS-assorted positive CR-1 cell subgroup in the U-87 MG cell line, co-expression of CR-1 and MDR-1 has been reported (Pojul Loying et al., 2015). In 2007, Hu et al. had already demonstrated that the drug-resistant leukaemia cell line chosen by Doxorubicin selection has higher CR-1 and MDR-1 expressions. Literature indicates a link between the transcriptional modulation of CR-1 and MDR-1 expressions and, like CR-1, MDR-1 also seems to be a target for HIF and  $\beta$ -catenin (Comerford et al., 2002) (T. Yamada et al., 2000). TGF- $\beta$  often stimulates MDR-1 expression, and intermodulation occurs between the TGF- $\beta$ /SMAD2/3 and the  $\beta$ -catenin pathways (Utsunomiya et al., 1997) (M. Zhang et al., 2010). In addition, AP-1 also regulates MDR-1 expression and interacts with SMAD (Daschner et al., 1999) (Liberati et al., 1999). Intriguingly, Hu et al. have demonstrated that on treatment with the anti-CR-1 antibody, a multidrug-resistant leukaemia cell line exhibited minor downregulation in MDR-1 expression (X. F. Hu et al., 2007). One can therefore hypothesize that the induction of MDR-1 expression in U-87 MG cells by CR-1 can eventuate via crosstalk involving transcription factors regulating MDR-1 expression as well as the ALK4/SMAD2/3 pathway

## 2.18. MDR-1 and HIF-1

Cancer cells experience a dynamic modification of their phenotype under hypoxia, a transition that is essential for cell sustainability under these regimes (Carnero & Leonart, 2016). One such survival cascade is triggered whenever the alpha subunit of the hypoxia-inducible factor (HIF) translocates from the cytoplasm to the nucleus to complex with the beta subunit forming an activated HIF complex transcription factor (Depping et al., 2008; Harris, 2002; Gregg L Semenza, 2003). This HIF complex binds specifically to the hypoxia sensitive elements (HREs) of target genes, including genes involved in invasion, proliferation, metabolism, and drug resistance, thereby triggering transcription (Harris, 2002; Gregg L Semenza, 2003; Brahimi-Horn et al., 2007; Jewell et al., 2001; Kizaka-Kondoh et al., 2003; Nanduri et al., 2008; Gregg L Semenza, 2008; Shannon et al., 2003). With very little oxygen accessible for energy acquirement by oxidative phosphorylation, such hypoxic cancerous cells return to aerobic metabolism for the generation of ATP which is known as the Pasteur and Warburg effect (Teicher et al., 2012). The initial reaction to the selection pressures dictates whether the cancer cell undergoes apoptosis, necrosis, becomes quiescent, propagates, or acquires MDR. One of the most characterized MDR operation principles is the up-regulation of ATP-Binding Cassette (ABC) transporters, and perhaps the most researched ABC transporter is P-glycoprotein (P-gp, MDR1, ABCB1) (Gillet et al., 2007) (Chinn & Kroetz, 2007). Cells that show elevated growth factor and receptor expression, nutrient import, aerobic glycolysis, DNA repair and enhanced ABC transporter activity, whilst simultaneously decreasing oxidative phosphorylation apoptosis and tumour microenvironment pH express elevated levels of MDR (Gottesman et al., 2002). Similarly, hypoxia alone can often be likely to elicit MDR through the transcriptional activity of HIF, that further stimulates MDR proteins and strategies (Trédan et al., 2007) (Harris, 2002) (Kizaka-Kondoh et al., 2003) (Shannon et al., 2003) (Brizel et al., 1996) (Vlahos et al., 1994) (J. M. Brown, 1990) (Höckel et al., 1999) (Nordmark et al., 1996) (Young & Hill, 1990). A wide variety of drugs can be efflux out by P-gp, and this efflux necessitates the consumption of two ATP molecules (Gottesman et al., 2002). MDR-1 is mostly launched with overexpression of P-gp. Still, other ABC transporters such as multidrug resistance protein 1 (MRP-1, ABCC1) or breast cancer resistance protein (BCRP, ABCG2) sometimes lead to the formation of MDR (Yagüe et al., 2007) (Gillet et al., 2007) (Buys et al., 2007) (Kimura et al., 2007) (Lemos et al., 2008). It is possible that certain tumors are induced by the deregulation of stem cells and is caused by the initiation of cancer stem cells. A subgroup of cancerous cells is indeed prone to developing stem-like

characteristics, and this subpopulation of cancer stem cells is highly probable to be MDR cells (Donnenberg & Donnenberg, 2005). MDR tumors can evolve stem-like characteristics and be classified as cancer stem cells. Various studies have consistently demonstrated that cell stressors, including hypoxia, that are successful in triggering cancer aggression and MDR phenotypes, frequently stimulate stem-like characteristics in cancer cells like that of the expression of the stem cell factor (SCF) (Harris, 2002)(Shannon et al., 2003)(Z.-B. Han et al., 2008). Moreover, hypoxic cells that are somewhat remote or temporarily cut off from the regional vascular system are often MDR cells where the acquisition of energy, nutrients and therapeutics is an obstacle.









### 3.1. Bacterial Strains Maintenance and Growth:

*E. coli* strains and clones were stored at -80 °C as glycerol stocks (20% glycerol) and were cultured at 37°C and 180 rpm for 12 h in LB medium (Himedia) or 2xTY medium (Himedia) containing ampicillin. *E. coli* strains used in this work, and the composition of culture media are mentioned in **Table 3.1** and **Table 3.2**, respectively.

**Table 3.1:** List of Bacterial Strains

SL. NO.	STRAIN	DESCRIPTION
1.	<i>Escherichia coli</i> DH5 $\alpha$	F' $\phi$ 80dlacZ $\Delta$ M15 $\Delta$ ( <i>lacZYA-argF</i> ) U169 <i>endA1 recA1 hsdR17</i> (rk-mk+) <i>deoR thi-1 phoA supE44 <math>\lambda</math>-gyrA96 relA1</i>
2.	<i>Escherichia coli</i> Rosetta Gami(DE3) (Novagen)	F- <i>ompT hsdSB</i> (rB- mB-) <i>gal dcm lacY1</i> <i>ahpC</i> (DE3) <i>gor522: Tn10 trxB pRARE</i> (CamR, KanR, TetR)

**Table 3.2:** Bacterial Culture Media

SL. NO.	MEDIUM	CONSTITUENTS	COMPOSITION	pH
1.	Luria Bertani broth (LB)	Tryptone	1.0%	7.2
		Yeast extract	0.5%	
		NaCl	0.5%	
2.	2X (Terrific Broth) (2X-TY)	Tryptone	1.6%	7.2
		Yeast extract	1.0%	
		NaCl	0.5%	

### 3.2. Human Cell Lines: Culturing, Passaging and Stock Making

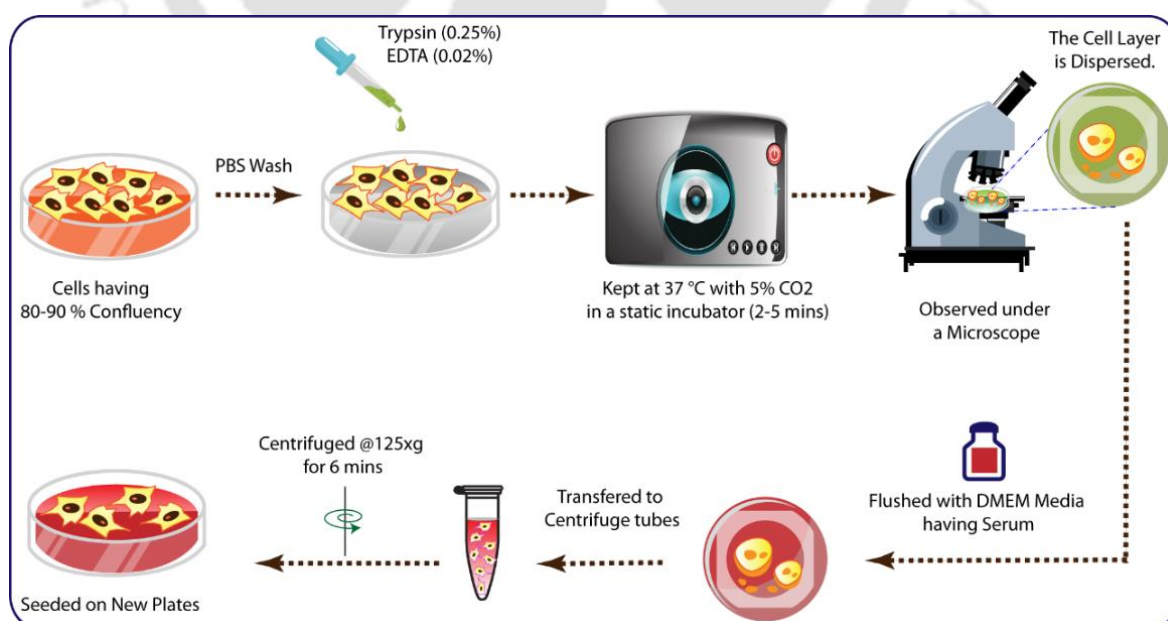
MCF-7 (Human breast cancer cell line) and HEK 293 (Human embryonic kidney cell line) were obtained from NCCS (National Centre for Cell Science), Pune, India. The cell lines were cultured in High Glucose DMEM media (Himedia) supplemented with 10% serum of bovine origin (FBS-South American) (Gibco), 3.7g/L NaHCO<sub>3</sub>, and 1X antibiotic-antimycotic solution (Gibco) and maintained at 37°C and 5% CO<sub>2</sub> in a static

incubator. The spent media was discarded and replenished with fresh media at time intervals for cell line maintenance, as mentioned in **Table 3.3**.

**Table 3.3:** Culture Conditions

SL. NO.	CELL LINE	SUB CULTIVATION RATIO	MEDIA RENEWAL
1.	MCF-7	1:4 to 1:8	Every 2 to 3 days
2.	HEK 293	1:3 to 1:6	2 to 3 times per week

Sub culturing of the cells was done once they reached 80-90% confluence. Firstly, the spent media was removed, and the monolayer was thoroughly washed with sterile PBS to eliminate any traces of serum containing the trypsin inhibitor. Now, 0.5 mL to 1 mL of Trypsin (0.25%) /EDTA (0.02%) (Sigma Aldrich) was added to the flask and placed at 37°C to facilitate dispersal. The flasks were observed under an inverted microscope after a few minutes to determine if the cell layer was scattered. The cells were now flushed with DMEM medium containing FBS and aspirated by gently pipetting. Approximately 30 percent of the cell suspension was added to a new flask with new growth media for HEK 293 cells, and cells were held in a static incubator at 37 °C with 5 percent CO<sub>2</sub>, as shown in Scheme 4.1. **Scheme 3.1**.



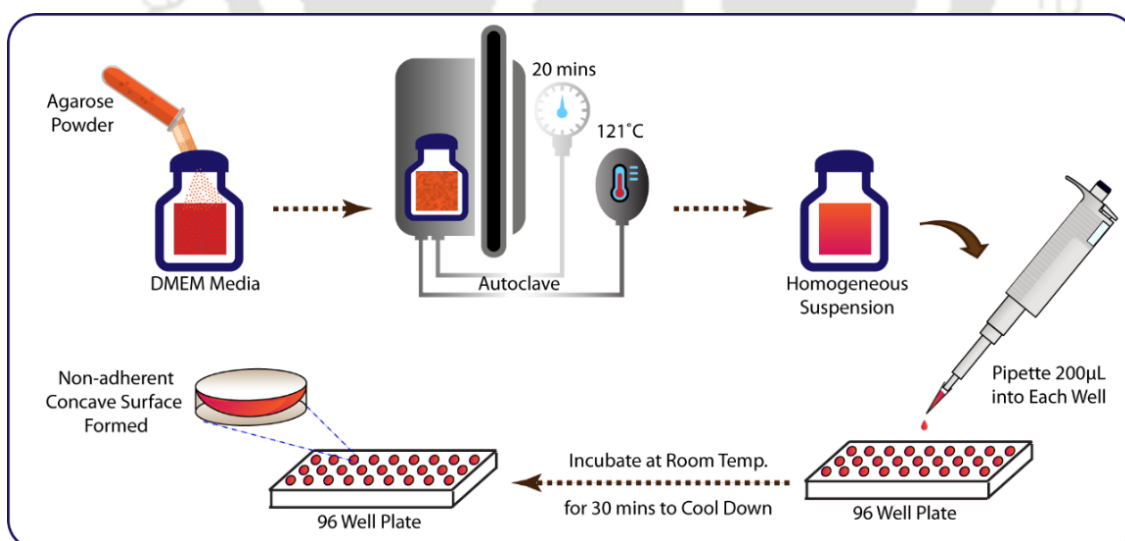
**Scheme 3.1:** Sub culturing of mammalian cell lines

However, for MCF7 cells, the cell suspension after aspiration was moved to a centrifuge tube and spun at approximately 600 xg for 6 minutes. The supernatant was removed, and a fresh growth medium was added to resuspend the cell pellet. From this, sufficient cell suspension aliquots to new culture vessels and held in a static incubator at 37 °C with 5 percent CO<sub>2</sub>.

For cryopreservation, a freezing medium containing fetal bovine serum supplemented with 5% (v/v) DMSO (Maerk) was used. For both the cell lines, the cells were centrifuged at 600 xg for 6 minutes, and the pellet was resuspended in the freezing medium and moved to the cryovial and kept liquid nitrogen for long-term preservation.

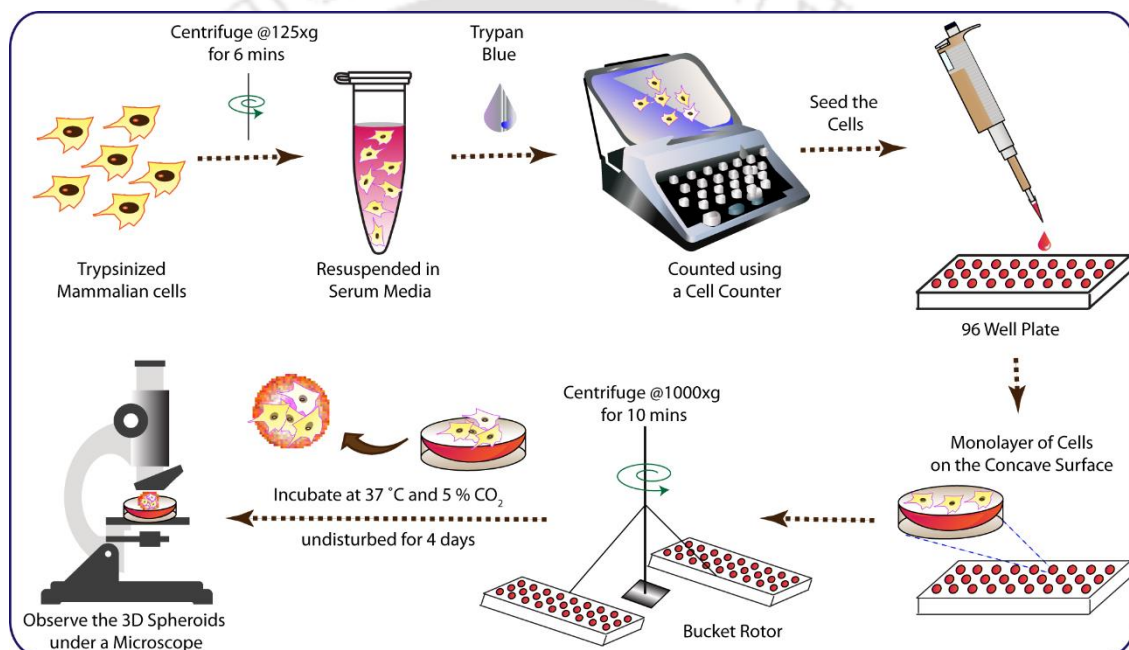
### 3.3. Spheroid Formation

For culturing of spheroids, a special semi solid 3D medium was made using agarose and DMEM. Agarose powder (Sigma Aldrich) was added to serum-free, liquid DMEM media in the proportion of 1% w/v and autoclaved at 121°C for 20 min to form a homogenous suspension. 50 µL of this suspension was pipetted into each well of 96-well plate and left at room temperature for few minutes to allow it to solidify as it cools down, leading to the formation of a non-adherent concave surface (**Scheme 3.2**).



**Scheme 3.2:** Formation of a special semi-solid medium for culturing of 3D spheroids.

In parallel, the cells were trypsinized using a standard method, as mentioned in section 4.2, re-suspended in fresh DMEM media containing 10% FBS and counted using the countess cell counter (Invitrogen). For unit HEK293 and MCF-7 spheroid formation,  $3 \times 10^4$  cells and  $2 \times 10^4$  cells were seeded in each well of the 96-well plate, respectively. This is followed by centrifugation of the 96 well plates in a swing bucket rotor at 1000xg for 10 min and incubation at 37°C and 5% CO<sub>2</sub> to allow undisturbed growth for a period of 4 days for stable spheroid formation. After the incubation period, the spheroids are then visualized using an inverted microscope to ascertain their morphology (**Scheme 3.3**).



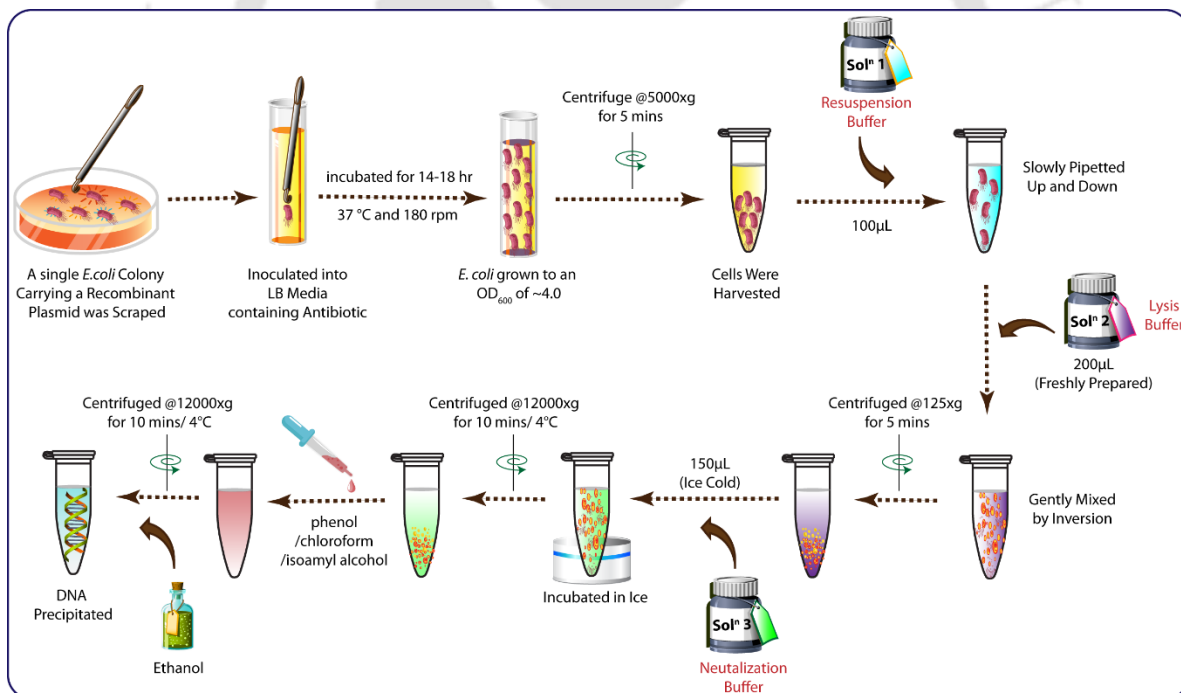
**Scheme 3.3:** Preparation of stable 3D spheroids.

### 3.4. Plasmid DNA Isolation

A test tube containing 5 mL LB media was inoculated with *E.coli* by using a sterile toothpick from the frozen stock and kept at 37 °C and 180 rpm and allowed to grow for 14-16 h. The Plasmid DNA Isolation was carried out using the HiPurA® Plasmid DNA Miniprep Purification Kit (Himedia) using the pre-made reagents provided by the manufacturer. The overnight recombinant *E. coli* culture was collected in a centrifuge tube and spun 3,000-5,000 x g for 5 minutes. The upper supernatant was discarded, and the cells pellet was resuspended in 100 µL of Resuspension solution (HP1) by slowly

pipetting until the cells were completely homogenous. This was followed by the addition of 250  $\mu\text{L}$  of Lysis solution (HP2) for lysis of the cells using an alkaline SDS lysis procedure. The contents were gently mixed by inversion of the tube (4-6 times) for a max of 5 minutes until the mixture became clear and viscous.

Further, 350  $\mu\text{L}$  of Neutralization Solution (HN3) was added to the tube and mixed by gently inverting the tube (4-6 times). This forms white cloudy precipitation, which was removed by centrifugation at 12000  $\times g$  for 15-20 min. The clear supernatant was then loaded onto the spin column and centrifuged at 12000  $\times g$  for a min. The follow-through was discarded, and the spin column was washed with Wash Solution (HPB) and centrifuged at 12000  $\times g$  for 1 min. Subsequently, the column was rewashed by Wash Solution (HPE). The empty column was centrifuged to dry the column. Finally, the plasmid DNA was eluted in 30-50  $\mu\text{L}$  of 10 mM Tris-Cl solution (pH 8.5) and stored in  $-20\text{ }^{\circ}\text{C}$  for further use. (Scheme 3.4).



**Scheme 3.4:** Recombinant Plasmid DNA Isolation

### 3.5. Plasmid Construct

The eukaryotic expression vector pCI-neo was obtained from Promega, Madison, WI. The full-length human CR-1 cDNA insert used in this study was a gift from Dr. D.

Salomon, NIH, USA. In order to obtain different clones, namely pCI-neo-CR-1(full length), pCI-neo- $\Delta$ CR-1(C-terminal truncated) and pCI-neo-EV (Empty vector). Different constructs were inserted into the eukaryotic expression vector by electroporation using a previously standardized protocol (Das et al., 2012). The plasmid vectors are listed in **Table 3.4**. Once the clones for CR-1 were obtained, we directly proceeded for the clone confirmation by colony PCR and restriction digestion.

**Table 3.4:** List of Plasmid Vectors

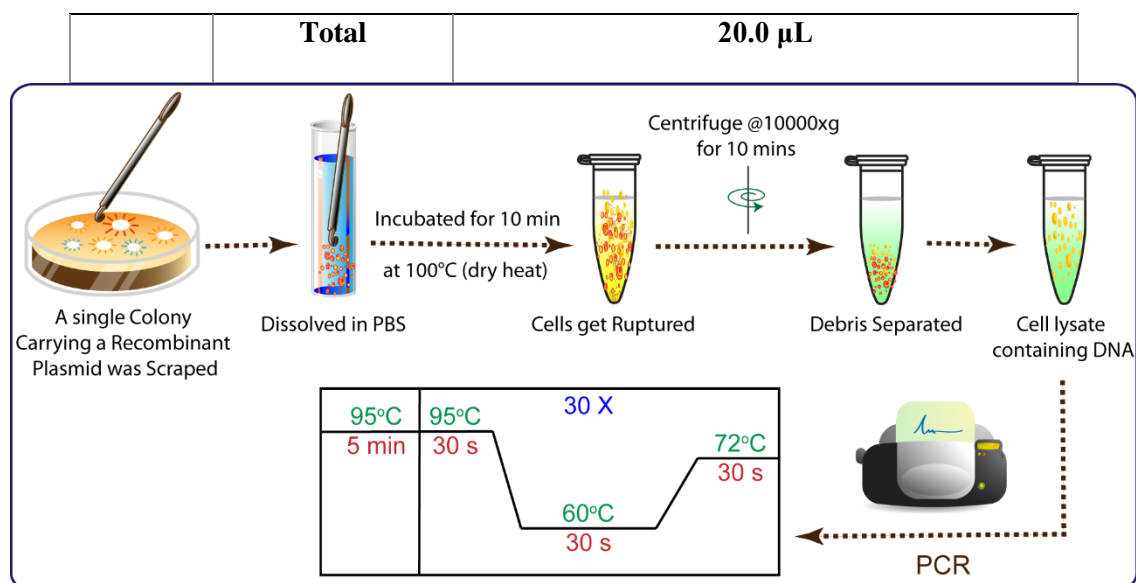
Sl. No.	Name	Use	Promoter	Selection marker	Cloning Site
1.	pCI-neo (Promega)	Mammalian Expression Vector	pCMV	Amp <sup>R</sup> , Neo <sup>R</sup>	Full-length CR1 cloned at EcoRI site
2.	pCI-neo (Promega)	Mammalian Expression Vector	pCMV	Amp <sup>R</sup> , Neo <sup>R</sup>	CR1 $\Delta$ C cloned at XhoI/NotI site

### 3.6. CR-1 Clone Confirmation by Colony PCR

CR-1 clone confirmation by done by Colony PCR. A minuscule amount of bacterial colony was taken and resuspended in PBS to form a homogeneous suspension. The vial was put in a heating block and heated to 100°C. Following this, the suspension was centrifuged at 10,000 rpm for 10 minutes to eliminate cell debris. The supernatant was moved to the new tube, and 1 $\mu$ L was used as a sample template for the reaction. A 20  $\mu$ L PCR reaction was set up (**Table 3.5**), and the cycling conditions were as shown in **Scheme 3.5**. PCR products have been resolved on agarose gel and analyzed for clone validation.

**Table 3.5:** Composition of the Reaction Mixture for Colony PCR

SL. NO.	COMPONENT	CONCENTRATION
1.	Template	1.00 $\mu$ L of Bacterial Colony Lysate
2.	Primer	2.00 $\mu$ L Fwd. +2.00 $\mu$ L Rev.
3.	2x Master Mix	10.00 $\mu$ L
4.	Water	5.0 $\mu$ L



**Scheme 3.5:** Colony PCR Protocol and Cycling Program

### 3.7. CR-1 Clone Confirmation by Restriction Digestion

Recombinant clones were further analyzed by digestion with restriction endonucleases. An aliquot of plasmid DNA ( $\sim 1 \mu\text{g}$ ) was digested overnight with the required amount of NEB Cut Smart restriction endonucleases. pCI-Neo-CR1 was digested by EcoR1, and pCI-Neo- $\Delta$ CR1 was digested by Xho1 and NOT1 according to the conditions specified by the manufacturer (**Table 3.6**). The reaction mixture was kept at 37 °C for 2 h and terminated by heating at 68 °C for 10 min. An aliquot was loaded on a 0.8 % agarose gel and resolved by electrophoresis for analysis of clone confirmation.

**Table 3.6.:** Composition of the Reaction Mixture for Restriction Digestion

SL. NO.	COMPONENT	CONCENTRATION
1.	Plasmid DNA	1.0 $\mu\text{g}$
2.	Cut Smart Restriction Enzyme	1.00 $\mu\text{L}$
3.	Cut Smart Buffer	2.00 $\mu\text{L}$
4.	Water	7.0 $\mu\text{L}$

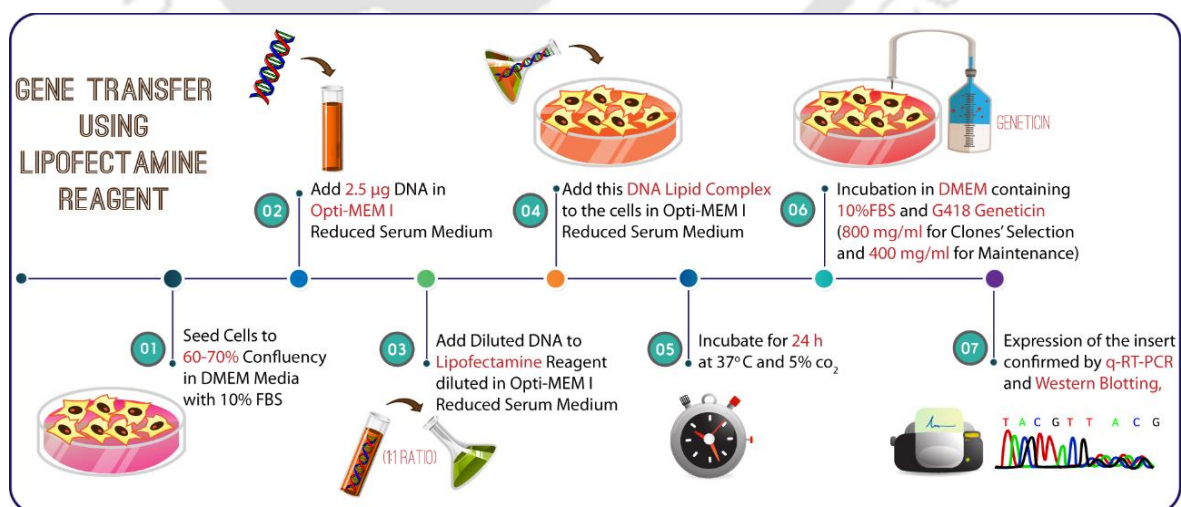
	<b>Total</b>	<b>20.0 <math>\mu</math>L</b>
--	--------------	-------------------------------

### 3.8. Transfection of CR-1 clone Vector Constructs into Mammalian Systems

MCF-7 and HEK293 cell lines were stably transfected with different CR-1 clones, namely pCI-neo-CR-1(full length), pCI-neo- $\Delta$ CR-1(C-terminal truncated) and pCI-neo-EV (Empty vector) (Table 4.5). The gene transfer was achieved using the Lipofectamine Reagent kit (Life Technologies, Inc.). The protocol followed was as follows:

On day 1, cells were trypsinized, counted and seeded in a 6-well plate.  $4 \times 10^4$  cells per well (MCF-7 cells) or  $0.5 - 1.25 \times 10^5$  cells per well (HEK 293 cells) were plated in 2 mL of DMEM medium with 10% FBS. The next day on which the cells reach 60–70% confluence is chosen as the day of transfection. At the same time, for each well, 2.5  $\mu$ g of plasmid DNA and 3.75  $\mu$ L P3000 reagent is diluted in 125  $\mu$ L of Opti-MEM I Reduced serum media without serum in separate Eppendorf tubes for each cell line. **(Scheme 3.6).**

Now for each well, 3.75  $\mu$ L of Lipofectamine (L3000) Reagent is added into the above diluted Opti-MEM: DNA solution in separate Eppendorf tubes, mixed gently and incubated for 10–15 minutes at room temperature to form DNA Lipofectamine complexes. After the 10–15 minutes of incubation is over, the DNA- Lipofectamine complex is added directly to each well containing cells 2 mL of Opti-MEM I reduced serum medium and mixed gently and kept in a CO<sub>2</sub> incubator for 24 h **(Scheme 3.6).**



**Scheme 3.6:** Procedure of Lipofectamine based transfection.

The transfected cells were subjected to selection for stable transfectomas using G418 as a selection marker. After 24 h, the spent media from the cells was flushed gently and replaced with 2 mL of DMEM with 10% serum of bovine origin containing 800 milligrams per mL G418 Geneticin (for clones' selection) (Invitrogen, Life Technologies, Inc.) The media was replenished every 72 h intervals, and in about 4 weeks' selection after transfection, only the drug resistant clones survived and formed visible distinct colonies. The stably transfected cells were picked up using sterile cotton swabs and inoculated into fresh 6 well plates having DMEM containing 10% fetal bovine serum and 400 milligrams per mL G418 Geneticin (for maintenance). CR-1 expression was confirmed by Real-Time PCR and Western blotting on mRNA and protein levels,aa respectively. **(Scheme 3.6).**

### 3.9. RNA Extraction

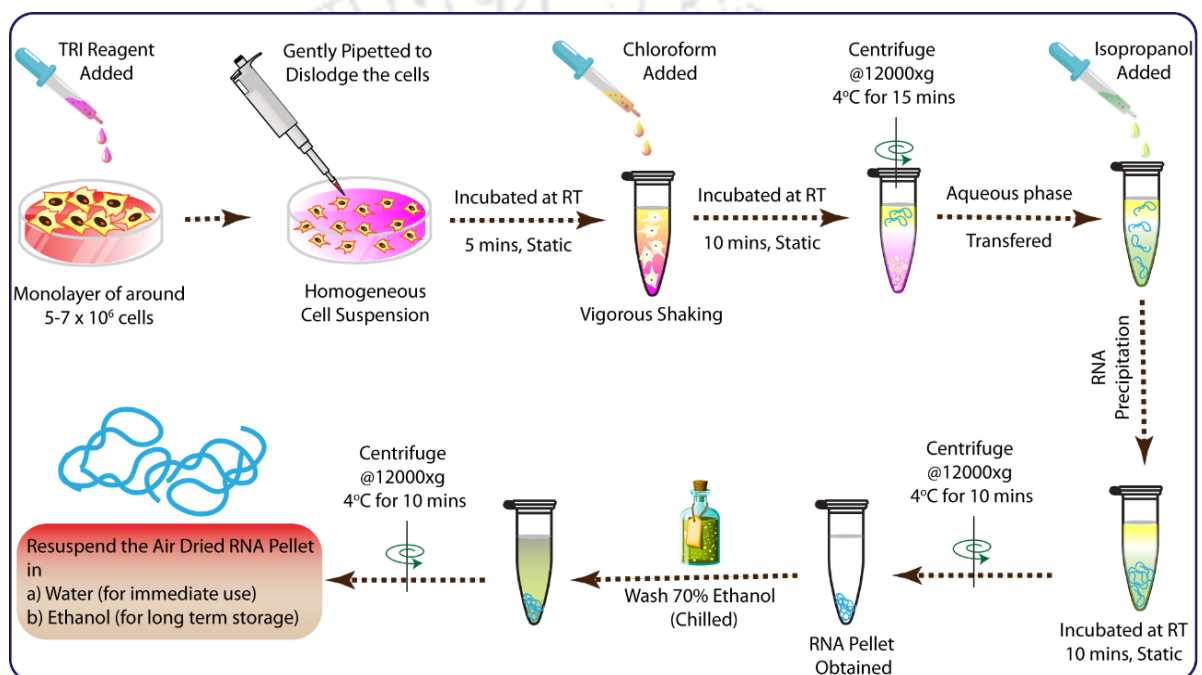
Prior to initiation of the RNA extraction process, all the non-disposable glassware and plastic ware were rinsed thoroughly with 0.1N NaOH/1mM EDTA and then incubated with diethyl pyrocarbonate (DEPC)-treated water overnight at 37 °C, to ensure that they are RNase-free. The treated consumables were autoclaved 30 minutes before use in order to eliminate any trace of DEPC. Total RNA was extracted by TRI reagent (Sigma). 25 cm<sup>2</sup> culture flasks having a monolayer of around 5-7 x 10<sup>6</sup> cells were flushed with 1 mL of TRI reagent.

After the addition of the reagent, it was gently pipetted to dislodge the cells and bring them in suspension to form a homogenous lysate. The cell suspensions were incubated at room temperature under static conditions for 5 minutes to ensure complete dissociation of the nucleoprotein complexes. Then, chloroform (200 µL) was added, and the tube was mixed by vigorous shaking for 30 secs. The sample tubes were subsequently incubated for 10 minutes at room temperature under static conditions. **(Scheme 3.7).**

The tube was then centrifuged at 12,000 g at 4 C for 15 minutes after incubation to achieve phase separation. The upper transparent phase containing the RNA was carefully moved to a new tube and was added to it with 0.5 mL of isopropanol to induce RNA precipitation. This suspension was again incubated for 10 min at room temperature with occasional mixing by inversion. The sample was now centrifuged at 12,000g for 10 min

at 4 °C to separate the supernatant, which was discarded finally and obtain the RNA in the pellet form (**Scheme 3.7**).

This RNA pellet was washed gently with 1mL of 75 % chilled ethanol and again subjected to centrifugation at 12,000 g for 10 min at 4 °C. The RNA pellet was either air-dried and dissolved in a suitable amount of sterile water and stored at –20 °C for immediate use or was suspended in ethanol for long-term storage at –70 °C (**Scheme 3.7**).



**Scheme 3.7:** Total RNA Extraction by TRIZOL Method

### 3.10. Removal of Genomic DNA Contamination from Isolated RNA

To get rid of the genomic DNA contamination that might coexist with the eluted RNA, each RNA sample was subjected to DNase treatment using Turbo DNase (Thermo Fisher Scientific, Waltham, MA, USA) according to the manufacturer's protocol with a few modifications. TURBO™ DNase is a higher catalytic efficiency genetically engineered type of bovine DNase I than traditional DNase I.

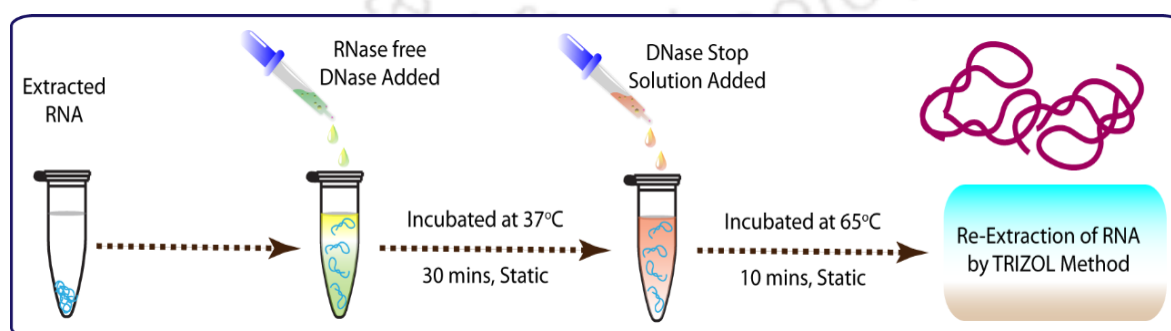
One unit of this DNase is known as the amount of enzyme needed to fully degrade 1 µg of DNA at 37 C in 10 minutes and is equivalent to 0.04 Kunitz units. DNase I is an endonuclease hydrolyzing the associations of phosphodiester generating

oligonucleotides with 5' phosphate and a free 3' hydroxyl group (Kunitz, 1950). DNase I can be used to cut chromatin, RNA: DNA hybrids, and single- and double-stranded DNA. The composition of the reaction mix was as given in **Table 3.7**.

**Table 3.7:** Composition of the Reaction Mixture for DNase treatment

SL. NO.	COMPONENT	CONCENTRATION
1.	RNA	50 -100 µg
2.	RNase-Free DNase 10X Reaction Buffer	5.00 µL
3.	RNase-Free DNase (1,000 U/mL)	5.00 µL
4.	Nuclease-free water to a final volume of	50.0 µL

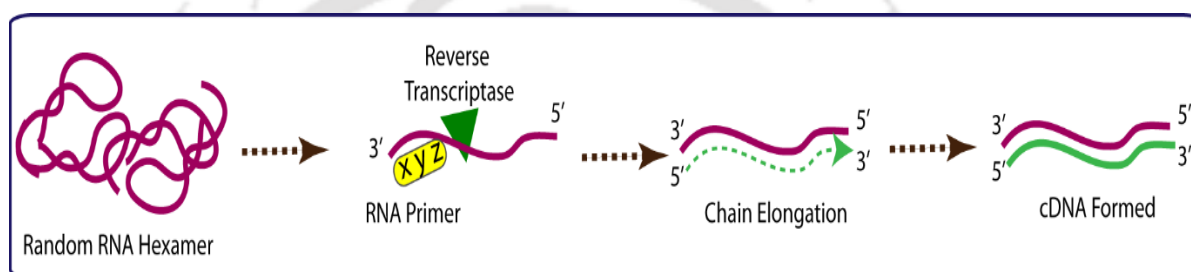
The reaction mixture was incubated under static conditions for 30 minutes at 37 °C. To end the reaction, 1µl of DNase Stop Solution has now been added, and the vial has been incubated at 65°C for 10 minutes to inactivate the DNase. After that, by repeating the same procedure as defined in the previous section, the RNA was re-extracted from the suspension using the TRI reagent. RNA samples free from DNA contamination were dissolved in nuclease-free water, and the RNA yield was quantified using IMPLEN NanoPhotometer® NP80. The RNA sample was diluted in water prior to RT-PCR to achieve a concentration that is compatible with this application (**Scheme 3.8**).



**Scheme 3.8:** Schematic illustrating DNase Treatment of RNA Samples Prior to RT-PCR.

### 3.11. cDNA Synthesis

This reaction was carried out to generate high yields of full-length cDNA from the extracted RNA using the Thermo Scientific Verso cDNA kit. Verso Reverse Transcriptase is an RNA-dependent DNA polymerase with slightly attenuated activity of RNase H. It is capable of synthesizing long strands of cDNA up to 11 kb at temperatures between 42 °C and 57 °C. Around 1 µg of total RNA was used for reverse transcription (Scheme 3.9). For a 20 µL of reaction, the sample mix was prepared as given in Table 3.8 and was subjected to the reverse transcription cycling program as shown in Table 3.9.



**Scheme 3.9:** Schematic illustrating the cDNA Synthesis Concept

**Table 3.8:** Reaction Mix Preparation for cDNA Synthesis

SL. NO.	COMPONENT	VOLUME	FINAL CONCENTRATION
1.	5X cDNA synthesis buffer	4 µL	1X
2.	dNTP Mix	2 µL	500 µM each
3.	RNA Primer*	1 µL	-
4.	RT Enhancer	1 µL	-
5.	Verso Enzyme Mix	1 µL	-
6.	Template (RNA)	1-5 µL	1 µg
7.	Water, nuclease-free	To 20 µL	-

**Table 3.9:** Reverse Transcription Cycling Program for cDNA Synthesis

SL. NO.	STEP	TEMPERATURE	TIME

1.	Random Hexamer Priming	25°C	10 min
2.	cDNA synthesis*	42°C	60 min
a3.	Inactivation	95°C	2 min

### 3.12. Quantitative Real-Time PCR

Power Track SYBR Green Master Mix (Applied Bio Systems™, Thermo Fisher Scientific) was used to perform qRT-PCR, triplicates were used for each sample, and 18s rRNA and GAPDH were used as endogenous control. 1–10 ng of cDNA was taken as the template per reaction depending on the yield. The reaction mix for the qRT-PCR was setup as depicted in **Table 3.10**.

**Table 3.10:** Reaction Mix Preparation for qRT-PCR

SL. NO.	COMPONENT	VOLUME
1.	Power Track™ SYBR™ Green Master Mix	10.0 µL
2.	Template (cDNA)	1.0 µL (from 1.0 ng/µL)
3.	Forward Primer	2.0 µL
4.	Reverse Primer	2.0 µL
5.	Water, nuclease-free	5.0 µL
	<b>Final Volume</b>	<b>20.0 µL</b>

No-template control (NTC) reactions containing all of the reaction components except for the sample (replaced with 1 µL water) was also setup along with the experimental triplicates to identify PCR contamination. The cycling conditions were as mentioned in **Table 3.11**. Primers used in this experiment are listed in **Appendix table A2**.

After completion of the reaction, the baseline and threshold cycles ( $C_t$ ) for the amplification curves were determined using the third-party instrument software (LinregPCR). Nonspecific amplification was also checked by using the melt curves generated at the end of the reaction. Relative quantitation was performed wherein the target was compared to an internal standard, using the comparative  $2^{-\Delta\Delta C_t}$  method.

**Table 3.11:** Standard cycling conditions are recommended for cDNA templates for qRT-PCR.

STEP	TEMPERATURE	DURATION	CYCLES
Enzyme Activation	95°C	2 min	1
Denaturation	95°C	30 sec	40
Annealing/Extension	95°C	1 min	
Melting	55 - 99°C	45 min (1°/min)	-

### 3.13. Protein Isolation

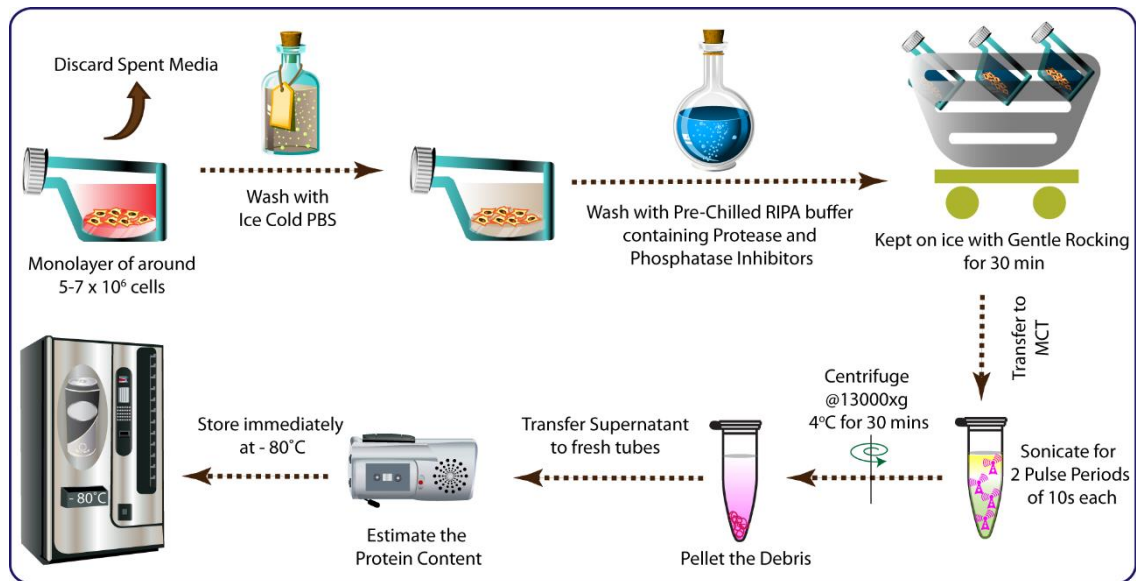
Using the RIPA (Radio immunoprecipitation assay), buffer isolation of total protein from mammalian cell lines was carried out, the composition of which is given in the appendix section. The media was discarded from the T25 culture flask, and cells were washed to remove the residual media with 2 mL of ice-cold PBS. 300 uL of pre-chilled RIPA buffer containing 1:10 ratio of protease inhibitor cocktail (Sigma Aldrich) and other freshly prepared phosphatase inhibitors like sodium fluoride (50 mM), PMSF (1 mM), sodium orthovanadate (1 mM), and EDTA (1 mM) was added to was added to each T25 flask. The composition of protease inhibitor cocktail was given in **Table 3.12**.

Now the flask was kept on ice in gentle rocking conditions for 30 min to allow the lysis of cells for the release of protein. After incubation on ice, the cells were scrapped and transferred to an MCT and sonicated in 2 pulse periods of 10s each. Following this, the

cell lysate was centrifuged for 30 min at 13,000 rpm, 4 °C, in order to remove the cell debris. The clear supernatant was transferred to multiple new tubes in small aliquots and stored immediately at -80 °C (**Scheme 3.10**). Concentrations of the protein were estimated by Lowry's Method for further experiments.

**Table 3.12:** *Specific properties of the components of the protease inhibitor cocktail :*

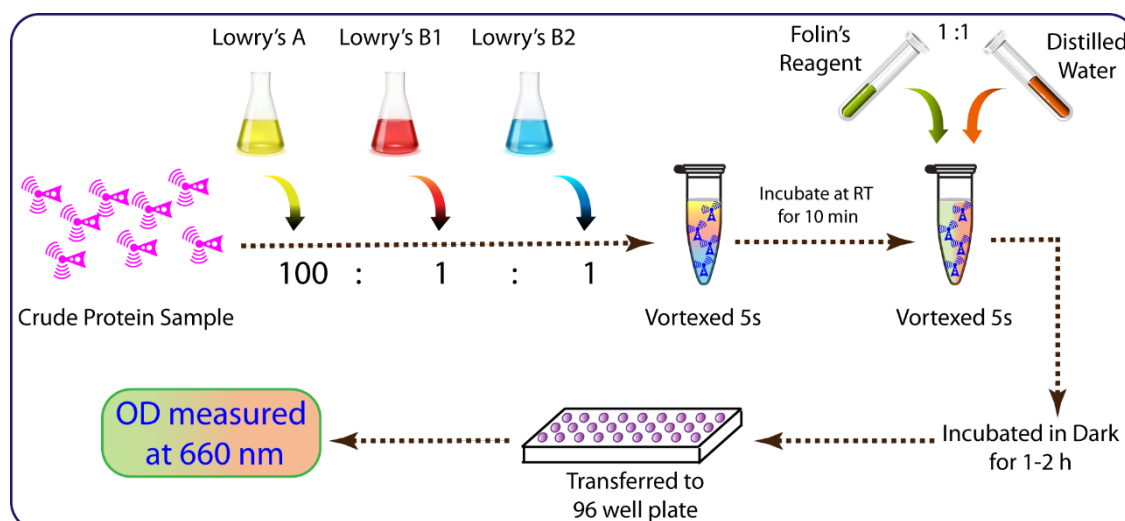
SL. NO.	COMPONENT	INHIBITOR OF	EXAMPLES
1.	AEBSF – [4-(2-Aminoethyl) Benzenesulfonyl Fluoride Hydrochloride]	Serine Proteases	Trypsin, Chymotrypsin, Plasmin, Kallikrein and Thrombin
2.	Aprotinin	Serine Proteases	Trypsin, Chymotrypsin, Plasmin, and Kallikrein; Human Leukocyte Elastase, But Not Pancreatic Elastase.
3.	Bestatin Hydrochloride	Amino peptidases	Leucine Amino peptidase and Alanyl Amino peptidase.1-4
4.	E-64 – [N-(Trans-Epoxy succinyl)-L-Leucine 4-Guanidinobutylamide]	Cysteine Proteases	Calpain, Papain, Cathepsin B, and Cathepsin L.
5.	Leupeptin Hemisulfate Salt	Both Serine And Cysteine Proteases	Plasmin, Trypsin, Papain, and Cathepsin B.
6.	Pepstatin A	Acid Proteases	Pepsin, Renin and Cathepsin D, and Many Microbial Aspartic Proteases



**Scheme 3.10:** Schematic illustrating the protein isolation protocol

### 3.14. Protein Estimation by Lowry' Method

The concentration of protein samples previously isolated by RIPA buffer was estimated according to Lowry's method with BSA protein as a standard. 200  $\mu\text{L}$  of diluted crude protein sample was mixed with 500  $\mu\text{L}$  of freshly prepared complex forming reagents composed of Lowry's A (2%  $\text{Na}_2\text{CO}_3$  in 0.1 N NaOH) + Lowry's B1 (2% potassium sodium tartrate) + Lowry's B2 (1.0%  $\text{CuSO}_4 \cdot 5\text{H}_2\text{O}$ ) in the ratio of 100:1:1. The reaction tubes were vortexed and kept at room temperature for 10 min. In the reaction mixture, 50  $\mu\text{L}$  of the freshly prepared diluted Folin reagent with distilled water (1:1) was applied and vortexed for 5 s. Then this reaction mixture was incubated for 1-2 h at room temperature in the dark. After incubation, 200  $\mu\text{L}$  of the reaction mixture of each sample was transferred to a 96-well plate, and the optical density was measured at 660 nm (**Scheme 3.11**).



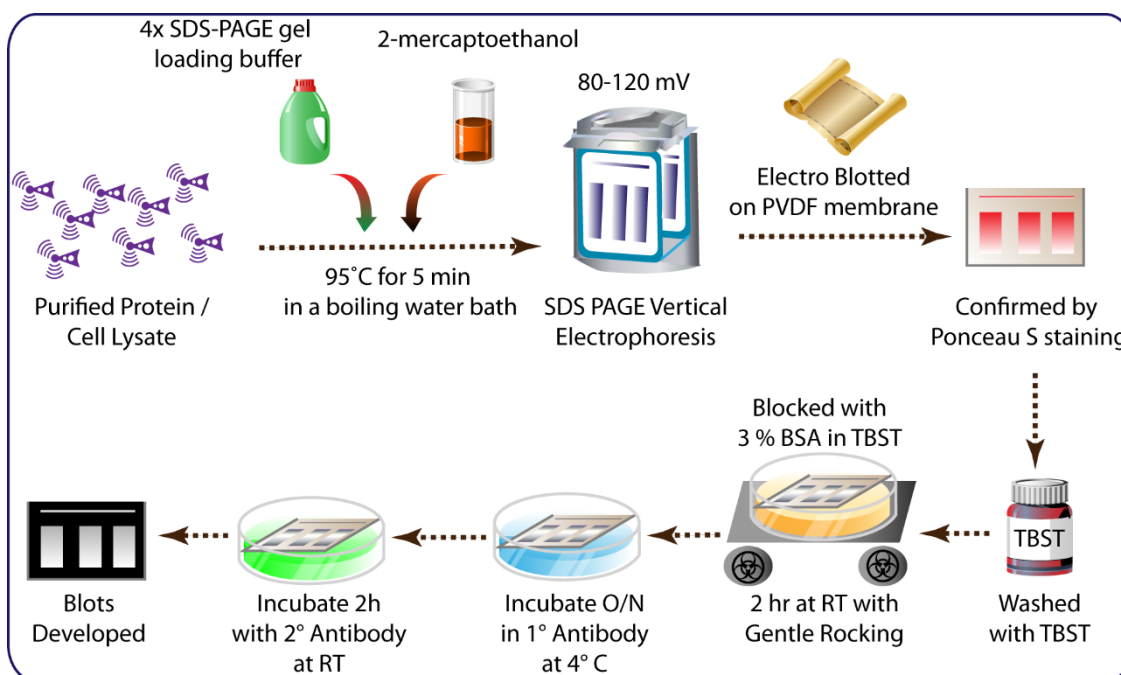
**Scheme 3.11:** Schematic illustrating the Protein Estimation by Lowry's method

### 3.15. SDS Page and Western Blotting

Western Blot was performed to analyze the protein level expression. First of all, the necessary amount of purified protein or cell lysate was mixed with a 4x SDS-PAGE gel loading buffer with a reduction agent (2-mercaptoethanol) and heated at 95°C for 5 min in a boiling water bath. The denatured protein samples along with standard SDS PAGE protein markers were loaded on the SDS PAGE apparatus, and electrophoresis was carried out using 5 % stacking and 8-12 % separating gels at the voltages of 80mV and 100-120mV for stacking and separating gel, respectively, in volt vertical electrophoresis system (G.E Healthcare).

Concentrated cell extract resolved on the 8-12 % SDS-PAGE gel was subsequently electro blotted on PVDF membrane (Millipore) by using the wet transfer module at 25 volts for 3 hr. Transfer of proteins on membrane was confirmed by Ponceau S staining, and the membrane was rinsed twice with TBST buffer to remove excess Ponceau S stain. The blot was later transferred in blocking solution (with 3 % BSA TBST) and then kept at rocker for 2 h at room temperature. The washed and blocked membranes were then exposed to a particular dilution of the primary antibody as required in 3 % BSA in TBST overnight in the cold room (2-8 °C). The next day, the blots were washed with TBST buffer thrice to remove unbound primary antibody followed by the addition of secondary antibody, which is coupled with horse radish peroxidase (HRP) and gently rocked at

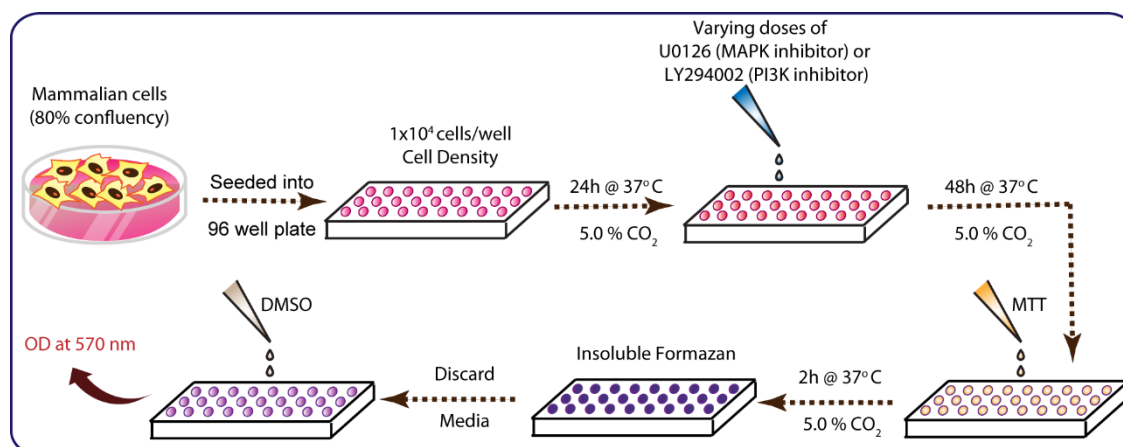
room temperature for 2 h. Different antibodies used in experiments are listed in **Appendix Table. A1**. After incubation, the blots were washed again thrice to remove the unbound secondary antibody. Finally, to develop the blots, a chemiluminescence based reagent was used (Super Signal West Dura, Thermo Scientific), and an image was taken using a gel documentation system (Bio-Rad gel documentation system) (**Scheme 3.12**). The images were processed using the inbuilt Image Lab software.



**Scheme 3.12:** Schematic illustrating the Protocol for western blotting

### 3.16. MTT Assay for Cytotoxicity

To determine the cytotoxicity of the inhibitors U0126 (MAPK inhibitor, sigma) and LY294002 (PI3K inhibitor, sigma) used in the study, MTT based cytotoxicity assay was done. Cells were seeded at  $1 \times 10^4$  cells in each well of 96-well plate and kept to grow for a day. The cells were then treated in triplicate with different doses of both the inhibitors in separate sets for 48 h. After completion of treatment, MTT was added to each well after diluting in fresh media. The sample plate was then kept in the CO<sub>2</sub> incubator for 2 h. Interaction of MTT with the viable cells results in the formation of violet Formazan crystals. Finally, to dissolve the Formazan crystals, DMSO was used, and optical density (OD) was measured at 570 nm to estimate viability. (**Scheme 3.13**). For each dose, 5 replicates were taken, and average OD was used for the calculation of the viability.

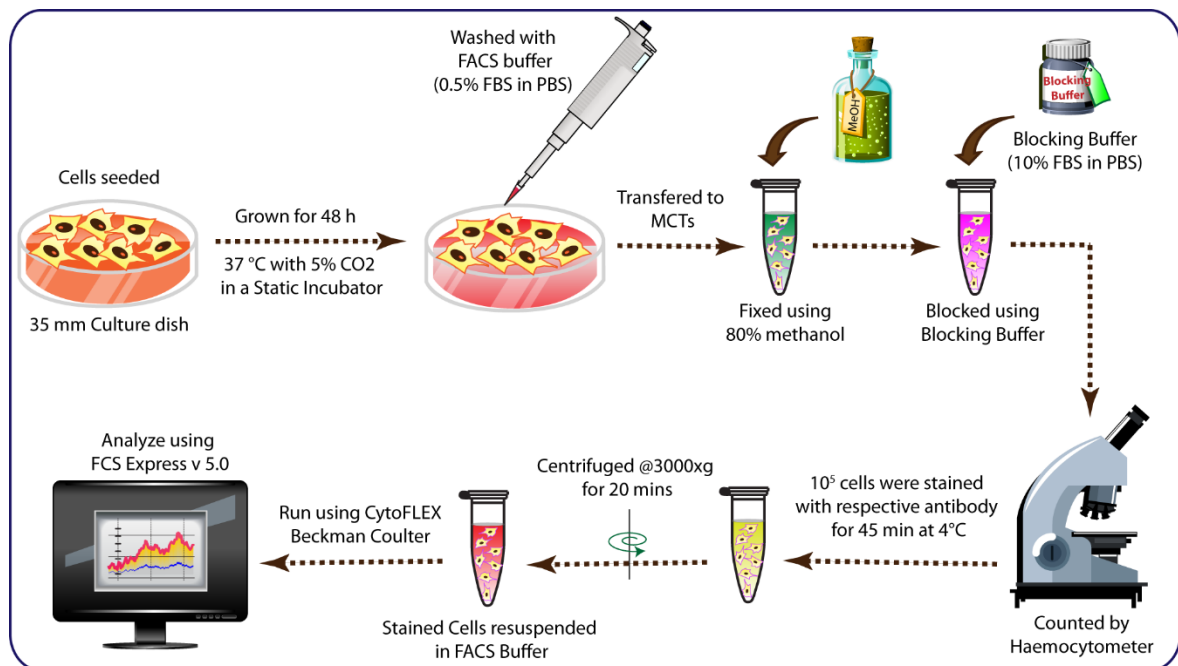


**Scheme 3.13:** Schematic illustrating the protocol of MTT assay for cytotoxicity assessment.

### 3.17. Flow Cytometry

For the detection of cell surface proteins, fluorophore tagged antibodies were used. Cells were seeded in a 35 mm dish and kept in the CO<sub>2</sub> incubator for 48 h. The attached cells were washed with FACS buffer (0.5% FBS in PBS) and removed by adding non-enzymatic buffer.

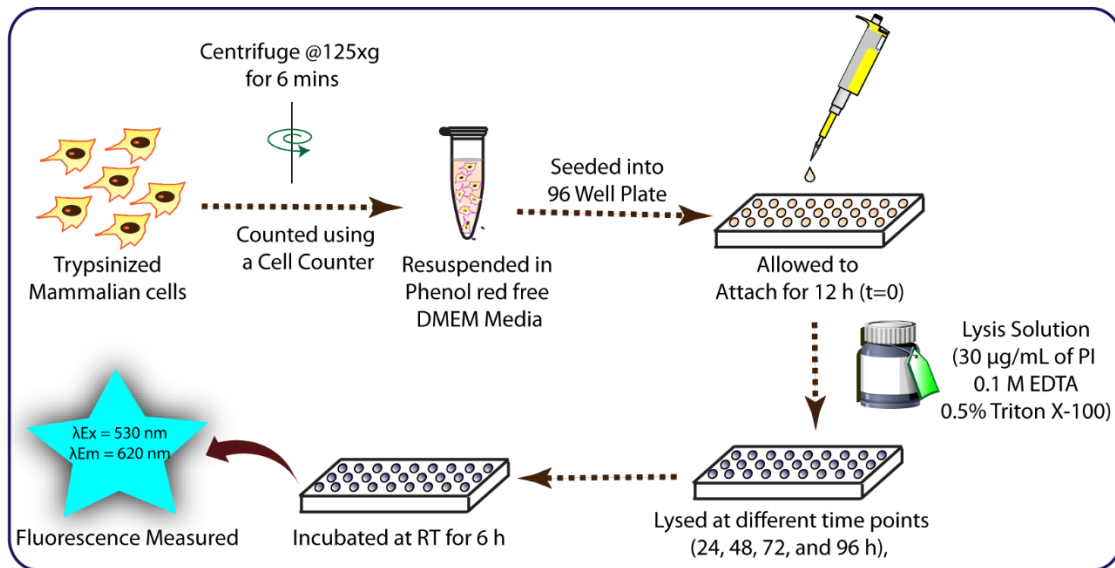
The Cells were fixed by using 80% methanol (final concentration) and kept for 20 min at -20°C. After fixation, the cells were washed 2 times with FACS buffer and incubated in blocking buffer (10% FBS in PBS) for 1 hr. Finally, counted by hemocytometer and  $10^5$  cells were stained with the respective antibody at 4 °C for 45 min, centrifuged at 3000 rpm for 20 min to remove excess antibody. Stained cells were re-suspended in FACS buffer were analysed using CytoFLEX (Beckman Coulter, Brea, CA, USA). The data was analyzed using FCS Express v 5.0 (**Scheme 3.14**).



**Scheme 3.14:** Schematic illustrating the Flow Cytometry protocol

### 3.18. Cell Proliferation Assay

To compare the proliferation rate between CR-1 transfected and EV-transfected cells, we used a Propidium iodide (PI) based cell proliferation assay (Dengler et al., 1995; Wan et al., 1994a). The cells were seeded at equal density in 96-well plates in Phenol red free DMEM media (Himedia) and allowed to attach for 12 h ( $t=0$ ). Further, the cells were allowed to grow and lysed by adding lysis solution (final concentration: 30  $\mu\text{g/mL}$  of PI, 0.5% Triton X-100, and 0.1 M EDTA) directly in the well, at different time points (from day 1 to 4), and kept for 6 h at room temperature. Finally, the fluorescence emission was measured at 530 nm excitation and 620 nm emission wavelength for each time point. The total number of cells present in each well at different time point was detected based on fluorescence intensity as depicted in **Scheme 3.15**.



**Scheme 3.15.:** Schematic illustrating the protocol of Cell Proliferation assay





## **RESULTS And DISCUSSION**

Human Cripto-1 is a member of the Epidermal Growth Factor-Cripto-FRL-1-cryptic (EGF-CFC) family of proteins, promoting cell proliferation, differentiation, and angiogenesis in the fetus (Bianco et al. 2010). Several signalling pathways critical for early embryonic development and regulating stem cell proliferation and differentiation have been shown to cross-talk with Cripto-1 (Bianco et al. 2005) (Bianco et al. 2010). Cripto-1 positive cells are found to regulate the expression of stem-cell-related genes in patient-derived tumour spheroids and exhibited increased clonogenic capacity (Francescangeli et al., 2015). In another study, the silencing of Cripto-1 results in the downregulation of well-established stemness markers like CD24, CD133, NANOG, NOTCH1, OCT4, SOX2 and chemoresistance-related genes ABCB1, ABCG2, ABCC6 in hepatocellular carcinoma (R. C. Lo et al., 2018). Conversely, under hypoxic conditions, Hypoxia-inducible factor-1 $\alpha$  (HIF-1 $\alpha$ ) was shown to induce the expression of OCT4, Nanog and SOX2 in ME180 cells (Mathieu et al., 2011). At the same, Qiang et al. 2012 have also depicted the role of HIF-1 $\alpha$  in the enrichment of GSC in Glioblastoma cells. Cripto-1 also plays an essential role in mES differentiation into Cardiomyocytes in the presence of HIF-1 $\alpha$  (Caterina Bianco et al., 2009)

In the present study, we hypothesize that under hypoxia, HIF-1 $\alpha$  interacts with cripto-1 by binding in its promoter region, and cripto-1 is the direct regulator of CSCs maintenance and chemoresistance related genes. To further our study, we used CoCl<sub>2</sub> (a chemical inducer of hypoxia) (Zhang et al., 2014) and 3D spheroid (Wartenberg et al., 2003) as two positive models for HIF-1 $\alpha$  whereas, recombinant CR-1 protein/TGF- $\beta$  (Loying et al., 2015) and Cripto-1 (CR-1) overexpressed system were used as positive models for CR-1. The human embryonic kidney cell line (HEK293) and Human embryonal carcinoma cell line (NTERA2) were used to explore the embryonic stem cell markers. In contrast, the Human Breast cancer cell line (MCF-7) was used to study cancer stem cell markers.

Cripto-1 is known to induce its own expression via ALK4/SMAD2/3 pathway in U-87MG cells via positive forward feed (P Loying et al., 2015). However, the expression of CR-1 does not increase after a certain level, indicating a possible negative stimulus within the cellular system. Hence, we hypothesize that the functioning of canonical oncogenic pathways, i.e., MAPK and PI3K pathways, might negatively impact the expression of CR-1. To clarify this, we blocked the MAPK and PI3K pathways by using

chemical inhibitors and check their effect on the expression of CR-1. To induce the CR-1 expression, we used TGF- $\beta$ , which is known to increase the expression of CR-1 (Shukla et al., 2008)

#### 4.1. Upregulation of CR-1 Expression by TGF- $\beta$ :

It has been established previously that TGF- $\beta$  induces CR-1 expression (Shukla et al., 2008). However, we further validated the previous finding in our cellular system. In this regard,  $4 \times 10^5$  NTERA-2 cells were seeded in a T-25 flask and allowed to grow for 24 h in DMEM media supplemented with 10% FBS. Later, the cells were serum-starved for 12 h in optimum media followed by treatment with TGF- $\beta$  for different concentration-dependent (10, 15, 20 ng/mL for 24 h) (Figure 4.1.A) and different time-dependent manner (10 ng/mL for 12, 24, 36 and 48 h) (Figure 4.1.B) in fresh optimum media.

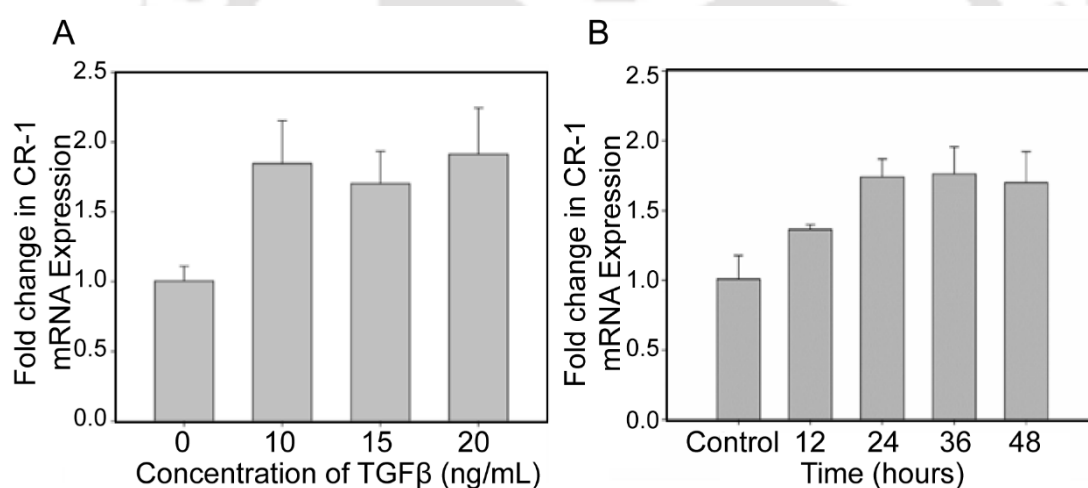


**Figure 4.1.** Upregulation of CR-1 expression by TGF- $\beta$  in NTERA-2 cell line analyzed by Real-Time PCR: A) different concentration of TGF- $\beta$  for 24 h and B) Treatment of 10 ng/mL of TGF- $\beta$  at different time points. Data represented are the mean of a triplicate sample, and the analysis was performed by using Kruskal-Wallis analysis of variance. The fold in the expression of CR-1 was statistically significant ( $p < 0.05$ ).

The samples were collected, and the CR-1 expression was analyzed using Real-time quantitative PCR. We observed a significant upregulation of CR-1 expression in treated

cells compared to untreated cells. Based on these experiments, the treatment dose of 10 ng/mL of TGF- $\beta$  for 24 h was chosen for further investigations (**Figure 4.2.A**).

Further, we checked the levels of TGF- $\beta$  induced CR-1 expression on protein level by flow cytometry (**Figure 4.2.B**). A significant shift in the histogram peak of TGF- $\beta$  treated cells stained with Phycoerythrin conjugated CR-1 antibody was observed. This implies that there was a substantial upregulation of protein was observed on TGF- $\beta$  treatment.

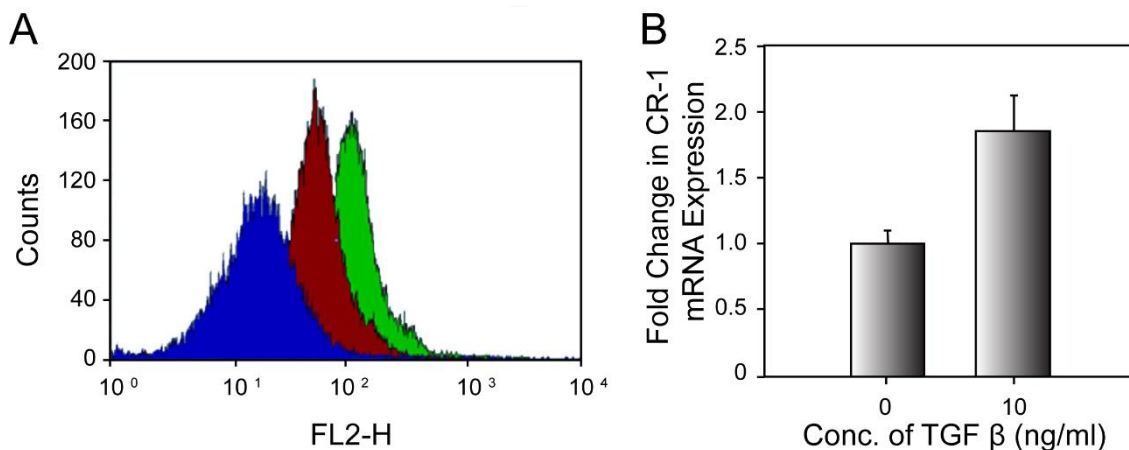


**Figure 4.2.** Upregulation of CR-1 expression by TGF- $\beta$  in NTERA-2 cell line: A) Protein level expression of CR-1 measured by Flow cytometer on treatment with 10 ng/mL of TGF- $\beta$  for 24 h in serum-free optimum media (colour code: green- treated stained, red-untreated stained and blue-untreated unstained) and B) Real-Time PCR based mRNA expression of CR-1 on treatment with 10 ng/mL of TGF- $\beta$ . 18s rRNA was used as an endogenous control. Data represented are the mean of a triplicate sample, and the analysis was performed using the Mann-Whitney U test. The fold in the expression of all the genes was statistically significant ( $p < 0.05$ ).

#### 4.2. Expression of CR-1 on MAPK and PI3K Pathway Inhibition:

Cripto-1 is known to autoregulate its expression by positive feedback circuit via ALK4/SMAD2/3 pathway (P Loyal et al., 2015). This study encouraged us to check whether either the MAPK pathway or PI3K pathway interact with Alk4/SMAD2/3 mediated CR-1 expression, which hinders the positive forward loop of CR-1. To verify this, we used U0126 which blocks the MAPK pathway by selectively inhibiting the intermediate molecule MEK1/2, whereas LY294002 was used to block the PI3K pathway inhibits PI3K itself. Before proceeding with the experiment, the inhibitors' cytotoxicity to NTERA-2 cells was determined using the MTT assay. The cells were treated with

different doses of inhibitors for 24 h in serum-free DMEM media (**Figure 4.3**). The doses at which the percentage cell viability was found to be more than 70% were selected for further experimentation. To understand the impact of MAPK and PI3K pathway on the expression of CR-1, NTERA-2 cells were treated with different doses of MAPK (U0126) and PI3K (LY294002) inhibitors, and the expression of CR-1 was quantified by Real-Time PCR. As shown in **Figure 4.4.A**, at lower doses (1  $\mu\text{M}$  and 5  $\mu\text{M}$ ) of U0126, the expression of CR-1 remains near to 1 fold or unchanged. However, at higher doses (10  $\mu\text{M}$  and 15  $\mu\text{M}$ ), the CR-1 expression gets significantly downregulated to 0.6 to 0.5 fold.

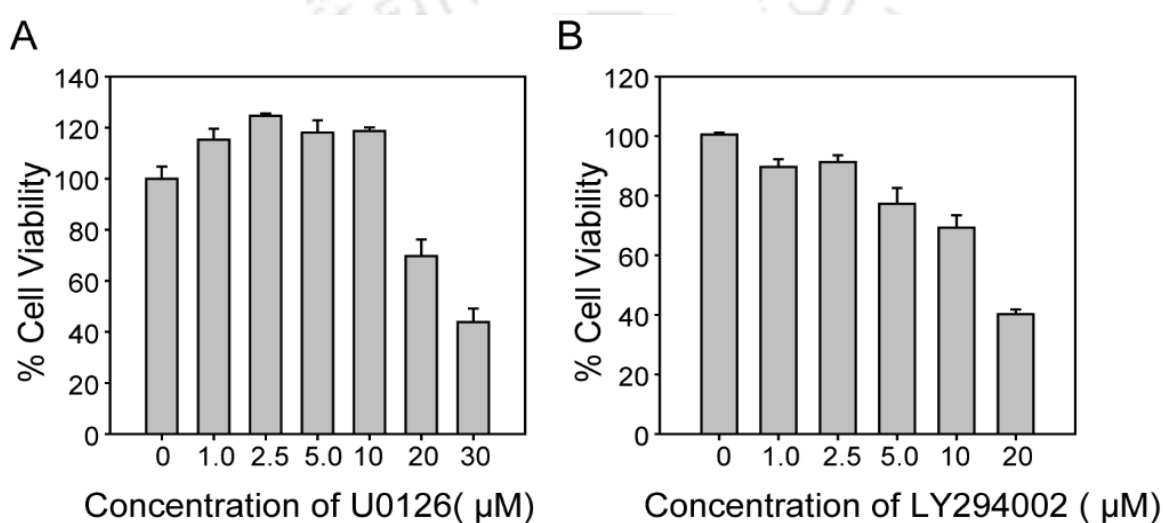


**Figure 4.3.** Cell viability of NTERA-2 cells treated with different doses of (A) U0126 and (B) LY294002. Cells were treated for 24 h in serum-free optimem media, and cell viability was measured by MTT assays.

Similarly, on treatment with LY294002, the expression of CR-1 remains unchanged or near to 1 fold. However, as shown in **Figure 4.4.B**, at the highest dose (20  $\mu\text{M}$ ), CR-1 expression was found to be downregulated to 0.5 fold. This may be due to higher cell death at 20  $\mu\text{M}$  dose, which was shown to reduce cell viability to ~40% in **Figure 4.3.B**. This data suggests that on complete blockage of MAPK and PI3K pathway, CR-1 expression also gets inhibited. This implies that the MAPK and PI3K pathways do not hinder the ALK4/SMAD2/3 mediated CR-1 expression. As both the MAPK and PI3K inhibitor, at a high dose, have reduced expression of CR-1, one may consider that there exists some positive regulation of expression of CR-1 by these two pathways.

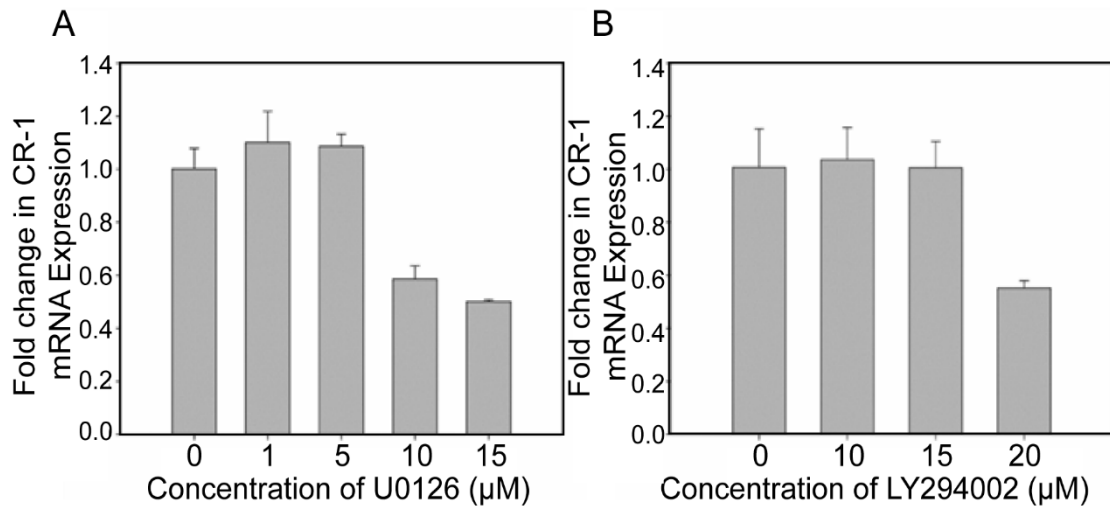


**Figure 4.4.** Expression of CR-1 on treatment with different doses of both the inhibitors: A) U0126 and B) LY294002. NTERA-2 cells were treated in serum-free optemem media for 24 h, and expression of CR-1 was quantified by Real-Time PCR. 18s rRNA was used as an endogenous control. Data represented are the mean of a triplicate sample, and the analysis was performed by using Kruskal-Wallis analysis of variance. The fold in the expression of CR-1 was statistically significant ( $p < 0.05$ ).

#### 4.3. TGF- $\beta$ Induced CR-1 Expression on MAPK & PI3K Pathway Blockage:

Our previous data depicted that TGF- $\beta$  was able to induce the expression of CR-1 in NTERA-2 cells, whereas, on blockage of the MAPK and PI3K pathways, the CR-1 expression gets downregulated. We went ahead to perform another experiment to understand the effect of TGF- $\beta$  on CR-1 expression in the presence of MAPK and PI3K pathway inhibitors. As observed in **Figure 4.5.A.**, the treatment with 10 ng/mL of TGF- $\beta$  alone for 24 h caused upregulation in the CR-1 expression by 2.4 fold, whereas on the contrary 24 h treatment with U0126 (15  $\mu$ M) caused downregulation of expression. However, on treatment with TGF- $\beta$  (10 ng/mL) combined with U0126 (15  $\mu$ M) for 24 h, downregulation in CR-1 expression was observed. Similarly, as shown in **Figure 4.5.B.**, varying doses of TGF- $\beta$  (10 and 15 ng/mL) exert the upregulation of CR-1 expression. In contrast, varying LY294002 (10 and 15  $\mu$ M) doses showed no change in CR-1 expression. However, the treatment of TGF- $\beta$  in combination with LY294002 blocks the TGF- $\beta$  induced CR-1 expression, which suggests the interaction of AKT and TGF- $\beta$ /ALK4/SMAD2/3 pathway.

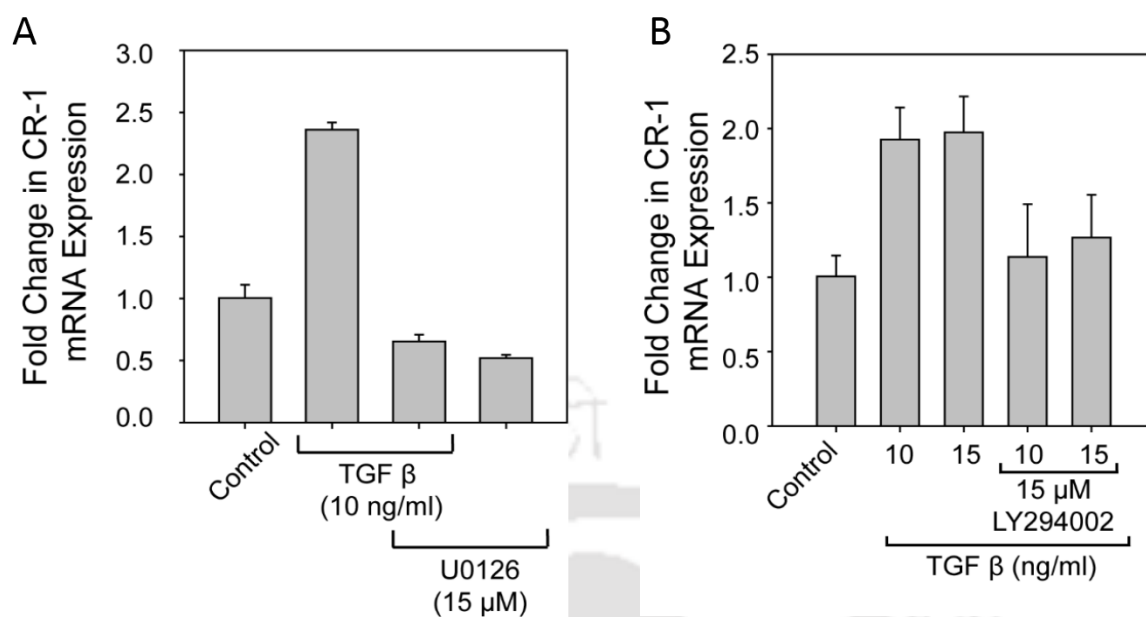


**Figure 4.5.** Expression of CR-1 on treatment with both the inhibitors in the presence or absence of TGF- $\beta$ : A) U0126 combined with TGF- $\beta$  and B) LY294002 combined with TGF- $\beta$ . NTERA-2 cells were treated in serum-free optemem media for 24 h, and the expression of CR-1 was quantified by Real-Time PCR. 18s rRNA was used as an endogenous control. Data represented are the mean of a triplicate sample, and the analysis was performed by using Kruskal-Wallis analysis of variance. The fold in the expression of CR-1 was statistically significant ( $p < 0.05$ ).

Altogether, we observed that the MAPK pathway blockage leads to downregulation of CR-1 expression while PI3K pathway inhibition hinders the TGF- $\beta$  induced CR-1 expression. Also, TGF- $\beta$  was unable to increase the expression of CR-1 in the presence of MAPK and PI3K inhibitors. The present data indicate that TGF- $\beta$ /ALK4/SMAD2/3 mediated CR-1 expression shows possible crosstalk between the MAPK/AKT and the TGF- $\beta$ /ALK4/SMAD2/3 pathways. However, previous literature reports (Bianco et al. 2002) have depicted ways of activating MAPK and AKT by CR-1, which do not require Nodal and ALK4.

#### 4.4. Induction of Cripto-1 Expression by Recombinant CR-1 in HEK293 Cells

Loying et al., 2015 discussed the upregulation of CR-1 expression by bacterial expressed recombinant GST tagged cripto-1 protein in U87MG cells. To replicate this model in our cell system, we chose HEK293 cells for our study based on the expression of all the

signalling molecules participating in ALK4/SMAD2/3 mediated CR-1 expression (Figure 4.6). HEK293 expresses a very high basal level of ALK4, SMAD2, SMAD3 and SMAD4 mRNA expression, while Nodal and Glypican-1 expression was comparatively low.

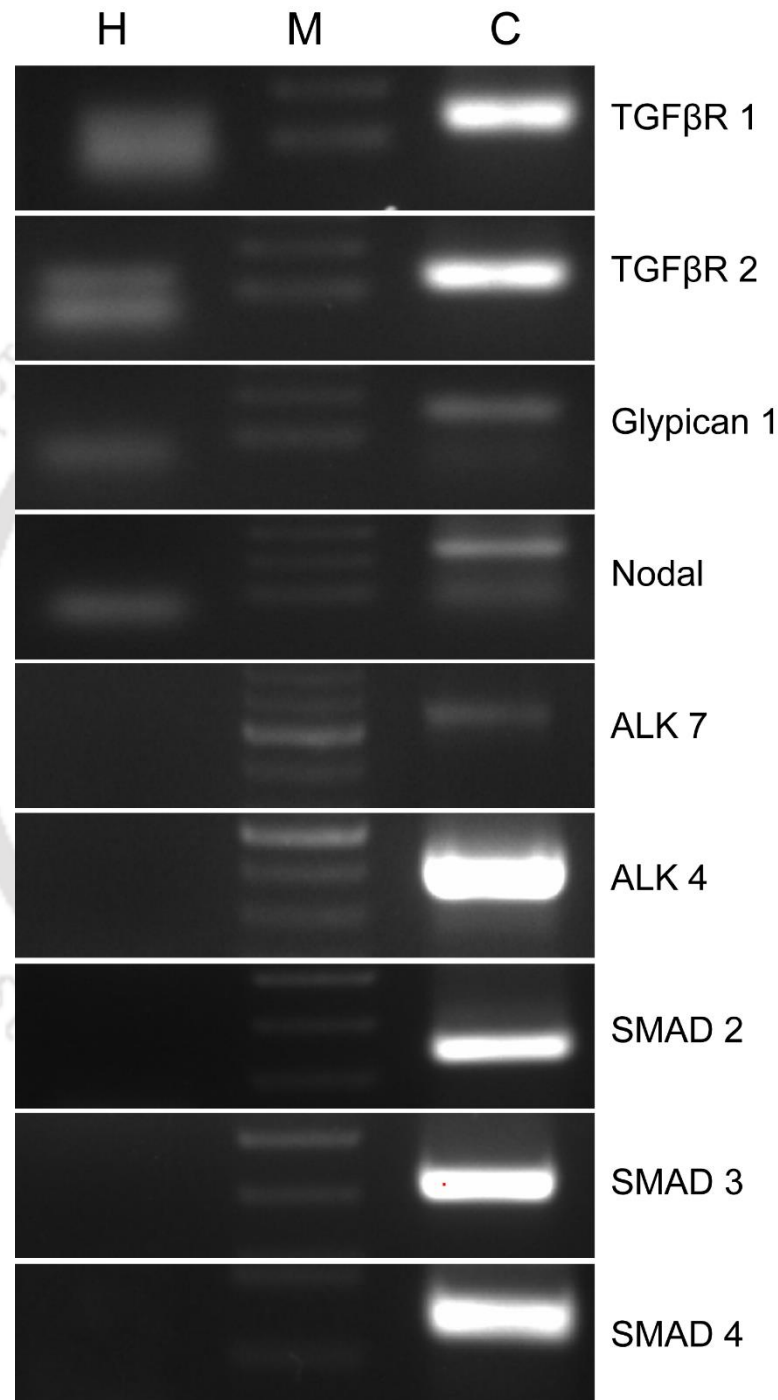


**Figure 4.6.** Components of ALK4/SMAD2/3 Pathway: Semi-quantitative PCR to check the expression of different molecules of the ALK4/SMAD2/3 pathway in HEK293 cells. Here H denotes Water control, M denotes 100 bp marker, and C represents cDNA

Subsequently, we treated the HEK293 cells with exogenous recombinant Cripto-1 protein (rCR-1) procured from R&D Systems. This rCR-1 is expressed in an insect cell line and contains 23-172 residues of human CR-1. On treatment with rCR-1 (50 ng/mL and 150 ng/mL) for 72 h in serum-free DMEM media, we observed a significant rise in CR-1 expression measured by Real-Time PCR (**Figure 4.7**). This further confirmed the suitability of HEK293 cells for our study.

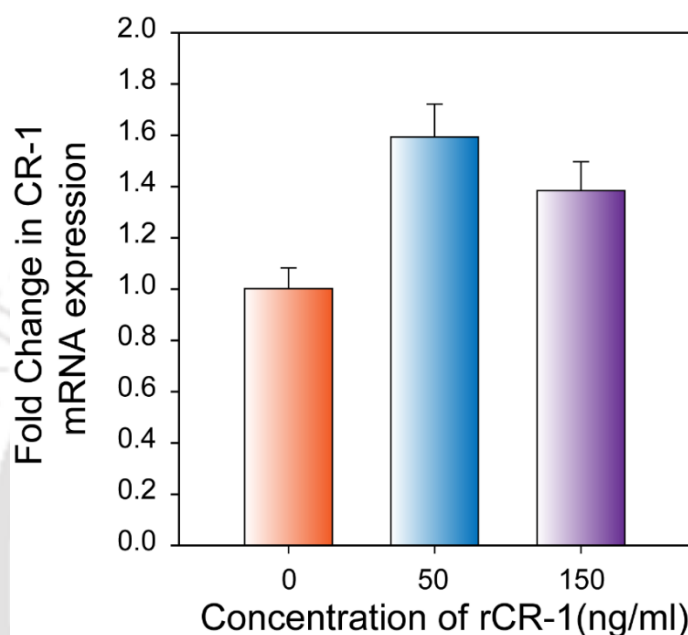


**Figure 4.7.** Expression of CR-1 on treatment with exogenous recombinant Cripto-1 protein (rCR-1). HEK293 cells were treated with 50ng/mL, and 150 ng/mL of dose in serum-free DMEM media for 72 h and expression of CR-1 was quantified by Real-Time PCR. 18s rRNA was used as an endogenous control. Data represented are the mean of a triplicate sample, and the analysis was performed by using Kruskal-Wallis analysis of variance. The fold in the expression of CR-1 was statistically significant ( $p < 0.05$ ).

#### 4.5. Generation of CR-1 Overexpressing Cell System:

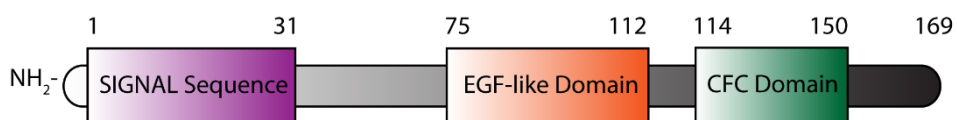
We observed that HEK293 cells express all the molecules required for ALK4/SMAD2/3 mediated induction of CR-1 expression. Subsequently, we also observed that the HEK293 cell shows induction of CR-1 expression on treatment with the exogenous recombinant cripto-1 protein expressed in an insect expression system. To further continue with our experiments, we decided to overexpress the CR-1 in HEK293 and MCF-7 cells to generate a mammalian cellular system. Structurally, the Cripto-1 proteins consist of three main domains an N-terminus signal sequence, a modified EGF-CFC

domain, and a hydrophobic C-terminus GPI moiety with varying lengths (Caterina Bianco et al., 2010b). The human cripto-1 protein exists in two forms based on the presence or absence of C-terminus GPI moiety. The membrane-bound form contains C-terminus GPI moiety, which helps the transmembrane anchorage of CR-1. At the same time, the form without C-terminus GPI moiety occurs in soluble form in the cells. It is also secreted by the cells in conditioned media during in-vitro cell culture (Kazuhide Watanabe et al., 2007). In our study, we worked with three different kinds of recombinant cripto-1, a) full-length CR-1, which consist of 1<sup>st</sup>-188<sup>th</sup> amino acids and all three domains, i.e., signalling domain, EGF-CFC domain and GPI moiety, b) C-terminus truncated CR-1, was called as  $\Delta$ CR-1 consists 1<sup>st</sup>-169<sup>th</sup> amino acids. It contains two domains signalling domain and EGF-CFC domain. c) Recombinant cripto-1 protein or rCR-1, which was expressed in the insect expression system. This protein consists of 31st- 172nd amino acids and has only one EGF-CFC domain shown in **Figure 4.8**.

#### A. Full length CR-1



#### B. C-terminus truncated CR-1 ( $\Delta$ CR-1)



#### C. Recombinant cripto-1 (rCR-1)

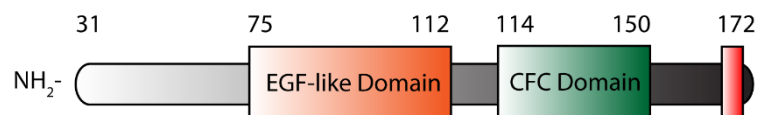


**Figure 4.8.** Different forms of CR-1 Protein used in the study. a) Full-length human CR-1 overexpressed in HEK293 and MCF-7 cells. b) C-terminal truncated human CR-1 ( $\Delta$ CR-1) overexpressed in HEK293 and MCF-7 cells. c) Recombinant CR-1 expressed in insect expression system procured from R&D Systems. Each block in the structure represents a protein domain, and the numbers above the blocks represent the number of amino acids arranged in sequence to form the particular domain.

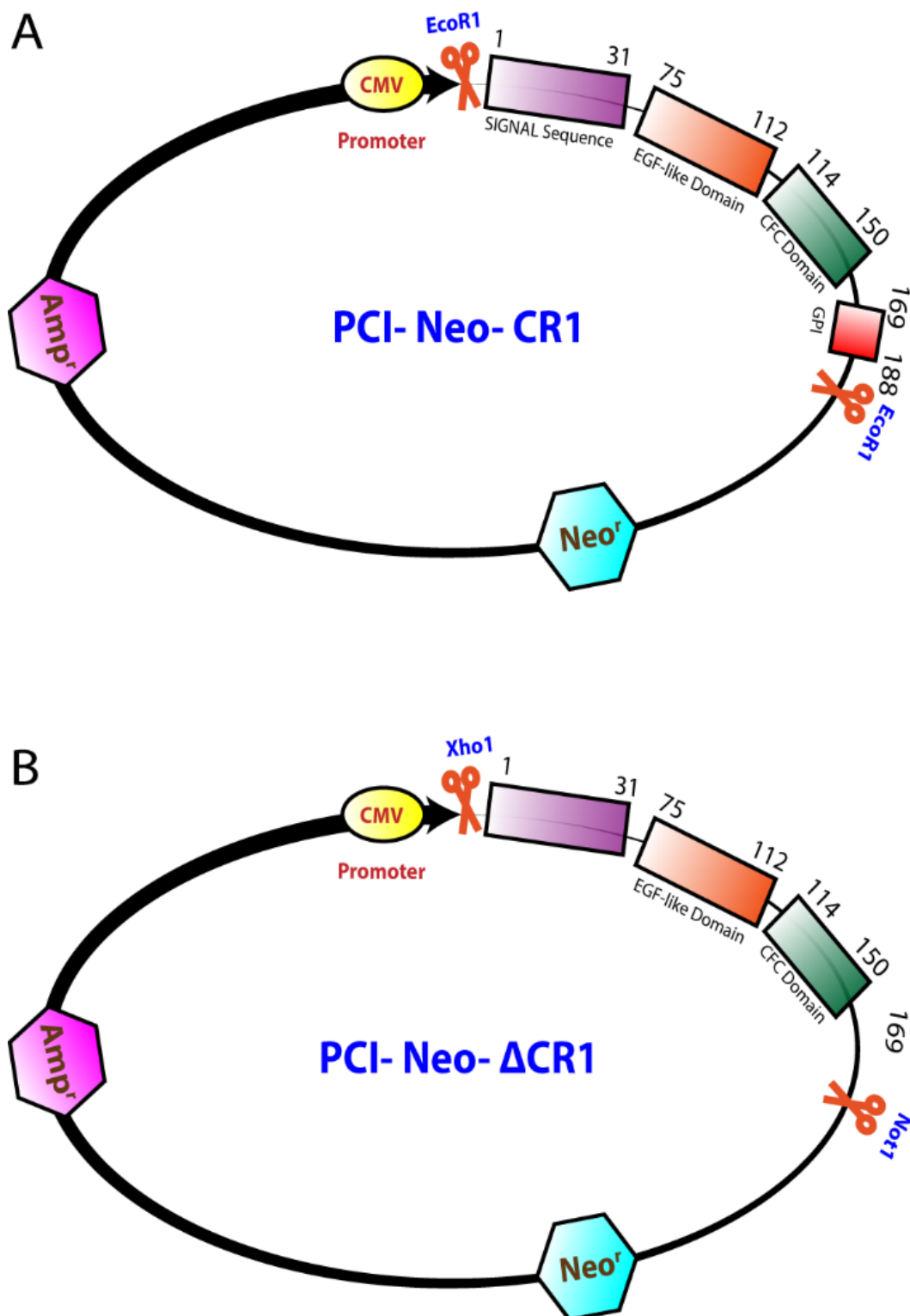


**Figure 4.9.** Schematic diagram of both the recombinant constructs: A) pCI-neo-CR-1 consists of Full-length human CR-1 gene and B) pCI-neo-ΔCR-1 contains C-terminal truncated human CR-1 gene. The vector consists of the CMV promoter, Amp<sup>r</sup> (ampicillin resistance gene for bacterial selection) and Neo<sup>r</sup> (Neomycin resistance gene as mammalian cells selection marker)

The full-length human CR-1 cDNA clone was generously gifted by Dr David Salomon, NIH, USA. This CR-1 cDNA fragment was inserted into the pCI-neo mammalian expression vector using restriction enzyme EcoRI from both ends. This construct was named pCI-neo-CR-1. The C-terminus truncated CR-1 was cloned previously in our lab by Das et al., 2012. The cloning strategy includes the amplification of DNA fragment corresponding to C-terminus truncated human CR-1 (1 - 169 amino acids) by PCR using pCI-neo-CR-1 as a template. The amplified product was inserted in the pCI-neo expression vector using restriction enzyme XhoI and NotI, and the resultant construct was called pCI-neo- $\Delta$ CR-1. **Figure 4.9** shows a schematic diagram of both the recombinant constructs.

The vector consists of CMV promoter, ampicillin resistance gene for bacterial selection and Neomycin resistance gene as mammalian cells selection marker. DNA sequencing was performed to confirm the insertion of the desired sequence into the vector. Further, the recombinant constructs were transformed into *E. Coli* (DH5 $\alpha$ ) by heat shock method, and glycerol stock (20% glycerol) were made and stored in -80 °C for long term use.

Further, these glycerol stocks were used to inoculate and revive the transformed clones in 2X TY media. The plasmid DNA was isolated from the bacterial culture grown overnight at 37 °C in the presence of ampicillin. The isolation of desired plasmid DNA was subjected to the Restriction digestion, and the digested products were separated using Agarose gel electrophoresis. As shown in **Figure 4.10**, the presence of the band near 500 bp in digested lane confirms plasmid DNA's authenticity. pCI-neo-CR-1 was digested by using EcoRI, whereas pCI-neo- $\Delta$ CR-1 was digested by XhoI and NotI restriction enzymes.

The HEK293 and MCF-7 cells were grown to 70 – 80 % confluence and transfected with pCI-neo-CR-1 and pCI-neo- $\Delta$ CR-1 along with pCI-neo empty vector using Lipofectamine based method. Subsequently, the cells were grown in DMEM containing Geneticin (G418) as a selection antibiotic. Geneticin is an analogue of neomycin which is more potent than conventional neomycin. The cells were further subcultured, and seeding density was so low that each well of the 96-well plate gets a single cell. Such seeding was done to obtain monoclonal clones for each recombinant construct.

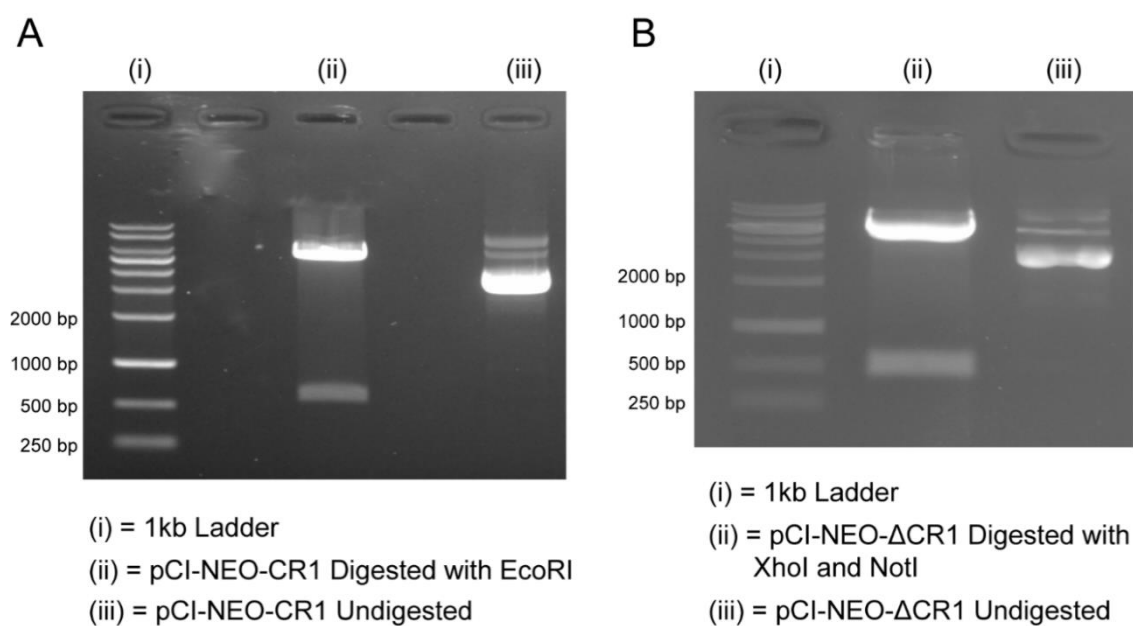


**Figure 4.10.** Confirmation of Plasmid DNA by Restriction Digestion: A) Restriction digestion of *pCI-neo-CR-1* by *EcoRI*. Lane 1 is 1 KB ladder; Lane 2 is digested plasmid with a fragment of 532 bp released at the bottom of the gel, and Lane 3 is an undigested circular plasmid. B) Restriction digestion of *pCI-neo-ΔCR-1* by *XhoI* and *NotI*. Lane 1 is 1 KB ladder; Lane 2 is digested plasmid with a fragment of 507 bp released at the bottom of the gel, and Lane 3 is an undigested circular plasmid.

The concentration of Geneticin for selection was determined by kill curve formation before the transfection. Transfected HEK293 cells were selected by treatment with 600  $\mu\text{g}/\text{mL}$  of Geneticin, whereas MCF-7 cells were selected using 800  $\mu\text{g}/\text{mL}$  of antibiotics for 4 - 8 weeks. On completion of selection, the CR-1 overexpression was measured by using Real-time PCR and western blotting. As shown in **Figure 4.11**, the transfected cells were highly overexpressed with *cripto-1* on mRNA level.

Further, we checked the protein expression of CR-1 in transfected cells **Figure 4.12**, and We observed that CR-1 transfection showed a significant increase in the expression of CR-1. The clones were named based on the construct present in them. HEK293 transfected with *pCI-neo-CR-1*, *pCI-neo-ΔCR-1* and *pCI-neo* empty vector were called HEK-CR1, HEK-ΔCR1 and HEK-EV, respectively. A similar naming pattern was followed for the MCF-7 cell line as well.

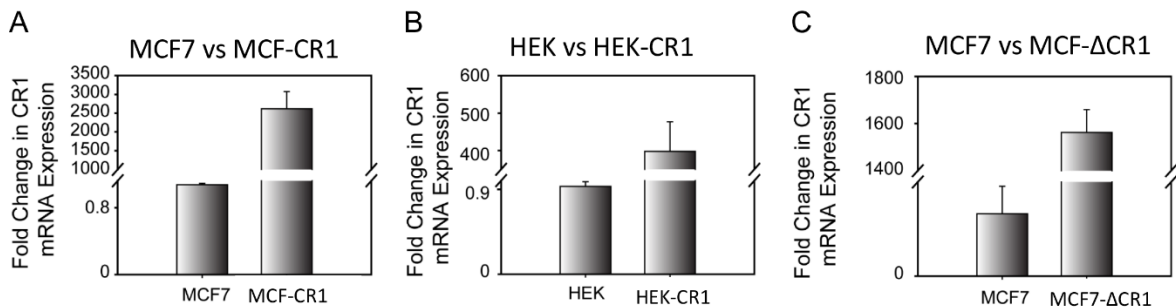


**Figure 4.11.** Generation of stably transfected clones: A) Expression of CR-1 in MCF-7 transfected with Full-length human CR-1 compared with untransfected MCF-7 cells. B) Expression of CR-1 in HEK293 transfected with Full-length human CR-1(HEK-CR-1) compared with untransfected HEK293 cells. C) Expression of CR-1 in MCF-7 transfected with C-terminal truncated human CR-1(MCF-ΔCR-1) compared with untransfected MCF-7 cells. Real-time PCR was used to measure the expression of CR-1 after 6-8 weeks of clonal selection by G-418 antibiotics

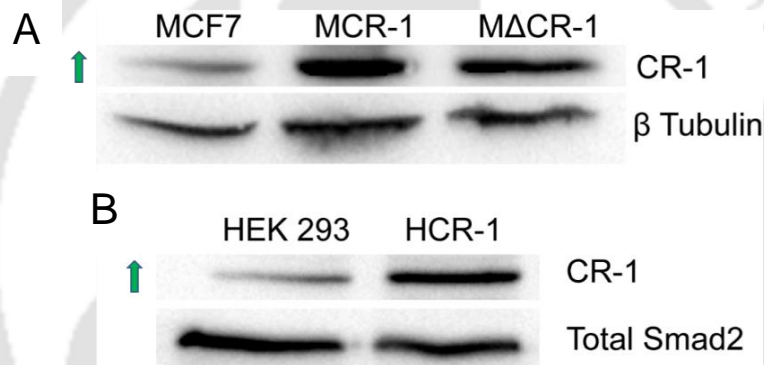


**Figure 4.12.** The expression of CR-1 was accessed by western blotting.  $\beta$ -actin and Total Smad2 were used as a loading control for MCF-7 clones and HEK293 clones, respectively. A) Protein level Expression of CR-1 in MCF-7 transfected with Full-length human CR-1 and C-terminal truncated CR-1 compared with untransfected MCF-7 cells. B) Protein level Expression of CR-1 in HEK293 transfected with Full-length human CR-1(HEK-CR-1) compared with untransfected HEK293 cells.

#### 4.6. Co-expression of HIF-1 $\alpha$ and MDR-1 on CR-1 Overexpression in HEK293:

During embryonic development in humans, cripto-1 plays a crucial role in the primitive streak formation, defining mesoderm and endoderm in gastrula and left/right asymmetry establishment for the developing organ (Caterina Bianco et al., 2010a). However, later life re-expression of cripto-1 has led to highly malignant cancer progression via adaptation of different ways like the stimulation of epithelial cells for epithelial to

mesenchymal transition, cell proliferation, angiogenesis and cancer stem cell expansion (C Bianco et al., 2005).

These phenomena were also acquired by HIF-1 $\alpha$  (Hypoxia-inducible factor-1 $\alpha$ ) for cancer maintenance and progression (Jing et al., 2019). In 2009, Bianco et al. demonstrated the importance of HIF-1 $\alpha$  as an aid of CR-1 during cardiomyocytes differentiation. HIF-1 $\alpha$  was found to regulate MDR-1 (multidrug resistance-1 / ABCB1 gene) in bladder cancer cell line, which was induced for MDR-1 expression by prolonged cisplatin treatment (Sun et al. Cripto-1 positive subpopulation isolated by cell sorting also have shown higher expression of MDR-1 in human glioblastoma cells (P Laying et al., 2015). These studies prompted us to explore the possible crosstalk between CR-1, HIF-1 and MDR-1.

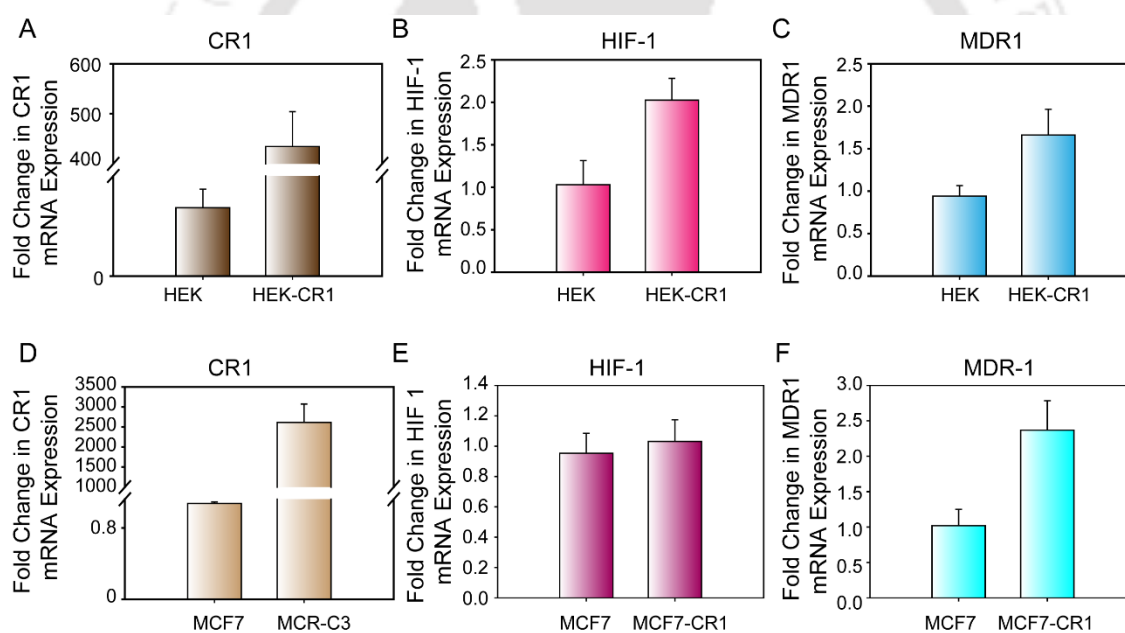


**Figure 4.13.** Co-expression of HIF-1 $\alpha$  and MDR-1 on CR-1 overexpression: A) Expression of CR-1 in HEK293 overexpressed with full-length human CR-1 by stable transfection. B) and C) represents the expression of HIF-1 $\alpha$  and MDR-1, respectively, on CR-1 overexpression in HEK293. D) Expression of CR-1 in MCF-7 overexpressed with full-length human CR-1 by stable transfection. E) and F) represents the expression of HIF-1 $\alpha$  and MDR-1, respectively, on CR-1 overexpression in MCF-7. The expression of genes was assessed by Real-Time PCR. 18s rRNA was used as endogenous control. Data represented are the mean of a triplicate sample, and the analysis was performed using the Mann-Whitney U test. The fold in the expression of all the genes was statistically significant ( $p < 0.05$ ), except HIF1- $\alpha$ (E) was non-significant.

To understand this, initially, we overexpressed HEK293, and MCF-7 cells with Full-length CR-1 (HEK-CR-1 and MCF-CR-1) and C-terminal truncated CR-1 (HEK- $\Delta$ CR-1 and MCF- $\Delta$ CR-1) by stable transfection. Subsequently, we checked the expression of HIF-1 $\alpha$  and MDR-1 in CR-1 overexpressed cells. We observed a significant upregulation in mRNA expression HIF-1 $\alpha$  and MDR-1 in HEK-CR-1, whereas MCF-CR-1 also showed significant upregulation of MDR-1 expression, but HIF-1 $\alpha$  expression remains unchanged on CR-1 overexpression in real-time PCR **Figure 4.13**.

Further, we checked the co-expression of HIF-1 $\alpha$  and MDR-1 on protein level via western blotting. As expected, HIF-1 $\alpha$  and MDR-1 expression were found to be upregulated in HEK-CR-1 and HEK- $\Delta$ CR-1. While MCF-CR-1 and MCF- $\Delta$ CR-1 showed upregulated MDR-1 expression (**Figure 4.14**.)

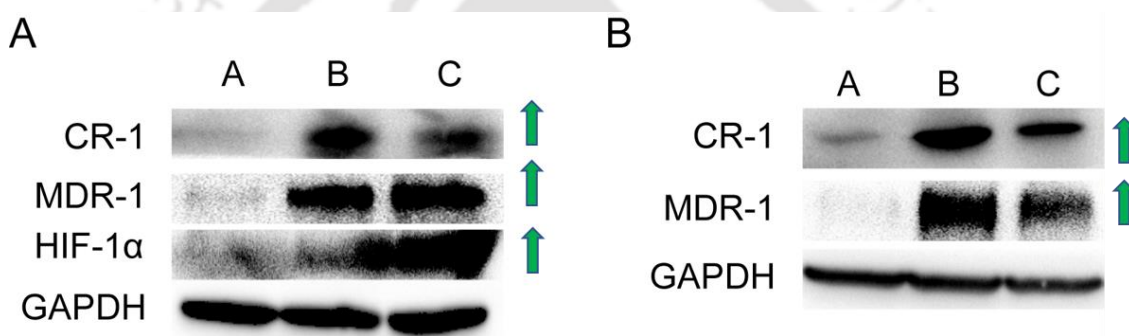


**Figure 4.14.** Western blotting shows the Co-expression of HIF-1 $\alpha$  and MDR-1 on protein level in CR-1 overexpression cells: A) Expression of CR-1, HIF-1 $\alpha$  and MDR-1 in HEK-CR-1 and HEK- $\Delta$ CR1 cells as compared to HEK-EV. Lane A, B, and C represents HEK-EV, HEK-CR-1 and HEK- $\Delta$ CR1 sample, respectively. B) Expression of CR-1 and MDR-1 in MCF-CR-1 and MCF- $\Delta$ CR1 cells compared to MCF-EV. Lane A, B, and C represents MCF-EV, MCF-CR-1 and MCF- $\Delta$ CR1 sample, respectively. GAPDH was used as the loading control.

Both CR-1 and  $\Delta$ CR-1 clones exhibited similar behavior, so we used only full-length CR-1 clones for most of the experiments. Altogether, the present data suggest CR-1 induces the expression of HIF-1 $\alpha$  and MDR-1 in HEK293 cells. However, CR-1 fails to induce HIF-1 $\alpha$  expression in MCF-7 cells.

#### 4.7. Cripto-1 Overexpression Induced HIF-1 $\alpha$ Expression Mediated by AKT Mitogenic Pathway:

In 2012, Jiao et al. depicted the chemical inhibition of the AKT pathway by LY294002 leads to downregulation of HIF1- $\alpha$ , which implicates the involvement of AKT in the

induction HIF-1 $\alpha$  and MDR-1 in the hepatocellular carcinoma cell line (HepG2 cells). Literature also suggests that Cripto-1 overexpression activates AKT and MAPK pathway in a mammary epithelial cell line (Eph4 cells) independent of the ALK4/Nodal/Smad2/3 pathway (Bianco et al., 2002). also demonstrated the activation of MAPK and PI3K pathway in U87MG cells.

To investigate the pathway with which cripto-1 induces the expression of HIF-1 $\alpha$  and MDR-1 in HEK293 cells, we checked the phosphorylation status of AKT and ERK in CR-1 overexpressed cells using western blotting. As shown in **Figure 4.15.A**, both AKT and ERK pathways get activated on CR-1 overexpression in HEK293 cells. Contrastingly, the CR-1 overexpressed MCF-7 cells (MCF-CR-1) show the dephosphorylation of AKT and ERK1/2 pathway compared to MCF-EV cells (**Figure 4.15.B.**)

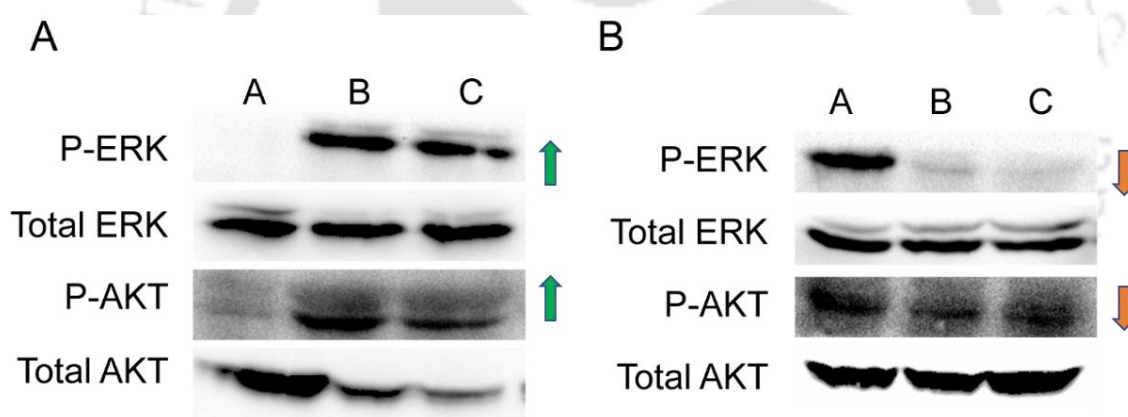


**Figure 4.15.** Western Blotting to detect the phosphorylation status of ERK and AKT (A) Expression of P-ERK and P-AKT in HEK-CR-1 and HEK- $\Delta$ CR1 cells compared to HEK-EV Lane A, B, and C represents HEK-EV, HEK-CR-1 and HEK- $\Delta$ CR1 sample, respectively. (B) Expression of P-ERK and P-AKT in MCF-CR-1 and MCF- $\Delta$ CR1 cells compared to MCF-EV. Lane A, B, and C represents MCF-EV, MCF-CR-1 and MCF- $\Delta$ CR1 sample, respectively. Total ERK and Total AKT were used as the loading control.

This behavior suggests the adaptation of alternate pathways by MCF-CR-1 for its mitogenic activity, and hence it fails to induce the expression of HIF1- $\alpha$  in the given system. In conclusion, the present data shows the involvement of AKT and ERK1/2 in the cripto-1 induced co-expression of HIF-1 $\alpha$  and MDR-1 gene in HEK-CR-1 cells.

#### 4.8. CR-1 Overexpression Induces the Cell Proliferation in HEK and MCF-7 Cells:

As previously depicted, CR-1 overexpression leads to the activation of AKT and ERK pathways in HEK293 clone cells. To further elucidate the effect of CR-1 overexpression on the cell proliferation rate of HEK293 and MCF-7 cells, we used a propidium iodide based assay (Wan et al. 1994).

The cells were seeded at low density in each well of 96-well plate in Phenol red-free DMEM media (10% FBS). The first fluorescence was measured immediately after the attachment of cells to get the initial seeding cell density's fluorescence intensity at (t=0) time point. As the cell grows, the fluorescence intensity was measured, after adding cell staining solution (final concentration: 30  $\mu\text{g}/\text{mL}$  of PI, 0.1 M EDTA, 0.5% Triton X-100) directly in the well for 10 min, at the different time points (24, 48, 72 and 96 h). The fluorescence emission was measured at each time point at 530 nm excitation and 620 nm emission wavelength.

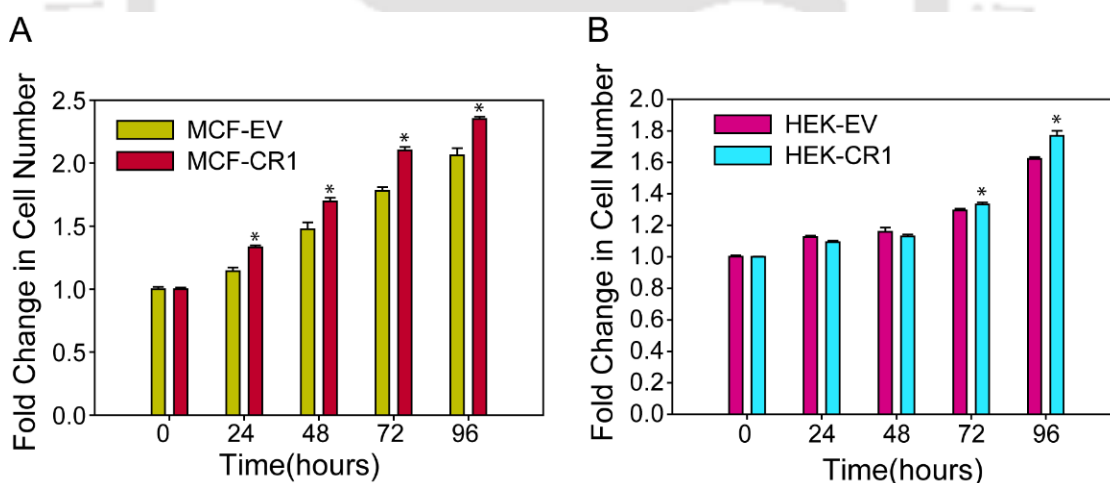


**Figure 4.16.** Cell proliferation assay: Cells were seeded in equal density in a 96-well plate in phenol red-free Serum media. Cells were lysed at a specific time point by adding the staining solution (composition: see methods section). Multiplate reader measured fluorescence intensity at 530 nm excitation and 620 nm emission wavelength. A) Fold change in Cell number compared between MCF-EV and MCF-CR1 B) Fold change in Cell number compared between HEK-EV between HEK-CR1

As shown in **Figure 4.16A**, the CR-1 overexpressed MCF-7 cells (MCF-CR-1) showed significantly higher cell proliferation than Empty vector-transfected MCF-7 (MCF-EV) cells. Immediately after 24 h, these cells started growing at a higher rate, and the proliferation rate increased after 72 and 96 h. In the case of HEK-CR-1 (**Figure 4.16B**), there was no significant difference in cell proliferation after 24 and 48 h, but after 72 h, the cell proliferation rate increased significantly.

The enhanced cell proliferation shown by HEK-CR-1 can be the attribute of activation of the AKT and ERK pathways. However, these pathways were found downregulated in MCF-CR-1. Still, it showed higher cell proliferation. This indicates the possibility of adaptation of alternate mitogenic pathways by MCF-CR-1.

#### **4.9. Effect of CR-1 Overexpression on Functional P-Glycoprotein Efflux Pump:**

We observed the induction of MDR-1(P-glycoprotein) expression in MCF-7 and HEK293 on CR-1 overexpression in previous experiments. To access the functional activity of MDR-1, we performed a drug sensitivity assay of CR-1 overexpressed cells with two standard anticancer drugs Paclitaxel and Doxorubicin. Paclitaxel is a mitotic inhibitor of cancer cells, whereas doxorubicin intercalates in cancer cells' DNA to exert their action. We performed the MTT assay to compare the drug resistance acquired by CR-1 overexpressed cells over empty vector transfected cells against the abovementioned anticancer drugs. The cells were seeded at equal density in 96-well plates and grown for 24 h. Subsequently, the cells were treated in DMEM (10% FBS) media containing different doses of drugs (Paclitaxel and Doxorubicin) for 48 h in separate sets. Five replicates for each dose were used.

As shown in **Figure 4.17 (A and B)**, we observed a significant increase in  $IC_{50}$  values of MCF-CR-1 when compared with MCF-EV against both drugs. The  $IC_{50}$  of paclitaxel increases from 34.5 nM (MCF-EV) to 43.6 nM (MCF-CR-1), and the  $IC_{50}$  of doxorubicin rises to 296.5 nM (MCF-CR-1) from 145.7 nM (MCF-EV), which indicates the acquisition of higher drug resistance by MCF-7 on CR-1 overexpression.

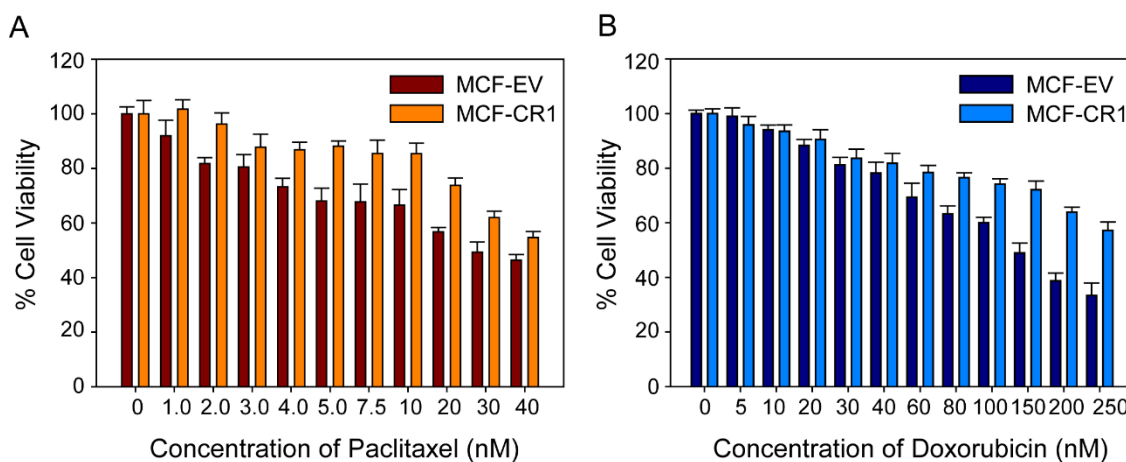


**Figure 4.17.** Cytotoxicity assay: To measure P-glycoprotein efflux pump activity in MCF-CR-1 cells compared to MCF-EV cells, the MTT assay was performed. A) % cell viability after treatment with different doses of Paclitaxel for 48 h B) % cell viability after treatment with different doses of Doxorubicin for 48 h. For each dose, five replicates were used, and the absorbance of DMSO dissolved formazan crystals was measured by the multiplate reader at 570 nM wavelength.

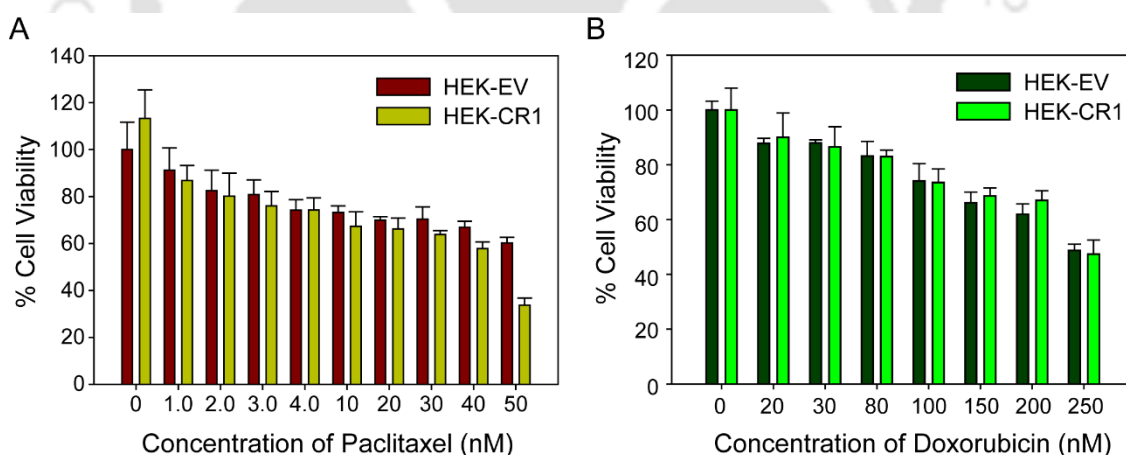


**Figure 4.18.** Cytotoxicity assay: To measure P-glycoprotein efflux pump activity in HEK-CR-1 cells compared to HEK-EV cells, the MTT assay was performed. A) % cell viability after treatment with different doses of Paclitaxel for 48 h B) % cell viability after treatment with different doses of Doxorubicin for 48 h. For each dose, five replicates were used, and the absorbance of DMSO dissolved formazan crystals was measured by the multiplate reader at 570 nm wavelength.

We also performed a similar experiment with HEK-CR-1 and HEK-EV (**Figure 4.18 A and B**). We observed a decrease in the IC<sub>50</sub> value of paclitaxel against HEK-CR-1 compared with HEK-EV. This indicates the increased susceptibility of HEK293 against paclitaxel on CR-1 overexpression. However, there was no significant difference observed in the IC<sub>50</sub> of Doxorubicin against HEK-CR-1 and HEK-EV.

Altogether, the present data imply that the acquisition of drug resistance against a single drug may vary with a cell-to-cell variation. In the MCF-7 clone (MCF-CR-1), the cells showed the expression of functionally active drug efflux pump, but in the HEK293 clone (HEK-CR-1), the cells seem to acquire drug resistance in some other way.

#### 4.10. CR-1 Modulates the CSC Markers' Expression:

Cripto-1 is well known for its stem cell maintenance and pluripotency properties (Caterina Bianco et al., 2010b). The cancer cells that exhibit the ability to regenerate solid tumours with original phenotypes in immune-deficient mice can be defined as cancer stem cells (CSCs) (Visvader et al., 2008). For the first time, CSCs were identified in the blood of acute myeloid leukaemia (AML) patients (Bonnet et al., 1997). Subsequently, CSCs associated with different body organs were identified in the brain, breast, head and neck, prostate, pancreas and lungs (Sheila K. Singh et al., 2004)(Al-Hajj et al., 2003). In 2011, Siva et al. demonstrated the importance of active expression of HIF-1 $\alpha$  for cripto-1/GRP78<sup>+</sup> signalling mediated maintenance of hematopoietic stem cells (HSCs).

To further explore the effect of Cripto-1 and HIF-1 $\alpha$  co-expression in our system. The CR-1 overexpressed cells were subjected to Real-Time PCR to detect the expression of cancer stem cell markers like CD24, CD44 and CD133. As shown in **Figure 4.19**, the CR-1 overexpressed cells (HEK-CR-1 and MCF-CR-1) show upregulation in the mRNA expression of CD24 and CD44 (**Figure 4.19.A, B, and D, E**). However, the expression of CD133 was found downregulated in HEK-CR-1 (**Figure 4.19.C**) and remain unchanged in MCF-CR-1 (**Figure 4.19.F**)

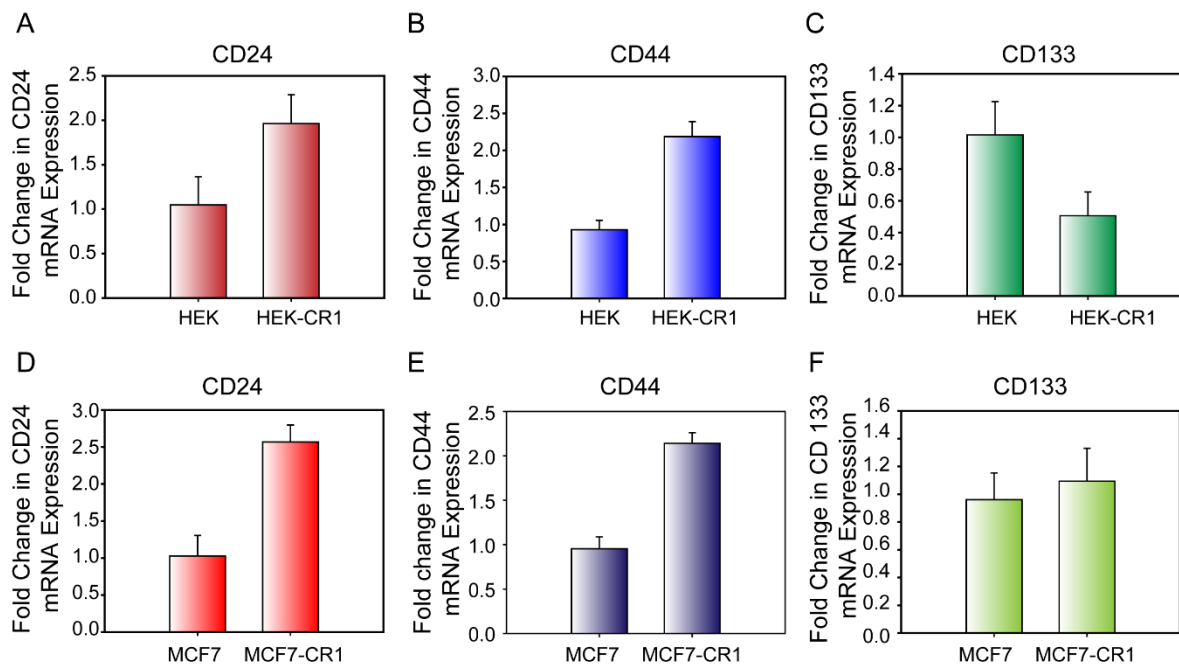


**Figure 4.19.** *CR-1 modulates the CSCs marker expression: To check this, the expression of cancer cell surface markers was measured using Real-time PCR: A) CD24, B) CD44, and C) CD133 represents the fold change in mRNA expression of HEK-CR-1 compared to HEK293 wild-type cells. While D) CD24 E) CD44 and F) CD133 represents the mRNA level expression in MCF-CR1 compared to MCF-7 wild-type cells. 18s rRNA was used as endogenous control. Data represented are the mean of a triplicate sample, and the analysis was performed using the Mann-Whitney U test. The fold in the expression of all the genes was statistically significant ( $p < 0.05$ ), except CD133(F) was non-significant.*

The effect of cripto-1 on cancer stem cells (CSCs) enrichment in HEK293 cells was further evaluated on treatment with recombinant cripto-1 protein for 72 h in serum-free DMEM media. Subsequently, the expression of CD24 and CD44 were measured by using Real-Time PCR **Figure 4.20**. We observed that the expression of CD44 and CD24 were found significantly upregulated at 50 ng/mL and 150 ng/mL doses of recombinant cripto-1 protein (rCR-1).

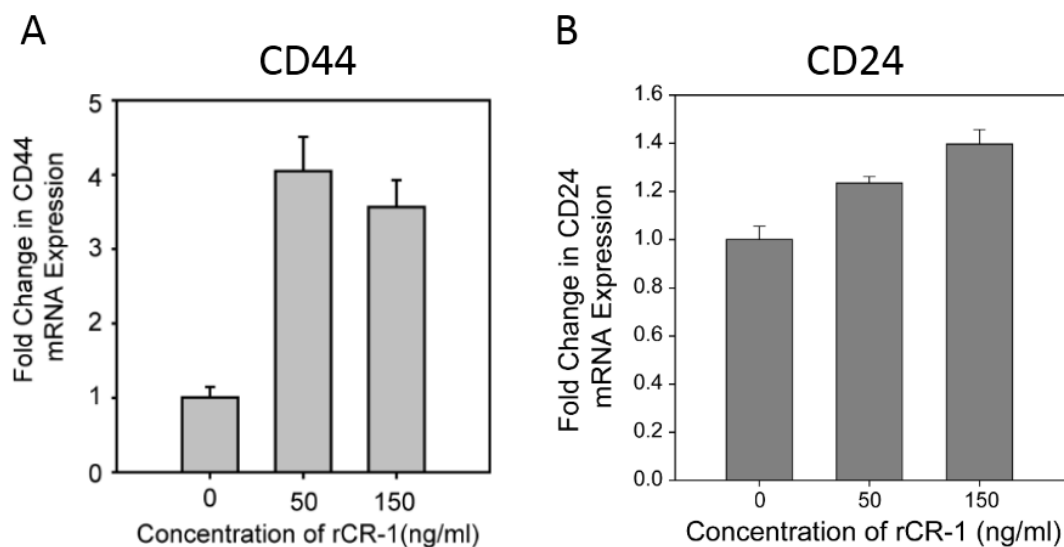


**Figure 4.20.** Effect of rCR-1 treatment on the CSCs modulation: The HEK293 cells were treated with two different doses of rCR-1 for 72 h in serum-free DMEM media, and the expression of cancer cell surface markers was measured by using Real-time PCR: A) CD24 and B) CD44 represents the fold change in mRNA expression in rCR-1 treated HEK293 as compared to untreated cells. 18s rRNA was used as the endogenous control. Data represented are the mean of a triplicate sample, and the analysis was performed by using Kruskal-Wallis analysis of variance. The fold in the expression of all the genes was statistically significant ( $p < 0.05$ ).

To verify CD44 and CD24 markers' active expression on protein level in recombinant CR-1 treated HEK293 cells, flow cytometry-based experiments were executed. As depicted in **Figure 4.21**, there was an evident shift in the median fluorescence intensity (MFI) of CD24 and CD44 towards the right side (denotes increase in expression) in a dose-dependent manner. This shows that CR-1 induces the expression of CD24 and CD44 at the protein level as well.

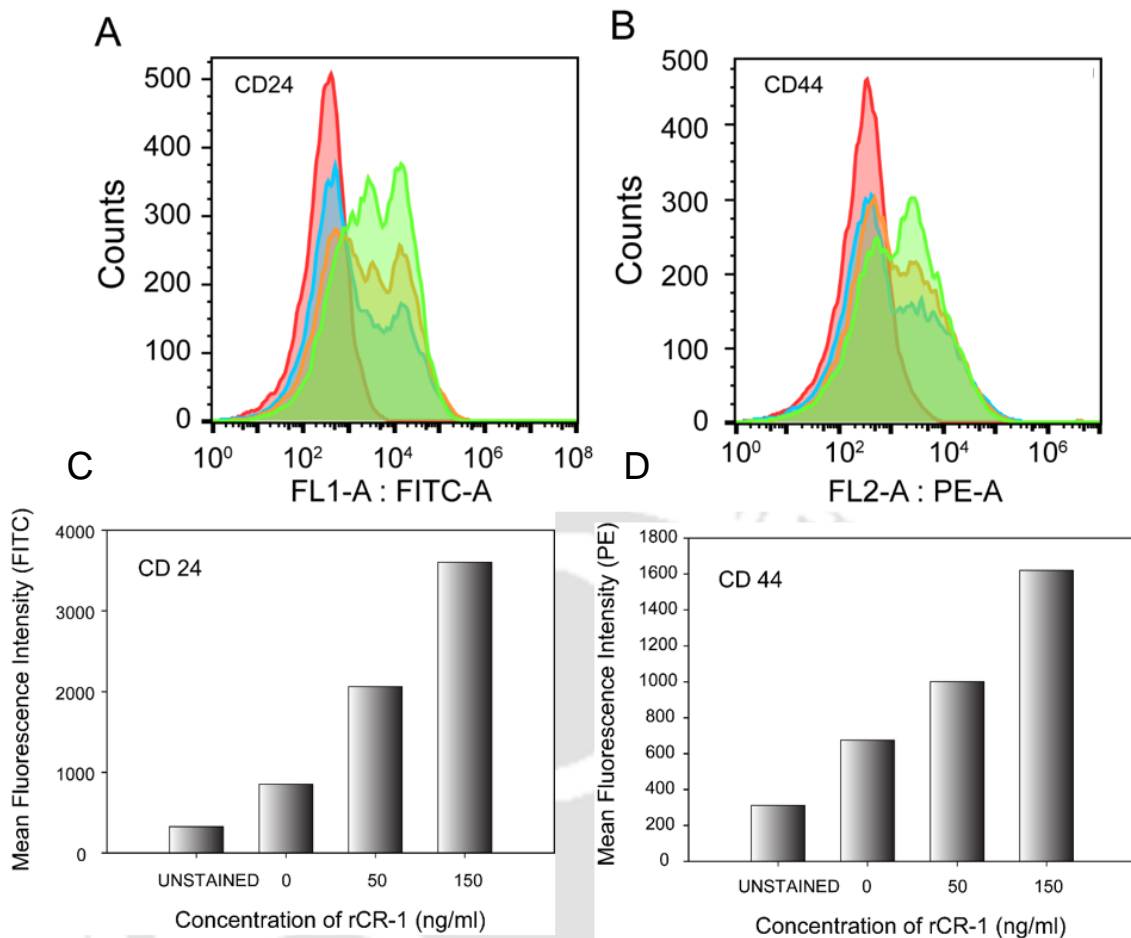


**Figure 4.21.** Flow cytometry analysis to detect the cell surface expression of CD24 and CD44: HEK293 treated with rCR-1 for 72 h in serum-free DMEM media and the expression of A) CD24 and B) CD44 was checked by FACS analysis. (Colour code: Red, Blue, Orange, and Green histograms represent Untreated Unstained, Untreated stained with antibody, 50 ng/mL of rCR-1 treated stained with antibody and 150ng/mL rCR-1 treated stained with antibody respectively). The increase in expression was denoted in terms of median fluorescence intensity (MFI), shown in C) MFI of CD24-FITC tagged and D) MFI of CD44-PE tagged.

Furthermore, we performed a dual colour flow cytometry to determine the side cell population's nature on cripto-1 induction in HEK293. We observed a dose-dependent increase in the CD44<sup>+</sup>CD24<sup>+</sup> subpopulation (**Figure 4.22**). In untreated group, the percentage of CD44<sup>+</sup>CD24<sup>+</sup> subpopulation was 15.61%, which significantly increases on treatment with recombinant cripto-1 protein to 20.06% (50 ng/mL) and 27.13% (150 ng/mL). Literature suggests that this type of CD44<sup>+</sup>CD24<sup>+</sup> subpopulation has also been previously identified in the gastric cancer cell line (AGS), where these subpopulations have exhibited the ability to grow a solid tumour in 50 % of NOD-SCID mice (6 out of

12) even when injected in as low as 200 cells/mice concentration, which is very high as compared to the CD44-CD24- subpopulation which developed tumour only in 8.3% of NOD-SCID mice after injecting 10,000 cells/mice (Zhang et al., 2011).

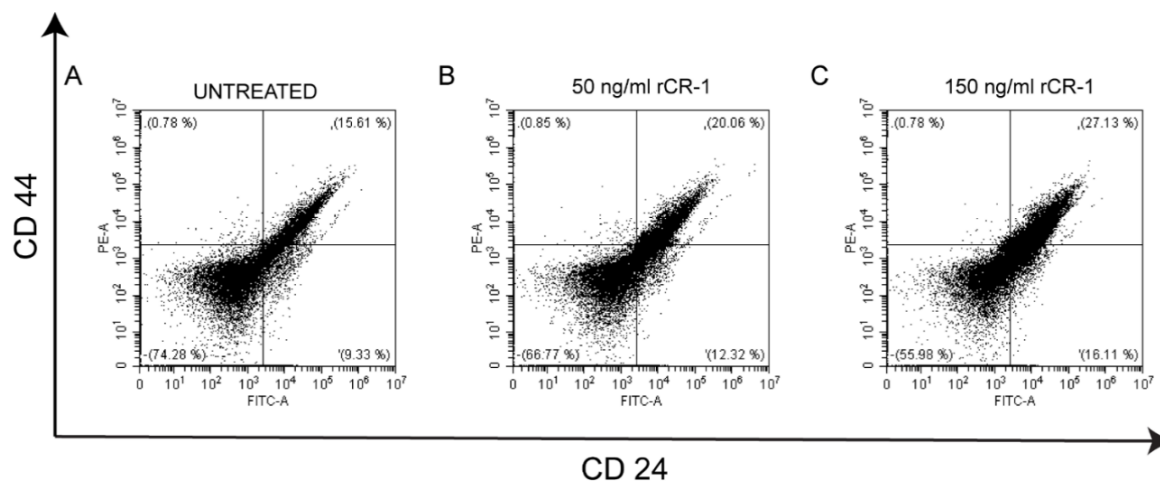


**Figure 4.22.** Dual colour flow cytometry to determine the side cell population's nature on treatment with recombinant cripto-1 in HEK293 cells. The cells were stained with CD24-FITC tagged, and CD44-PE tagged. The dot plots represent A) Untreated group, B) 50 ng/mL rCR-1 treated and C) 150 ng/mL rCR-1 treated. The fluorescence spillover was removed using the compensation matrix. The percentage of CD44<sup>+</sup>/CD24<sup>+</sup> subpopulation increases in a dose-dependent manner.

Further literature reports state that the Cervical squamous cell carcinoma cell line (SiHa) also contains a CD44<sup>+</sup>CD24<sup>+</sup> subpopulation which is highly resistant to radiotherapy and does not undergo cell apoptosis irradiation. SiHa CD44<sup>+</sup>CD24<sup>+</sup> subpopulation also displays the competence to develop a tumour in nude mice (Liu et al., 2016). TGF- $\beta$ , a known inducer of CR-1, also induces the proliferation of CD24<sup>+</sup> and CD44<sup>+</sup> subpopulation in the human embryonal carcinoma cell line (NTERA2).

As shown in **Figure 4.23**, treatment with 10 ng/mL of TGF- $\beta$  for 24 h, the CR-1<sup>+</sup> subpopulation increased by ~2%. This induction of CR-1 expression ultimately triggered the expression of CD24 and CD44 on the cell surface. The CD24<sup>+</sup> subpopulation increased by ~ 61% whereas CD44<sup>+</sup> subpopulation increased by ~19.7 %. Altogether, the cripto-1 induced increase in CD44<sup>+</sup>CD24<sup>+</sup> subpopulation in HEK293 and NTERA2 suggests the involvement of cripto-1 in the modulation of CSCs population within the cell line.

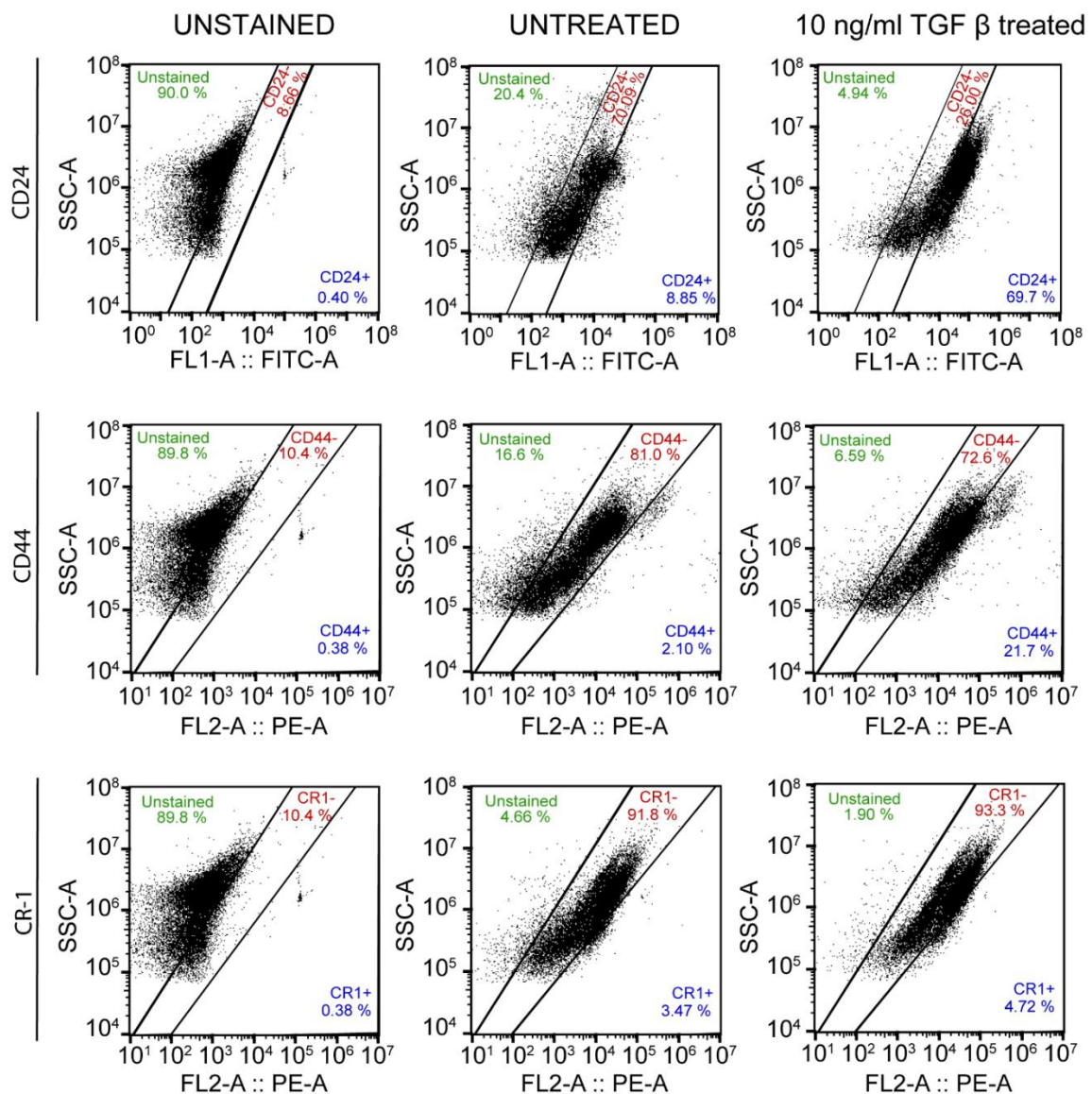


**Figure 4.23.** Flow cytometry to detect the CSCs marker expression: The NTERA2 cells were treated with 10ng/mL of TGF- $\beta$  for 24 h in serum-free optimen media. The top row represents the expression of CD24-FITC tagged, the middle row represents the expression of CD44-PE tagged, and the bottom row represents the expression of CR-1-PE tagged.

#### 4.11. Association of Cripto-1 with Embryonic Stem Cells Markers:

The stemness markers are the genes that are responsible for the maintenance of pluripotency. Some of these markers also act as transcription factors and regulate the expression of cripto-1 in adult stem cells. Knockout of cripto-1 decreased self-

renewability in embryonic stem cells of fish (Fiorenzano et al., 2016). CR-1<sup>High</sup> cells isolated by fluorescence-activated cell sorting from Embryonal carcinoma cells (NTERA2 and NCCIT cells) shows higher expression of OCT4, Nanog, Sox2, Leafy and Nodal as compared to CR-1<sup>Low</sup> (K Watanabe et al. 2010). A recent report (Park et al., 2018) has identified the putative promoter binding site of OCT4 in the CR-1 promoter. The overexpression of OCT4 induces the transactivation of CR-1, while the shRNA inhibition of OCT4 leads to the downregulation of CR-1. To further investigate the correlation of embryonic stem cell (ESC) genes with cripto-1 and HIF-1 $\alpha$  co-expression in HEK293 cells. We decided to check the expression of OCT4, Nanog and Sox2 in CR-1 overexpressed cells (HEK293 and MCF-7) by Real-Time PCR. We observed that the OCT4 expression was significantly upregulated in both HEK-CR-1 and MCF-CR-1 (Figure 4.24.A and D). At the same time, the Nanog shows no change in its expression

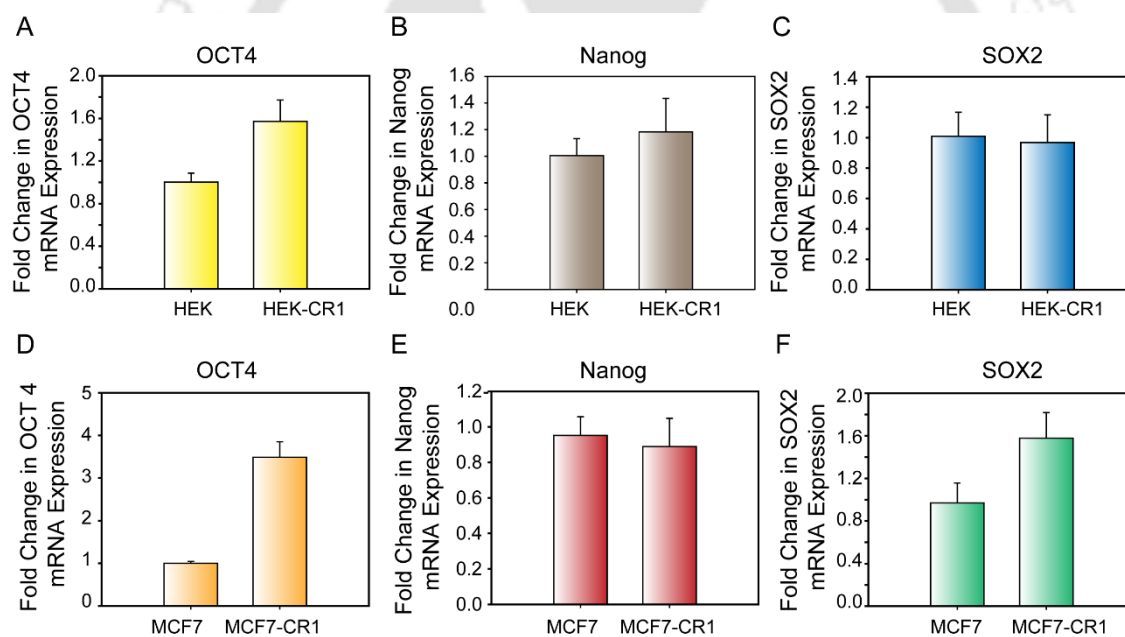


**Figure 4.24.** CR-1 overexpression induces the ESCs markers expression: To check this, the expression of embryonic stem cell markers was measured by using Real-time PCR: A) OCT4, B) Nanog, and C) SOX2 represents the fold change in mRNA expression in HEK-CR1 as compared to HEK293 wild-type cells. While D) OCT4 E) Nanog and F) SOX2 represents the mRNA level expression in MCF-CR1 compared to MCF-7 wild-type cells. 18s rRNA was used as endogenous control. Data represented are the mean of a triplicate sample, and the analysis was performed using the Mann Whitney U test. The expression of OCT4(A, D) and SOX2(F) were statistically significant ( $p < 0.05$ ) in both HEK293 and MCF-7 clones. In contrast, the fold change in expression of Nanog (B, C) and SOX2(C) is not significant.

on CR-1 overexpression (**Figure 4.24.B and E**). However, the expression of Sox2 was found upregulated in MCF-CR-1(**Figure 4.24.F**) but remain unchanged in HEK-CR-1. We also observed significant upregulation in ESC genes expression on treatment with different doses of recombinant CR-1(rCR-1) protein. As shown in **Figure 4.25**, the expression levels of Nanog and OCT4 was found to be upregulated on treatment with 50ng/mL of rCR-1 for 72 h in serum-free DMEM media.

However, the upregulation in Sox2 expression was not significant. The present data indicate that the expression of CR-1 is closely correlated with the expression of OCT4 in HEK293 and MCF-7 cells, which implies that OCT4 is the critical regulator of CR-1 expression.

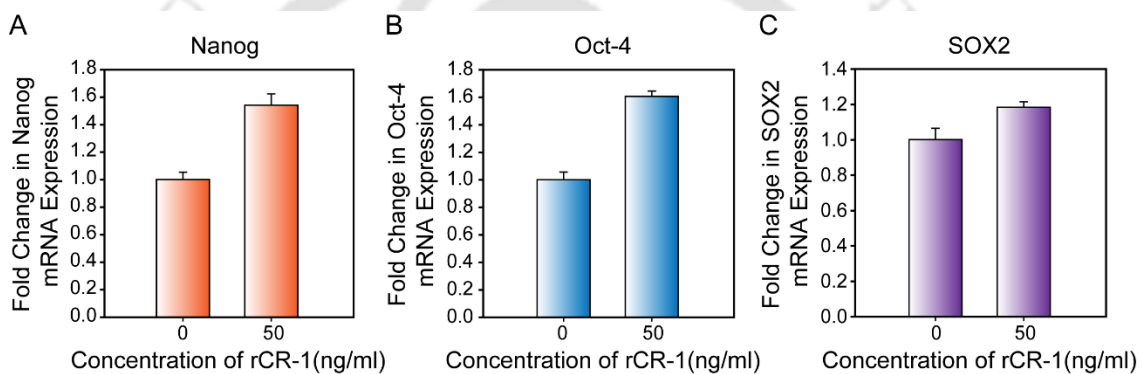


**Figure 4.25.** Effect of rCR-1 treatment on ESCs markers expression: The HEK293 cells were treated with two different doses of rCR-1 for 72 h in serum-free DMEM media, and the expression of cancer cell surface markers was measured by using Real-time PCR: A) OCT4 B) Nanog and C) SOX2 represents the fold change in mRNA expression in rCR-1 treated HEK293 as compared to untreated cells. 18s rRNA was used as the endogenous control. Data represented are the mean of a triplicate sample, and the analysis was performed using the Mann Whitney U test. The fold in the expression of OCT4 and Nanog genes was statistically significant ( $p < 0.05$ ), whereas the fold change in SOX2 expression was insignificant.

#### 4.12. In Hypoxic-like Condition, HIF-1 $\alpha$ Induces the Expression of CR-1:

In HEK293 cells, overexpression of CR-1 induces the expression of HIF-1 $\alpha$ , which indicates the presence of crosstalk between these two molecules. However, the exact interplay and regulations between these two molecules are yet to be determined. To further investigate this, we chose an experimental model which can be used as a positive control for hypoxia. We used CoCl<sub>2</sub>, a chemical inducer of hypoxia, which induces the

hypoxia-like condition by inhibiting the prolyl hydroxylase enzyme, which degrades HIF-1 $\alpha$  (Doublier et al., 2012).

To check the expression of cripto-1 in HEK293 cells under hypoxia-like conditions, the cells were treated with 150  $\mu$ M of CoCl<sub>2</sub> for 24 h in DMEM media supplemented with 10 % FBS (Fetal bovine serum). As expected, **Figure 4.26. A** shows the induction of HIF-1 $\alpha$  expression in the HEK293 cell. This induction of HIF-1 $\alpha$  expression was accompanied by the upregulation in the expression of CR-1 and MDR-1 (**Figure 4.26.B and C**)

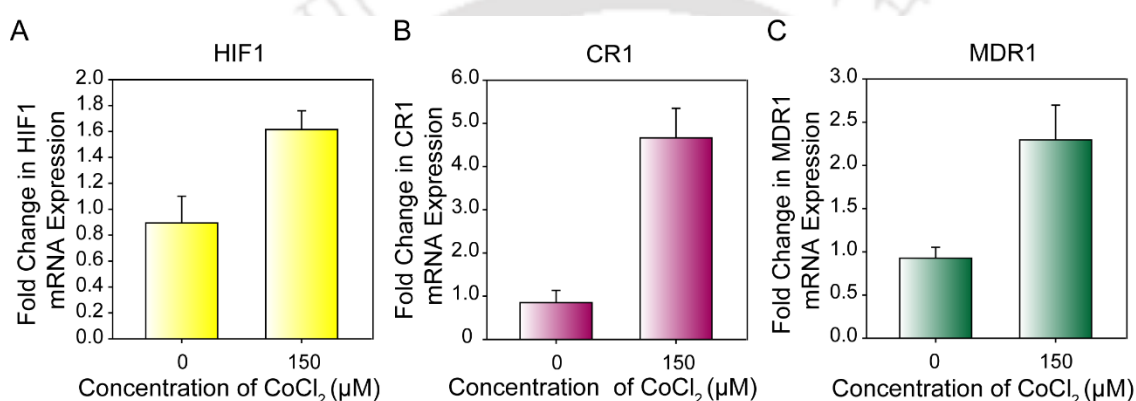


**Figure 4.26.** Effect of Cobalt Chloride on co-expression of CR-1 and HIF-1 $\alpha$ : The HEK293 cells were treated with CoCl<sub>2</sub> for 24 h in serum DMEM media, and the mRNA expression was measured by using Real-time PCR: A) HIF-1 $\alpha$  B) CR-1 and C) MDR-1 represents the fold change in mRNA expression in CoCl<sub>2</sub> treated HEK293 as compared to untreated cells. 18s rRNA was used as the endogenous control. Data represented are the mean of a triplicate sample, and the analysis was performed using the Mann Whitney U test. The fold in the expression of all the genes was statistically significant ( $p < 0.05$ ).

Furthermore, Cripto-1 also shows high transcriptional activity on treatment with CoCl<sub>2</sub> (C Bianco et al., 2009). Consequently, The induction of HIF-1 $\alpha$  expression by CoCl<sub>2</sub> treatment has been reported to produce doxorubicin-resistant MCF-7 cells (Doublier et al., 2012). HEK293 and MCF-7 cells were treated with different doses of CoCl<sub>2</sub> (0, 100, 150, and 200  $\mu$ M) for 24 h and cells lysate was prepared using RIPA buffer (Radio immunoprecipitation assay buffer). The protein expression of genes was analyzed using western blotting.

As shown in **Figure 4.27.A.**, the expression of HIF-1 $\alpha$  was found to increase in a dose-dependent manner. In HEK293 cells, with hypoxia induction, the expression of CR-1 and MDR-1 also increases in a dose-dependent pattern. Similarly, In MCF-7 cells, the expression of MDR-1 also increases gradually in a dose-dependent manner (**Figure 4.27.B**). In summary, the present data depicts the co-expression of CR-1 and MDR-1 on the induction of HIF-1 $\alpha$  expression by CoCl<sub>2</sub> exposure.

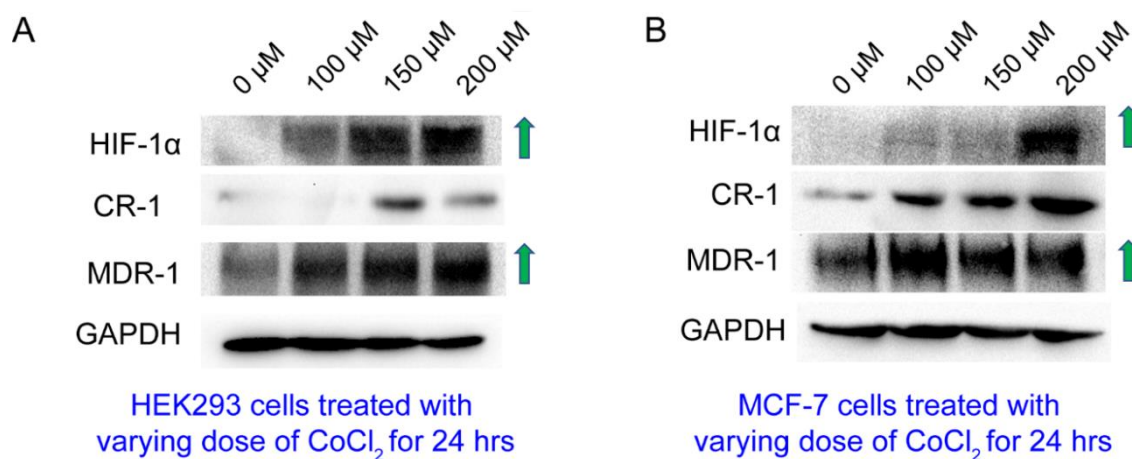


**Figure 4.27.** Western blotting to show the Co-expression of HIF-1 $\alpha$  and CR-1 in Cobalt chloride treated HEK293 cells: A) Expression of CR-1, HIF-1 $\alpha$  and MDR-1 on treatment with different dose of CoCl<sub>2</sub> in HEK293 cells as compared to untreated. B) Expression of CR-1 and MDR-1 on treatment with different doses of CoCl<sub>2</sub> in MCF-7 cells compared to untreated. GAPDH was used as the loading control.

#### 4.13. Effect of CoCl<sub>2</sub> on the Activation of AKT/ERK Pathways:

To investigate the effect of CoCl<sub>2</sub> treatment on the phosphorylation pattern of AKT and ERK, the cells were treated with CoCl<sub>2</sub> in a concentration-dependent manner (0, 100, 150 and 200 μM) for 24 h in DMEM media supplemented with 10% FBS.

Literature reports have suggested that the treatment with CoCl<sub>2</sub> leads to the activation of AKT and ERK pathway (S. Choi et al., 2016) (Ardyanto et al., 2006). In agreement with this report, **Figure 4.28.B** shows that on the treatment of MCF-7 cells with different concentrations of CoCl<sub>2</sub>, an induction in the activation of AKT and ERK pathway in a dose-dependent manner was observed.

Surprisingly, as shown in **Figure 4.28.A**, HEK293 cells also depict the upregulated phosphorylation of AKT and ERK pathways on exposure with different doses of  $\text{CoCl}_2$ . Altogether, the present data suggest the AKT and ERK pathway's involvement in the activation of HIF-1 $\alpha$  expression by  $\text{CoCl}_2$ .

However, in 2002, xx et al. indicated that few cells might not show activation of the AKT pathway on treatment with  $\text{CoCl}_2$ , which can be due to the cell type-specific variation. In another study, the Cobalt chloride induced HIF-1 $\alpha$  expression was shown to get downregulated on chemical inhibition of the AKT pathway by LY294002 (Ardyanto et al., 2006). This indicated the presence of correlation between HIF-1 $\alpha$  and AKT activation in cancer cells.

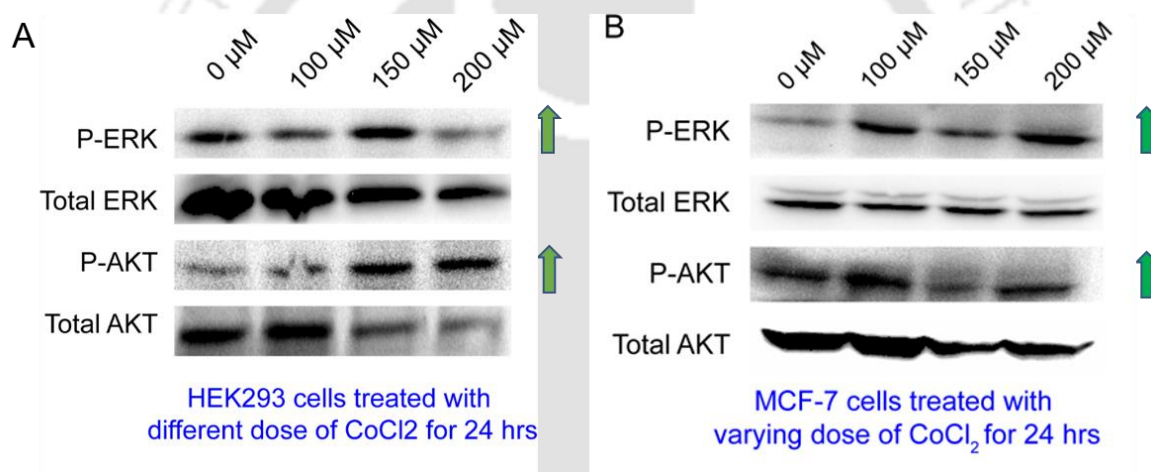


**Figure 4.28.** Western Blotting to detect the phosphorylation status of ERK and AKT in  $\text{CoCl}_2$  treated HEK293 cells (A) Expression of P-ERK and P-AKT on treatment with different doses of  $\text{CoCl}_2$  in HEK293 cells as compared to untreated. (B) Expression of P-ERK and P-AKT on treatment with different doses of  $\text{CoCl}_2$  in MCF-7 cells compared to untreated. Total ERK and Total AKT were used as the loading control.

#### 4.14. Expression Studies of CSC and ESC markers on Cells Subjected to $\text{CoCl}_2$ Treatment:

As demonstrated earlier in the present work, the overexpression of CR-1 leads to the induction of HIF-1 $\alpha$  in the HEK293 cells. Later on, this co-expression of CR-1 and HIF-1 $\alpha$  promoted chemoresistance (induction of MDR-1 expression) and CSCs modulation in HEK293. Similarly, the upregulation of HIF-1 $\alpha$ , under  $\text{CoCl}_2$ -induced hypoxia-like

condition, was shown the co-expression of CR-1 in HEK293. To further explore the effect of  $\text{CoCl}_2$  treatment on CSCs marker expression, the HEK293 cells were treated with  $150 \mu\text{M}$  of  $\text{CoCl}_2$  for 24 h in DMEM media supplemented with 10 % FBS. The expression of CSC markers like CD44, CD24 and CD133 was measured using Real-Time PCR. A significant upregulation in the expression of CD24 and CD44 was observed as expected (**Figure 4.29.A and B**). However, there was no significant change observed in the expression of CD133 (**Figure 4.29.C**).

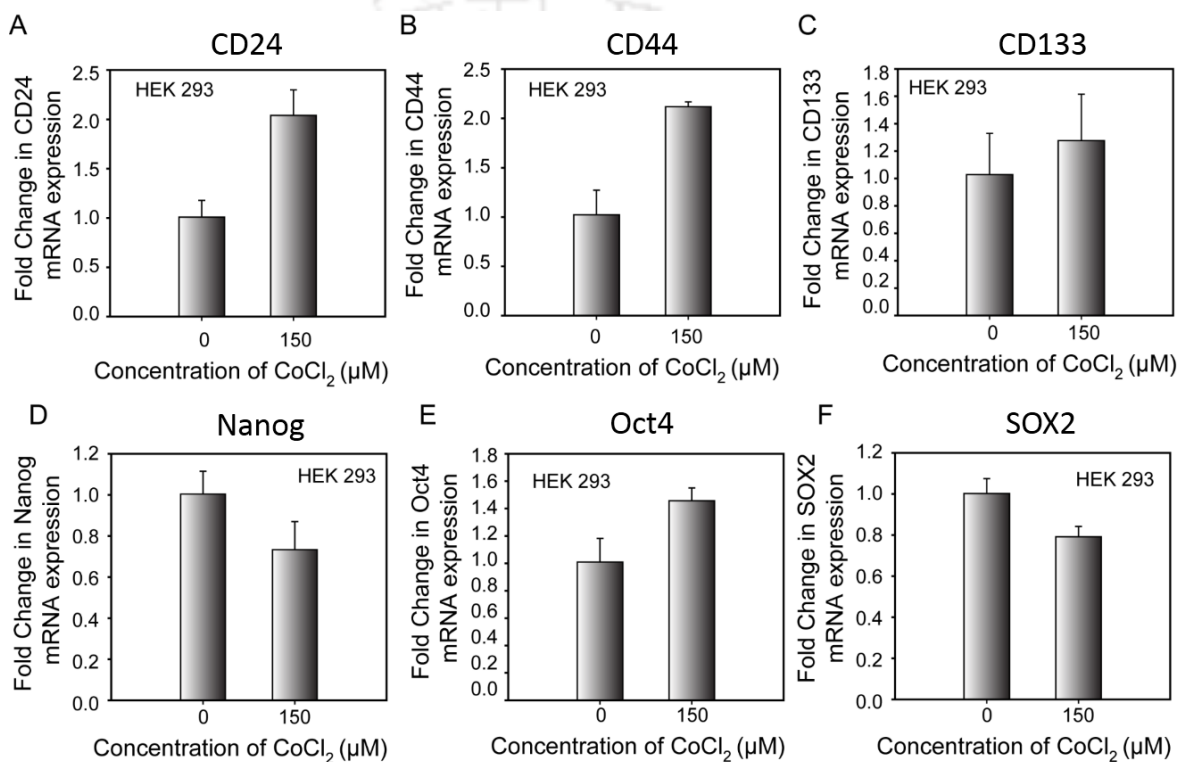


**Figure 4.29.** Effect of Cobalt Chloride on CSCs and ESCs markers: The HEK293 cells were treated with  $\text{CoCl}_2$  for 24 h in serum DMEM media, and the mRNA expression was measured by using Real-time PCR: A) CD24 B) CD44 C) CD133 D) Nanog E) OCT4 and F) SOX2 represents the fold change in mRNA expression in  $\text{CoCl}_2$  treated HEK293 as compared to untreated cells. 18s rRNA was used as endogenous control. Data represented is the mean of a triplicate sample, and the analysis was performed using the Mann Whitney U test. The fold in the expression of CD24, CD44 and OCT4 were statistically significant ( $p < 0.05$ ), whereas fold change in CD133, Nanog, and SOX2 was non-significant.

The Cobalt chloride induced hypoxia was previously reported to promote the expression of CD24, CD133, CD44 and SOX2 in chick embryos (Bauer et al., 2014). Another study

has also demonstrated the induction of CD44 expression and cell cycle arrest in multiple myeloma cell lines (U266) by using  $\text{CoCl}_2$  to induce hypoxia-like conditions (S. Bae et al., 2012).

Subsequently, ESC expression (embryonic stem cells) markers were also analysed using real-time PCR in hypoxia-induced HEK293 cells. As shown in **Figure 4.29 D, E and F**, the treatment with  $\text{CoCl}_2$  for hypoxia induction led to the upregulation of OCT4 expression. Alternately, the expression of Nanog and SOX2 were shown slightly downregulated or unchanged. However, OCT4, Nanog and SOX2 expression was found upregulation in human prostate cancer cell line (PC-3, DU-145 and LnCAP), when grown under hypoxic condition (1 %  $\text{O}_2$ ) and inhibition of HIF-1 $\alpha$  and HIF-2 $\alpha$  leads to the downregulation of SOX2 (K. Bae et al., 2016).

The present data indicate that under hypoxic condition, upregulation of OCT4, CD24 and CD44 occurs in HEK 293 cells. Similar findings were observed in CR-1 overexpressed HEK293, which suggest the possible role of CR-1 and HIF-1 $\alpha$  co-expression in the acquisition of chemoresistance and CSCs enrichment.

#### **4.15. Expression of CR-1 in 2D Monolayer vs 3D Spheroids Model:**

We have previously demonstrated the co-expression of cripto-1 and HIF-1 $\alpha$  in the Cobalt chloride induced hypoxia model. To further verify the co-expression of CR-1 and HIF-1 $\alpha$ , we have chosen another hypoxia positive model, i.e., 3D spheroids. For the formation of 3D spheroids, the cells were allowed to be grown in a 96-well plate coated with 1% agarose solution in serum-free DMEM media for at least 4 days. **Figure 4.30B** shows a representative image of the 3D spheroid of HEK293 cells.

We went ahead to study the expression of CR-1 in HEK293 spheroids grown for different time points by using Real-Time PCR. As shown in **Figure 4.31. (A and B)**, with the increase in age (in days) of spheroids, the expression of CR-1 also increases compared to monolayer due to the generation of more and more hypoxia core.

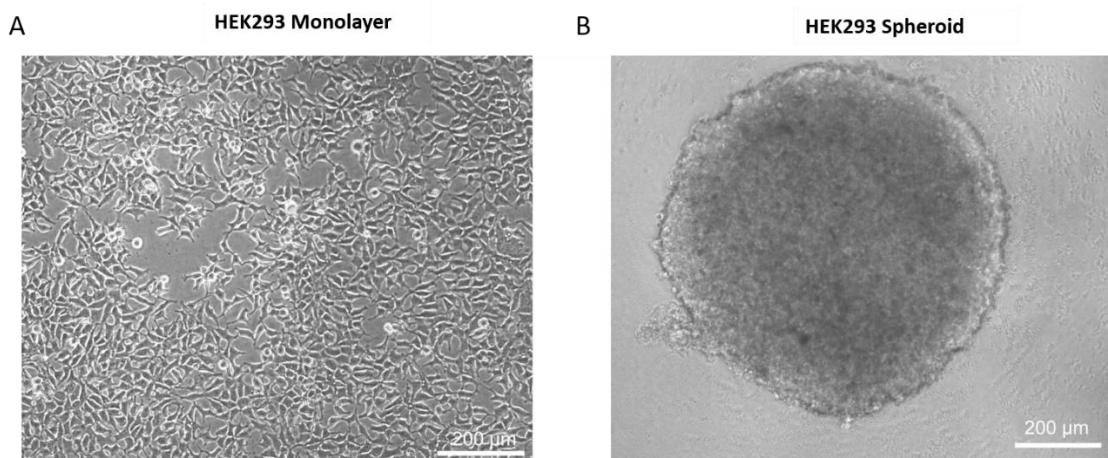


**Figure 4.30.** Bright-field microscopic image showing morphological differences between HEK293 Monolayer vs 3D Spheroids. The scale bar of the image is 200 μm.

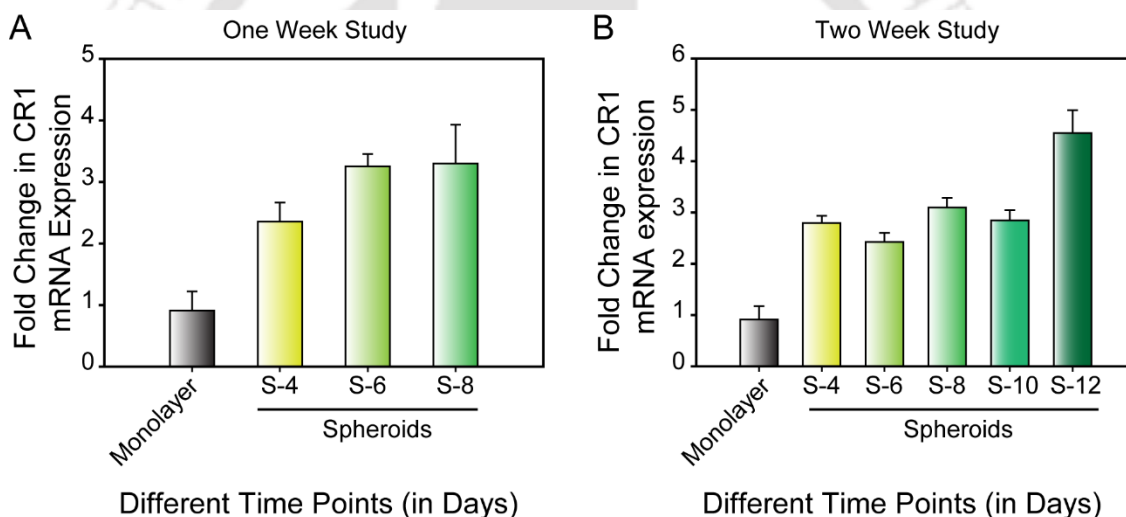


**Figure 4.31.** Expression of CR-1 in 2D monolayer vs 3D spheroids: The HEK293 cells were allowed to grow up to different time points, and Real-Time PCR measured the fold change in mRNA expression. A) And B) represents the induction of CR-1 expression in 3D spheroids grown for different time points. S-4, S-6 and S-8 represent the spheroids grown for 4, 6, and 8 days respectively. 18s rRNA was used as endogenous control. Data represented are the mean of a triplicate sample, and the analysis was performed by using Kruskal-Wallis analysis of variance. The fold in the expression of all the genes was statistically significant ( $p < 0.05$ ).

We further compared the co-expression of CR-1 and HIF-1 $\alpha$  between the monolayer (2D) and spheroids (3D) model. Spheroids are known to have a hypoxic core (Kolenda et al., 2011), **Figure 4.32. (B and E)**, represents a significant rise in the expression of HIF-1 $\alpha$  in spheroids compared to the monolayer.

The expression of HIF1 $\alpha$  and MDR-1 remain the same in both EV and CR-1 transfected cells **Figure 4.32. (B, C, E and F)**. However, as seen in **Figure 4.32. (A and D)**, the expression of CR-1 was found to be a bit higher in HEK-CR-1 spheroids as compared to the HEK-EV spheroids. This may be due to the formation of more hypoxic core in the HEK-CR-1 spheroids than the HEK-EV spheroids, which results in higher expression of HIF-1 $\alpha$ , which further induces the expression of CR-1.

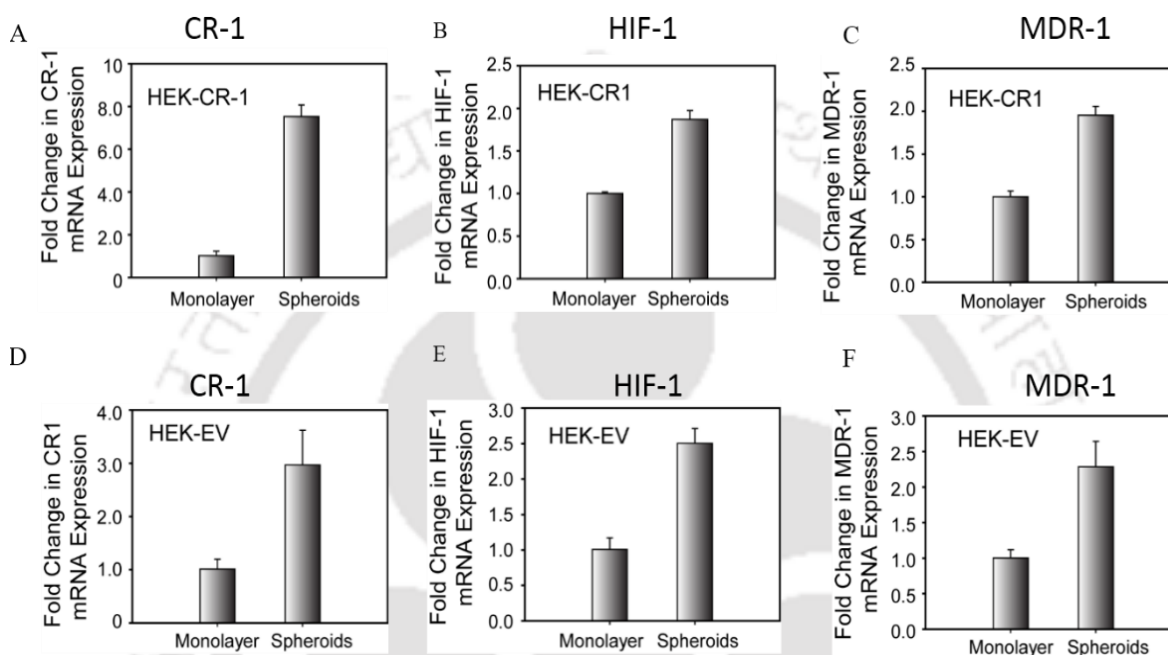


**Figure 4.32.** Co-expression of CR-1 and HIF-1 $\alpha$  in 3D spheroids was detected by using Real-Time PCR. The Top row bar plot represents the fold change in expression of A) CR-1, B) HIF-1 $\alpha$ , and C) MDR-1 in the HEK-CR-1 spheroids compared to HEK-CR-1 monolayer. The bottom row bar plot represents the fold change in expression of D) CR-1 E) HIF-1 $\alpha$  and D) MDR-1 in the HEK-EV spheroids compared to the HEK-EV monolayer. 18s rRNA was used as endogenous control. Data represented are the mean of a triplicate sample, and the analysis was performed using the Mann Whitney U test. The fold in the expression of all the genes was statistically significant ( $p < 0.05$ ).

Furthermore, the co-expression of CR-1 and HIF-1 $\alpha$  was verified on the protein level by using western blotting. As shown in **Figure 4.33.A**, a significant rise in the expression of CR-1, HIF-1 $\alpha$  and MDR-1 was observed in HEK293 cells compared to the monolayer. Similarly, MCF-7 spheroids, **Figure 4.33.B**, also show significant upregulation in the expression of CR-1, HIF-1 $\alpha$  and MDR-1 compared to MCF-7 monolayer. Earlier studies have been showing a correlation between HIF-1 $\alpha$ , MDR-1 and ESCs markers(OCT4,

Nanog and SOX2)(Mathieu et al., 2011) (M. D. R. Gene et al., 2002) in 3D spheroids. However, there are no concrete reports on the co-expression of HIF-1 $\alpha$  and CR-1 in spheroids so far. Alternately, the expression of MDR-1 was shown to co-express with HIF-1 $\alpha$  in triple-negative breast cancer cell lines (Samanta et al., 2014). Simultaneously, the MDR-1 expression was also shown to co-express with CR-1 in CR-1- positive cells isolated by FACS from C8161 cells and exhibit the ability to form the sphere. Taken together, our data represent the upregulation of CR-1 expression in spheroids with hypoxic core, which further induces the expression of MDR-1, CSCs and ESCs markers to promoter proliferation, migration and invasion in cancer cells.

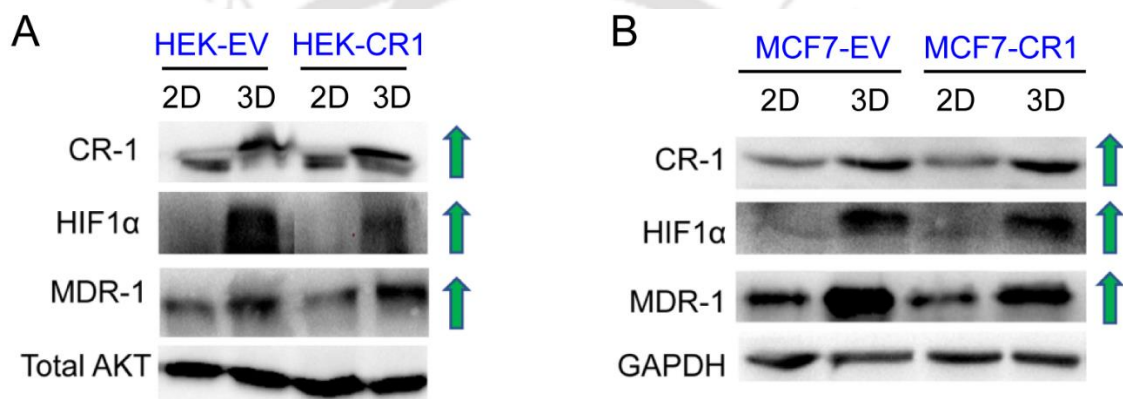


**Figure 4.33.** Western blotting shows the Co-expression of HIF-1 $\alpha$  and CR-1 in 3D spheroids: **A)** Expression of CR-1, HIF-1 $\alpha$  and MDR-1 in monolayer vs spheroids comparison of HEK293 clones. **B)** Expression of CR-1, HIF-1 $\alpha$  and MDR-1 in monolayer vs spheroids comparison of MCF7 clones. GAPDH and Total AKT were used as the loading control.

#### 4.16. Studies on the Activation of ERK in the 3D Spheroid Model:

To elucidate the pathways which were followed in 3D spheroids for the co-expression of CR-1 and HIF-1 $\alpha$ . We investigated the phosphorylation pattern of canonical oncogenic pathways, i.e., the ERK pathway, which mainly mediates cancer cells' growth, maintenance, and proliferation.

As evident from **Figure 4.34.A**, the ERK pathways get highly phosphorylated in the spheroids generated from the different clones of HEK293 cells (HEK-EV and HEK-CR-1). Simultaneously, P-ERK expression was also upregulated in CR-1 transfected cells compared to EV transfected HEK293. This indicates the pro-proliferative activity of CR-1 in HEK293 cells. Likewise, MCF-7 spheroids also show the activation of the ERK

pathway, as evident from **Figure 4.34.B**. Contrastingly, the MCF-CR-1 cells do not display any change in P-ERK expression compared to MCF-EV cells.

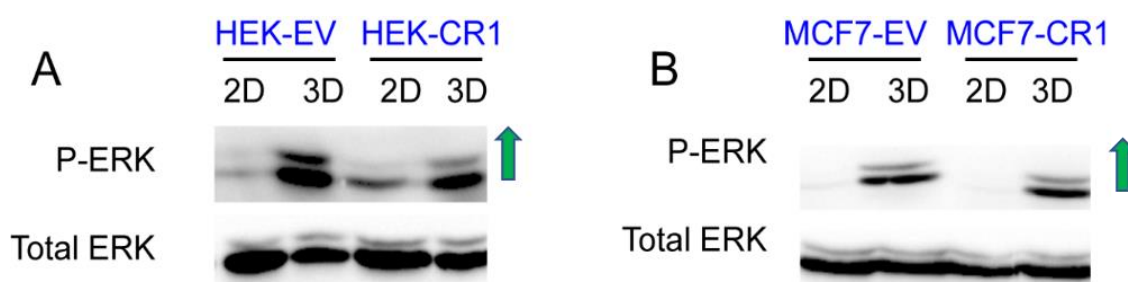


**Figure 4.34.** Western Blotting to detect the phosphorylation status of ERK (A) Expression of P-ERK in monolayer vs spheroids comparison of HEK293 clones. (B) Expression of P-ERK in monolayer vs spheroids comparison of MCF-7 clones. Total ERK was used as the loading control

As per literature, most previous studies have reported the activation of the MAPK pathway in spheroids compared with monolayer cells (Da He et al., 2017). Surprisingly, the chemical inhibition of the MAPK pathway leads to the activation of the AKT pathway (Tavana et al., 2020) and a reduction in spheroids' size (Sarah J. Harmych et al. This represents the shifting of the cell from one pathway to another for growth and survival.

#### 4.17. The Fate of CSC and ESC Markers in the 3D Spheroids Hypoxic Model:

Spheroids are known to have a hypoxic core and proliferative ring across the periphery. Most CSCs exist at the peripheral ring, and treatment with anticancer agents like paclitaxel and cisplatin has been observed to reduce spheroids' size by affecting the periphery population, not the spheroid core (Reynolds et al., 2017). Literature reports suggest that spheroids grown in serum-free media containing different additive growth factors like FGF, EGF, Insulin and hydrocortisone, exhibit enriched CSCs population compared to the spheroids grown in regular serum media (Herheliuk et al., 2019). Spheroids formed from cells derived from colorectal cancer patients show a higher percentage of CR-1 positive population. These CR-1<sup>+</sup> cells have been seen to exhibit higher level expression of intestinal stemness markers like Nanog, Lgr5 and EphB2, whereas the corresponding spheroids showed upregulation of CD44, CD133, SOX2 and bmi (Francescangeli et al., 2015).

As depicted previously, the co-expression of CR-1 and HIF-1 $\alpha$  induces the CSCs and ESC population and chemoresistance in the cells. To verify the occurrence of CSCs in 3D spheroids, we analyzed the expression of different CSCs markers (CD24, CD44, and CD133) and ESCs markers (OCT4, Nanog, and SOX2). We performed quantitative Real-time PCR based studies to compare these markers' expression between 2D monolayer and 3D spheroids to check the expression. As shown in **Figure 4.35 (A, B, and C)**, we observed significant upregulation in the expression levels of CD24, CD44 and CD133.

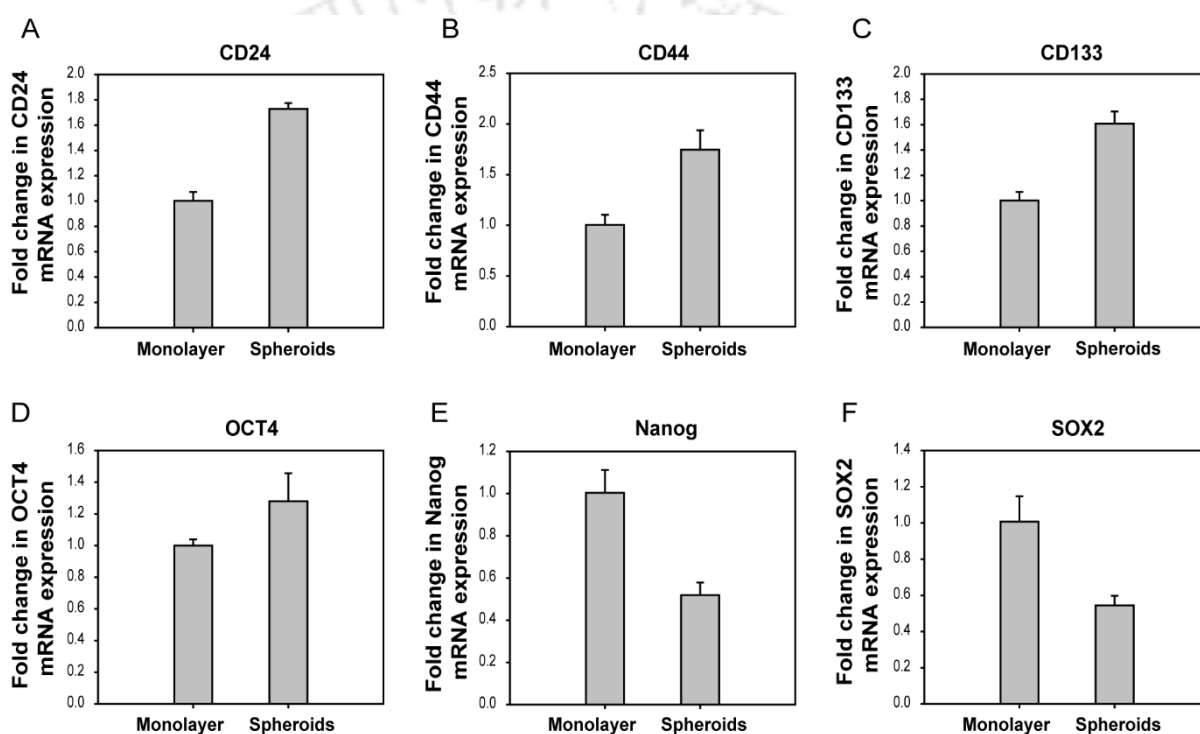


**Figure 4.35.** CSCs and ESCs markers expression in 3D spheroids: The HEK293 spheroids were formed after 4 days of cell seeding. The expression of CSC and ESC markers spheroids was compared by monolayer and detected by using Real-time PCR: A) CD24 B) CD44 C) CD133 D) OCT4 E) Nanog and F) SOX2 represents the fold change in mRNA expression in spheroids as compared to HEK293 monolayer. 18s rRNA was used as endogenous control. Data represented are the mean of a triplicate sample, and the analysis was performed using the Mann Whitney U test. The fold in the expression of all the genes was statistically significant ( $p < 0.05$ ).

Subsequently, we also checked the expression of ESCs marker, i.e., OCT4, Nanog and SOX2 in 3D spheroids compared to the 2D monolayer of HEK293 cells. As depicted in

**Figure 4.35. (D, E, and F)** we observed significantly higher expression of OCT4, whereas Nanog and SOX2 were found downregulated in 3D spheroids.

Literature suggests that single-celled spheroids (SS) derived from gastric adenocarcinoma cell lines (SNU-638 and SNU-484) exhibited higher expression of Nanog and SOX2 as compared to parental cells or Traditional spheroids (TS). In contrast, the expression of OCT4 remains unchanged or downregulated (J. W. Lee et al., 2018). Consistent with our finding, H. Liu et al., in 2016, previously demonstrated the occurrence of CD44+/CD24+ population highly resistant to radiotherapy and chemotherapy in Cervical cancer cell line (SiHa cell). This CD44+/CD24+ population was shown to resist apoptosis and have a Higher expression of surviving OCT4 and Bcl2.

#### **4.18. Effect of CR-1 Overexpression on 3D Spheroids:**

In continuation of our work, we further explore the effect of CR-1 overexpression in spheroid formation. We observed that both HEK-CR-1 and wild-type HEK293 cells show spheroid forming capacity in 4 days. However, the HEK-CR-1 clone forms more hypoxia core visually (data not shown). Subsequently, the expression of CR-1, HIF-1 $\alpha$ , and MDR-1 was measured by Real-Time PCR. In **Figure 4.36.B.**, we observed that HEK-CR-1 cells show significantly higher expression of CR-1 compared to wild-type HEK293. The observation was obviously due to the overexpression of CR-1 in HEK293 cells by stable transfection. However, In **Figure 4.36.A.**, the expression of HIF-1 $\alpha$  was significantly upregulated in HEK-CR-1 compared with wild-type. This further confirms our hypothesis that CR-1 overexpression induces HIF-1 $\alpha$  expression.

Likewise, HEK-CR-1 cells, wild-type HEK293, also formed a hypoxic core, but a bigger hypoxic core was observed in the latter. Subsequently, we also compared the expression of CSCs marker CD24, OCT4 and chemoresistant gene MDR-1. As shown in **Figure 4.36. (C, D, and E)** the expression of MDR-1 and CD24 was found upregulated in HEK-CR-1 as compared to wild-type HEK293 cells. The spheroids derived from CR-1-positive cells also showed upregulation of MDR-1 in concurrence to what has been previously reported by (Luigi Strizzi et al., 2013) and CSCs enrichment in Colorectal cancer cells (Francescangeli et al., 2015). However, The expression of OCT4 remained the same or marginally downregulated in HEK-CR-1, which indicates the regulation of

OCT4 by HIF-2 $\alpha$  as also seen in the literature (Covello et al., 2006). The expression of OCT4 was also shown to downregulate on siRNA inhibition of HIF1 $\alpha$ , HIF2 $\alpha$  and HIF $\beta$ , which was in concurrence with (Mathieu et al., 2011).

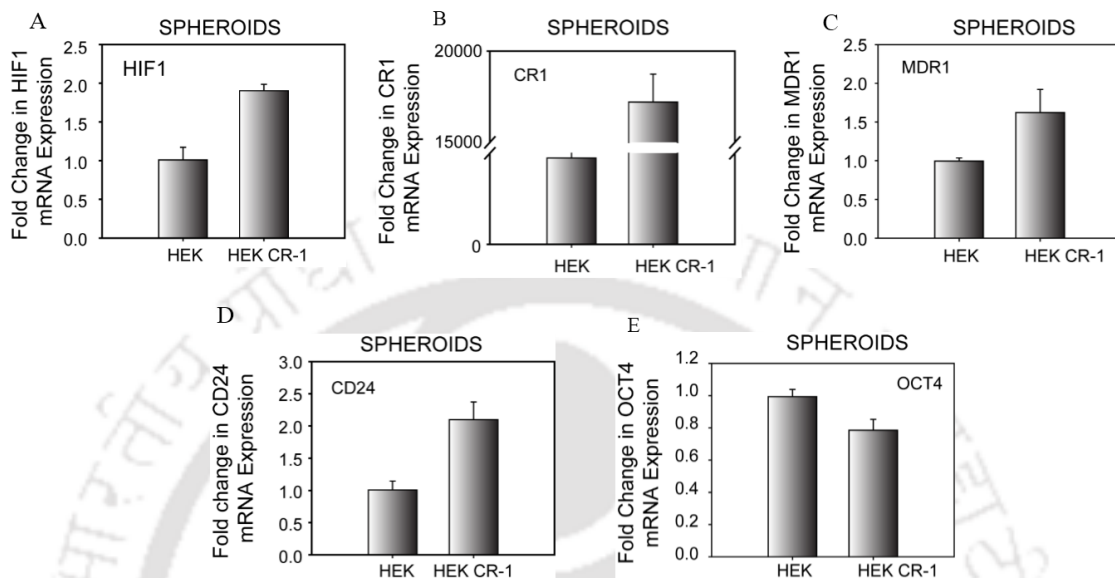


**Figure 4.36.** Effect of CR-1 overexpression on 3D spheroids: The spheroids were formed after 4 days of cell seeding. The expression of CR-1, HIF-1 $\alpha$  and MDR-1 was analyzed in the HEK-CR-1 spheroids as compared to HEK293 spheroids and detected by using Real-time PCR: A) HIF-1 $\alpha$  B) CR-1 C) MDR-1 D) CD24 and E) OCT4 represents the fold change in mRNA expression in HEK-CR-1 spheroids as compared to HEK293 spheroids. 18s rRNA was used as endogenous control. Data represented is the mean of triplicate sample and the analysis was performed by using Mann Whitney U test. The fold in expression of HIF-1 $\alpha$ , CR-1, MDR-1 and CD24 were statistically significant ( $p < 0.05$ ), whereas fold change in OCT-4 expression was not significant ( $p > 0.05$ ).

**CONCLUSION**

**And**

**FUTURE PERSPECTIVES**





## 5.1. Conclusion and Future perspectives:

In the present study, we investigated the role of the MAPK and AKT pathways in regulating cripto-1 expression. We had observed that inhibition of MAPK pathway and PI3K pathway reduced expression of CR-1, mostly at higher doses of inhibitors. However, TGF- $\beta$ , the known inducer of CR-1 expression, failed to cause induction in presence of the inhibitors of these two pathways. These observations indicate that both MAPK and PI3K pathway has some positive modulatory effect on TGF- $\beta$ /ALK4/SMAD2/3 pathway-mediated expression of CR-1. In some experimental systems, CR-1 is known to induce activation of MAPK and PI3K pathways through some SMAD-independent mechanisms. Following those observations along with ours in the present work, one may suggest that CR-1 have multiple autoregulatory pathways involving TGF- $\beta$ , MAPK and PI3K pathways.

We also studied the interplay between cripto-1 and HIF-1 $\alpha$  and their role in the maintenance and proliferation of embryonic/cancer stem cells and chemoresistance in HEK293 cells. We observed the co-expression of HIF-1 $\alpha$  and MDR-1 expression in cripto-1 overexpressing cells. The CR-1 overexpressing cells also show upregulated expression of cancer stem cell markers (CD44, CD24, and CD133) and ESCs marker (OCT-4 and Nanog). HEK293 cells also show higher CSCs and ESCs expression on treatment with recombinant cripto-1 protein. Cancer stem cell markers are associated with highly progressive and metastatic cancer. However, the expression of these markers is not universal to all types of cancer. Hence, it is challenging to target CSCs markers for prognosis and management of cancer of different origins. On the other hand, cripto-1 is a known modulator of CSCs and ESCs markers in various types of cancer, making it an attractive target for cancer prognosis and therapeutics.

Subsequently, the enhanced activity proliferative pathway, i.e., MAPK and AKT pathways, were shown in CR-1 overexpressing HEK293 cells. The CR-1 overexpressing cells also shows a higher proliferation rate compared to empty vector-transfected cells. Moreover, the drug sensitivity assay reveals that MCF-CR-1 cells show higher resistance than MCF-EV cells against the paclitaxel and doxorubicin treatment.

In contrast, HIF-1 $\alpha$  is also reported to be associated with the regulation of CSCs and ESCs marker expression. To further elucidate the correlation of HIF-1 $\alpha$  and CR-1 with the expression of CSCs, ESCs markers and MDR-1, we used cobalt chloride (a chemical

inducer of hypoxia) and 3D spheroid (hypoxia core) as the hypoxic models. On treatment with  $\text{CoCl}_2$ , the HIF-1 $\alpha$  increases along with that enhanced coexpression of CR-1 and MDR-1 was also observed in HEK293 cells. Subsequently, upregulation in CD44, CD24 and OCT-4 expression was also observed. Moreover, both MAPK and AKT pathways were shown activated under hypoxia-like conditions induced by  $\text{CoCl}_2$  treatment.

Furthermore, 3D spheroids formed by HEK293 and MCF-7 cells show an upregulation of CR-1 expression compared to the 2D monolayer. The expression of CR-1 increases with age (in days) of spheroids as the older spheroids forms a more hypoxic core. This further correlates the expression of CR-1 and HIF-1 $\alpha$ . The early embryonic development, which CR-1 mediates, also occurs under hypoxic conditions. Therefore, the formation of the hypoxia core in the tumour might be one of the several reasons for the reappearance of CR-1 expression in adults. 3D spheroids also show increased expression of MDR-1, OCT4 and CSCs markers (CD24, CD44 and CD133). We also observed the MAPK pathway activity in 3D spheroids compared to monolayer, which contributes to the proliferation of the periphery of the spheroids.

We also compared the expression of HIF-1 $\alpha$ , CR-1 and MDR-1 between the HEK-EV and HEK-CR-1 spheroids. We observed HEK-CR-1 spheroids shows higher expression of HIF-1 $\alpha$  and MDR-1 compared to HEK-EV spheroids. The possible reason for this is that the spheroids formed from HEK-CR-1 always have a bigger hypoxic core compared to HEK-EV spheroids.

Overall, the present study provides curial information about the regulation of CR-1 expression and its effect on the other oncogenic molecules. We have shown the coexpression of CR-1 and HIF-1 $\alpha$  and their implication on the CSCs/ESCs and chemoresistance. However, it is yet to explore whether CR-1 directly controls the expression of MDR-1, CSC/ESC marker or it is mediated by HIF-1 $\alpha$ . Gene silencing and dominant negative mice models can be a good approach to explore these phenomena. Understanding of exact regulators of these phenomena may help in targeting cancer in a better way.





## Bibliography

Aasen, T., Raya, A., Barrero, M. J., Garreta, E., Consiglio, A., Gonzalez, F., Vassena, R., Bilić, J., Pekarik, V., Tiscornia, G., Edel, M., Boué, S., & Belmonte, J. C. I. (2008). Efficient and rapid generation of induced pluripotent stem cells from human keratinocytes. *Nature Biotechnology*, *26*(11), 1276–1284.  
<https://doi.org/10.1038/nbt.1503>

Abell, A. N., & Johnson, G. L. (2014). Implications of Mesenchymal Cells in Cancer Stem Cell Populations: Relevance to EMT. *Current Pathobiology Reports*, *2*(1), 21–26. <https://doi.org/10.1007/s40139-013-0034-7>

Ackland, M. L., Newgreen, D. F., Fridman, M., Waltham, M. C., Arvanitis, A., Minichiello, J., Price, J. T., & Thompson, E. W. (2003). Epidermal Growth Factor-Induced Epithelio-Mesenchymal Transition in Human Breast Carcinoma Cells. *Laboratory Investigation*, *83*(3), 435–448.  
<https://doi.org/10.1097/01.LAB.0000059927.97515.FD>

Adamson, E. D., Minchiotti, G., & Salomon, D. S. (2002). Cripto: A tumor growth factor and more. *Journal of Cellular Physiology*, *190*(3), 267–278.  
<https://doi.org/10.1002/jcp.10072>

Adkins, H. B., Bianco, C., Schiffer, S. G., Rayhorn, P., Zafari, M., Cheung, A. E., Orozco, O., Olson, D., De Luca, A., Chen, L. L., Miatkowski, K., Benjamin, C., Normanno, N., Williams, K. P., Jarpe, M., LePage, D., Salomon, D., & Sanicola, M. (2003). Antibody blockade of the Cripto CFC domain suppresses tumour cell growth in vivo. *The Journal of Clinical Investigation*, *112*(4), 575–587.  
<https://doi.org/10.1172/JCI17788>

Agani, F. (n.d.). Oxygen-independent regulation of HIF-1: novel involvement of PI3K/AKT/mTOR pathway in cancer. In *Current cancer drug targets* (Vol. 13, Issue 3, pp. 245–251). <https://doi.org/info:doi/>

Agliano, A., Calvo, A., & Box, C. (2017). The challenge of targeting cancer stem cells to halt metastasis. *Seminars in Cancer Biology*, *44*, 25–42.  
<https://doi.org/10.1016/j.semcancer.2017.03.003>

Al-Fahdawi, A. R. M. G., Hamad, M. A., & Al-Hadithy, E. M. R. (2019).

- Teratocarcinoma-derived growth factor-1 (TDGF-1): A guide molecule for monitoring the treatment success of Iraqi patients with colorectal carcinoma. *Indian Journal of Forensic Medicine and Toxicology*, 13(4), 1085–1089.  
<https://doi.org/10.5958/0973-9130.2019.00444.4>
- Al-Hajj, M., Wicha, M. S., Benito-Hernandez, A., Morrison, S. J., & Clarke, M. F. (2003). Prospective identification of tumorigenic breast cancer cells. *Proceedings of the National Academy of Sciences*, 100(7), 3983–3988.  
<https://doi.org/10.1073/pnas.0530291100>
- Al-Hajj, Muhammad, & Clarke, M. F. (2004). Self-renewal and solid tumor stem cells. *Oncogene*, 23(43 REV. ISS. 6), 7274–7282.  
<https://doi.org/10.1038/sj.onc.1207947>
- Alam, M. J., Takahashi, R., Afify, S. M., Oo, A. K. K., Kumon, K., Nawara, H. M., Khayrani, A. C., Du, J., Zahra, M. H., Seno, A., Salomon, D. S., & Seno, M. (2018). Exogenous cripto-1 suppresses self-renewal of cancer stem cell model. *International Journal of Molecular Sciences*, 19(11).  
<https://doi.org/10.3390/ijms19113345>
- ALHulais, R. A., & Ralph, S. J. (2019). Cancer stem cells, stemness markers and selected drug targeting: metastatic colorectal cancer and cyclooxygenase-2/prostaglandin E2 connection to WNT as a model system. *Journal of Cancer Metastasis and Treatment*, 2019. <https://doi.org/10.20517/2394-4722.2018.71>
- Alowaidi, F., Hashimi, S. M., Alqurashi, N., Wood, S. A., & Wei, M. Q. (2019). Cripto-1 overexpression in U87 glioblastoma cells activates MAPK, focal adhesion and ErbB pathways. *Oncology Letters*, 18(3), 3399–3406.  
<https://doi.org/10.3892/ol.2019.10626>
- Ambudkar, S. V, Kimchi-Sarfaty, C., Sauna, Z. E., & Gottesman, M. M. (2003). P-glycoprotein: from genomics to mechanism. *Oncogene*, 22(47), 7468–7485.  
<https://doi.org/10.1038/sj.onc.1206948>
- Angelini, A., Di Febbo, C., Ciofani, G., Di Nisio, M., Baccante, G., Di Ilio, C., Cuccurullo, F., & Porreca, E. (2005). Inhibition of P-glycoprotein-mediated multidrug resistance by unfractionated heparin. A new potential chemosensitizer

- for cancer therapy. *Cancer Biology and Therapy*, 4(3), 313–317.  
<https://doi.org/10.4161/cbt.4.3.1503>
- Aplin, A. E., Kaplan, F. M., & Shao, Y. (2011). Mechanisms of resistance to RAF inhibitors in melanoma. *Journal of Investigative Dermatology*, 131(9), 1817–1820. <https://doi.org/10.1038/jid.2011.147>
- Ardyanto, T. D. W. I., Osaki, M., & Tokuyasu, N. (2006). *CoCl<sub>2</sub>-induced HIF-1 expression correlates with proliferation and apoptosis in MKN-1 cells: A possible role for the PI3K/Akt pathway*. 549–555.
- Ayob, A. Z., & Ramasamy, T. S. (2018). Cancer stem cells as key drivers of tumour progression. *Journal of Biomedical Science*, 25(1), 1–18.  
<https://doi.org/10.1186/s12929-018-0426-4>
- Bae, K. M., Dai, Y., Vieweg, J., & Siemann, D. W. (2016). Hypoxia regulates SOX2 expression to promote prostate cancer cell invasion and sphere formation. *American Journal of Cancer Research*, 6(5), 1078–1088.
- Bae, S., Jeong, H., Cha, H. W. A. J. U. N., Kim, K., Choi, Y. M. I. N., An, I., Koh, H. J., Lim, D. A. E. J. I. N., Lee, S., & An, S. (2012). *The hypoxia-mimetic agent cobalt chloride induces cell cycle arrest and alters gene expression in U266 multiple myeloma cells*. *Mm*, 1180–1186. <https://doi.org/10.3892/ijmm.2012.1115>
- Baldassarre, G., Tucci, M., Lembo, G., Pacifico, F. M., Dono, R., Lago, C. T., Barra, A., Bianco, C., Viglietto, G., Salomon, D., & Persico, M. G. (2001). A truncated form of teratocarcinoma-derived growth factor-1 (cripto-1) mRNA expressed in human colon carcinoma cell lines and tumors. *Tumour Biology: The Journal of the International Society for Oncodevelopmental Biology and Medicine*, 22(5), 286–293. <https://doi.org/10.1159/000050629>
- Bandeira, C. L., Urban Borbely, A., Pulcineli Vieira Francisco, R., Schultz, R., Zugaib, M., & Bevilacqua, E. (2014). Tumorigenic factor CRIPTO-1 Is immunolocalized in extravillous cytotrophoblast in placenta creta. *BioMed Research International*, 2014. <https://doi.org/10.1155/2014/892856>
- Bao, B., Ahmad, A., Azmi, A. S., Ali, S., & Sarkar, F. H. (2013). Overview of cancer stem cells (CSCS) and mechanisms of their regulation: Implications for cancer

- therapy. *Current Protocols in Pharmacology*, SUPPL.61, 1–18.  
<https://doi.org/10.1002/0471141755.ph1425s61>
- Bauer, N., Liu, L., Aleksandrowicz, E., & Herr, I. (2014). Establishment of hypoxia induction in an in vivo animal replacement model for experimental evaluation of pancreatic cancer. *Oncology Reports*, 32(1), 153–158.  
<https://doi.org/10.3892/or.2014.3196>
- Benita, Y., Kikuchi, H., Smith, A. D., Zhang, M. Q., Chung, D. C., & Xavier, R. J. (2009). An integrative genomics approach identifies Hypoxia Inducible Factor-1 (HIF-1)-target genes that form the core response to hypoxia. *Nucleic Acids Research*, 37(14), 4587–4602. <https://doi.org/10.1093/nar/gkp425>
- Berra, E., Benizri, E., Ginouvès, A., Volmat, V., Roux, D., & Pouyssegur, J. (2003). HIF prolyl-hydroxylase 2 is the key oxygen sensor setting low steady-state levels of HIF-1 $\alpha$  in normoxia. *EMBO Journal*, 22(16), 4082–4090.  
<https://doi.org/10.1093/emboj/cdg392>
- Bianco, C., Adkins, H., & Wechselberger, C. (2002). Cripto-1 activates nodal-and ALK4-dependent and-independent signalling pathways in mammary epithelial Cells. *And Cellular Biology*. <http://mcb.asm.org/content/22/8/2586.short>
- Bianco, C., Castro, N., & Baraty, C. (2013). Regulation of human Cripto-1 expression by nuclear receptors and DNA promoter methylation in human embryonal and breast cancer cells. *Journal of Cellular*.  
<http://onlinelibrary.wiley.com/doi/10.1002/jcp.24271/full>
- Bianco, C., Cotten, C., Lonardo, E., & Strizzi, L. (2009). Cripto-1 is required for hypoxia to induce cardiac differentiation of mouse embryonic stem cells. *The American Journal Of*.  
<http://www.sciencedirect.com/science/article/pii/S0002944010607237>
- Bianco, C., Strizzi, L., Ebert, A., & Chang, C. (2005). Role of human cripto-1 in tumor angiogenesis. *Journal of The*. <http://jnci.oxfordjournals.org/content/97/2/132.short>
- Bianco, C., Strizzi, L., Normanno, N., & Khan, N. (2005). Cripto-1: an oncofetal gene with many faces. *Curr Top Dev*.  
<https://books.google.co.in/books?hl=en&lr=&id=5mrkoiZAXX4C&oi=fnd&pg=P>

A85&dq=Cripto-

1:+an+oncofetal+gene+with+many+faces&ots=zDEyxiwTi&sig=9A6HTFptR4  
HBBXR6iF7GChAkn94

Bianco, C, Wechselberger, C., Ebert, A., & Khan, N. (2001). Identification of Cripto-1 in human milk. *Breast Cancer Research*.  
<http://link.springer.com/article/10.1023/A:1010648923432>

Bianco, Caterina, Adkins, H. B., Wechselberger, C., Seno, M., Normanno, N., De Luca, A., Sun, Y., Khan, N., Kenney, N., Ebert, A., Williams, K. P., Sanicola, M., & Salomon, D. S. (2002). Cripto-1 Activates Nodal- and ALK4-Dependent and -Independent Signalling Pathways in Mammary Epithelial Cells. *Molecular and Cellular Biology*, 22(8), 2586–2597. <https://doi.org/10.1128/mcb.22.8.2586-2597.2002>

Bianco, Caterina, Castro, N. P., Baraty, C., Rollman, K., Held, N., Rangel, M. C., Karasawa, H., Gonzales, M., Strizzi, L., & Salomon, D. S. (2013). Regulation of human Cripto-1 expression by nuclear receptors and DNA promoter methylation in human embryonal and breast cancer cells. *Journal of Cellular Physiology*, 228(6), 1174–1188. <https://doi.org/10.1002/jcp.24271>

Bianco, Caterina, Cotten, C., Lonardo, E., Strizzi, L., Baraty, C., Mancino, M., Gonzales, M., Watanabe, K., Nagaoka, T., Berry, C., Arai, A. E., Minchiotti, G., & Salomon, D. S. (2009). Cripto-1 is required for hypoxia to induce cardiac differentiation of mouse embryonic stem cells. *American Journal of Pathology*, 175(5), 2146–2158. <https://doi.org/10.2353/ajpath.2009.090218>

Bianco, Caterina, Mysliwiec, M., Watanabe, K., Mancino, M., Nagaoka, T., Gonzales, M., & Salomon, D. S. (2008). Activation of a Nodal-independent signalling pathway by Cripto-1 mutants with impaired activation of a Nodal-dependent signalling pathway. *FEBS Letters*, 582(29), 3997–4002.  
<https://doi.org/10.1016/j.febslet.2008.10.052>

Bianco, Caterina, Rangel, M. C., Castro, N. P., Nagaoka, T., Rollman, K., Gonzales, M., & Salomon, D. S. (2010a). Malignant Progression. *The American Journal of Pathology*, 177(2), 532–540. <https://doi.org/10.2353/ajpath.2010.100102>

- Bianco, Caterina, Rangel, M. C., Castro, N. P., Nagaoka, T., Rollman, K., Gonzales, M., & Salomon, D. S. (2010b). Role of Cripto-1 in stem cell maintenance and malignant progression. *American Journal of Pathology*, *177*(2), 532–540.  
<https://doi.org/10.2353/ajpath.2010.100102>
- Bianco, Caterina, & Salomon, D. S. (2010). Targeting the embryonic gene Cripto-1 in cancer and beyond. *Expert Opinion on Therapeutic Patents*, *20*(12), 1739–1749.  
<https://doi.org/10.1517/13543776.2010.530659>
- Bianco, Caterina, Strizzi, L., Ebert, A., Chang, C., Rehman, A., Normanno, N., Guedez, L., Salloum, R., Ginsburg, E., Sun, Y., Khan, N., Hirota, M., Wallace-Jones, B., Wechselberger, C., Vonderhaar, B. K., Tosato, G., Stetler-Stevenson, W. G., Sanicola, M., & Salomon, D. S. (2005). Role of human cripto-1 in tumor angiogenesis. *Journal of the National Cancer Institute*, *97*(2), 132–141.  
<https://doi.org/10.1093/jnci/dji011>
- Bianco, Caterina, Strizzi, L., Normanno, N., Khan, N., & Salomon, D. S. (2005). Cripto-1: An Oncofetal Gene with Many Faces. In *Current Topics in Developmental Biology* (Vol. 67, Issue 04). Elsevier Masson SAS.  
[https://doi.org/10.1016/S0070-2153\(05\)67003-2](https://doi.org/10.1016/S0070-2153(05)67003-2)
- Bianco, Caterina, Strizzi, L., Rehman, A., Normanno, N., Wechselberger, C., Sun, Y., Khan, N., Hirota, M., Adkins, H., Williams, K., Margolis, R. U., Sanicola, M., & Salomon, D. S. (2003). *Advances in Brief A Nodal- and ALK4-independent Signalling Pathway Activated by Cripto-1 through*. *153035*, 1192–1197.
- Bolós, V., Grego-Bessa, J., & de la Pompa, J. L. (2007). Notch Signalling in Development and Cancer. *Endocrine Reviews*, *28*(3), 339–363.  
<https://doi.org/10.1210/er.2006-0046>
- Bonnet, D., & Dick, J. E. (1997). Human acute myeloid leukemia is organized as a hierarchy that originates from a primitive hematopoietic cell. *Nature Medicine*, *3*(7), 730–737. <https://doi.org/10.1038/nm0797-730>
- Bonnet D, D. J. (1997). Human acute myeloid leukemia is organized as a hierarchy that originates from a primitive hematopoietic cell. *Nat Med.*, *3*, 730–737.
- Bononi, A., Agnoletto, C., De Marchi, E., Marchi, S., Patergnani, S., Bonora, M.,

- Giorgi, C., Missiroli, S., Poletti, F., Rimessi, A., & Pinton, P. (2011). Protein kinases and phosphatases in the control of cell fate. *Enzyme Research*, 2011(1). <https://doi.org/10.4061/2011/329098>
- Boutros, T., Chevet, E., & Metrakos, P. (2008). Mitogen-Activated Protein (MAP) kinase/MAP kinase phosphatase regulation: Roles in cell growth, death, and cancer. *Pharmacological Reviews*, 60(3), 261–310. <https://doi.org/10.1124/pr.107.00106>
- Boyer, B., Vallés, A. M., & Edme, N. (2000). Induction and regulation of epithelial–mesenchymal transitions. *Biochemical Pharmacology*, 60(8), 1091–1099. [https://doi.org/https://doi.org/10.1016/S0006-2952\(00\)00427-5](https://doi.org/https://doi.org/10.1016/S0006-2952(00)00427-5)
- Brahimi-Horn, M. C., Chiche, J., & Pouysségur, J. (2007). Hypoxia and cancer. *Journal of Molecular Medicine (Berlin, Germany)*, 85(12), 1301–1307. <https://doi.org/10.1007/s00109-007-0281-3>
- Brandt, R., Normannos, N., Gullickll, W. J., Lin, J., Harkins, R., Schneider, D., Jones, B., Ciardiello, F., Persico, M. G., Armenantego, F., Kims, N., & David, S. (1994). Identification and Biological Characterization of an Epidermal. *J. Biol. Chem.*, 269(25), 17320–17328.
- Brennan, J., Lu, C. C., Norris, D. P., Rodriguez, T. A., Beddington, R. S. P., & Robertson, E. J. (2001). Nodal signalling in the epiblast patterns the early mouse embryo. *Nature*, 411(6840), 965–969. <https://doi.org/10.1038/35082103>
- Brizel, D. M., Scully, S. P., Harrelson, J. M., Layfield, L. J., Bean, J. M., Prosnitz, L. R., & Dewhirst, M. W. (1996). Tumor oxygenation predicts for the likelihood of distant metastases in human soft tissue sarcoma. *Cancer Research*, 56(5), 941–943.
- Brown, J. M. (1990). Tumor hypoxia, drug resistance, and metastases. *Journal of the National Cancer Institute*, 82(5), 338–339. <https://doi.org/10.1093/jnci/82.5.338>
- Brown, L. M., Cowen, R. L., Debray, C., Eustace, A., Erler, J. T., Sheppard, F. C. D., Parker, C. A., Stratford, I. J., & Williams, K. J. (2006). Reversing hypoxic cell chemoresistance in vitro using genetic and small molecule approaches targeting hypoxia inducible factor-1. *Molecular Pharmacology*, 69(2), 411–418.

<https://doi.org/10.1124/mol.105.015743>

- Bruhn, O., & Cascorbi, I. (2014). Polymorphisms of the drug transporters ABCB1, ABCG2, ABCC2 and ABCC3 and their impact on drug bioavailability and clinical relevance. *Expert Opinion on Drug Metabolism and Toxicology*, 10(10), 1337–1354. <https://doi.org/10.1517/17425255.2014.952630>
- Bruick, R. K., & McKnight, S. L. (2001). A Conserved Family of Prolyl-4-Hydroxylases That Modify HIF. *Science*, 294(5545), 1337 LP – 1340. <https://doi.org/10.1126/science.1066373>
- Buys, T. P. H., Chari, R., Lee, E. H. L., Zhang, M., MacAulay, C., Lam, S., Lam, W. L., & Ling, V. (2007). Genetic changes in the evolution of multidrug resistance for cultured human ovarian cancer cells. *Genes, Chromosomes & Cancer*, 46(12), 1069–1079. <https://doi.org/10.1002/gcc.20492>
- Calabrese, C., Poppleton, H., Kocak, M., Hogg, T. L., Fuller, C., Hamner, B., Oh, E. Y., Gaber, M. W., Finklestein, D., Allen, M., Frank, A., Bayazitov, I. T., Zakharenko, S. S., Gajjar, A., Davidoff, A., & Gilbertson, R. J. (2007). A Perivascular Niche for Brain Tumor Stem Cells. *Cancer Cell*, 11(1), 69–82. <https://doi.org/10.1016/j.ccr.2006.11.020>
- Carnero, A., & Leonart, M. (2016). The hypoxic microenvironment: A determinant of cancer stem cell evolution. *Inside the Cell*, 1(2), 96–105. <https://doi.org/10.1002/icl3.1039>
- Casaroli–Marano, R. P., Pagan, R., & Vilaró, S. (1999). Epithelial–Mesenchymal Transition in Proliferative Vitreoretinopathy: Intermediate Filament Protein Expression in Retinal Pigment Epithelial Cells. *Investigative Ophthalmology & Visual Science*, 40(9), 2062–2072.
- Chailier, P. (1999). Ontogeny of EGF receptors in the human gut. *Frontiers in Bioscience*, 4(1–3), d87. <https://doi.org/10.2741/Chailier>
- Chambers, A. F., Groom, A. C., & MacDonald, I. C. (2002). Dissemination and growth of cancer cells in metastatic sites. *Nature Reviews Cancer*, 2(8), 563–572. <https://doi.org/10.1038/nrc865>

- Chandel, N. S., & Budinger, G. R. S. (2007). The cellular basis for diverse responses to oxygen. *Free Radical Biology and Medicine*, *42*(2), 165–174.  
<https://doi.org/10.1016/j.freeradbiomed.2006.10.048>
- Chang, G., Zhang, H., Wang, J., Zhang, Y., Xu, H., Wang, C., Zhang, H., Ma, L., Li, Q., & Pang, T. (2013). CD44 targets Wnt/ $\beta$ -catenin pathway to mediate the proliferation of K562 cells. *Cancer Cell International*, *13*(1), 117.  
<https://doi.org/10.1186/1475-2867-13-117>
- Chen, C., Zhao, S., Karnad, A., & Freeman, J. W. (2018). The biology and role of CD44 in cancer progression: Therapeutic implications. *Journal of Hematology and Oncology*, *11*(1), 1–23. <https://doi.org/10.1186/s13045-018-0605-5>
- Chen, D., & Wang, C.-Y. (2019). Targeting cancer stem cells in squamous cell carcinoma. *Precision Clinical Medicine*, *2*(3), 152–165.  
<https://doi.org/10.1093/pcmedi/pbz016>
- Chen, H., Kuo, H., Chen, W., Wu, F., Yang, Y., & Ho, H. (2009). A reduced oxygen tension ( 5 %) is not beneficial for maintaining human embryonic stem cells in the undifferentiated state with short splitting intervals. *Stem Cells*, *24*(1), 71–80.  
<https://doi.org/10.1093/humrep/den345>
- Chen, J., Ding, Z., Peng, Y., Pan, F., Li, J., Zou, L., Zhang, Y., & Liang, H. (2014). HIF-1 $\alpha$  inhibition reverses multidrug resistance in colon cancer cells via downregulation of MDR1/P-Glycoprotein. *PLoS ONE*, *9*(6).  
<https://doi.org/10.1371/journal.pone.0098882>
- Chen, W., Dong, J., Haiech, J., Kilhoffer, M. C., & Zeniou, M. (2016). Cancer stem cell quiescence and plasticity as major challenges in cancer therapy. *Stem Cells International*, *2016*. <https://doi.org/10.1155/2016/1740936>
- Chen, X., Wan, L., Wang, W., Xi, W. J., Yang, A. G., & Wang, T. (2020). Re-recognition of pseudogenes: From molecular to clinical applications. *Theranostics*, *10*(4), 1479–1499. <https://doi.org/10.7150/thno.40659>
- Chen, Y., & Schier, A. F. (2002). Lefty proteins are long-range inhibitors of Squint-mediated Nodal signalling. *Current Biology*, *12*(24), 2124–2128.  
[https://doi.org/10.1016/S0960-9822\(02\)01362-3](https://doi.org/10.1016/S0960-9822(02)01362-3)

- Cheng-Jun Hu,\*† Aneesa Sataur,‡ Liyi Wang,‡ Hongqing Chen, and M. C. S. (2007). The N-Terminal Transactivation Domain Confers Target Gene Specificity of Hypoxia-inducible Factors HIF-1<sub>Δ</sub> and HIF-2<sub>Δ</sub>. *Molecular Biology of the Cell*, 18(December), 986–994. <https://doi.org/10.1091/mbc.E06>
- Chinn, L. W., & Kroetz, D. L. (2007). ABCB1 pharmacogenetics: progress, pitfalls, and promise. *Clinical Pharmacology and Therapeutics*, 81(2), 265–269. <https://doi.org/10.1038/sj.clpt.6100052>
- Cho, Y., & Kim, Y. K. (2020). Cancer Stem Cells as a Potential Target to Overcome Multidrug Resistance. *Frontiers in Oncology*, 10(June), 1–10. <https://doi.org/10.3389/fonc.2020.00764>
- Choi, C.-H. (2005). ABC transporters as multidrug resistance mechanisms and the development of chemosensitizers for their reversal. *Cancer Cell International*, 5(1), 30. <https://doi.org/10.1186/1475-2867-5-30>
- Choi, S., Lee, K., Lee, J. H., Kang, H. J., Lee, M. J., Kim, H. Y., & Park, K. (2016). *Suppression of Akt-HIF-1* □ *signalling axis by diacetyl atractylodiol inhibits hypoxia-induced angiogenesis*. 49(9), 508–513.
- Ciccodicola, A., Dono, R., Obici, S., Simeone, A., Zollo, M., & Graziella Persico, M. (1989). Molecular characterization of a gene of the “EGF family” expressed in undifferentiated human NTERA2 teratocarcinoma cells. *EMBO Journal*, 8(7), 1987–1991. <https://doi.org/10.1002/j.1460-2075.1989.tb03605.x>
- Ciccodicola, A., Dono, R., Obici, S., Simeone, A., Zollo, M., & Persico, M. G. (1989). Molecular characterization of a gene of the ‘EGF family’ expressed in undifferentiated human NTERA2 teratocarcinoma cells. *The EMBO Journal*, 8(7), 1987–1991. <https://doi.org/10.1002/j.1460-2075.1989.tb03605.x>
- Clark, A. S., West, K., Streicher, S., & Dennis, P. A. (2002). Constitutive and Inducible Akt Activity Promotes Resistance to Chemotherapy, Trastuzumab, or Tamoxifen in Breast Cancer Cells. *Molecular Cancer Therapeutics*, 1(9), 707 LP – 717. <http://mct.aacrjournals.org/content/1/9/707.abstract>
- Cocciadiferro, L., Miceli, V., Kang, K.-S., Polito, L. M., Trosko, J. E., & Carruba, G. (2009). Profiling Cancer Stem Cells in Androgen-Responsive and Refractory

- Human Prostate Tumor Cell Lines. *Annals of the New York Academy of Sciences*, 1155(1), 257–262. <https://doi.org/10.1111/j.1749-6632.2009.03696.x>
- Comerford, K. M., Wallace, T. J., Karhausen, J., Louis, N. A., Montalto, M. C., & Colgan, S. P. (2002). Hypoxia-inducible factor-1-dependent regulation of the multidrug resistance (MDR1) gene. *Cancer Research*, 62(12), 3387–3394.
- Compernelle, V., Brusselmans, K., Acker, T., Hoet, P., Tjwa, M., Beck, H., Plaisance, S., Dor, Y., Keshet, E., Lupu, F., Nemery, B., Dewerchin, M., Van Veldhoven, P., Plate, K., Moons, L., Collen, D., & Carmeliet, P. (2002). Loss of HIF-2 $\alpha$  and inhibition of VEGF impair fetal lung maturation, whereas treatment with VEGF prevents fatal respiratory distress in premature mice. *Nature Medicine*, 8(7), 702–710. <https://doi.org/10.1038/nm721>
- CORTEGOSO, A. V. B., LAUREANO, N. K., SILVA, A. D. da, DANILEVICZ, C. K., MAGNUSSON, A. S., VISIOLI, F., & RADOS, P. V. (2017). Cell proliferation markers at the invasive tumor front of oral squamous cell carcinoma: comparative analysis in relation to clinicopathological parameters of patients. *Journal of Applied Oral Science*, 25(3), 318–323. <https://doi.org/10.1590/1678-7757-2016-0238>
- Covello, K. L., Kehler, J., Yu, H., Gordan, J. D., Arsham, A. M., Hu, C., Labosky, P. A., Simon, M. C., & Keith, B. (2006). *HIF-2  $\alpha$  regulates Oct-4 : effects of hypoxia on stem cell function , embryonic development , and tumor growth*. 557–570. <https://doi.org/10.1101/gad.1399906.Sox2>
- Cripto-, H. (2012). *Molecular Signalling Pathways of Recombinant Dedicated to my parents for their love , encouragement and support . March*.
- D'Andrea, D., Liguori, G. L., Le Good, J. A., Lonardo, E., Andersson, O., Constam, D. B., Persico, M. G., & Minchiotti, G. (2008). Cripto promotes A-P axis specification independently of its stimulatory effect on Nodal autoinduction. *Journal of Cell Biology*, 180(3), 597–605. <https://doi.org/10.1083/jcb.200709090>
- Da He, RE-Xian wang, jian-ping Mao, Bin Xiao, Da-Fu Chen, wei tian. (n.d.). *Three-dimensional spheroid culture promotes the stemness maintenance of cranial stem cells by activating PI3K AKT and suppressing NF- $\kappa$  B pathways Elsevier*

*Enhanced Reader.pdf.*

- Dandachi, N., Hauser-Kronberger, C., Moré, E., Wiesener, B., Hacker, G. W., Dietze, O., & Wirl, G. (2001). Co-expression of tenascin-C and vimentin in human breast cancer cells indicates phenotypic transdifferentiation during tumour progression: correlation with histopathological parameters, hormone receptors, and oncoproteins. *The Journal of Pathology*, *193*(2), 181–189.  
[https://doi.org/10.1002/1096-9896\(2000\)9999:9999::AID-PATH752>3.0.CO;2-V](https://doi.org/10.1002/1096-9896(2000)9999:9999::AID-PATH752>3.0.CO;2-V)
- Das, A. B., Loying, P., & Bose, B. (2012). Human recombinant Cripto-1 increases doubling time and reduces proliferation of HeLa cells independent of pro-proliferation pathways. *Cancer Letters*, *318*(2), 189–198.  
<https://doi.org/10.1016/j.canlet.2011.12.013>
- Daschner, P. J., Ciolino, H. P., Plouzek, C. A., & Yeh, G. C. (1999). Increased AP-1 activity in drug resistant human breast cancer MCF-7 cells. *Breast Cancer Research and Treatment*, *53*(3), 229–240.  
<https://doi.org/10.1023/A:1006138803392>
- Davis, J. E., Kirk, J., Ji, Y., & Tang, D. G. (2019). Tumor Dormancy and Slow-Cycling Cancer Cells. In J. S. Rhim, A. Dritschilo, & R. Kremer (Eds.), *Human Cell Transformation: Advances in Cell Models for the Study of Cancer and Aging* (pp. 199–206). Springer International Publishing. [https://doi.org/10.1007/978-3-030-22254-3\\_15](https://doi.org/10.1007/978-3-030-22254-3_15)
- De Angelis, M. L., Francescangeli, F., La Torre, F., & Zeuner, A. (2019). Stem cell plasticity and dormancy in the development of cancer therapy resistance. *Frontiers in Oncology*, *9*(JULY), 1–14. <https://doi.org/10.3389/fonc.2019.00626>
- De Castro, N. P., Rangel, M. C., Nagaoka, T., Salomon, D. S., & Bianco, C. (2010). Cripto-1: An embryonic gene that promotes tumorigenesis. *Future Oncology*, *6*(7), 1127–1142. <https://doi.org/10.2217/fon.10.68>
- De Santis, M. L., Martinez-Lacaci, I., Bianco, C., Seno, M., Wallace-Jones, B., Kim, N., Ebert, A., Wechselberger, C., & Salomon, D. S. (2000). Cripto-1 induces apoptosis in HC-11 mouse mammary epithelial cells. *Cell Death and*

- Differentiation*, 7(2), 189–196. <https://doi.org/10.1038/sj.cdd.4400588>
- De Wert, G., & Mummery, C. (2003). Human embryonic stem cells: Research, ethics and policy. *Human Reproduction*, 18(4), 672–682.  
<https://doi.org/10.1093/humrep/deg143>
- Deeley, R. G., & Cole, S. P. C. (1997). Function, evolution and structure of multidrug resistance protein (MRP). *Seminars in Cancer Biology*, 8(3), 193–204.  
<https://doi.org/10.1006/scbi.1997.0070>
- Dekanty, A., Lavista-Llanos, S., Irisarri, M., Oldham, S., & Wappner, P. (2005). The insulin-PI3K/TOR pathway induces a HIF-dependent transcriptional response in *Drosophila* by promoting nuclear localization of HIF- $\alpha$ /Sima. *Journal of Cell Science*, 118(23), 5431 LP – 5441. <https://doi.org/10.1242/jcs.02648>
- Dellinger, M. T., & Brekken, R. A. (2011). Phosphorylation of Akt and ERK1/2 Is Required for VEGF-A/VEGFR2-Induced Proliferation and Migration of Lymphatic Endothelium. *PLOS ONE*, 6(12), 1–9.  
<https://doi.org/10.1371/journal.pone.0028947>
- Dengler, W. A., Schulte, J., Berger, D. P., Mertelsmann, R., & Fiebig, H. H. (1995). Development of a propidium iodide fluorescence assay for proliferation and cytotoxicity assays. *Anti-Cancer Drugs*, 6(4), 522–532.  
<https://doi.org/10.1097/00001813-199508000-00005>
- Depping, R., Steinhoff, A., Schindler, S. G., Friedrich, B., Fagerlund, R., Metzen, E., Hartmann, E., & Köhler, M. (2008). Nuclear translocation of hypoxia-inducible factors (HIFs): involvement of the classical importin alpha/beta pathway. *Biochimica et Biophysica Acta*, 1783(3), 394–404.  
<https://doi.org/10.1016/j.bbamcr.2007.12.006>
- Dhillon, A. S., Hagan, S., Rath, O., & Kolch, W. (2007). MAP kinase signalling pathways in cancer. *Oncogene*, 26(22), 3279–3290.  
<https://doi.org/10.1038/sj.onc.1210421>
- Di Bari, M. G., Ginsburg, E., Plant, J., Strizzi, L., Salomon, D. S., & Vonderhaar, B. K. (2009). Msx2 induces epithelial-mesenchymal transition in mouse mammary epithelial cells through upregulation of Cripto-1. *Journal of Cellular Physiology*,

- 219(3), 659–666. <https://doi.org/10.1002/jcp.21712>
- Ding, J., Yang, L., Yan, Y. T., Chen, A., Desai, N., Wynshaw-Boris, A., & Shen, M. M. (1998). Cripto is required for correct orientation of the anterior-posterior axis in the mouse embryo. *Nature*, 395(6703), 702–707. <https://doi.org/10.1038/27215>
- Dituri, F., Mazzocca, A., Giannelli, G., & Antonaci, S. (2011). PI3K functions in cancer progression, anticancer immunity and immune evasion by tumors. *Clinical and Developmental Immunology*, 2011. <https://doi.org/10.1155/2011/947858>
- Dobbin, Z. C., & Landen, C. N. (2013). The importance of the PI3K/AKT/MTOR pathway in the progression of ovarian cancer. *International Journal of Molecular Sciences*, 14(4), 8213–8227. <https://doi.org/10.3390/ijms14048213>
- Dong, Y., Liao, H., Yu, J., Fu, H., Zhao, D., Gong, K., Wang, Q., & Duan, Y. (2019). Incorporation of drug efflux inhibitor and chemotherapeutic agent into an inorganic/organic platform for the effective treatment of multidrug resistant breast cancer. *Journal of Nanobiotechnology*, 17(1), 1–15. <https://doi.org/10.1186/s12951-019-0559-y>
- Donnenberg, V. S., & Donnenberg, A. D. (2005). Multiple drug resistance in cancer revisited: the cancer stem cell hypothesis. *Journal of Clinical Pharmacology*, 45(8), 872–877. <https://doi.org/10.1177/0091270005276905>
- Dono, R., Montuori, N., Rocchi, M., De Ponti-Zilli, L., Ciccodicola, A., & Persico, M. G. (1991). Isolation and characterization of the CRIPTO autosomal gene and its X-linked related sequence. *American Journal of Human Genetics*, 49(3), 555–565.
- Dono, Rosanna, Scalera, L., Pacifico, F., Acampora, D., & Persico, M. G. (1993). *The murine cripto gene : expression during mesoderm induction and early heart morphogenesis*. 1168, 1157–1168.
- Dörfel, M. J., Lyon, G. J., Friedrich, U. A., Zedan, M., Hessling, B., Fenzl, K., Gillet, L., Knop, M., Kramer, G., Bukau, B., Jeong, J.-W., Bae, M.-H. M.-K., Ahn, M.-Y., Kim, S.-H., Sohn, T.-K., Bae, M.-H. M.-K., Yoo, M.-A., Song, E. J., Lee, K.-J., ... Seo, J. H. (2013). Regulation and Destabilization of HIF-1 $\alpha$  by ARD1-Mediated Acetylation. *Cell*, 32(2), 5270–5277. <http://dx.doi.org/10.1038/s12276-018-0100-7><http://dx.doi.org/10.1016/j.gene.2015.04.085>

- Doublier, S., Belisario, D. C., Polimeni, M., Annaratone, L., Riganti, C., Allia, E., Ghigo, D., Bosia, A., & Sapino, A. (2012). HIF-1 activation induces doxorubicin resistance in MCF7 3-D spheroids via P-glycoprotein expression: A potential model of the chemo-resistance of invasive micropapillary carcinoma of the breast. *BMC Cancer*, *12*, 1–15. <https://doi.org/10.1186/1471-2407-12-4>
- Doyle, L. A., Yang, W., Abruzzo, L. V, Krogmann, T., Gao, Y., Rishi, A. K., & Ross, D. D. (1998). A multidrug resistance transporter from human MCF-7 breast cancer cells. *Proceedings of the National Academy of Sciences*, *95*(26), 15665 LP – 15670. <https://doi.org/10.1073/pnas.95.26.15665>
- Du, B., & Shim, J. S. (2016). Targeting epithelial-mesenchymal transition (EMT) to overcome drug resistance in cancer. *Molecules*, *21*(7). <https://doi.org/10.3390/molecules21070965>
- Dudu, V., Pantazis, P., & González-Gaitán, M. (2004). Membrane traffic during embryonic development: Epithelial formation, cell fate decisions and differentiation. *Current Opinion in Cell Biology*, *16*(4), 407–414. <https://doi.org/10.1016/j.ceb.2004.06.008>
- Dumontet, C., & Jordan, M. A. (2010). Microtubule-binding agents: a dynamic field of cancer therapeutics. *Nature Reviews. Drug Discovery*, *9*(10), 790–803. <https://doi.org/10.1038/nrd3253>
- Dunwoodie, S. L. (2009). The Role of Hypoxia in Development of the Mammalian Embryo. *Developmental Cell*, *17*(6), 755–773. <https://doi.org/10.1016/j.devcel.2009.11.008>
- Dvorak, H. F., Nagy, J. A., & Dvorak, A. M. (1991). Structure of solid tumors and their vasculature: implications for therapy with monoclonal antibodies. *Cancer Cells (Cold Spring Harbor, N.Y. : 1989)*, *3*(3), 77–85.
- Ebert, A., Wechselberger, C., Frank, S., & Wallace-Jones, B. (1999). Cripto-1 induces phosphatidylinositol 3'-kinase-dependent phosphorylation of AKT and glycogen synthase kinase 3 $\beta$  in human cervical carcinoma cells. *Cancer Research*. <http://cancerres.aacrjournals.org/content/59/18/4502.short>
- Ebert, A., Wechselberger, C., Nees, M., & Clair, T. (2000). Cripto-1-induced increase

- in vimentin expression is associated with enhanced migration of human Caski cervical carcinoma cells. *Experimental Cell*.  
<http://www.sciencedirect.com/science/article/pii/S001448270094881X>
- Edy Susanto, M. (2010). Stem Cell Biology in Health and Disease. In T. Dittmar & K. S. Zanker (Eds.), *Journal of Chemical Information and Modeling* (Vol. 53, Issue 9). Springer Netherlands. <https://doi.org/10.1007/978-90-481-3040-5>
- Eini, R., Stoop, H., Gillis, A. J. M., Biermann, K., Dorssers, L. C. J., & Looijenga, L. H. J. (2014). *Role of SOX2 in the Etiology of Embryonal Carcinoma , Based on Analysis of the NCCIT and NT2 Cell Lines*. 9(1).  
<https://doi.org/10.1371/journal.pone.0083585>
- Elçin, Y. M., Inanç, B., & Elçin, A. E. (2010). Human embryonic stem cell differentiation on periodontal ligament fibroblasts. In *Methods in molecular biology (Clifton, N.J.)* (Vol. 584). [https://doi.org/10.1007/978-1-60761-369-5\\_14](https://doi.org/10.1007/978-1-60761-369-5_14)
- Engineering, G., & Ireland, S. B. (2015). *The overexpression of SOX2 affects the migration of human teratocarcinoma cell line NT2 / D1*. 87, 389–405.
- Englund, M. C. O., Sartipy, P., & Hyllner, J. (2011). Human embryonic stem cells. *Regenerative Medicine: From Protocol to Patient*, 10, 169–186.  
[https://doi.org/10.1007/978-90-481-9075-1\\_7](https://doi.org/10.1007/978-90-481-9075-1_7)
- Escuin, D., Kline, E. R., & Giannakakou, P. (2005). Both microtubule-stabilizing and microtubule-destabilizing drugs inhibit hypoxia-inducible factor-1 $\alpha$  accumulation and activity by disrupting microtubule function. *Cancer Research*, 65(19), 9021–9028. <https://doi.org/10.1158/0008-5472.CAN-04-4095>
- Evans, M. J., & Kaufman, M. H. (1981). Establishment in culture of pluripotential cells from mouse embryos. *Nature*, 292(5819), 154–156.  
<https://doi.org/10.1038/292154a0>
- Ezashi, T., Das, P., & Roberts, R. M. (2005). Low O<sub>2</sub> tensions and the prevention of differentiation of hES cells. *Proceedings of the National Academy of Sciences of the United States of America*, 102(13), 4783–4788.  
<https://doi.org/10.1073/pnas.0501283102>

- Fan, C.-F., Miao, Y., Lin, X.-Y., Zhang, D., & Wang, E.-H. (2014). Expression of a phosphorylated form of ATF4 in lung and non-small cell lung cancer tissues. *Tumor Biology*, 35(1), 765–771. <https://doi.org/10.1007/s13277-013-1104-5>
- Federici, G., Espina, V., Liotta, L., & Edmiston, K. H. (2011). Breast cancer stem cells: a new target for therapy. *Oncology (Williston Park, N.Y.)*, 25(1), 25–28, 30. <https://doi.org/10.3390/biomedicines6030077>
- Fiorenzano, A., Pascale, E., D’Aniello, C., Acampora, D., Bassalart, C., Russo, F., Andolfi, G., Biffoni, M., Francescangeli, F., Zeuner, A., Angelini, C., Chazaud, C., Patriarca, E. J., Fico, A., & Minchiotti, G. (2016). Cripto is essential to capture mouse epiblast stem cell and human embryonic stem cell pluripotency. *Nature Communications*, 7. <https://doi.org/10.1038/ncomms12589>
- Fletcher, J. I., Haber, M., Henderson, M. J., & Norris, M. D. (2010). ABC transporters in cancer: More than just drug efflux pumps. *Nature Reviews Cancer*, 10(2), 147–156. <https://doi.org/10.1038/nrc2789>
- Flügel, D., Görlach, A., Michiels, C., & Kietzmann, T. (2007). Glycogen Synthase Kinase 3 Phosphorylates Hypoxia-Inducible Factor 1 $\alpha$  and Mediates Its Destabilization in a VHL-Independent Manner. *Molecular and Cellular Biology*, 27(9), 3253 LP – 3265. <https://doi.org/10.1128/MCB.00015-07>
- Foley, S. F., Van Vlijmen, H. W. T., Boynton, R. E., Adkins, H. B., Cheung, A. E., Singh, J., Sanicola, M., Young, C. N., & Wen, D. (2003). The CRIPTO/FRL-1/CRYPTIC (CFC) domain of human cripto: Functional and structural insights through disulfide structure analysis. *European Journal of Biochemistry*, 270(17), 3610–3618. <https://doi.org/10.1046/j.1432-1033.2003.03749.x>
- Francescangeli, F., Contavalli, P., De Angelis, M. L., Baiocchi, M., Gambarà, G., Pagliuca, A., Fiorenzano, A., Prezioso, C., Boe, A., Todaro, M., Stassi, G., Castro, N. P., Watanabe, K., Salomon, D. S., De Maria, R., Minchiotti, G., & Zeuner, A. (2015). Dynamic regulation of the cancer stem cell compartment by Cripto-1 in colorectal cancer. *Cell Death and Differentiation*, 22(10), 1700–1713. <https://doi.org/10.1038/cdd.2015.19>
- Friedmann-Morvinski, D., & Verma, I. M. (2014). Dedifferentiation and

- reprogramming: Origins of cancer stem cells. *EMBO Reports*, 15(3), 244–253.  
<https://doi.org/10.1002/embr.201338254>
- Fuchs, B., Ostmeier, H., & Suter, L. (1991). p-glycoprotein expression in malignant melanoma. *Journal of Cancer Research and Clinical Oncology*, 117(2), 168–171.  
<https://doi.org/10.1007/BF01613142>
- Fukuda, R., Hirota, K., Fan, F., Jung, Y. Do, Ellis, L. M., & Semenza, G. L. (2002). Insulin-like Growth Factor 1 Induces Hypoxia-inducible Factor 1-mediated Vascular Endothelial Growth Factor Expression, Which is Dependent on MAP Kinase and Phosphatidylinositol 3-Kinase Signalling in Colon Cancer Cells\*. *Journal of Biological Chemistry*, 277(41), 38205–38211.  
<https://doi.org/https://doi.org/10.1074/jbc.M203781200>
- Funa, N. S., Schachter, K. A., Lerdrup, M., Ekberg, J., Hess, K., Dietrich, N., Honoré, C., Hansen, K., & Semb, H. (2015).  $\beta$ -Catenin Regulates Primitive Streak Induction through Collaborative Interactions with SMAD2/SMAD3 and OCT4. *Cell Stem Cell*, 16(6), 639–652. <https://doi.org/10.1016/j.stem.2015.03.008>
- Furman, P. A., Fyfe, J. A., St Clair, M. H., Weinhold, K., Rideout, J. L., Freeman, G. A., Lehrman, S. N., Bolognesi, D. P., Broder, S., & Mitsuya, H. (1986). Phosphorylation of 3'-azido-3'-deoxythymidine and selective interaction of the 5'-triphosphate with human immunodeficiency virus reverse transcriptase. *Proceedings of the National Academy of Sciences*, 83(21), 8333 LP – 8337. <https://doi.org/10.1073/pnas.83.21.8333>
- Galian, C., Björkholm, P., Bulleid, N., & Von Heijne, G. (2012). Efficient glycosylphosphatidylinositol (GPI) modification of membrane proteins requires a C-terminal anchoring signal of marginal hydrophobicity. *Journal of Biological Chemistry*, 287(20), 16399–16409. <https://doi.org/10.1074/jbc.M112.350009>
- Gan, Q., Yoshida, T., McDonald, O. G., & Owens, G. K. (2007). Concise Review: Epigenetic Mechanisms Contribute to Pluripotency and Cell Lineage Determination of Embryonic Stem Cells. *Stem Cells*, 25(1), 2–9.  
<https://doi.org/10.1634/stemcells.2006-0383>
- Gang, W., Wang, J. J., Fu, X. L., Rui, G., & Tony To, S. S. (2017). Advances in the

- targeting of HIF-1 $\alpha$  and future therapeutic strategies for glioblastoma multiforme (Review). In *Oncology Reports* (Vol. 37, Issue 2, pp. 657–670).  
<https://doi.org/10.3892/or.2016.5309>
- Gao, M., Liang, J., Lu, Y., Guo, H., German, P., Bai, S., Jonasch, E., Yang, X., Mills, G. B., & Ding, Z. (2014). Site-specific activation of AKT protects cells from death induced by glucose deprivation. *Oncogene*, *33*(6), 745–755.  
<https://doi.org/10.1038/onc.2013.2>
- Gasser, M., Zhan, Q., Jordan, S., & Duncan, L. M. (2013). *19\_715 (6).Pdf. 451(7176)*, 345–349. <https://doi.org/10.1038/nature06489>.Identification
- Gawlik-Rzemieniewska, N., & Bednarek, I. (2016). The role of NANOG transcriptional factor in the development of malignant phenotype of cancer cells. *Cancer Biology and Therapy*, *17*(1), 1–10.  
<https://doi.org/10.1080/15384047.2015.1121348>
- Gene, M. D. R., Comerford, K. M., Wallace, T. J., Louis, N. A., Montalto, M. C., & Colgan, S. P. (2002). *Hypoxia-inducible Factor-1-dependent Regulation of the Multidrug Resistance*. 3387–3394.
- Gene, N., Mem-, C., & Sato, M. (2010). *Teratocarcinoma-Derived Growth Factor-Tissue-Specific Vascular Endothelial Signals and Vector Targeting , Part B Cripto*.
- Gillet, J.-P., Efferth, T., & Remacle, J. (2007). Chemotherapy-induced resistance by ATP-binding cassette transporter genes. *Biochimica et Biophysica Acta*, *1775*(2), 237–262. <https://doi.org/10.1016/j.bbcan.2007.05.002>
- Gillis, A. J. M., Stoop, H., Biermann, K., van Gurp, R. J. H. L. M., Swartzman, E., Cribbes, S., Ferlinz, A., Shannon, M., Oosterhuis, J. W., & Looijenga, L. H. J. (2011). Expression and interdependencies of pluripotency factors LIN28, OCT3/4, NANOG and SOX2 in human testicular germ cells and tumours of the testis. *International Journal of Andrology*, *34*(4pt2), e160–e174.  
<https://doi.org/10.1111/j.1365-2605.2011.01148.x>
- Glumac, P. M., & LeBeau, A. M. (2018). The role of CD133 in cancer: a concise review. *Clinical and Translational Medicine*, *7*(1), 18.

<https://doi.org/10.1186/s40169-018-0198-1>

Gottesman, M. M., Fojo, T., & Bates, S. E. (2002). Multidrug resistance in cancer: Role of ATP-dependent transporters. *Nature Reviews Cancer*, 2(1), 48–58.

<https://doi.org/10.1038/nrc706>

Gottesman, M. M., & Pastan, I. (1993). MULTIDRUG RESISTANCE MULTIDRUG TRANSPORTER1. *Annual Review of Biochemistry*, 62, 385–427.

Gottesman, M. M., & Pastan, I. H. (2015). The Role of Multidrug Resistance Efflux Pumps in Cancer: Revisiting a JNCI Publication Exploring Expression of the MDR1 (P-glycoprotein) Gene. *Journal of the National Cancer Institute*, 107(9), 4–6. <https://doi.org/10.1093/jnci/djv222>

Grandage, V. L., Gale, R. E., Linch, D. C., & Khwaja, A. (2005). PI3-kinase/Akt is constitutively active in primary acute myeloid leukaemia cells and regulates survival and chemoresistance via NF- $\kappa$ B, MAPkinase and p53 pathways. *Leukemia*, 19(4), 586–594. <https://doi.org/10.1038/sj.leu.2403653>

Gray, P. C., & Vale, W. (2012). Cripto/GRP78 modulation of the TGF- $\beta$  pathway in development and oncogenesis. In *FEBS Letters* (Vol. 586, Issue 14, pp. 1836–1845). <https://doi.org/10.1016/j.febslet.2012.01.051>

Grille, S. J., Bellacosa, A., Upson, J., Klein-Szanto, A. J., van Roy, F., Lee-Kwon, W., Donowitz, M., Tsihchlis, P. N., & Larue, L. (2003). The Protein Kinase Akt Induces Epithelial Mesenchymal Transition and Promotes Enhanced Motility and Invasiveness of Squamous Cell Carcinoma Lines. *Cancer Research*, 63(9), 2172 LP – 2178. <http://cancerres.aacrjournals.org/content/63/9/2172.abstract>

Gritsman, K., Zhang, J., Cheng, S., Heckscher, E., Talbot, W. S., & Schier, A. F. (1999). The EGF-CFC protein one-eyed pinhead is essential for nodal signalling. *Cell*, 97(1), 121–132. [https://doi.org/10.1016/S0092-8674\(00\)80720-5](https://doi.org/10.1016/S0092-8674(00)80720-5)

Gu, P., Goodwin, B., Chung, A. C.-K., Xu, X., Wheeler, D. A., Price, R. R., Galardi, C., Peng, L., Latour, A. M., Koller, B. H., Gossen, J., Kliewer, S. A., & Cooney, A. J. (2005). Orphan Nuclear Receptor LRH-1 Is Required To Maintain Oct4 Expression at the Epiblast Stage of Embryonic Development. *Molecular and Cellular Biology*, 25(9), 3492 LP – 3505. <https://doi.org/10.1128/MCB.25.9.3492->

3505.2005

Gu, P., LeMenuet, D., Chung, A. C.-K., Mancini, M., Wheeler, D. A., & Cooney, A. J. (2005). Orphan Nuclear Receptor GCNF Is Required for the Repression of Pluripotency Genes during Retinoic Acid-Induced Embryonic Stem Cell Differentiation. *Molecular and Cellular Biology*, 25(19), 8507 LP – 8519. <https://doi.org/10.1128/MCB.25.19.8507-8519.2005>

Gu, P., Xu, X., Le Menuet, D., Chung, A. C.-K., & Cooney, A. J. (2011). Differential Recruitment of Methyl CpG-Binding Domain Factors and DNA Methyltransferases by the Orphan Receptor Germ Cell Nuclear Factor Initiates the Repression and Silencing of Oct4. *STEM CELLS*, 29(7), 1041–1051. <https://doi.org/https://doi.org/10.1002/stem.652>

Gutting, T., Burgermeister, E., Härtel, N., & Ebert, M. P. (2019). Checkpoints and beyond – Immunotherapy in colorectal cancer. *Seminars in Cancer Biology*, 55(April 2018), 78–89. <https://doi.org/10.1016/j.semcancer.2018.04.003>

Han, L., Shi, S., Gong, T., Zhang, Z., & Sun, X. (2013). Cancer stem cells: therapeutic implications and perspectives in cancer therapy. *Acta Pharmaceutica Sinica B*, 3(2), 65–75. <https://doi.org/10.1016/j.apsb.2013.02.006>

Han, Z.-B., Ren, H., Zhao, H., Chi, Y., Chen, K., Zhou, B., Liu, Y., Zhang, L., Xu, B., Liu, B., Yang, R., & Han, Z.-C. (2008). Hypoxia-inducible factor (HIF)-1 alpha directly enhances the transcriptional activity of stem cell factor (SCF) in response to hypoxia and epidermal growth factor (EGF). *Carcinogenesis*, 29(10), 1853–1861. <https://doi.org/10.1093/carcin/bgn066>

Hanahan, D., & Weinberg, R. A. (2011). Hallmarks of cancer: The next generation. *Cell*, 144(5), 646–674. <https://doi.org/10.1016/j.cell.2011.02.013>

Harris, A. L. (2002). Hypoxia--a key regulatory factor in tumour growth. *Nature Reviews. Cancer*, 2(1), 38–47. <https://doi.org/10.1038/nrc704>

Hauswirth, A. W., Florian, S., Printz, D., Sotlar, K., Krauth, M. T., Fritsch, G., Scherthaner, G. H., Wacheck, V., Selzer, E., Sperr, W. R., & Valent, P. (2007). Expression of the target receptor CD33 in CD34 +/CD38 -/CD123 + AML stem cells. *European Journal of Clinical Investigation*, 37(1), 73–82.

<https://doi.org/10.1111/j.1365-2362.2007.01746.x>

Hazrati, L. N., Van Cauwenberghe, C., Brooks, P. L., Brouwers, N., Ghani, M., Sato, C., Cruts, M., Sleegers, K., St. George-Hyslop, P., Van Broeckhoven, C., & Rogaeva, E. (2012). Genetic association of CR1 with Alzheimer's disease: A tentative disease mechanism. *Neurobiology of Aging*, *33*(12), 2949.e5-2949.e12. <https://doi.org/10.1016/j.neurobiolaging.2012.07.001>

He, S., Liu, F., Xie, Z., Zu, X., Xu, W., & Jiang, Y. (2010). P-Glycoprotein/MDR1 regulates pokemon gene transcription through p53 expression in human breast cancer cells. *International Journal of Molecular Sciences*, *11*(9), 3039–3051. <https://doi.org/10.3390/ijms11093039>

Hentschke, M., Kurth, I., & Borgmeyer, U. (2006). Germ cell nuclear factor is a repressor of CRIPTO-1 and CRIPTO-3. *Journal of Biological Chemistry*. <http://www.jbc.org/content/281/44/33497.short>

Hentschke, Moritz, Kurth, I., Borgmeyer, U., & Hübner, C. A. (2006). Germ cell nuclear factor is a repressor of CRIPTO-1 and CRIPTO-3. *Journal of Biological Chemistry*, *281*(44), 33497–33504. <https://doi.org/10.1074/jbc.M606975200>

Herheliuk, T., Perepelytsina, O., Ugnivenko, A., Ostapchenko, L., & Sydorenko, M. (2019). Investigation of multicellular tumor spheroids enriched for a cancer stem cell phenotype. *Stem Cell Investigation*, *6*(August), 1–13. <https://doi.org/10.21037/sci.2019.06.07>

Herreros-Villanueva, M., Zhang, J. S., Koenig, A., Abel, E. V., Smyrk, T. C., BamLet, W. R., De Narvajas, A. A. M., Gomez, T. S., Simeone, D. M., Bujanda, L., & Billadeau, D. D. (2013). SOX2 promotes dedifferentiation and imparts stem cell-like features to pancreatic cancer cells. *Oncogenesis*, *2*(June). <https://doi.org/10.1038/oncsis.2013.23>

Herrington, E. E., Ram, T. G., Salomon, D. S., Johnson, G. R., Gullick, W. J., Kenney, N., & Hosick, H. L. (1997). Expression of epidermal growth factor-related proteins in the aged adult mouse mammary gland and their relationship to tumorigenesis. In *Journal of Cellular Physiology* (Vol. 170, Issue 1, pp. 47–56). [https://doi.org/10.1002/\(SICI\)1097-4652\(199701\)170:1<47::AID-JCP6>3.0.CO;2-](https://doi.org/10.1002/(SICI)1097-4652(199701)170:1<47::AID-JCP6>3.0.CO;2-)

## L

- Höckel, M., Schlenger, K., Höckel, S., & Vaupel, P. (1999). Hypoxic cervical cancers with low apoptotic index are highly aggressive. *Cancer Research*, *59*(18), 4525–4528.
- Hoffman, E. C., Reyes, H., Chu, F. F., Sander, F., Conley, L. H., Brooks, B. A., & Hankinson, O. (1991). Cloning of a factor required for activity of the Ah (dioxin) receptor. *Science*, *252*(5008), 954 LP – 958.  
<https://doi.org/10.1126/science.1852076>
- Hogenesch, J. B., Chan, W. K., Jackiw, V. H., Brown, R. C., Gu, Y.-Z., Pray-Grant, M., Perdew, G. H., & Bradfield, C. A. (1997). Characterization of a Subset of the Basic-Helix-Loop-Helix-PAS Superfamily That Interacts with Components of the Dioxin Signalling Pathway\*. *Journal of Biological Chemistry*, *272*(13), 8581–8593. <https://doi.org/10.1074/jbc.272.13.8581>
- Holland, J. D., Klaus, A., Garratt, A. N., & Birchmeier, W. (2013). Wnt signalling in stem and cancer stem cells. *Current Opinion in Cell Biology*, *25*(2), 254–264.  
<https://doi.org/10.1016/j.ceb.2013.01.004>
- Holmquist-Mengelbier, L., Fredlund, E., Löfstedt, T., Noguera, R., Navarro, S., Nilsson, H., Pietras, A., Vallon-Christersson, J., Borg, Å., Gradin, K., Poellinger, L., & Pahlman, S. (2006). Recruitment of HIF-1 $\alpha$  and HIF-2 $\alpha$  to common target genes is differentially regulated in neuroblastoma: HIF-2 $\alpha$  promotes an aggressive phenotype. In *Cancer Cell* (Vol. 10, Issue 5, pp. 413–423).  
<https://doi.org/10.1016/j.ccr.2006.08.026>
- Holohan, C., Van Schaeybroeck, S., Longley, D. B., & Johnston, P. G. (2013). Cancer drug resistance: an evolving paradigm. *Nature Reviews Cancer*, *13*(10), 714–726.  
<https://doi.org/10.1038/nrc3599>
- Hough, S. R., Thornton, M., Mason, E., Mar, J. C., Wells, C. A., & Pera, M. F. (2014). Single-cell gene expression profiles define self-renewing, pluripotent, and lineage primed states of human pluripotent stem cells. *Stem Cell Reports*, *2*(6), 881–895.  
<https://doi.org/10.1016/j.stemcr.2014.04.014>
- Hsu, Y. C., Pasolli, H. A., & Fuchs, E. (2011). Dynamics between stem cells, niche,

- and progeny in the hair follicle. *Cell*, 144(1), 92–105.  
<https://doi.org/10.1016/j.cell.2010.11.049>
- Hu, C.-J., Wang, L.-Y., Chodosh, L. A., Keith, B., & Simon, M. C. (2003). Differential Roles of Hypoxia-Inducible Factor 1 $\alpha$  (HIF-1 $\alpha$ ) and HIF-2 $\alpha$  in Hypoxic Gene Regulation. *Molecular and Cellular Biology*, 23(24), 9361–9374.  
<https://doi.org/10.1128/mcb.23.24.9361-9374.2003>
- Hu, C., Wang, L., Chodosh, L. a, Keith, B., & Simon, M. C. (2003). Differential Roles of Hypoxia-Inducible Factor 1 alpha ( HIF-1 alpha ) and HIF-2 alpha in Hypoxic Gene Regulation. *Molecular and Cellular Biology*, 23(24), 9361–9374.  
<https://doi.org/10.1128/MCB.23.24.9361>
- Hu, X. F., Li, J., Yang, E., Vandervalk, S., & Xing, P. X. (2007). Anti-Cripto Mab inhibit tumour growth and overcome MDR in a human leukaemia MDR cell line by inhibition of Akt and activation of JNK/SAPK and bad death pathways. *British Journal of Cancer*, 96(6), 918–927. <https://doi.org/10.1038/sj.bjc.6603641>
- Hu, Xiu Feng, & Xing, P. X. (2005). Cripto as a target for cancer immunotherapy. *Expert Opinion on Therapeutic Targets*, 9(2), 383–394.  
<https://doi.org/10.1517/14728222.9.2.383>
- Huang, L. E., Gu, J., Schau, M., & Bunn, H. F. (1998). Regulation of hypoxia-inducible factor 1 $\alpha$  is mediated by an O<sub>2</sub>-dependent degradation domain via the ubiquitin-proteasome pathway. *Proceedings of the National Academy of Sciences of the United States of America*, 95(14), 7987–7992.  
<https://doi.org/10.1073/pnas.95.14.7987>
- Huntly, B. J. P., & Gilliland, D. G. (2005). Leukaemia stem cells and the evolution of cancer-stem-cell research. *Nature Reviews Cancer*, 5(4), 311–321.  
<https://doi.org/10.1038/nrc1592>
- Hur, E., Chang, K. Y., Lee, E., Lee, S. K., & Park, H. (2001). Mitogen-activated protein kinase kinase inhibitor PD98059 blocks the trans-activation but not the stabilization or DNA binding ability of Hypoxia-inducible factor-1 $\alpha$ . *Molecular Pharmacology*, 59(5), 1216–1224. <https://doi.org/10.1124/mol.59.5.1216>
- Inoshima, I., Inoshima, N., Wilke, G., Powers, M., Frank, K., Wang, Y., &

- Wardenburg, J. B. (2012). *Teratoma Formation: A Tool for Monitoring Pluripotency in Stem Cell Research Raman*. *17*(10), 1310–1314.  
<https://doi.org/10.1002/9780470151808.sc04a08s32.Teratoma>
- Ischenko, I., Zhi, J., Moll, U. M., Nemaierova, A., & Petrenko, O. (2013). Direct reprogramming by oncogenic Ras and Myc. *Proceedings of the National Academy of Sciences of the United States of America*, *110*(10), 3937–3942.  
<https://doi.org/10.1073/pnas.1219592110>
- Iyer, N. V., Kotch, L. E., Agani, F., Leung, S. W., Laughner, E., Wenger, R. H., Gassmann, M., Gearhart, J. D., Lawler, A. M., Yu, A. Y., & Semenza, G. L. (1998). Cellular and developmental control of O<sub>2</sub> homeostasis by hypoxia-inducible factor 1 $\alpha$ . *Genes and Development*, *12*(2), 149–162.  
<https://doi.org/10.1101/gad.12.2.149>
- Jaakkola, P., Mole, D. R., Tian, Y.-M., Wilson, M. I., Gielbert, J., Gaskell, S. J., Kriegsheim, A. von, Hebestreit, H. F., Mukherji, M., Schofield, C. J., Maxwell, P. H., Pugh, ‡ Christopher W, & Ratcliffe, ‡ Peter J. (2001). Targeting of HIF- $\alpha$  to the von Hippel-Lindau Ubiquitylation Complex by O<sub>2</sub>-Regulated Prolyl Hydroxylation. *Science*, *292*(5516), 468 LP – 472.  
<https://doi.org/10.1126/science.1059796>
- Jacobson, A. C., & Weis, J. H. (2008). Comparative Functional Evolution of Human and Mouse CR1 and CR2. *The Journal of Immunology*, *181*(5), 2953–2959.  
<https://doi.org/10.4049/jimmunol.181.5.2953>
- Jaggupilli, A., & Elkord, E. (2012). Significance of CD44 and CD24 as cancer stem cell markers: An enduring ambiguity. *Clinical and Developmental Immunology*, *2012*. <https://doi.org/10.1155/2012/708036>
- Jerabek, S., Merino, F., Schöler, H. R., & Cojocaru, V. (2014). OCT4: Dynamic DNA binding pioneers stem cell pluripotency. *Biochimica et Biophysica Acta - Gene Regulatory Mechanisms*, *1839*(3), 138–154.  
<https://doi.org/10.1016/j.bbagr.2013.10.001>
- Jewell, U. R., Kvietikova, I., Scheid, A., Bauer, C., Wenger, R. H., & Gassmann, M. (2001). Induction of HIF-1 $\alpha$  in response to hypoxia is instantaneous. *FASEB*

- Journal : Official Publication of the Federation of American Societies for Experimental Biology*, 15(7), 1312–1314.
- Jhaveri, N., Chen, T. C., & Hofman, F. M. (2016). Tumor vasculature and glioma stem cells: Contributions to glioma progression. *Cancer Letters*, 380(2), 545–551. <https://doi.org/10.1016/j.canlet.2014.12.028>
- Jiang, B. H., Rue, E., Wang, G. L., Roe, R., & Semenza, G. L. (1996). Dimerization, DNA binding, and transactivation properties of hypoxia- inducible factor 1. *Journal of Biological Chemistry*, 271(30), 17771–17778. <https://doi.org/10.1074/jbc.271.30.17771>
- Jiang, T., & Qiu, Y. (2003). Interaction between Src and a C-terminal Proline-rich Motif of Akt Is Required for Akt Activation\*. *Journal of Biological Chemistry*, 278(18), 15789–15793. <https://doi.org/https://doi.org/10.1074/jbc.M212525200>
- Jiao, M. I. N., & Nan, K. (2012). *Activation of PI3 kinase / Akt / HIF-1  $\alpha$  pathway contributes to hypoxia-induced epithelial-mesenchymal transition and chemoresistance in hepatocellular carcinoma*. 461–468. <https://doi.org/10.3892/ijo.2011.1197>
- Jin, X., Jin, X., Jung, J. E., Beck, S., & Kim, H. (2013). Cell surface Nestin is a biomarker for glioma stem cells. *Biochemical and Biophysical Research Communications*, 433(4), 496–501. <https://doi.org/10.1016/j.bbrc.2013.03.021>
- Jing, X., Yang, F., Shao, C., Wei, K., Xie, M., Shen, H., & Shu, Y. (2019). Role of hypoxia in cancer therapy by regulating the tumor microenvironment. *Molecular Cancer*, 18(1), 1–15. <https://doi.org/10.1186/s12943-019-1089-9>
- Johansson, M., & Karlsson, A. (1996). Cloning and expression of human deoxyguanosine kinase cDNA. *Proceedings of the National Academy of Sciences*, 93(14), 7258 LP – 7262. <https://doi.org/10.1073/pnas.93.14.7258>
- Johnson, S. E., Rothstein, J. L., & Knowles, B. B. (1994). Expression of epidermal growth factor family gene members in early mouse development. *Developmental Dynamics*, 201(3), 216–226. <https://doi.org/10.1002/aja.1002010305>
- Joyce, H., McCann, A., Clynes, M., & Larkin, A. (2015). Influence of multidrug

- resistance and drug transport proteins on chemotherapy drug metabolism. *Expert Opinion on Drug Metabolism and Toxicology*, 11(5), 795–809.  
<https://doi.org/10.1517/17425255.2015.1028356>
- Kamdje, A. H. N., Kamga, P. T., Simo, R. T., Vecchio, L., Etet, P. F. S., Muller, J. M., Bassi, G., Lukong, E., Goel, R. K., Amvene, J. M., & Krampera, M. (2017). Developmental pathways associated with cancer metastasis: Notch, Wnt, and Hedgehog. *Cancer Biology and Medicine*, 14(2), 109–120.  
<https://doi.org/10.20892/j.issn.2095-3941.2016.0032>
- Kannan, S., Santis, M. De, Lohmeyer, M., & Riese, D. (1997). Cripto enhances the tyrosine phosphorylation of Shc and activates mitogen-activated protein kinase (MAPK) in mammary epithelial cells. *Journal of Biological Chemistry*.  
<http://www.jbc.org/content/272/6/3330.short>
- Kasai, T., Chen, L., Mizutani, A., Kudoh, T., Murakami, H., Fu, L., & Seno, M. (2014). Cancer stem cells converted from pluripotent stem cells and the cancerous niche. *Journal of Stem Cells and Regenerative Medicine*, 10(1), 2–7.  
<https://doi.org/10.46582/jsrm.1001002>
- Kashyap, V., Rezende, N. C., Scotland, K. B., Shaffer, S. M., Persson, J. L., Gudas, L. J., & Mongan, N. P. (2009). Regulation of Stem cell pluripotency and differentiation involves a mutual regulatory circuit of the Nanog, OCT4, and SOX2 pluripotency transcription factors with polycomb Repressive Complexes and Stem Cell microRNAs. *Stem Cells and Development*, 18(7), 1093–1108.  
<https://doi.org/10.1089/scd.2009.0113>
- Katayama, K., Noguchi, K., & Sugimoto, Y. (2014). Regulations of P-Glycoprotein/ABCB1/MDR1 in Human Cancer Cells. *New Journal of Science*, 2014, 1–10. <https://doi.org/10.1155/2014/476974>
- Katoh & Katoh. (2008). Hedgehog signalling, epithelial-to-mesenchymal transition and miRNA (Review). *International Journal of Molecular Medicine*, 22(4), 271–275.  
[https://doi.org/10.3892/ijmm\\_00000019](https://doi.org/10.3892/ijmm_00000019)
- Keith, B., Johnson, R. S., & Simon, M. C. (2012). HIF1  $\alpha$  and HIF2  $\alpha$ : sibling rivalry in hypoxic tumour growth and progression. In *Nature Reviews Cancer* (Vol. 12,

- Issue 1, pp. 9–22). <https://doi.org/10.1038/nrc3183>
- Kelber, J. A., Panopoulos, A. D., Shani, G., Booker, E. C., Belmonte, J. C., Vale, W. W., & Gray, P. C. (2009). Blockade of Cripto binding to cell surface GRP78 inhibits oncogenic Cripto signalling via MAPK/PI3K and Smad2/3 pathways. *Oncogene*, 28(24), 2324–2336. <https://doi.org/10.1038/onc.2009.97>
- Kimura, Y., Morita, S., Matsuo, M., & Ueda, K. (2007). Mechanism of multidrug recognition by MDR1/ABCB1. *Cancer Science*, 98(9), 1303–1310. <https://doi.org/10.1111/j.1349-7006.2007.00538.x>
- Kinoshita, T. (2014). Enzymatic mechanism of GPI anchor attachment clarified. *Cell Cycle*, 13(12), 1838–1839. <https://doi.org/10.4161/cc.29379>
- Kizaka-Kondoh, S., Inoue, M., Harada, H., & Hiraoka, M. (2003). Tumor hypoxia: a target for selective cancer therapy. *Cancer Science*, 94(12), 1021–1028. <https://doi.org/10.1111/j.1349-7006.2003.tb01395.x>
- Klapper, L. N., Kirschbaum, L. N., Sela, M., & Yarden, Y. (1999). Biochemical and clinical implications of the ErbB/HER signalling network of growth factor receptors. *Advances in Cancer Research*, 77, 25–79. [https://doi.org/10.1016/S0065-230X\(08\)60784-8](https://doi.org/10.1016/S0065-230X(08)60784-8)
- Klauzinska, M., Castro, N. P., Rangel, M. C., Spike, B. T., Gray, P. C., Bertolette, D., Cuttitta, F., & Salomon, D. (2014). The multifaceted role of the embryonic gene Cripto-1 in cancer, stem cells and epithelial-mesenchymal transition. *Seminars in Cancer Biology*, 29, 51–58. <https://doi.org/10.1016/j.semcancer.2014.08.003>
- Klonisch, T., Wiehac, E., Hombach-Klonisch, S., Ande, S. R., Wesselborg, S., Schulze-Osthoff, K., & Los, M. (2008). Cancer stem cell markers in common cancers - therapeutic implications. *Trends in Molecular Medicine*, 14(10), 450–460. <https://doi.org/10.1016/j.molmed.2008.08.003>
- Knizetova, P., Ehrmann, J., Hlobilkova, A., Vancova, I., Kalita, O., Kolar, Z., & Bartek, J. (2008). Autocrine regulation of glioblastoma cell-cycle progression, viability and radioresistance through the VEGF-VEGFR2 (KDR) interplay. *Cell Cycle*, 7(16), 2553–2561. <https://doi.org/10.4161/cc.7.16.6442>

- Koivunen, P., Hirsilä, M., Günzler, V., Kivirikko, K. I., & Myllyharju, J. (2004). Catalytic Properties of the Asparaginyl Hydroxylase (FIH) in the Oxygen Sensing Pathway Are Distinct from Those of Its Prolyl 4-Hydroxylases. *Journal of Biological Chemistry*, 279(11), 9899–9904. <https://doi.org/10.1074/jbc.M312254200>
- Kolenda, J., Skov, S., & Charlotte, J. (2011). *Effects of hypoxia on expression of a panel of stem cell and chemoresistance markers in glioblastoma-derived spheroids*. 43–58. <https://doi.org/10.1007/s11060-010-0357-8>
- Koop, S., MacDonald, I. C., Luzzi, K., Schmidt, E. E., Morris, V. L., Grattan, M., Khokha, R., Chambers, A. F., & Groom, A. C. (1995). Fate of Melanoma Cells Entering the Microcirculation: Over 80% Survive and Extravasate. *Cancer Research*, 55(12), 2520–2523.
- Kotch, L. E., Iyer, N. V., Laughner, E., & Semenza, G. L. (1999). Defective vascularization of HIF-1 $\alpha$ -null embryos is not associated with VEGF deficiency but with mesenchymal cell death. *Developmental Biology*, 209(2), 254–267. <https://doi.org/10.1006/dbio.1999.9253>
- Kreso, A., & Dick, J. E. (2014). Evolution of the cancer stem cell model. *Cell Stem Cell*, 14(3), 275–291. <https://doi.org/10.1016/j.stem.2014.02.006>
- Kristensen, T., Jensen, H. K., & Munch-Petersen, B. (1994). Overexpression of human thymidine kinase mRNA without corresponding enzymatic activity in patients with chronic lymphatic leukemia. *Leukemia Research*, 18(11), 861–866. [https://doi.org/https://doi.org/10.1016/0145-2126\(94\)90168-6](https://doi.org/https://doi.org/10.1016/0145-2126(94)90168-6)
- Kypta, R. M., & Waxman, J. (2012). Wnt/ $\beta$ -catenin signalling in prostate cancer. *Nature Reviews. Urology*, 9(8), 418–428. <https://doi.org/10.1038/nrurol.2012.116>
- Labhasetwar, V. (2011). Drug resistance in cancer therapy. *Drug Delivery and Translational Research*, 1(6), 407–408. <https://doi.org/10.1007/s13346-011-0047-x>
- Lando, D., Peet, D. J., Gorman, J. J., Whelan, D. A., Whitelaw, M. L., & Bruick, R. K. (2002). FIH-1 is an asparaginyl hydroxylase enzyme that regulates the transcriptional activity of hypoxia-inducible factor. *Genes and Development*,

- 16(12), 1466–1471. <https://doi.org/10.1101/gad.991402>
- Lapidot, T., Sirard, C., Vormoor, J., Murdoch, B., Hoang, T., Caceres-Cortes, J., Minden, M., Paterson, B., Caligiuri, M. A., & Dick, J. E. (1994). A cell initiating human acute myeloid leukaemia after transplantation into SCID mice. *Nature*, 367(6464), 645–648. <https://doi.org/10.1038/367645a0>
- Lebedeva, I. V., Pande, P., & Patton, W. F. (2011). Sensitive and specific fluorescent probes for functional analysis of the three major types of Mammalian ABC transporters. *PLoS ONE*, 6(7). <https://doi.org/10.1371/journal.pone.0022429>
- Lee, C. H. (2010). Reversing agents for ATP-binding cassette drug transporters. In *Methods in molecular biology (Clifton, N.J.)* (Vol. 596). [https://doi.org/10.1007/978-1-60761-416-6\\_14](https://doi.org/10.1007/978-1-60761-416-6_14)
- Lee, J. T., Steelman, L. S., & McCubrey, J. A. (2004). Phosphatidylinositol 3'-kinase activation leads to multidrug resistance protein-1 expression and subsequent chemoresistance in advanced prostate cancer cells. *Cancer Research*, 64(22), 8397–8404. <https://doi.org/10.1158/0008-5472.CAN-04-1612>
- Lee, J. W., Sung, J. S., Park, Y. S., Chung, S., & Kim, Y. H. (2018). Isolation of spheroid-forming single cells from gastric cancer cell lines: Enrichment of cancer stem-like cells. *BioTechniques*, 65(4), 197–203. <https://doi.org/10.2144/btn-2018-0046>
- Lee, Sau Har, Reed-Newman, T., Anant, S., & Ramasamy, T. S. (2020). Regulatory Role of Quiescence in the Biological Function of Cancer Stem Cells. *Stem Cell Reviews and Reports*, 16(6), 1185–1207. <https://doi.org/10.1007/s12015-020-10031-8>
- Lee, Seung Hoon, Cho, Y. S., Shim, C. S., Kim, J. S., Choi, J. J., Oh, S. H., Kim, J. W., Zhang, W., & Lee, J. H. (2001). Aberrant expression of Smad4 results in resistance against the growth-inhibitory effect of transforming growth factor- $\beta$  in the SiHa human cervical carcinoma cell line. *International Journal of Cancer*, 94(4), 500–507. <https://doi.org/10.1002/ijc.1494>
- Lemos, C., Jansen, G., & Peters, G. J. (2008). Drug transporters: recent advances concerning BCRP and tyrosine kinase inhibitors. *British Journal of Cancer*, 98(5),

- 857–862. <https://doi.org/10.1038/sj.bjc.6604213>
- Lengyel, E. (2010). Ovarian cancer development and metastasis. *American Journal of Pathology*, 177(3), 1053–1064. <https://doi.org/10.2353/ajpath.2010.100105>
- Li, F., Sonveaux, P., Rabbani, Z. N., Liu, S., Yan, B., Huang, Q., Vujaskovic, Z., Dewhirst, M. W. W., & Li, C. Y. (2007). Regulation of HIF-1 $\alpha$  Stability through S-Nitrosylation. *Molecular Cell*, 26(1), 63–74. <https://doi.org/10.1016/j.molcel.2007.02.024>
- Li, J., Xu, Y., Long, X. D., Wang, W., Jiao, H. K., Mei, Z., Yin, Q. Q., Ma, L. N., Zhou, A. W., Wang, L. S., Yao, M., Xia, Q., & Chen, G. Q. (2014). Cbx4 governs HIF-1 $\alpha$  to potentiate angiogenesis of hepatocellular carcinoma by its SUMO E3 ligase activity. *Cancer Cell*, 25(1), 118–131. <https://doi.org/10.1016/j.ccr.2013.12.008>
- Li, L., Qi, L., Liang, Z., Song, W., Liu, Y., Wang, Y., Sun, B., Zhang, B., & Cao, W. (2015). Transforming growth factor- $\beta$ 1 induces EMT by the transactivation of epidermal growth factor signalling through HA/CD44 in lung and breast cancer cells. In *International Journal of Molecular Medicine* (Vol. 36, Issue 1, pp. 113–122). <https://doi.org/10.3892/ijmm.2015.2222>
- Li, M., Knight, D. A., Smyth, M. J., & Stewart, T. J. (2012). Sensitivity of a novel model of mammary cancer stem cell-like cells to TNF-related death pathways. *Cancer Immunology, Immunotherapy*, 61(8), 1255–1268. <https://doi.org/10.1007/s00262-012-1200-1>
- Li, X., Lewis, M. T., Huang, J., Gutierrez, C., Osborne, C. K., Wu, M. F., Hilsenbeck, S. G., Pavlick, A., Zhang, X., Chamness, G. C., Wong, H., Rosen, J., & Chang, J. C. (2008). Intrinsic resistance of tumorigenic breast cancer cells to chemotherapy. *Journal of the National Cancer Institute*, 100(9), 672–679. <https://doi.org/10.1093/jnci/djn123>
- Li, Z., Bao, S., Wu, Q., Wang, H., Eyler, C., Sathornsumetee, S., Shi, Q., Cao, Y., Lathia, J., McLendon, R. E., Hjelmeland, A. B., & Rich, J. N. (2009). Hypoxia-Inducible Factors Regulate Tumorigenic Capacity of Glioma Stem Cells. *Cancer Cell*, 15(6), 501–513. <https://doi.org/10.1016/j.ccr.2009.03.018>

- Liberati, N. T., Datto, M. B., Frederick, J. P., Shen, X., Wong, C., Rougier-Chapman, E. M., & Wang, X. F. (1999). Smads bind directly to the Jun family of AP-1 transcription factors. *Proceedings of the National Academy of Sciences of the United States of America*, *96*(April), 4844–4849.  
<https://doi.org/10.1073/pnas.96.9.4844>
- Lin, Q., Kim, Y., Alarcon, R. M., & Yun, Z. (2008). Oxygen and cell fate decisions. *Gene Regulation and Systems Biology*, *2008*(2), 43–51.  
<https://doi.org/10.4137/grsb.s434>
- Lin, S., Koh, J. J., Aung, T. T., Lim, F., Li, J., Zou, H., Wang, L., Lakshminarayanan, R., Verma, C., Wang, Y., Tan, D. T. H., Cao, D., Beuerman, R. W., Ren, L., & Liu, S. (2017). Symmetrically Substituted Xanthone Amphiphiles Combat Gram-Positive Bacterial Resistance with Enhanced Membrane Selectivity. *Journal of Medicinal Chemistry*, *60*(4), 1362–1378.  
<https://doi.org/10.1021/acs.jmedchem.6b01403>
- Linardi, R. L., & Natalini, C. C. (2006). Multi-drug resistance (MDR1) gene and P-glycoprotein influence on pharmacokinetic and pharmacodynamic of therapeutic drugs. *Ciencia Rural*, *36*(1), 336–341. <https://doi.org/10.1590/s0103-84782006000100056>
- Lister, R., Pelizzola, M., Kida, Y. S., Hawkins, R. D., Nery, J. R., Hon, G., Antosiewicz-Bourget, J., O'Malley, R., Castanon, R., Klugman, S., Downes, M., Yu, R., Stewart, R., Ren, B., Thomson, J. A., Evans, R. M., & Ecker, J. R. (2011). Hotspots of aberrant epigenomic reprogramming in human induced pluripotent stem cells. *Nature*, *471*(7336), 68–73. <https://doi.org/10.1038/nature09798>
- Lisy, K., & Peet, D. J. (2008). Turn me on: Regulating HIF transcriptional activity. *Cell Death and Differentiation*, *15*(4), 642–649. <https://doi.org/10.1038/sj.cdd.4402315>
- Liu, Changjiang, Shi, Y., Du, Y., Ning, X., Liu, N., Huang, D., Liang, J., Xue, Y., & Fan, D. (2005). Dual-specificity phosphatase DUSP1 protects overactivation of hypoxia-inducible factor 1 through inactivating ERK MAPK. *Experimental Cell Research*, *309*(2), 410–418.  
<https://doi.org/https://doi.org/10.1016/j.yexcr.2005.06.022>

- Liu, Cong, Krishnan, J., & Xu, X. Y. (2015). Intrinsic and induced drug resistance mechanisms: in silico investigations at the cellular and tissue scales. *Integrative Biology*, 7(9), 1044–1060. <https://doi.org/10.1039/C5IB00088B>
- Liu, H., & Bian, L. (2016). *CD44+/CD24+ cervical cancer cells resist radiotherapy and exhibit properties of cancer stem cells*. 20, 1745–1754.
- Liu, Q., Cui, X., Yu, X., Bian, B., Qian, F., Hu, X., Ji, C., & Yang, L. (2017). *Cripto-1 acts as a functional marker of cancer stem-like cells and predicts prognosis of the patients in esophageal squamous cell carcinoma*. 1–12. <https://doi.org/10.1186/s12943-017-0650-7>
- Liu, Q., Cui, X., Yu, X., Bian, B. S. J., Qian, F., Hu, X. gang, Ji, C. dong, Yang, L., Ren, Y., Cui, W., Zhang, X., Zhang, P., Wang, J. M., Cui, Y. hong, & Bian, X. wu. (2017). *Cripto-1 acts as a functional marker of cancer stem-like cells and predicts prognosis of the patients in esophageal squamous cell carcinoma*. *Molecular Cancer*, 16(1), 1–12. <https://doi.org/10.1186/s12943-017-0650-7>
- Lo, R. C. L., Leung, C. O. N., Chan, K. K. S., Ho, D. W. H., Wong, C. M., Lee, T. K. W., & Ng, I. O. L. (2018). *Cripto-1 contributes to stemness in hepatocellular carcinoma by stabilizing Dishevelled-3 and activating Wnt/ $\beta$ -catenin pathway*. *Cell Death and Differentiation*, 25(8), 1426–1441. <https://doi.org/10.1038/s41418-018-0059-x>
- Lo, R. C., Leung, C. O., Chan, K. K., Ho, D. W., Wong, C., Lee, T. K., & Ng, I. O. (2018). *Cripto-1 contributes to stemness in hepatocellular carcinoma by stabilizing Dishevelled-3 and activating Wnt /  $\beta$  -catenin pathway*.
- Loh, C. Y., Chai, J. Y., Tang, T. F., Wong, W. F., Sethi, G., Shanmugam, M. K., Chong, P. P., & Looi, C. Y. (2019). *The E-Cadherin and N-Cadherin Switch in Epithelial-to-Mesenchymal Transition: Signalling, Therapeutic Implications, and Challenges*. In *Cells* (Vol. 8, Issue 10). <https://doi.org/10.3390/cells8101118>
- Loh, Y. H., Wu, Q., Chew, J. L., Vega, V. B., Zhang, W., Chen, X., Bourque, G., George, J., Leong, B., Liu, J., Wong, K. Y., Sung, K. W., Lee, C. W. H., Zhao, X. D., Chiu, K. P., Lipovich, L., Kuznetsov, V. A., Robson, P., Stanton, L. W., ... Ng, H. H. (2006). *The Oct4 and Nanog transcription network regulates*

- pluripotency in mouse embryonic stem cells. *Nature Genetics*, 38(4), 431–440.  
<https://doi.org/10.1038/ng1760>
- Lonardo, E., Hermann, P. C., Mueller, M. T., Huber, S., Balic, A., Miranda-Lorenzo, I., Zagorac, S., Alcala, S., Rodriguez-Arabaolaza, I., Ramirez, J. C., Torres-Ruiz, R., Garcia, E., Hidalgo, M., Cebrián, D. Á., Heuchel, R., Löhr, M., Berger, F., Bartenstein, P., Aicher, A., & Heeschen, C. (2011). Nodal/activin signalling drives self-renewal and tumorigenicity of pancreatic cancer stem cells and provides a target for combined drug therapy. *Cell Stem Cell*, 9(5), 433–446.  
<https://doi.org/10.1016/j.stem.2011.10.001>
- Loying, P., Manhas, J., Sen, S., & Bose, B. (2015). Autoregulation and heterogeneity in expression of human Cripto-1. *PloS One*.  
<http://journals.plos.org/plosone/article?id=10.1371/journal.pone.0116748>
- Loying, Pojul, Manhas, J., Sen, S., & Bose, B. (2015). Autoregulation and heterogeneity in expression of human Cripto-1. *PLoS ONE*, 10(2), 1–17.  
<https://doi.org/10.1371/journal.pone.0116748>
- Lu, J. F., Pokharel, D., & Bebawy, M. (2015). MRP1 and its role in anticancer drug resistance. *Drug Metabolism Reviews*, 47(4), 406–419.  
<https://doi.org/10.3109/03602532.2015.1105253>
- Lu, W., & Kang, Y. (2019). Epithelial-Mesenchymal Plasticity in Cancer Progression and Metastasis. *Developmental Cell*, 49(3), 361–374.  
<https://doi.org/10.1016/j.devcel.2019.04.010>
- Lugowska, I., Kosela-Paterczyk, H., Kozak, K., & Rutkowski, P. (2015). Trametinib: A MEK inhibitor for management of metastatic melanoma. *OncoTargets and Therapy*, 8, 2251–2259. <https://doi.org/10.2147/OTT.S72951>
- Luo, M., & Guan, J.-L. (2010). Focal adhesion kinase: A prominent determinant in breast cancer initiation, progression and metastasis. *Cancer Letters*, 289(2), 127–139. <https://doi.org/https://doi.org/10.1016/j.canlet.2009.07.005>
- Luzzi, K. J., MacDonald, I. C., Schmidt, E. E., Kerkvliet, N., Morris, V. L., Chambers, A. F., & Groom, A. C. (1998). Multistep nature of metastatic inefficiency: Dormancy of solitary cells after successful extravasation and limited survival of

- early micrometastases. *American Journal of Pathology*, 153(3), 865–873.  
[https://doi.org/10.1016/S0002-9440\(10\)65628-3](https://doi.org/10.1016/S0002-9440(10)65628-3)
- Magee, J. A., Piskounova, E., & Morrison, S. J. (2012). Cancer Stem Cells: Impact, Heterogeneity, and Uncertainty. *Cancer Cell*, 21(3), 283–296.  
<https://doi.org/10.1016/j.ccr.2012.03.003>
- Mahmoudian, R. A., Abbaszadegan, M. R., Forghanifard, M. M., Moghbeli, M., Moghbeli, F., Chamani, J., & Gholamin, M. (2017). Biological and clinicopathological significance of Cripto-1 expression in the progression of human ESCC. *Reports of Biochemistry and Molecular Biology*, 5(2), 83–90.  
<https://doi.org/10.1016/j.jocit.2017.04.036>
- Makino, Y., Kanopka, A., Wilson, W. J., Tanaka, H., & Poellinger, L. (2002). Inhibitory PAS domain protein (IPAS) is a hypoxia-inducible splicing variant of the hypoxia-inducible factor-3 $\alpha$  locus. *Journal of Biological Chemistry*, 277(36), 32405–32408. <https://doi.org/10.1074/jbc.C200328200>
- Mancino, M., Esposito, C., Watanabe, K., Nagaoka, T., Gonzales, M., Bianco, C., Normanno, N., Salomon, D. S., & Strizzi, L. (2009). Neuronal guidance protein netrin-1 induces differentiation in human embryonal carcinoma cells. *Cancer Research*, 69(5), 1717–1721. <https://doi.org/10.1158/0008-5472.CAN-08-2985>
- Mancino, M., Strizzi, L., Wechselberger, C., Watanabe, K., Gonzales, M., Hamada, S., Normanno, N., Salomon, D. S., & Bianco, C. (2008). Regulation of human Cripto-1 gene expression by TGF- $\beta$ 1 and BMP-4 in embryonal and colon cancer cells. *Journal of Cellular Physiology*, 215(1), 192–203.  
<https://doi.org/10.1002/jcp.21301>
- Månsson, E., Flordal, E., Liliemark, J., Spasokoukotskaja, T., Elford, H., Lagercrantz, S., Eriksson, S., & Albertioni, F. (2003). Down-regulation of deoxycytidine kinase in human leukemic cell lines resistant to cladribine and clofarabine and increased ribonucleotide reductase activity contributes to fludarabine resistance. *Biochemical Pharmacology*, 65(2), 237–247.  
[https://doi.org/https://doi.org/10.1016/S0006-2952\(02\)01484-3](https://doi.org/https://doi.org/10.1016/S0006-2952(02)01484-3)
- Mao, Q., & Unadkat, J. D. (2005). Role of the breast cancer resistance protein

- (ABCG2) in drug transport. *AAPS Journal*, 7(1), 118–133.  
<https://doi.org/10.1208/aapsj070112>
- Maria Cristina, Rangel Nadia, P. Castro, Hideaki Karasawa, Tadahiro Nagaoka, David S. Salomon, C. B. (2012). Stem Cells and Cancer Stem Cells, Volume 2. In M. A. Hayat (Ed.), *Journal of Chemical Information and Modeling* (1st ed., Vol. 53, Issue 9). Springer Netherlands. <https://doi.org/10.1007/978-94-007-2016-9>
- Marjanovic, N. D., Weinberg, R. A., & Chaffer, C. L. (2013). Cell plasticity and heterogeneity in cancer. *Clinical Chemistry*, 59(1), 168–179.  
<https://doi.org/10.1373/clinchem.2012.184655>
- Martin, G. R. (1981). Isolation of a pluripotent cell line from early mouse embryos cultured in medium conditioned by teratocarcinoma stem cells. *Proceedings of the National Academy of Sciences of the United States of America*, 78(12 II), 7634–7638. <https://doi.org/10.1073/pnas.78.12.7634>
- Massagué, J., & Xi, Q. (2012). TGF- $\beta$  control of stem cell differentiation genes. *FEBS Letters*, 586(14), 1953–1958. <https://doi.org/10.1016/j.febslet.2012.03.023>
- Mathieu, J., Zhang, Z., Nelson, A., Lamba, D. A., Reh, T. A., Ware, C., & Ruohola-Baker, H. (2013). Hypoxia induces re-entry of committed cells into pluripotency. *Stem Cells*, 31(9), 1737–1748. <https://doi.org/10.1002/stem.1446>
- Mathieu, J., Zhang, Z., Zhou, W., Wang, A. J., Heddleston, J. M., Pinna, C. M. A., Hubaud, A., Stadler, B., Choi, M., Bar, M., Tewari, M., Liu, A., Vessella, R., Rostomily, R., Born, D., Horwitz, M., Ware, C., Blau, C. A., Cleary, M. A., ... Ruohola-Baker, H. (2011). HIF induces human embryonic stem cell markers in cancer cells. *Cancer Research*, 71(13), 4640–4652. <https://doi.org/10.1158/0008-5472.CAN-10-3320>
- Mazure, N. M., Brahimi-Horn, M. C., Berta, M. A., Benizri, E., Bilton, R. L., Dayan, F., Ginouvès, A., Berra, E., & Pouyssegur, J. (2004). HIF-1: master and commander of the hypoxic world: A pharmacological approach to its regulation by siRNAs. *Biochemical Pharmacology*, 68(6), 971–980.  
<https://doi.org/https://doi.org/10.1016/j.bcp.2004.04.022>
- McAuliffe, P., Meric-Bernstam, F., Mills, G., & Gonzalez-Angulo, A. (2010).

- Deciphering the role of PI3K/Akt/mTOR pathway in breast cancer biology and pathogenesis. *Clinical Breast Cancer*, 10(SUPPL. 3), S59–S65.  
<https://doi.org/10.3816/CBC.2010.s.013>
- McCubrey, J. A., Rakus, D., Gizak, A., Steelman, L. S., Abrams, S. L., Lertpiriyapong, K., Fitzgerald, T. L., Yang, L. V., Montalto, G., Cervello, M., Libra, M., Nicoletti, F., Scalisi, A., Torino, F., Fenga, C., Neri, L. M., Marmioli, S., Cocco, L., & Martelli, A. M. (2016). Effects of mutations in Wnt/ $\beta$ -catenin, hedgehog, Notch and PI3K pathways on GSK-3 activity—Diverse effects on cell growth, metabolism and cancer. *Biochimica et Biophysica Acta (BBA) - Molecular Cell Research*, 1863(12), 2942–2976. <https://doi.org/10.1016/j.bbamcr.2016.09.004>
- Miharada, K., Karlsson, G., Rehn, M., Rörby, E., Siva, K., Cammenga, J., & Karlsson, S. (2011). Cripto regulates hematopoietic stem cells as a hypoxic-niche-related factor through cell surface receptor GRP78. *Cell Stem Cell*, 9(4), 330–344.  
<https://doi.org/10.1016/j.stem.2011.07.016>
- Milane, L., Ganesh, S., Shah, S., Duan, Z. F., & Amiji, M. (2011). Multi-modal strategies for overcoming tumor drug resistance: Hypoxia, the Warburg effect, stem cells, and multifunctional nanotechnology. *Journal of Controlled Release*, 155(2), 237–247. <https://doi.org/10.1016/j.jconrel.2011.03.032>
- Minchiotti, G., Manco, G., Parisi, S., Lago, C. T., Rosa, F., & Graziella Persico, M. (2001). Structure–function analysis of the EGF-CFC family member Cripto identifies residues essential for nodal signalling. *Development*, 128(22), 4501–4510.
- Minet, E., Arnould, T., Michel, G., Roland, I., Mottet, D., Raes, M., Remacle, J., & Michiels, C. (2000). ERK activation upon hypoxia: Involvement in HIF-1 activation. *FEBS Letters*, 468(1), 53–58. [https://doi.org/10.1016/S0014-5793\(00\)01181-9](https://doi.org/10.1016/S0014-5793(00)01181-9)
- Mitra, A., Mishra, L., & Li, S. (2015). EMT, CTCs and CSCs in tumor relapse and drug-resistance. *Oncotarget*, 6(13), 10697–10711.  
<https://doi.org/10.18632/oncotarget.4037>
- Mohyeldin, A., Garzón-Muvdi, T., & Quiñones-Hinojosa, A. (2010). Oxygen in stem

- cell biology: A critical component of the stem cell niche. *Cell Stem Cell*, 7(2), 150–161. <https://doi.org/10.1016/j.stem.2010.07.007>
- Moitra, K. (2015). Overcoming Multidrug Resistance in Cancer Stem Cells. *BioMed Research International*, 2015, 635745. <https://doi.org/10.1155/2015/635745>
- Mokhtari, R. B., Homayouni, T. S., Baluch, N., Morgatskaya, E., Kumar, S., Das, B., & Yeger, H. (2017). Combination therapy in combating cancer SYSTEMATIC REVIEW: COMBINATION THERAPY IN COMBATING CANCER BACKGROUND. *Oncotarget*, 8(23), 38022–38043.
- Mole, D. R., Blancher, C., Copley, R. R., Pollard, P. J., Gleadle, J. M., Ragousis, J., & Ratcliffe, P. J. (2009). Genome-wide association of hypoxia-inducible factor (HIF)-1 $\alpha$  and HIF-2 $\alpha$  DNA binding with expression profiling of hypoxia-inducible transcripts. *Journal of Biological Chemistry*, 284(25), 16767–16775. <https://doi.org/10.1074/jbc.M901790200>
- Molinas, A., Sicard, G., & Jakob, I. (2012). Functional evidence of multidrug resistance transporters (MDR) in rodent olfactory epithelium. *PLoS ONE*, 7(5). <https://doi.org/10.1371/journal.pone.0036167>
- Morkel, M., Huelsken, J., Wakamiya, M., & Ding, J. (2003).  $\beta$ -catenin regulates *Cripto*-and *Wnt3*-dependent gene expression programs in mouse axis and mesoderm formation. <http://dev.biologists.org/content/130/25/6283.short>
- Mottet, D., Dumont, V., Deccache, Y., Demazy, C., Ninane, N., Raes, M., & Michiels, C. (2003). Regulation of hypoxia-inducible factor-1 $\alpha$  protein level during hypoxic conditions by the phosphatidylinositol 3-kinase/Akt/glycogen synthase kinase 3 $\beta$  pathway in HepG2 cells. *Journal of Biological Chemistry*, 278(33), 31277–31285. <https://doi.org/10.1074/jbc.M300763200>
- Mottet, D., Michel, G., Renard, P., Ninane, N., Raes, M., & Michiels, C. (2003). Role of ERK and calcium in the hypoxia-induced activation of HIF-1. *Journal of Cellular Physiology*, 194(1), 30–44. <https://doi.org/10.1002/jcp.10176>
- Multiforme, G. (2015). *Functional Identification of Cripto-1 ( Tdgf1 ) Role in. 1.*
- Muraoka-Cook, R. S., Feng, S. M., Strunk, K. E., & Earp, S. H. (2008). ErbB4/HER4:

- Role in mammary gland development, differentiation and growth inhibition. *Journal of Mammary Gland Biology and Neoplasia*, 13(2), 235–246.  
<https://doi.org/10.1007/s10911-008-9080-x>
- Mylonis, I., Chachami, G., Paraskeva, E., & Simos, G. (2008). Atypical CRM1-dependent Nuclear Export Signal Mediates Regulation of Hypoxia-inducible Factor-1 $\alpha$  by MAPK\*. *Journal of Biological Chemistry*, 283(41), 27620–27627.  
<https://doi.org/https://doi.org/10.1074/jbc.M803081200>
- Mylonis, I., Chachami, G., Samiotaki, M., Panayotou, G., Paraskeva, E., Kalousi, A., Georgatsou, E., Bonanou, S., & Simos, G. (2006). Identification of MAPK Phosphorylation Sites and Their Role in the Localization and Activity of Hypoxia-inducible Factor-1 $\alpha$ \*. *Journal of Biological Chemistry*, 281(44), 33095–33106.  
<https://doi.org/https://doi.org/10.1074/jbc.M605058200>
- Nagaoka, T., Karasawa, H., Castro, N. P., Rangel, M. C., Salomon, D. S., & Bianco, C. (2012). An evolving web of signalling networks regulated by Cripto-1. *Growth Factors*, 30(1), 13–21. <https://doi.org/10.3109/08977194.2011.641962>
- Nagaoka, T., Karasawa, H., Turbyville, T., Rangel, M. C., Castro, N. P., Gonzales, M., Baker, A., Seno, M., Lockett, S., Greer, Y. E., Rubin, J. S., Salomon, D. S., & Bianco, C. (2013). Cripto-1 enhances the canonical Wnt/ $\beta$ -catenin signalling pathway by binding to LRP5 and LRP6 co-receptors. *Cellular Signalling*, 25(1), 178–189. <https://doi.org/10.1016/j.cellsig.2012.09.024>
- Nanduri, J., Yuan, G., Kumar, G. K., Semenza, G. L., & Prabhakar, N. R. (2008). Transcriptional responses to intermittent hypoxia. *Respiratory Physiology & Neurobiology*, 164(1–2), 277–281. <https://doi.org/10.1016/j.resp.2008.07.006>
- Naumov, G. N., Bender, E., Zurakowski, D., Kang, S. Y., Sampson, D., Flynn, E., Watnick, R. S., Straume, O., Akslen, L. A., Folkman, J., & Almog, N. (2006). A model of human tumor dormancy: An angiogenic switch from the nonangiogenic phenotype. *Journal of the National Cancer Institute*, 98(5), 316–325.  
<https://doi.org/10.1093/jnci/djj068>
- Neo, S. Y., Zhang, Y., Yaw, L. P., Li, P., & Lin, S. C. (2000). Axin-induced apoptosis depends on the extent of its JNK activation and its ability to down-regulate beta-

- catenin levels. *Biochemical and Biophysical Research Communications*, 272(1), 144–150. <https://doi.org/10.1006/bbrc.2000.2751>
- Neradil, J., & Veselska, R. (2015). Nestin as a marker of cancer stem cells. *Cancer Science*, 106(7), 803–811. <https://doi.org/10.1111/cas.12691>
- Nogales, E., Grayer Wolf, S., Khan, I. A., Ludueña, R. F., & Downing, K. H. (1995). Structure of tubulin at 6.5 Å and location of the taxol-binding site. *Nature*, 375(6530), 424–427. <https://doi.org/10.1038/375424a0>
- Nomura, Y., Ishikawa, M., Yashiro, Y., Sanggarnjanavanich, S., Yamaguchi, T., Arai, C., Noda, K., Takano, Y., Nakamura, Y., & Hanada, N. (2012). Human periodontal ligament fibroblasts are the optimal cell source for induced pluripotent stem cells. *Histochemistry and Cell Biology*, 137(6), 719–732. <https://doi.org/10.1007/s00418-012-0923-6>
- Nordsmark, M., Overgaard, M., & Overgaard, J. (1996). Pretreatment oxygenation predicts radiation response in advanced squamous cell carcinoma of the head and neck. *Radiotherapy and Oncology : Journal of the European Society for Therapeutic Radiology and Oncology*, 41(1), 31–39. [https://doi.org/10.1016/s0167-8140\(96\)91811-3](https://doi.org/10.1016/s0167-8140(96)91811-3)
- Noris, M., & Remuzzi, G. (2013). Overview of complement activation and regulation. *Seminars in Nephrology*, 33(6), 479–492. <https://doi.org/10.1016/j.semnephrol.2013.08.001>
- Normanno, N., De Luca, A., Bianco, C., Maiello, M. R., Carriero, M. V., Rehman, A., Wechselberger, C., Arra, C., Strizzi, L., Sanicola, M., & Salomon, D. S. (2004). Cripto-1 Overexpression Leads to Enhanced Invasiveness and Resistance to Anoikis in Human MCF-7 Breast Cancer Cells. *Journal of Cellular Physiology*, 198(1), 31–39. <https://doi.org/10.1002/jcp.10375>
- O'Brien-Ball, C., & Biddle, A. (2017). Reprogramming to developmental plasticity in cancer stem cells. *Developmental Biology*, 430(2), 266–274. <https://doi.org/10.1016/j.ydbio.2017.07.025>
- O'Driscoll, L., & Clynes, M. (2006). Molecular markers of multiple drug resistance in breast cancer. *Chemotherapy*, 52(3), 125–129. <https://doi.org/10.1159/000092540>

- Ortiz-Barahona, A., Villar, D., Pescador, N., Amigo, J., & del Peso, L. (2010). Genome-wide identification of hypoxia-inducible factor binding sites and target genes by a probabilistic model integrating transcription-profiling data and in silico binding site prediction. *Nucleic Acids Research*, *38*(7), 2332–2345. <https://doi.org/10.1093/nar/gkp1205>
- Parat, M.-O., & Riggins, G. J. (2012). Caveolin-1, caveolae, and glioblastoma. *Neuro-Oncology*, *14*(6), 679–688. <https://doi.org/10.1093/neuonc/nos079>
- Parisi, S., D'Andrea, D., Lago, C. T., Adamson, E. D., Persico, M. G., & Minchiotti, G. (2003). Nodal-dependent Cripto signalling promotes cardiomyogenesis and redirects the neural fate of embryonic stem cells. *Journal of Cell Biology*, *163*(2), 303–314. <https://doi.org/10.1083/jcb.200303010>
- Park, S. W., Do, H. J., Han, M. H., Choi, W., & Kim, J. H. (2018). The expression of the embryonic gene Cripto-1 is regulated by OCT4 in human embryonal carcinoma NCCIT cells. In *FEBS Letters* (Vol. 592, Issue 1, pp. 24–35). <https://doi.org/10.1002/1873-3468.12935>
- Pastushenko, I., & Blanpain, C. (2019). EMT Transition States during Tumor Progression and Metastasis. *Trends in Cell Biology*, *29*(3), 212–226. <https://doi.org/10.1016/j.tcb.2018.12.001>
- Patrick H. Maxwell\*, M. S. W., Gin-Wen Chang\*, Steven C. Clifford†, E. C. V., Matthew E. Cockman‡, C. C. W., Christopher W. Pugh‡, E. R. M., & Ratcliffe\*‡, & P. J. (2019). *Tumour Suppressor*. *44*(0), 271–275.
- Pei, D., & Weiss, S. J. (1995). Furin-dependent intracellular activation of the human stromelysin-3 zymogen. In *Nature* (Vol. 375, Issue 6528, pp. 244–247). <https://doi.org/10.1038/375244a0>
- Pellegrini, F., & Budman, D. R. (2005). Review: Tubulin Function, Action of Antitubulin Drugs, and New Drug Development. *Cancer Investigation*, *23*(3), 264–273. <https://doi.org/10.1081/CNV-200055970>
- Peng, J., Zhang, L., Drysdale, L., & Fong, G.-H. (2000). The transcription factor EPAS-1/hypoxia-inducible factor 2 $\alpha$  plays an important role in vascular remodeling. *Proceedings of the National Academy of Sciences*, *97*(15), 8386 LP –

8391. <https://doi.org/10.1073/pnas.140087397>

Pereira, N., Cristina, M., Nagaoka, T., Karasawa, H., S., D., & Bianco, C. (2011). Cripto-1: At the Crossroads of Embryonic Stem Cells and Cancer. *Embryonic Stem Cells - Basic Biology to Bioengineering*, May 2014. <https://doi.org/10.5772/22800>

Pérez-Pomares, J. M., & Muñoz-Chápuli, R. (2002). Epithelial–mesenchymal transitions: A mesodermal cell strategy for evolutive innovation in Metazoans. *The Anatomical Record*, 268(3), 343–351. <https://doi.org/https://doi.org/10.1002/ar.10165>

Persico, M. Graziella, Liguori, G. L., Parisi, S., D'Andrea, D., Salomon, D. S., & Minchiotti, G. (2001). Cripto in tumors and embryo development. *Biochimica et Biophysica Acta - Reviews on Cancer*, 1552(2), 87–93. [https://doi.org/10.1016/S0304-419X\(01\)00039-7](https://doi.org/10.1016/S0304-419X(01)00039-7)

Persico, Maria Graziella, Liguori, G. L., Parisi, S., D'Andrea, D., Salomon, D. S., Minchiotti, G., Niemeyer, C. C., Spencer-Dene, B., Wu, J. X., Adamson, E. D., Persico, M. G., Adamson, E. D., Baldassarre, G., Romano, A., Armenante, F., Rambaldi, M., Paoletti, I., Sandomenico, C., Pepe, S., ... Salomon, D. S. (1998). Preneoplastic mammary tumor markers: Cripto and amphiregulin are overexpressed in hyperplastic stages of tumor progression in transgenic mice. *Molecular Oncology*, 5(4), 440–449. <https://doi.org/10.5958/0973-9130.2019.00444.4>

Petty, A. P., Garman, K. L., Winn, V. D., Spidel, C. M., & Lindsey, J. S. (2007). Overexpression of carcinoma and embryonic cytotrophoblast cell-specific Mig-7 induces invasion and vessel-like structure formation. *American Journal of Pathology*, 170(5), 1763–1780. <https://doi.org/10.2353/ajpath.2007.060969>

Pilgaard, L., Mortensen, J. H., Henriksen, M., Olesen, P., Sørensen, P., Laursen, R., Vyberg, M., Agger, R., Zachar, V., Moos, T., & Duroux, M. (2014). *Cripto-1 Expression in Glioblastoma Multiforme*. 24, 360–370. <https://doi.org/10.1111/bpa.12131>

Polakis, P. (2012). Wnt signalling in cancer. *Cold Spring Harbor Perspectives in*

- Biology*, 4(5). <https://doi.org/10.1101/cshperspect.a008052>
- Powis, G., & Kirkpatrick, L. (2004). Hypoxia inducible factor-1 $\alpha$  as a cancer drug target. *Molecular Cancer Therapeutics*, 3(5), 647 LP – 654.  
<http://mct.aacrjournals.org/content/3/5/647.abstract>
- Putnam, A. J. (2014). The instructive role of the vasculature in stem cell niches. *Biomater. Sci.*, 2(11), 1562–1573. <https://doi.org/10.1039/C4BM00200H>
- Qian, C. N., Tan, M. H., Yang, J. P., & Cao, Y. (2016). Revisiting tumor angiogenesis: Vessel co-option, vessel remodeling, and cancer cell-derived vasculature formation. *Chinese Journal of Cancer*, 35(2), 2–7. <https://doi.org/10.1186/s40880-015-0070-2>
- Qiang, L., Wu, T., Zhang, H. W., Lu, N., Hu, R., Wang, Y. J., Zhao, L., Chen, F. H., Wang, X. T., You, Q. D., & Guo, Q. L. (2012). HIF-1 $\alpha$  is critical for hypoxia-mediated maintenance of glioblastoma stem cells by activating Notch signalling pathway. In *Cell Death and Differentiation* (Vol. 19, Issue 2, pp. 284–294). <https://doi.org/10.1038/cdd.2011.95>
- Rangel, M. C., Karasawa, H., Castro, N. P., Nagaoka, T., Salomon, D. S., & Bianco, C. (2012). Role of Cripto-1 during epithelial-to-mesenchymal transition in development and cancer. *American Journal of Pathology*, 180(6), 2188–2200. <https://doi.org/10.1016/j.ajpath.2012.02.031>
- Raya, A., Kawakami, Y., Rodríguez-Esteban, C., Büscher, D., Koth, C. M., Itoh, T., Morita, M., Raya, R. M., Dubova, I., Bessa, J. G., De la Pompa, J. L., & Izpisua Belmonte, J. C. (2003). Notch activity induces Nodal expression and mediates the establishment of left-right asymmetry in vertebrate embryos. *Genes and Development*, 17(10), 1213–1218. <https://doi.org/10.1101/gad.1084403>
- Reynolds, D. S., Tevis, K. M., Blessing, W. A., Colson, Y. L., Zaman, M. H., & Grinstaff, M. W. (2017). Breast Cancer Spheroids Reveal a Differential Cancer Stem Cell Response to Chemotherapeutic Treatment. *Scientific Reports*, 7(1), 1–12. <https://doi.org/10.1038/s41598-017-10863-4>
- Ricci-Vitiani, L., Pallini, R., Biffoni, M., Todaro, M., Invernici, G., Cenci, T., Maira, G., Parati, E. A., Stassi, G., Larocca, L. M., & De Maria, R. (2010). Tumour

- vascularization via endothelial differentiation of glioblastoma stem-like cells. *Nature*, 468(7325), 824–828. <https://doi.org/10.1038/nature09557>
- Richard, D. E., Berra, E., Gothié, E., Roux, D., & Pouyssegur, J. (1999). p42/p44 Mitogen-activated Protein Kinases Phosphorylate Hypoxia-inducible Factor 1 $\alpha$  (HIF-1 $\alpha$ ) and Enhance the Transcriptional Activity of HIF-1\*. *Journal of Biological Chemistry*, 274(46), 32631–32637. <https://doi.org/https://doi.org/10.1074/jbc.274.46.32631>
- Rippon, H. J., & Bishop, A. E. (2004). Embryonic stem cells. *Cell Proliferation*, 37(1), 23–34. <https://doi.org/10.1111/j.1365-2184.2004.00298.x>
- Robey, R. W., Shukla, S., Steadman, K., Obrzut, T., Finley, E. M., Ambudkar, S. V., & Bates, S. E. (2007). Inhibition of ABCG2-mediated transport by protein kinase inhibitors with a bisindolylmaleimide or indolocarbazole structure. *Molecular Cancer Therapeutics*, 6(6), 1877 LP – 1885. <https://doi.org/10.1158/1535-7163.MCT-06-0811>
- Röpke, M., Boltze, C., Neumann, H. W., Roessner, A., & Schneider-Stock, R. (2003). Genetic and epigenetic alterations in tumor progression in a dedifferentiated chondrosarcoma. *Pathology Research and Practice*, 199(6), 437–444. <https://doi.org/10.1078/0344-0338-00443>
- Ruas, J. L., Poellinger, L., & Pereira, T. (2002). Functional analysis of hypoxia-inducible factor-1 $\alpha$ -mediated transactivation: Identification of amino acid residues critical for transcriptional activation and/or interaction with creb-binding protein. *Journal of Biological Chemistry*, 277(41), 38723–38730. <https://doi.org/10.1074/jbc.M205051200>
- Ruggiero, D., Nappo, S., Nutile, T., Sorice, R., Talotta, F., Giorgio, E., Bellenguez, C., Leutenegger, A. L., Liguori, G. L., & Ciullo, M. (2015). Genetic Variants Modulating CRIPTO Serum Levels Identified by Genome-Wide Association Study in Cilento Isolates. *PLoS Genetics*, 11(1), 1–19. <https://doi.org/10.1371/journal.pgen.1004976>
- Saccone, S., Rapisarda, A., Motta, S., Dono, R., Persico, G. M., & Della Valle, G. (1995). Regional localization of th human EGF-like growth factor CRIPTO gene

- (TDGF-1) to chromosome 3p21. *Human Genetics*, 95(2), 229–230.  
<https://doi.org/10.1007/BF00209409>
- Saeed, M., Zeino, M., Kadioglu, O., Volm, M., & Efferth, T. (2014). Overcoming of P-glycoprotein-mediated multidrug resistance of tumors in vivo by drug combinations. *Synergy*, 1(1), 44–58. <https://doi.org/10.1016/j.synres.2014.07.002>
- Sakuma, R., Ohnishi, Y. I., Meno, C., Fujii, H., Juan, H., Takeuchi, J., Ogura, T., Li, E., Miyazono, K., & Hamada, H. (2002). Inhibition of Nodal signalling by Lefty mediated through interaction with common receptors and efficient diffusion. *Genes to Cells*, 7(4), 401–412. <https://doi.org/10.1046/j.1365-2443.2002.00528.x>
- Salomon, D. S., Bianco, C., Ebert, A. D., Khan, N. I., De Santis, M., Normanno, N., Wechselberger, C., Seno, M., Williams, K., Sanicola, M., Foley, S., Gullick, W. J., & Persico, G. (2000). The EGF-CFC family: Novel epidermal growth factor-related proteins in development and cancer. *Endocrine-Related Cancer*, 7(4), 199–226. <https://doi.org/10.1677/erc.0.0070199>
- Samanta, D., Gilkesa, D. M., Chaturvedia, P., Xiang, L., & Semenza, G. L. (2014). Hypoxia-inducible factors are required for chemotherapy resistance of breast cancer stem cells. *Proceedings of the National Academy of Sciences of the United States of America*, 111(50), E5429–E5438.  
<https://doi.org/10.1073/pnas.1421438111>
- Sanchez-Vega, F., Mina, M., Armenia, J., Chatila, W. K., Luna, A., La, K. C., Dimitriadou, S., Liu, D. L., Kantheti, H. S., Saghafeinia, S., Chakravarty, D., Daian, F., Gao, Q., Bailey, M. H., Liang, W. W., Foltz, S. M., Shmulevich, I., Ding, L., Heins, Z., ... Schultz, N. (2018). Oncogenic Signalling Pathways in The Cancer Genome Atlas. *Cell*, 173(2), 321–337.e10.  
<https://doi.org/10.1016/j.cell.2018.03.035>
- Sang, N., Stiehl, D. P., Bohensky, J., Leshchinsky, I., Srinivas, V., & Caro, J. (2003). MAPK Signalling Up-regulates the Activity of Hypoxia-inducible Factors by Its Effects on p300\*. *Journal of Biological Chemistry*, 278(16), 14013–14019.  
<https://doi.org/https://doi.org/10.1074/jbc.M209702200>
- Saraswathy, M., & Gong, S. (2013). Different strategies to overcome multidrug

- resistance in cancer. *Biotechnology Advances*, 31(8), 1397–1407.  
<https://doi.org/10.1016/j.biotechadv.2013.06.004>
- Sato, J., Karasawa, H., Suzuki, T., Nakayama, S., Katagiri, M., Maeda, S., Ohnuma, S., Motoi, F., Naitoh, T., & Unno, M. (2020). The Function and Prognostic Significance of Cripto-1 in Colorectal Cancer. *Cancer Investigation*, 38(4), 214–227. <https://doi.org/10.1080/07357907.2020.1741604>
- Savagner, P. (2001). Leaving the neighborhood: Molecular mechanisms involved during epithelial-mesenchymal transition. *BioEssays*, 23(10), 912–923.  
<https://doi.org/10.1002/bies.1132>
- Sawamiphak, S., Seidel, S., Essmann, C. L., Wilkinson, G. A., Pitulescu, M. E., Acker, T., & Acker-Palmer, A. (2010). Ephrin-B2 regulates VEGFR2 function in developmental and tumour angiogenesis. *Nature*, 465(7297), 487–491.  
<https://doi.org/10.1038/nature08995>
- Saygin, C., Matei, D., Majeti, R., Reizes, O., & Lathia, J. D. (2019). Targeting Cancer Stemness in the Clinic: From Hype to Hope. *Cell Stem Cell*, 24(1), 25–40.  
<https://doi.org/10.1016/j.stem.2018.11.017>
- Scheuermann, T. H., Tomchick, D. R., Machius, M., Guo, Y., Bruick, R. K., & Gardner, K. H. (2009). Artificial ligand binding within the HIF2 $\alpha$  PAS-B domain of the HIF2 transcription factor. *Proceedings of the National Academy of Sciences of the United States of America*, 106(2), 450–455.  
<https://doi.org/10.1073/pnas.0808092106>
- Schier, A. F., & Shen, M. M. (2000). Nodal signalling in vertebrate development. *Nature*, 403(6768), 385–389. <https://doi.org/10.1038/35000126>
- Schofield, C. J., & Ratcliffe, P. J. (2004). Oxygen sensing by HIF hydroxylases. *Nature Reviews Molecular Cell Biology*, 5(5), 343–354. <https://doi.org/10.1038/nrm1366>
- Schulenburg, A., Blatt, K., Cerny-Reiterer, S., Sadovnik, I., Herrmann, H., Marian, B., Grunt, T. W., Zielinski, C. C., & Valent, P. (2015). Cancer stem cells in basic science and in translational oncology: Can we translate into clinical application? *Journal of Hematology and Oncology*, 8(1), 1–21. <https://doi.org/10.1186/s13045-015-0113-9>

- Scognamiglio, B., Baldassarre, G., Cassano, C., Tucci, M., Montuori, N., Dono, R., Lembo, G., Barra, A., Lago, C. T., Viglietto, G., Rocchi, M., & Persico, M. G. (1999). Assignment of human teratocarcinoma derived growth factor (TDGF) sequences to chromosomes 2q37, 3q22, 6p25 and 19q13.1. *Cytogenetics and Cell Genetics*, 84(3–4), 220–224. <https://doi.org/10.1159/000015263>
- Scortegagna, M., Ding, K., Oktay, Y., Gaur, A., Thurmond, F., Yan, L.-J., Marck, B. T., Matsumoto, A. M., Shelton, J. M., Richardson, J. A., Bennett, M. J., & Garcia, J. A. (2003). Multiple organ pathology, metabolic abnormalities and impaired homeostasis of reactive oxygen species in *Epas1*<sup>-/-</sup> mice. *Nature Genetics*, 35(4), 331–340. <https://doi.org/10.1038/ng1266>
- Sebastiano, V., Dalvai, M., Gentile, L., Schubart, K., Sutter, J., Wu, G. M., Tapia, N., Esch, D., Ju, J. Y., Hübner, K., Bravo, M. J. A., Schöler, H. R., Cavaleri, F., & Matthias, P. (2010). Oct1 regulates trophoblast development during early mouse embryogenesis. *Development*, 137(21), 3551–3560. <https://doi.org/10.1242/dev.047027>
- Secades, P., de Santa-María, I. S., Merlo, A., Suarez, C., & Chiara, M.-D. (2015). In vitro study of normoxic epidermal growth factor receptor-induced hypoxia-inducible factor-1-alpha, vascular endothelial growth factor, and BNIP3 expression in head and neck squamous cell carcinoma cell lines: Implications for anti-epidermal growth fact. *Head & Neck*, 37(8), 1150–1162. <https://doi.org/https://doi.org/10.1002/hed.23733>
- Seidel, S., Garvalov, B. K., Wirta, V., Von Stechow, L., Schänzer, A., Meletis, K., Wolter, M., Sommerlad, D., Henze, A. T., Nistér, M., Reifenberger, G., Lundeberg, J., Frisén, J., & Acker, T. (2010). A hypoxic niche regulates glioblastoma stem cells through hypoxia inducible factor 2 $\alpha$ . *Brain*, 133(4), 983–995. <https://doi.org/10.1093/brain/awq042>
- Seidensticker, M., & Behrens, J. (2000). Biochemical interactions in the wnt pathway. *Et Biophysica Acta (BBA)-Molecular Cell ...*. <http://www.sciencedirect.com/science/article/pii/S0167488999001585>
- Sekido, Y., Ahmadian, M., Wistuba, I. I., Latif, F., Bader, S., Wei, M. H., Duh, F. M., Gazdar, A. F., Lerman, M. I., & Minna, J. D. (1998). Cloning of a breast cancer

- homozygous deletion junction narrows the region of search for a 3p21.3 tumor suppressor gene. *Oncogene*, 16(24), 3151–3157.  
<https://doi.org/10.1038/sj.onc.1201858>
- Sell, S. (2010). On the stem cell origin of cancer. *American Journal of Pathology*, 176(6), 2584–2594. <https://doi.org/10.2353/ajpath.2010.091064>
- Semenza, G L, & Wang, G. L. (1992). A nuclear factor induced by hypoxia via de novo protein synthesis binds to the human erythropoietin gene enhancer at a site required for transcriptional activation. *Molecular and Cellular Biology*, 12(12), 5447–5454. <https://doi.org/10.1128/mcb.12.12.5447>
- Semenza, Gregg L., Nejfelt, M. K., Chi, S. M., & Antonarakis, S. E. (1991). Hypoxia-inducible nuclear factors bind to an enhancer element located 3' to the human erythropoietin gene. *Proceedings of the National Academy of Sciences of the United States of America*, 88(13), 5680–5684.  
<https://doi.org/10.1073/pnas.88.13.5680>
- Semenza, Gregg L. (2003). Targeting HIF-1 for cancer therapy. *Nature Reviews. Cancer*, 3(10), 721–732. <https://doi.org/10.1038/nrc1187>
- Semenza, Gregg L. (2008). Hypoxia-inducible factor 1 and cancer pathogenesis. *IUBMB Life*, 60(9), 591–597. <https://doi.org/10.1002/iub.93>
- Seoane, J., & Gomis, R. R. (2017). *and Cancer Progression*. 1–30.
- Serrano, F., Calatayud, C. F., Blazquez, M., Torres, J., Castell, J. V., & Bort, R. (2013). Gata4 blocks somatic cell reprogramming by directly repressing Nanog. *Stem Cells*, 31(1), 71–82. <https://doi.org/10.1002/stem.1272>
- Shani, G., Fischer, W., & Justice, N. (2008). GRP78 and Cripto form a complex at the cell surface and collaborate to inhibit transforming growth factor  $\beta$  signalling and enhance cell growth. *And Cellular Biology*.  
<http://mcb.asm.org/content/28/2/666.short>
- Shannon, A. M., Bouchier-Hayes, D. J., Condrón, C. M., & Toomey, D. (2003). Tumour hypoxia, chemotherapeutic resistance and hypoxia-related therapies. *Cancer Treatment Reviews*, 29(4), 297–307. <https://doi.org/10.1016/s0305->

7372(03)00003-3

- Sheila K. Singh, Cynthia Hawkins, Ian D. Clarke, Jeremy A. Squire, Jane Bayani, Takuichiro Hide, R. Mark Henkelman, M. D. C. & P. B. D. (2004). Identification of human brain tumour initiating cells. *Nature*, 432(November).  
<https://doi.org/10.1038/nature03031.1>.
- Shen, M. M. (2007). Nodal signalling: Development roles and regulation. *Development*, 134(6), 1023–1034. <https://doi.org/10.1242/dev.000166>
- Shen, M. M., Wang, H., & Leder, P. (1997). A differential display strategy identifies Cryptic, a novel EGF-related gene expressed in the axial and lateral mesoderm during mouse gastrulation. *Development*, 124(2), 429–442.
- Shi, J.-Y., Shi, Z.-Z., Zhang, S.-J., Zhu, Y.-M., Gu, B.-W., Li, G., Bai, X.-T., Gao, X.-D., Hu, J., Jin, W., Huang, W., Chen, Z., & Chen, S.-J. (2004). Association between single nucleotide polymorphisms in deoxycytidine kinase and treatment response among acute myeloid leukaemia patients. *Pharmacogenetics and Genomics*, 14(11).  
[https://journals.lww.com/jpharmacogenetics/Fulltext/2004/11000/Association\\_between\\_single\\_nucleotide.7.aspx](https://journals.lww.com/jpharmacogenetics/Fulltext/2004/11000/Association_between_single_nucleotide.7.aspx)
- Shi, Yan, Desponts, C., Do, J. T., Hahm, H. S., Schöler, H. R., & Ding, S. (2008). Induction of Pluripotent Stem Cells from Mouse Embryonic Fibroblasts by Oct4 and Klf4 with Small-Molecule Compounds. *Cell Stem Cell*, 3(5), 568–574.  
<https://doi.org/10.1016/j.stem.2008.10.004>
- Shi, Ying, Bao, Y. L., Wu, Y., Yu, C. L., Huang, Y. X., Sun, Y., Zheng, L. H., & Li, Y. X. (2011). Alantolactone inhibits cell proliferation by interrupting the interaction between Cripto-1 and activin receptor type II A in activin signalling pathway. *Journal of Biomolecular Screening*, 16(5), 525–535.  
<https://doi.org/10.1177/10870571111398486>
- Shibue, T., & Weinberg, R. A. (2017). EMT, CSCs, and drug resistance: The mechanistic link and clinical implications. *Nature Reviews Clinical Oncology*, 14(10), 611–629. <https://doi.org/10.1038/nrclinonc.2017.44>
- Shukla, A., Ho, Y., Liu, X., Ryscavage, A., & Glick, A. B. (2008). Cripto-1 alters

- keratinocyte differentiation via blockade of transforming growth factor- $\beta$ 1 signalling: Role in skin carcinogenesis. *Molecular Cancer Research*, 6(3), 509–516. <https://doi.org/10.1158/1541-7786.MCR-07-0396>
- Simões, P. D., & Ramos, T. (2007). Human pluripotent embryonal carcinoma NTERA2 cl.D1 cells maintain their typical morphology in an angiomyogenic medium. *Journal of Negative Results in BioMedicine*, 6(1), 5. <https://doi.org/10.1186/1477-5751-6-5>
- Singh, A. M., Reynolds, D., Cliff, T., Ohtsuka, S., Mattheyses, A. L., Sun, Y., Menendez, L., Kulik, M., & Dalton, S. (2012). Signalling network crosstalk in human pluripotent cells: A Smad2/3-regulated switch that controls the balance between self-renewal and differentiation. *Cell Stem Cell*, 10(3), 312–326. <https://doi.org/10.1016/j.stem.2012.01.014>
- Singh, A., & Settleman, J. (2010). EMT, cancer stem cells and drug resistance: An emerging axis of evil in the war on cancer. *Oncogene*, 29(34), 4741–4751. <https://doi.org/10.1038/onc.2010.215>
- Sirard, C., De La Pompa, J. L., Elia, A., Itie, A., Mirtsos, C., Cheung, A., Hahn, S., Wakeham, A., Schwartz, L., Kern, S. E., Rossant, J., & Mak, T. W. (1998). The tumor suppressor gene Smad4/Dpc4 is required for gastrulation and later for anterior development of the mouse embryo. *Genes and Development*, 12(1), 107–119. <https://doi.org/10.1101/gad.12.1.107>
- Siva, K., & Miharada, K. (2011). *Article Cripto Regulates Hematopoietic Stem Cells as a Hypoxic-Niche-Related Factor through Cell Surface Receptor GRP78*. <https://doi.org/10.1016/j.stem.2011.07.016>
- Sonia Prado-lopez; ana conesa et al Miodrag stojkovic. (2010). *Hypoxia Promotes Efficient Differentiation of Human Embryonic* (pp. 407–418). Stem cells. <https://doi.org/doi:10.1002/stem.295> STEM
- Souquet, B., Tourpin, S., Messiaen, S., Moison, D., Habert, R., & Livera, G. (2012). Nodal signalling regulates the entry into meiosis in fetal germ cells. *Endocrinology*, 153(5), 2466–2473. <https://doi.org/10.1210/en.2011-2056>
- Sousa, E. R., Zoni, E., Karkampouna, S., Manna, F. La, Gray, P. C., Menna, M. De, &

- Julio, M. K. De. (2020). A multidisciplinary review of the roles of cripto in the scientific literature through a bibliometric analysis of its biological roles. *Cancers*, 12(6), 1–19. <https://doi.org/10.3390/cancers12061480>
- Spasokoukotskaja, T., Arnér, E. S. J., Brosjö, O., Gunvén, P., Juliusson, G., Liliemark, J., & Eriksson, S. (1995). Expression of deoxycytidine kinase and phosphorylation of 2-chlorodeoxyadenosine in human normal and tumour cells and tissues. *European Journal of Cancer*, 31(2), 202–208. [https://doi.org/https://doi.org/10.1016/0959-8049\(94\)00435-8](https://doi.org/https://doi.org/10.1016/0959-8049(94)00435-8)
- Steinert, P., & Roop, D. (1988). Molecular and cellular biology of intermediate filaments. *Annual Review of Biochemistry*. <http://www.annualreviews.org/doi/pdf/10.1146/annurev.bi.57.070188.003113>
- Strizzi, L, Bianco, C., & Normanno, N. (2004). Epithelial mesenchymal transition is a characteristic of hyperplasias and tumors in mammary gland from MMTV-Cripto-1 transgenic mice. *Journal of Cellular*. <http://onlinelibrary.wiley.com/doi/10.1002/jcp.20062/full>
- Strizzi, Luigi, Abbott, D. E., Salomon, D. S., & Hendrix, M. J. C. (2008). Potential for cripto-1 in defining stem cell-like characteristics in human malignant melanoma. *Cell Cycle*, 7(13), 1931–1935. <https://doi.org/10.4161/cc.7.13.6236>
- Strizzi, Luigi, Bianco, C., Normanno, N., & Salomon, D. (2005). Cripto-1: A multifunctional modulator during embryogenesis and oncogenesis. *Oncogene*, 24(37), 5731–5741. <https://doi.org/10.1038/sj.onc.1208918>
- Strizzi, Luigi, Margaryan, N., Gilgur, A., Hardy, K., Salomon, D. S., Hendrix, M. J. C., Strizzi, L., Margaryan, N., Gilgur, A., Hardy, K., Salomon, D. S., Hendrix, M. J. C., Strizzi, L., Margaryan, N. V., Gilgur, A., Hardy, K. M., Normanno, N., Salomon, D. S., & Hendrix, M. J. C. (2013). *The significance of a Cripto-1-positive subpopulation of human melanoma cells exhibiting stem cell-like characteristics* *The significance of a Cripto-1-positive subpopulation of human melanoma cells exhibiting stem cell-like characteristics*. 4101(November 2016). <https://doi.org/10.4161/cc.24601>
- Strizzi, Luigi, Margaryan, N. V., Gilgur, A., Hardy, K. M., Normanno, N., Salomon, D.

- S., & Hendrix, M. J. C. (2013). The significance of a Cripto-1 positive subpopulation of human melanoma cells exhibiting stem cell-like characteristics. *Cell Cycle*, 12(9), 1450–1456. <https://doi.org/10.4161/cc.24601>
- Strizzi, Luigi, Postovit, L. M., Margaryan, N. V., Seftor, E. A., Abbott, D. E., Seftor, R. E. B., Salomon, D. S., & Hendrix, M. J. C. (2007). Emerging roles of nodal and cripto-1: From embryogenesis to breast cancer progression. *Breast Disease*, 29(February), 91–103. <https://doi.org/10.3233/bd-2008-29110>
- Sun, Yi, Guan, Z., Liang, L., Cheng, Y., Zhou, J., Li, J., & Xu, Y. (2016). HIF-1 $\alpha$ /MDR1 pathway confers chemoresistance to cisplatin in bladder cancer. *Oncology Reports*, 35(3), 1549–1556. <https://doi.org/10.3892/or.2015.4536>
- Sun, Yong, Xing, X., Liu, Q., Wang, Z., Xin, Y., Zhang, P., Hu, C., & Liu, Y. (2015). Hypoxia-induced autophagy reduces radiosensitivity by the HIF-1 $\alpha$ /miR-210/Bcl-2 pathway in colon cancer cells. In *International Journal of Oncology* (Vol. 46, Issue 2, pp. 750–756). <https://doi.org/10.3892/ijo.2014.2745>
- Tabata, T., & Takei, Y. (2004). Morphogens, their identification and regulation. *Development*, 131(4), 703–712. <https://doi.org/10.1242/dev.01043>
- Takahashi, K., & Yamanaka, S. (2006). Induction of Pluripotent Stem Cells from Mouse Embryonic and Adult Fibroblast Cultures by Defined Factors. *Cell*, 126(4), 663–676. <https://doi.org/10.1016/j.cell.2006.07.024>
- Takebe, N., Harris, P. J., Warren, R. Q., & Ivy, S. P. (2011). Targeting cancer stem cells by inhibiting Wnt, Notch, and Hedgehog pathways. *Nature Reviews Clinical Oncology*, 8(2), 97–106. <https://doi.org/10.1038/nrclinonc.2010.196>
- Tavana, H. (2020). *Modeling Adaptive Resistance of KRAS Mutant Colorectal Cancer to*.
- Teicher, B. A., Linehan, W. M., & Helman, L. J. (2012). Targeting Cancer Metabolism. *Clinical Cancer Research*, 18(20), 5537 LP – 5545. <https://doi.org/10.1158/1078-0432.CCR-12-2587>
- Thiery, J. P. (2002). Epithelial-mesenchymal transitions in tumor progression. *Nature Reviews Cancer*, 2(6), 442–454. <https://doi.org/10.1038/nrc822>

- Thiery, J. P., & Chopin, D. (1999). Epithelial cell plasticity in development and tumor progression. *Cancer and Metastasis Reviews*, *18*(1), 31–42.  
<https://doi.org/10.1023/A:1006256219004>
- Tian, H., McKnight, S. L., & Russell, D. W. (1997). Endothelial PAS domain protein 1 (EPAS1), a transcription factor selectively expressed in endothelial cells. *Genes and Development*, *11*(1), 72–82. <https://doi.org/10.1101/gad.11.1.72>
- Todaro, M., Gaggianesi, M., Catalano, V., Benfante, A., Iovino, F., Biffoni, M., Apuzzo, T., Sperduti, I., Volpe, S., Cocorullo, G., Gulotta, G., Dieli, F., De Maria, R., & Stassi, G. (2014). CD44v6 is a marker of constitutive and reprogrammed cancer stem cells driving colon cancer metastasis. *Cell Stem Cell*, *14*(3), 342–356.  
<https://doi.org/10.1016/j.stem.2014.01.009>
- Trédan, O., Galmarini, C. M., Patel, K., & Tannock, I. F. (2007). Drug resistance and the solid tumor microenvironment. *Journal of the National Cancer Institute*, *99*(19), 1441–1454. <https://doi.org/10.1093/jnci/djm135>
- Treins, C., Giorgetti-Peraldi, S., Murdaca, J., Monthouël-Kartmann, M.-N., & Van Obberghen, E. (2005). Regulation of Hypoxia-Inducible Factor (HIF)-1 Activity and Expression of HIF Hydroxylases in Response to Insulin-Like Growth Factor I. *Molecular Endocrinology*, *19*(5), 1304–1317. <https://doi.org/10.1210/me.2004-0239>
- Tsou, S. H., Chen, T. M., Hsiao, H. T., & Chen, Y. H. (2015). A critical dose of doxorubicin is required to alter the gene expression profiles in MCF-7 cells acquiring multidrug resistance. *PLoS ONE*, *10*(1), 1–24.  
<https://doi.org/10.1371/journal.pone.0116747>
- Tsuchida, K., Nakatani, M., Yamakawa, N., Hashimoto, O., Hasegawa, Y., & Sugino, H. (2004). Activin isoforms signal through type I receptor serine/threonine kinase ALK7. *Molecular and Cellular Endocrinology*, *220*(1–2), 59–65.  
<https://doi.org/10.1016/j.mce.2004.03.009>
- Uchino, M., Kojima, H., Wada, K., Imada, M., Onoda, F., Satofuka, H., Utsugi, T., & Murakami, Y. (2010). Nuclear  $\beta$ -catenin and CD44 upregulation characterize invasive cell populations in non-aggressive MCF-7 breast cancer cells. *BMC*

- Cancer*, 10. <https://doi.org/10.1186/1471-2407-10-414>
- Utsunomiya, Y., Hasegawa, H., Yanagisawa, K., & Fujita, S. (1997). Enhancement of *mdr1* gene expression by transforming growth factor- $\beta$ 1 in the new adriamycin-resistant human leukemia cell line ME-F2/ADM [2]. *Leukemia*, 11(6), 894–895. <https://doi.org/10.1038/sj.leu.2400663>
- Vaidyanathan, A., Sawers, L., Gannon, A. L., Chakravarty, P., Scott, A. L., Bray, S. E., Ferguson, M. J., & Smith, G. (2016). ABCB1 (MDR1) induction defines a common resistance mechanism in paclitaxel- and olaparib-resistant ovarian cancer cells. *British Journal of Cancer*, 115(4), 431–441. <https://doi.org/10.1038/bjc.2016.203>
- Van Der Schoor, L. W. E., Verkade, H. J., Kuipers, F., & Jonker, J. W. (2015). New insights in the biology of ABC transporters ABCC2 and ABCC3: Impact on drug disposition. *Expert Opinion on Drug Metabolism and Toxicology*, 11(2), 273–293. <https://doi.org/10.1517/17425255.2015.981152>
- van der Zee, M., Jia, Y., Wang, Y., Heijmans-Antonissen, C., Ewing, P. C., Franken, P., DeMayo, F. J., Lydon, J. P., Burger, C. W., Fodde, R., & Blok, L. J. (2013). Alterations in Wnt- $\beta$ -catenin and Pten signalling play distinct roles in endometrial cancer initiation and progression. *The Journal of Pathology*, 230(1), 48–58. <https://doi.org/10.1002/path.4160>
- Van Vlijmen, H. W. T., Gupta, A., Narasimhan, L. S., & Singh, J. (2004). A Novel Database of Disulfide Patterns and its Application to the Discovery of Distantly Related Homologs. *Journal of Molecular Biology*, 335(4), 1083–1092. <https://doi.org/10.1016/j.jmb.2003.10.077>
- Vellonen, K. S., Honkakoski, P., & Urtti, A. (2004). Substrates and inhibitors of efflux proteins interfere with the MTT assay in cells and may lead to underestimation of drug toxicity. *European Journal of Pharmaceutical Sciences : Official Journal of the European Federation for Pharmaceutical Sciences*, 23(2), 181–188. <https://doi.org/10.1016/j.ejps.2004.07.006>
- Visvader, J. E., & Lindeman, G. J. (2008). Cancer stem cells in solid tumours: accumulating evidence and unresolved questions. *Nature Reviews Cancer*, 8(10),

- 755–768. <https://doi.org/10.1038/nrc2499>
- Vlahos, C. J., Matter, W. F., Hui, K. Y., & Brown, R. F. (1994). A specific inhibitor of phosphatidylinositol 3-kinase, 2-(4-morpholinyl)- 8-phenyl-4H-1-benzopyran-4-one (LY294002). *Journal of Biological Chemistry*, 269(7), 5241–5248.
- Vogelstein, B., & Kinzler, K. W. (2004). *OUR TENTH YEAR Cancer genes and the pathways they control*. 10(8), 789–799. <https://doi.org/10.1038/nm1087>
- Wainwright, E. N., & Scaffidi, P. (2017). Epigenetics and Cancer Stem Cells: Unleashing, Hijacking, and Restricting Cellular Plasticity. *Trends in Cancer*, 3(5), 372–386. <https://doi.org/10.1016/j.trecan.2017.04.004>
- Wakao, S., Kitada, M., Kuroda, Y., Ogura, F., Murakami, T., Niwa, A., & Dezawa, M. (2012). Morphologic and Gene Expression Criteria for Identifying Human Induced Pluripotent Stem Cells. *PLoS ONE*, 7(12). <https://doi.org/10.1371/journal.pone.0048677>
- Waldrip, W. R., Bikoff, E. K., Hoodless, P. A., Wrana, J. L., & Robertson, E. J. (1998). Smad2 signalling in extraembryonic tissues determines anterior-posterior polarity of the early mouse embryo. *Cell*, 92(6), 797–808. [https://doi.org/10.1016/S0092-8674\(00\)81407-5](https://doi.org/10.1016/S0092-8674(00)81407-5)
- Wan, C. P., Sigh, R. V., & Lau, B. H. S. (1994a). A simple fluorometric assay for the determination of cell numbers. *Journal of Immunological Methods*, 173(2), 265–272. [https://doi.org/10.1016/0022-1759\(94\)90305-0](https://doi.org/10.1016/0022-1759(94)90305-0)
- Wan, C. P., Sigh, R. V., & Lau, B. H. S. (1994b). *OF METHODS A simple fluorometric assay for the determination of cell numbers*. 1759(94).
- Wang, D., Plukker, J. T. M., & Coppes, R. P. (2017). Cancer stem cells with increased metastatic potential as a therapeutic target for esophageal cancer. *Seminars in Cancer Biology*, 44(March), 60–66. <https://doi.org/10.1016/j.semcancer.2017.03.010>
- Wang, Dantong, Malo, D., & Hekimi, S. (2010). Elevated Mitochondrial Reactive Oxygen Species Generation Affects the Immune Response via Hypoxia-Inducible Factor-1 $\alpha$  in Long-Lived Mcl1 +/- Mouse Mutants. *The Journal of Immunology*,

- 184(2), 582–590. <https://doi.org/10.4049/jimmunol.0902352>
- Wang, J., Su, C., Neuhard, J., & Eriksson, S. (2000). Expression of human mitochondrial thymidine kinase in escherichia coli: correlation between the enzymatic activity of pyrimidine nucleoside analogues and their inhibitory effect on bacterial growth. *Biochemical Pharmacology*, 59(12), 1583–1588. [https://doi.org/https://doi.org/10.1016/S0006-2952\(00\)00285-9](https://doi.org/https://doi.org/10.1016/S0006-2952(00)00285-9)
- Wang, K., Wu, X., Wang, J., & Huang, J. (2013). Cancer stem cell theory: Therapeutic implications for nanomedicine. *International Journal of Nanomedicine*, 8, 899–908. <https://doi.org/10.2147/IJN.S38641>
- Wang, X., Zhang, H., & Chen, X. (2019). Drug resistance and combating drug resistance in cancer. *Cancer Drug Resistance*. <https://doi.org/10.20517/cdr.2019.10>
- Wartenberg, M., Ling, F. C., Klein, F., Acker, H., Petrat, K., & Sauer, H. (2003). *Regulation of the multidrug resistance transporter P-glycoprotein in multicellular tumor spheroids by hypoxia-inducible factor-1 and reactive oxygen species. 1*. <https://doi.org/10.1096/fj.02-0358fje>
- Watanabe, K., Meyer, M., Strizzi, L., & Lee, J. (2010). Cripto-1 is a cell surface marker for a tumorigenic, undifferentiated subpopulation in human embryonal carcinoma cells. *Cells*. <http://onlinelibrary.wiley.com/doi/10.1002/stem.463/full>
- Watanabe, Kazuhide, Bianco, C., Strizzi, L., Hamada, S., Mancino, M., Bailly, V., Mo, W., Wen, D., Miatkowski, K., Gonzales, M., Sanicola, M., Seno, M., & Salomon, D. S. (2007). Growth factor induction of cripto-1 shedding by glycosylphosphatidylinositol-phospholipase D and enhancement of endothelial cell migration. *Journal of Biological Chemistry*, 282(43), 31643–31655. <https://doi.org/10.1074/jbc.M702713200>
- Watanabe, Kazuhide, Meyer, M. J., Strizzi, L., Lee, J. M., Gonzales, M., Bianco, C., Nagaoka, T., Farid, S. S., Margaryan, N., Hendrix, M. J. C., Vonderhaar, B. K., & Salomon, D. S. (2010). Cripto-1 is a cell surface marker for a tumorigenic, undifferentiated subpopulation in human embryonal carcinoma cells. *Stem Cells*, 28(8), 1303–1314. <https://doi.org/10.1002/stem.463>

- Watt, F. M., & Driskell, R. R. (2010). The therapeutic potential of stem cells. *Philosophical Transactions of the Royal Society B: Biological Sciences*, 365(1537), 155–163. <https://doi.org/10.1098/rstb.2009.0149>
- Wechselberger, C., Strizzi, L., Kenney, N., Hirota, M., Sun, Y., Ebert, A., Orozco, O., Bianco, C., Khan, N. I., Wallace-Jones, B., Normanno, N., Adkins, H., Sanicola, M., & Salomon, D. S. (2005). Human Cripto-1 overexpression in the mouse mammary gland results in the development of hyperplasia and adenocarcinoma. *Oncogene*, 24(25), 4094–4105. <https://doi.org/10.1038/sj.onc.1208417>
- Wenger, R. H. (2000). Mammalian oxygen sensing, signalling and gene regulation. *Journal of Experimental Biology*, 203(8), 1253–1263. <https://doi.org/10.5167/uzh-1436>
- Wong, W. W., Cahill, J. M., Rosen, M. D., Kennedy, C. A., Bonaccio, E. T., Morris, M. J., Wilson, J. G., Klickstein, L. B., & Fearon, D. T. (1989). Structure of the human CR1 gene. Molecular basis of the structural and quantitative polymorphisms and identification of a new CR1-like allele. *Journal of Experimental Medicine*, 169(3), 847–863. <https://doi.org/10.1084/jem.169.3.847>
- Wu, D., Shi, Z., Xu, H., Chen, R., Xue, S., & Sun, X. (2017). Knockdown of Cripto-1 inhibits the proliferation, migration, invasion, and angiogenesis in prostate carcinoma cells. *Journal of Biosciences*, 42(3), 405–416. <https://doi.org/10.1007/s12038-017-9700-y>
- Wu, Z., Li, G., Wu, L., Weng, D., Li, X., & Yao, K. (2009). Cripto-1 overexpression is involved in the tumorigenesis of nasopharyngeal carcinoma. *BMC Cancer*, 9, 315. <https://doi.org/10.1186/1471-2407-9-315>
- Xiao, Y.-F., Yong, X., Tang, B., Qin, Y., Zhang, J.-W., Zhang, D., Xie, R., & Yang, S.-M. (2016). Notch and Wnt signalling pathway in cancer: Crucial role and potential therapeutic targets (Review). *Int J Oncol*, 48(2), 437–449. <https://doi.org/10.3892/ijo.2015.3280>
- Xing, P. X., Hu, X. F., Pietersz, G. A., Hosick, H. L., & McKenzie, I. F. C. (2004). Cripto: A Novel Target for Antibody-Based Cancer Immunotherapy. *Cancer Research*, 64(11), 4018 LP – 4023. <https://doi.org/10.1158/0008-5472.CAN-03->

3888

- Xu, Chun-hua, Sheng, Z., & Hu, H. (2014). *Elevated expression of Cripto-1 correlates with poor prognosis in non-small cell lung cancer*. <https://doi.org/10.1007/s13277-014-2039-1>
- Xu, Chunhui, Liguori, G., Persico, M. G., & Adamson, E. D. (1999). Abrogation of the Cripto gene in mouse leads to failure of postgastrulation morphogenesis and lack of differentiation of cardiomyocytes. *Development*, *126*(3), 483–494.
- Xu, H., Tian, Y., Yuan, X., Liu, Y., Wu, H., Liu, Q., Wu, G. S., & Wu, K. (2016). Enrichment of CD44 in basal-type breast cancer correlates with EMT, cancer stem cell gene profile, and prognosis. *OncoTargets and Therapy*, *9*, 431–444. <https://doi.org/10.2147/OTT.S97192>
- Xu, P., Wang, M., Jiang, Y., Ouyang, J., & Chen, B. (2017). The association between expression of hypoxia inducible factor-1 $\alpha$  and multi-drug resistance of acute myeloid leukemia. *Translational Cancer Research*, *6*(1), 198–205. <https://doi.org/10.21037/tcr.2017.01.10>
- Xu, X., Ho, W., Zhang, X., Bertrand, N., & Farokhzad, O. (2015). Cancer nanomedicine: From targeted delivery to combination therapy. *Trends in Molecular Medicine*, *21*(4), 223–232. <https://doi.org/10.1016/j.molmed.2015.01.001>
- Xue, Y., Chen, S., Chen, W., Wu, G., Liao, Y., Xu, J., & Tang, H. (2019). *Cripto-1 expression in patients with clear cell renal cell carcinoma is associated with poor disease outcome*. *6*, 1–17.
- Yagüe, E., Arance, A., Kubitzka, L., O'Hare, M., Jat, P., Ogilvie, C. M., Hart, I. R., Higgins, C. F., & Raguz, S. (2007). Ability to acquire drug resistance arises early during the tumorigenesis process. *Cancer Research*, *67*(3), 1130–1137. <https://doi.org/10.1158/0008-5472.CAN-06-2574>
- Yamada, T., Takaoka, A. S., Naishiro, Y., Hayashi, R., Maruyama, K., Maesawa, C., Ochiai, A., & Hirohashi, S. (2000). Transactivation of the Multidrug Resistance 1 gene by T-cell factor 4/ $\beta$ -catenin complex in early colorectal carcinogenesis. *Cancer Research*, *60*(17), 4761–4766.

- Yamada, Yasuhiro, Yoshimi, N., Sugie, S., Suzui, M., Matsunaga, K., Kawabata, K., Hara, A., & Mori, H. (1999).  $\beta$ -Catenin (Ctnnb1) Gene Mutations in Diethylnitrosamine (DEN)-induced Liver Tumors in Male F344 Rats. *Japanese Journal of Cancer Research*, 90(8), 824–828.  
<https://doi.org/https://doi.org/10.1111/j.1349-7006.1999.tb00822.x>
- Yamada, Yosuke, Haga, H., & Yamada, Y. (2014). Concise Review: Dedifferentiation Meets Cancer Development: Proof of Concept for Epigenetic Cancer. *STEM CELLS Translational Medicine*, 3(10), 1182–1187.  
<https://doi.org/10.5966/sctm.2014-0090>
- Yan, Y.-T., Liu, J.-J., Luo, Y., E, C., Haltiwanger, R. S., Abate-Shen, C., & Shen, M. M. (2002). Dual Roles of Cripto as a Ligand and Coreceptor in the Nodal Signalling Pathway. *Molecular and Cellular Biology*, 22(13), 4439–4449.  
<https://doi.org/10.1128/mcb.22.13.4439-4449.2002>
- Yang, K., Wang, X., Zhang, H., Wang, Z., Nan, G., Zhang, F., Mohammed, M. K., Haydon, R. C., Luu, H. H., & Bi, Y. (2016). *tumorigenesis : Implications in targeted cancer therapies*. 96(2), 116–136.  
<https://doi.org/10.1038/labinvest.2015.144.The>
- Yeo, C.-Y., & Whitman, M. (2001). Nodal Signals to Smads through Cripto-Dependent and Cripto-Independent Mechanisms. *Molecular Cell*, 7(5), 949–957.  
[https://doi.org/10.1016/S1097-2765\(01\)00249-0](https://doi.org/10.1016/S1097-2765(01)00249-0)
- Yoon, D., Pastore, Y. D., Divoky, V., Liu, E., Mlodnicka, A. E., Rainey, K., Ponka, P., Semenza, G. L., Schumacher, A., & Prchal, J. T. (2006). Hypoxia-inducible Factor-1 Deficiency Results in Dysregulated Erythropoiesis Signalling and Iron Homeostasis in Mouse Development\*. *Journal of Biological Chemistry*, 281(35), 25703–25711. <https://doi.org/https://doi.org/10.1074/jbc.M602329200>
- Young, S. D., & Hill, R. P. (1990). Effects of reoxygenation on cells from hypoxic regions of solid tumors: anticancer drug sensitivity and metastatic potential. *Journal of the National Cancer Institute*, 82(5), 371–380.  
<https://doi.org/10.1093/jnci/82.5.371>
- Yu, E. W., McDermott, G., Zgurskaya, H. I., Nikaido, H., & Koshland Jr., D. E.

- (2003). Structural basis of multiple drug-binding capacity of the AcrB multidrug efflux pump. *Science*, *300*(5621), 976–980.  
<https://doi.org/10.1126/science.1083137>
- Yu, J., Vodyanik, M. A., Smuga-Otto, K., Antosiewicz-Bourget, J., Frane, J. L., Tian, S., Nie, J., Jonsdottir, G. A., Ruotti, V., Stewart, R., Slukvin, I. I., & Thomson, J. A. (2007). Induced pluripotent stem cell lines derived from human somatic cells. *Science*, *318*(5858), 1917–1920. <https://doi.org/10.1126/science.1151526>
- Zhang, C., Li, C., & He, F. (2011). Identification of CD44+CD24+ gastric cancer stem cells. 1679–1686. <https://doi.org/10.1007/s00432-011-1038-5>
- Zhang, M., Wang, M., Tan, X., Li, T. F., Zhang, Y. E., & Chen, D. (2010). Smad3 prevents  $\beta$ -catenin degradation and facilitates  $\beta$ -catenin nuclear translocation in chondrocytes. *Journal of Biological Chemistry*, *285*(12), 8703–8710.  
<https://doi.org/10.1074/jbc.M109.093526>
- Zhang, Y., Wang, X., Meister, E. A., Gong, K., & Yan, S. (2014). The Effects of CoCl<sub>2</sub> on HIF-1  $\alpha$  Protein under Experimental Conditions of Autoprogressive Hypoxia Using Mouse Models. *Ca 1*, 10999–11012. <https://doi.org/10.3390/ijms150610999>
- Zhang, Y. Y., Mi, X. G., Song, Z. B., Li, Y. X., YingShi, & Niu, J. Q. (2018). Cripto-1 promotes resistance to drug-induced apoptosis by activating the TAK-1/NF- $\kappa$ B/survivin signalling pathway. *Biomedicine and Pharmacotherapy*, *104*(May), 729–737. <https://doi.org/10.1016/j.biopha.2018.05.063>
- Zhao, J., Du, F., Shen, G., Zheng, F., & Xu, B. (2015). The role of hypoxia-inducible factor-2 in digestive system cancers. *Cell Death and Disease*, *6*(1), 1–9.  
<https://doi.org/10.1038/cddis.2014.565>
- Zhongwu Guo. (2013). Synthetic Studies of Glycosylphosphatidylinositol (GPI) Anchors and GPI-Anchored Peptides, Glycopeptides, and Proteins. *Curr Org Synth.*, *23*(1), 1–7. <https://doi.org/10.2174/1570179411310030003.Synthetic>
- Zhou, B. B. S., Zhang, H., Damelin, M., Geles, K. G., Grindley, J. C., & Dirks, P. B. (2009). Tumour-initiating cells: Challenges and opportunities for anticancer drug discovery. *Nature Reviews Drug Discovery*, *8*(10), 806–823.  
<https://doi.org/10.1038/nrd2137>

- Zhou, G., Golden, T., Aragon, I. V., & Honkanen, R. E. (2004). Ser/Thr Protein Phosphatase 5 Inactivates Hypoxia-induced Activation of an Apoptosis Signal-regulating Kinase 1/MKK-4/JNK Signalling Cascade\*. *Journal of Biological Chemistry*, 279(45), 46595–46605.  
<https://doi.org/https://doi.org/10.1074/jbc.M408320200>
- Zhou, Y., Xia, L., Wang, H., Oyang, L., Su, M., Liu, Q., Lin, J., Tan, S., Tian, Y., Liao, Q., & Cao, D. (2018). Cancer stem cells in progression of colorectal cancer. *Oncotarget*, 9(70), 33403–33415. <https://doi.org/10.18632/oncotarget.v9i70>
- Zimmerer, R. M., Korn, P., Demougin, P., Kampmann, A., Kokemüller, H., Eckardt, A. M., Gellrich, N.-C., & Tavassol, F. (2013). Functional features of cancer stem cells in melanoma cell lines. *Cancer Cell International*, 13(1), 78.  
<https://doi.org/10.1186/1475-2867-13-78>



# APPENDIX

---

**Bacterial growth media:** 2X TY media [Tryptone, yeast extract, Sodium Chloride (NaCl)] and Agar (bacteriological culture grade), Ampicillin from Himedia India.

**Mamalian Cell culture media:** Dulbecco's Modified Eagle Medium (DMEM), Phosphate buffer saline (PBS) (Himedia, India), 1X antibiotics and antimycotic solution and Trypsin-EDTA (Invitrogen, USA), Fetal bovine serum (Gibco, USA) and Sodium bicarbonate (Sigma-Aldrich, USA).

**3D Spheroids culture:** Complete DMEM media without serum, and molecular grade agarose powder both from Himedia, India.

**Plasmid DNA Isolation and Restriction Digestion:** HiPurA® Plasmid DNA Miniprep Purification Kit from Himedia, India, pCI-Neo Plasmid gifted by Prof. David Salomon, NIH, USA, and EcoRI, NotI, and xhoI restriction enzymes from NEB, USA.

**Colony PCR:** 2X PCR TaqMixture, 1 KB DNA ladder, Tris Acetate EDTA (TAE) buffer Agarose powder and 2X TY media from Himedia, India.

**Transfection:** Lipofectamine 3000 from Invitrogen, USA, Optimen media and Geneticin antibiotic for clonal selection both from Gibco, USA.

**RNA Extraction and DNase Treatment:** Trizol reagent from Sigma-Aldrich, USA, molecular grade Chloroform, Isopropanol, Ethanol from Himedia, India, and TURBO DNA-free™ Kit from Invitrogen, USA.

**cDNA Synthesis and qPCR:** Verso cDNA synthesis kit and PowerTrack Sybr Green master mix both from Themoscientific, USA.

**Protein Isolation:**

RIPA Buffer, Phenylmethylsulfonyl fluoride (PMSF), Sodium Orthovanadate, Sodium Fluoride, Ethylenediaminetetraacetic acid (EDTA) all from Himedia, India, and Protease Inhibitor cocktail from Sigma-Aldrich, USA.

**Protein Estimation by Lowry's method:**

Lowry's A [2% Sodium carbonate ( $\text{Na}_2\text{CO}_3$ ) in 0.1 N sodium hydroxide (NaOH)], Lowry's B1 (2% potassium sodium tartrate), Lowry's B2 [1.0% Copper sulphate ( $\text{CuSO}_4 \cdot 5\text{H}_2\text{O}$ )] from Himedia, India, and Lowry's E (Folin's reagent) from Sigma-Aldrich, USA.

**MTT Assay:**

DMEM media and 3-(4,5-dimethylthiazol-2-yl)-2,5-diphenyl tetrazolium bromide (MTT) from Himedia, India, LY294002 (PI3K inhibitor), U0126 (MAPK inhibitor) from Sigma-Aldrich, USA.

**Cell proliferation assay:**

Propidium iodide, Triton X-100 and EDTA from Himedia, India.

**SDS PAGE and Western Blotting:**

Acrylamide, Bis-acrylamide, Ammonium persulphate (APS), TEMED, Ponceau solution from Sigma-Aldrich, USA, Sodium dodecyl sulphate (SDS), Tris-HCl powder, 5X Gel Running Buffer, Sample Loading Buffer, Transfer Buffer, TBS solution, Tween 20 from Himedia, India, PVDF membrane (0.2  $\mu\text{m}$ ) from Milipore, U.S.A. and Whatman blotting paper from Whatman, USA, SuperSignal West Dura ECL kit from ThermoScientific, USA.

**Composition of Buffers/Solution:**

**Tris-EDTA (TE) buffer:** 0.01 M Tris-HCl (pH 7.4), 0.001 M sodium EDTA (pH 8.0)

**50X Tris Acetate EDTA (TAE) buffer:** 24.2 g Tris base, 5.71 mL CH<sub>3</sub>COOH, 10 mL of 0.5 M EDTA.

**Phosphate buffer saline (PBS):** 0.137 M NaCl, 2.68 mM KCl, 7.98 mM Na<sub>2</sub>HPO<sub>4</sub>, 1.4 mM KH<sub>2</sub>PO<sub>4</sub>, pH 7.2.

**TBS:** 50mM tris base, and 150mM NaCl

**TBST:** TBS containing 0.1% Tween-20

**RIPA Buffer:** 50 mM Tris-HCl, pH 7.5, 150 mM NaCl, 1% Nonidet P40, 0.5% sodium deoxycholate, 0.1% SDS.

**30% acrylamide-bisacrylamide solution (100mL):** 29.2 g Acrylamide, 0.8 g Bisacrylamide.

**Tris.HCl, pH 6.8, 0.5 M (100 mL):** 6.06 g of Tris base, pH adjusted to 6.8 with 2 N HCl.

**Tris.HCl, pH 8.8, 1.5 M (100 mL):** 18.18 g of Tris base, pH adjusted to 8.8 with 2 N HCl.

**Gel Running Buffer:** 25 mM Tris base, 250 mM, 0.1% SDS

**Sample Loading Buffer (1X):** 50 mM Tris-HCl pH 6.8, 2% SDS, 10% glycerol, 1% β-mercaptoethanol, 0.02 % bromophenol blue.

**Transfer Buffer:** 25 mM Tris base, 39 mM Glycine, 20 % Methanol.

**Blocking solution:** 5% nonfat milk in PBST or 5% BSA in TBST.

**Table A1: List of Antibodies**

S.NO.	NAME	Source/Type	Working dilution	Working condition	Use
1	Anti-human Cripto-1 (Abcam, ab19917)	Rat/ Monoclonal	1:3000	Overnight/ 4 °C	WB
2	Anti-human MDR-1 (Cell signalling #13342)	Rat/ Monoclonal	1:3000	Overnight/ 4 °C	WB
3	Anti-human HIF-1 $\alpha$ (Cell signalling #36169)	Rat/ Monoclonal	1:3000	Overnight/ 4 °C	WB
4	Anti-human $\beta$ -tubulin (Cell signalling, #2128)	Rat/ Monoclonal	1:3000	Overnight/ 4 °C	WB
5	Anti-human phospho- p44/42 MAPK (Erk1/2) (Thr202/Tyr204) (Cell signalling, U.S.A, # 4370)	Rat/ Monoclonal	1:3000	Overnight/ 4 °C	WB
6	Anti-human p44/42 MAPK (Erk1/2) (Cell Signalling, U.S.A, # 4695)	Rat/ Monoclonal	1:3000	Overnight/ 4 °C	WB
7	Anti-human Phospho-Akt (Ser473) (Cell Signalling, U.S.A, # 4060)	Rat/ Monoclonal	1:3000	Overnight/ 4 °C	WB

S.NO.	NAME	Source/Type	Working dilution	Working condition	Use
8	Anti-human Akt (pan) (Cell Signalling, U.S.A, # 4691)	Rat/ Monoclonal	1:3000	Overnight/ 4 °C	WB
9	Anti-human GAPDH (Cell Signalling, U.S.A, # 2118)	Rat/ Monoclonal	1:3000	Overnight/ 4 °C	WB
10	Anti-Rabbit-HRP (Cell Signalling, U.S.A, # 7074)	Mouse/Polyclonal	1:5000	2 h/ Room temperature	WB
11	Anti-human CD44 (PE Conjugate) (Cell signalling, #88151)	Rat /monoclonal	1:100	1 h/ 4 °C	Flow
12	Anti-human CD24 (Abcam, #ab134375)	Mouse/Monoclonal	1:100	1 h/ 4 °C	Flow
13	Anti-human Cripto-1 (R&D system, #FAB2772P)	Mouse/monoclonal	1:100	1 h/ 4 °C	Flow

Table A2: List of Primers

S.No.	Gene of Interest	Gene
1	Cripto-1	Forward: TGGCCCGCTTCTCTTACAGTG Reverse: CCCCAGATGGACGAGCAAAT
2	MDR-1	Forward: CCCATCATTGCAATAGCAGG Reverse: TGTTCAAACCTTCTGCTCCTGA
3	HIF-1 $\alpha$	Forward: CATAAAGTCTGCAACATGGAAGGT Reverse: ATTTGATGGGTGAGGAATGGGTT
4	18s rRNA	Forward: GTAACCCGTTGAACCCATT Reverse: CCATCCAATCGGTAGTAGCG
5	CD24	Forward: GCGGACTTTTCTTTTGGGGG Reverse: AATCTGCGTGGGTAGGAGCA
6	CD44	Forward: AGCAAACACAACCTCTGGTCCTA Reverse: TTTTCTTCTGCCACAGCTTCTTC
7	CD133	Forward: CAG AGT ACA ACG CCA AAC CA Reverse: AAA TCA CGA TGA GGG TCA GC
8	Oct-4	Forward: GCAGCGACTATGCACAACGA Reverse: CCAGAGTGGTGACGGAGACA
9	SOX2	Forward: TACAGCATGTCCTACTCGCAG Reverse: GAGGAAGAGGTAACCACAGGG
10	Nanog	Forward: AATACCTCAGCCTCCAGCAGATG Reverse: TGCGTACACACCATTGCTATTCTT





# PUBLICATIONS

---

## Publications from Thesis Work:

Gurjar, S.S. and Bose B. (2021). *HIF-1 $\alpha$  recruits cripto-1 to execute its primary functions like enrichment of Cancer Stem Cells (CSCs) and increased resistance to drugs in HEK293 cells.* (Manuscript under preparation).

## Conference Proceedings:

Presented a paper titled “*Oncofetal gene Cripto-1 Induces Expression of Cancer Stem Cell Markers*” at the, *37th Annual Conference of the Indian Association for Cancer Research (37th IACR Convention) “From Cancer Biology to Precision Oncology”* held at Bose Institute, Unified Academic Campus, Kolkata, Feb 23 -25, 2018.

## Publications from Collaborative Work:

1. Pant, R., Jangra, A., Kwatra, M., Singh, T., Kushwah P., Bezbaruah B.K., **Gurjar, S.S.**, Phukan, S. (2017) *Cognitive Deficits Induced by Combined Exposure of Stress and Alcohol Mediated through Oxidative Stress-PARP Pathway In the Hippocampus. Neuroscience Letters*, 653,208-214.
2. Jangra, A., Sriram, C.S., Dwivedi, **Gurjar, S.S.**, Hussain M.I., Borah, P., Lahkar, M. (2017) *Sodium Phenylbutyrate and Edaravone Abrogate Chronic Restraint Stress-Induced Behavioral Deficits: Implication of Oxido-Nitrosative, Endoplasmic Reticulum Stress Cascade, and Neuroinflammation. Cellular and Molecular Neurobiology*, 37,65-81.
3. Sriram, C.S., Jangra, A., **Gurjar, S.S.**, Mohan, P., Bezbaruah B.K. (2016) *Edaravone Abrogates LPS-induced Behavioral Anomalies, Neuroinflammation and PARP-1. Physiology & Behavior*, 154, 135-144.

4. Sulakhiya, K., Keshavlal, G.P., Bezbaruah, B.B., Dwivedi, S., **Gurjar, S.S.**, Munde, N., Jangra, A., Lahkar, M., Gogoi, R. (2016) *Lipopolysaccharide Induced Anxiety-and Depressive-Like Behaviour In Mice are Prevented by Chronic Pre-Treatment of Esculetin. Neuroscience Letters*, 611, 106-111.
5. Jangra, A., Dwivedi, S., Sriram, C.S., **Gurjar, S.S.**, Kwatra, M., Sulakhiya, K., Baruah, C.C., Lahkar, M. (2016) *Honokiol Abrogates Chronic Restraint Stress-Induced Cognitive Impairment and Depressive-Like Behaviour by Blocking Endoplasmic Reticulum Stress in the Hippocampus of Mice. European Journal of Pharmacology*, 770, 25-32.
6. Jangra, A., Kasbe, P., Pandey, S.N., Dwivedi, S., **Gurjar, S.S.**, Kwatra, M., Mishra, M., Venu, A.K., Sulakhiya, K., Gogoi, R., Sarma, N., Bezbaruah B.K., Lahkar, M. (2015) *Hesperidin and Silibinin Ameliorate Aluminum-Induced Neurotoxicity: Modulation of Antioxidants and Inflammatory Cytokines Level in Mice Hippocampus. Biological Trace Element Research*, 168 (2), 462-471.
7. Sriram, C.S., Jangra, A., **Gurjar, S.S.**, Hussain, M.I., Borah, P, Lahkar, M., Mohan, P., Bezbaruah B.K. (2015). *Poly (ADP-Ribose) Polymerase-1 Inhibitor, 3-Aminobenzamide Pretreatment Ameliorates Lipopolysaccharide-Induced Neurobehavioral and Neurochemical Anomalies in Mice. Pharmacology Biochemistry and Behavior*, 133, 83-9.
8. Sulakhiya, K., Kumar, P., **Gurjar, S.S.**, Baruah, C.C., Hazarika, N.K. (2015). *Beneficial Effect of Honokiol on Lipopolysaccharide Induced Anxiety-Like Behavior and Liver Damage in Mice. Pharmacology Biochemistry and Behavior*, 132, 79-87.
9. Sriram, C.S., Jangra, A., Madhana, R.M., **Gurjar, S.S.**, Mohan, P., Bezbaruah B.K. (2015). *Multiple Facets of Poly (ADP-Ribose) Polymerase-1 in Neurological Diseases. Neural Regeneration Research*, 10 (1), 49.